

QUANTITATIVE PROTEOMIC ANALYSIS OF THE HUMAN IMMUNE RESPONSE  
FOLLOWING INFLUENZA VACCINATION

By

Allison C. Galassie

Dissertation

Submitted to the Faculty of the  
Graduate School of Vanderbilt University  
in partial fulfillment of the requirements

for the degree of

DOCTOR OF PHILOSOPHY

in

Chemistry

May, 2017

Nashville, Tennessee

Approved:

Andrew J. Link, Ph.D.

C. Buddy Creech, M.D.

John A. McLean, Ph.D.

David W. Wright, Ph.D.

## ACKNOWLEDGMENTS

The work presented in this dissertation could not have been possible without the generous financial support of Vanderbilt University and the Immunobiology of Blood and Vascular Systems training program (IBVSTP) grant (5T32HL069765-12). The IBVSTP grant's Inflammation Forum gave me the opportunity to expand my knowledge into the field of immunology, a brand new field to me. The forum also gave me many opportunities to present my work to other members and get helpful feedback along the way. I really have the IBVSTP to thank for the confidence in my public speaking skills.

There have been a number of people who helped guide me through graduate school. First, I would like to thank my PhD advisor, Dr. Andrew Link for giving me the opportunity to train and work under his guidance. I came to his lab in the Department of Pathology, Microbiology, and Immunology with no significant knowledge in any of those subjects, yet he gave me the opportunity to expand my knowledge base and become a mixture of an immunological chemist and chemical immunologist. His advice and critiques have helped me grow as a person and confident scientist. I would especially like to thank him for providing me with the wonderful opportunities for me to learn and present my work at many conferences around the nation.

I would like to thank the members of my doctoral committee Drs. John McLean, David Wright, and Buddy Creech. While still stressful, committee meetings and exams were lightened by your presence and humor. I am very grateful for your advice on how to tell the analytical story of my research, the push to present for the chemistry forum, and the friendly conversations had along the way. I would also like to thank all of the collaborators who have made my life interesting over the past few years: Dr. Leigh Howard, Dr. Kathryn Edwards, Johannes Goll, Travis Jensen, Dr. Sebastian Joyce, Dr. James Thomas, Dr. Nripesh Prasad, Dr. Mark Boothby, and Dr. Tom Dever. Each project offered new challenges and interesting biology for me to learn.

Thank you to the Link Lab members, both former and current, for helping me on this journey. Dr. Parimal Samir took me under his wing during my rotation and taught me everything he knew about being the main operator of our mass spectrometers. Being very well read, he was the first one to tell me about newly published research and taught me the benefit of being well read outside of my focus. He also provided me a lot of help and advice regarding my projects and politely pointed out the flaws before someone else did. Dr. Kristen Hoek helped me immensely with understanding the biological aspects of my project, the cell work project that is still in its initial stages, and the editing of manuscripts. I would like to extend my thanks to the rest of the Link Lab members I've had the pleasure of working with: Drs. Chris Browne, Tara Allos, and Xinnan Niu.

On a personal note, I would like to thank Alexis Wong, Lauren Gibson, Brad Durbin, Bryson Howard, Chad Chumbley, and Jessica Moore for not only being colleagues but also friends. Alexis and Lauren – Thank you for bringing me up when I was down and celebrating with me when things were perfectly right. I could not have asked for better friends during the most trying years of my life. Now we just need to get going on those Nashville bucketlists! Brad and Bryson – Thank you for always being funny and making sure I was social every once in a while. Chad – Thank you for not assuming I was a stalker when I not only chose the same graduate school as you, but the same apartment complex as well. I am forever grateful for being able to call you over to kill giant spiders for me and for the board game fun on snow days. Jessica – Thank you for making me an honorary Caprioli lab member during ASMS conferences and making sure I was never kidnapped when returning to my hotel. Through you, I met a number of other Caprioli group members to talk to and I never felt awkward or unwelcome at all.

The decision to come to graduate school was not easy, but various people helped with the decision. I would like to thank my high school teachers and college professors for the support and guidance. Mr. Spigner – I can trace where I am today back to the pivotal moment in your 9<sup>th</sup> grade physical science class when I discovered that chemistry was my passion. Dr. Vance – Thank you for helping me realize that I will be even more valuable to the forensic science community with a

graduate degree. Dr. Darrin Smith – Thank you for allowing me to conduct undergraduate research with you. It was a difficult project, but gave me helpful insights into what real chemistry research is like. I look forward to bumping into you at future ASMS conferences. Dr. Lori Smith – Thank you for taking a chance on me as an intern and then allowing me to continue as a part-time technician. I have a much stronger stomach thanks to you and a horse placenta in a blender. The experience I gained at the UK VDL is unquantifiable. Thank you for your influence and continued friendship. Lindsay Huffman – Thank you for being my Colonel Camp buddy and first Eastern Kentucky friend. I cannot imagine what EKU would have been like without you. Thank you for being so supportive of what I'm doing and encouraging me. Ethan Kilgore – Most people thought we were crazy when we decided to try long distance while both being in PhD programs, however we have made it work and are better for it. While vastly different than what you study, you never once have minded helping me talk through an experiment issue or practice a presentation, even when you have other things to do. No one understands the ups and downs in my life quite like you do. Thank you for the support, encouragement, and companionship.

Finally, I would like to thank my family for their love and support. Adrienne – thanks for being a great sister and lamenting with me from time to time about the difficulties of graduate school. Mom and Dad – I would not have made it this far without you and your encouraging Winnie the Pooh and Willy Wonka quotes. You have supported every decision I made, even when it meant leaving home at 16 to go to the special math and science school. Thanks for raising me to be the person I am today. I am eternally grateful for everything you have done and provided for me. I love you.

## TABLE OF CONTENTS

	Page
ACKNOWLEDGMENTS .....	ii
LIST OF FIGURES .....	vii
LIST OF TABLES .....	ix
ABBREVIATIONS .....	xi
 Chapter	
I. INTRODUCTION .....	1
Introduction to influenza.....	1
Immune responses to infections and vaccines.....	4
A brief history of influenza vaccines.....	8
Vaccine adjuvants .....	9
Systems biology in the study of vaccines.....	11
Proteomics in systems vaccinology .....	13
Quantitative Proteomic Methods and iTRAQ .....	14
Scope of this work .....	18
Acknowledgements.....	19
References .....	19
II. A CELL-BASED SYSTEMS BIOLOGY ASSESSMENT OF HUMAN BLOOD TO MONITOR PROTEOMIC IMMUNE RESPONSES AFTER INFLUENZA VACCINATION .....	28
Introduction.....	28
Methods and Materials .....	30
Seasonal TIV vaccination of human volunteers and blood collection .....	30
Immune cell isolation .....	31
iTRAQ experiment preparation .....	31
Quantitative proteomic analysis .....	32
Comparative and differential analysis .....	33
Visualization of proteins across the human genome .....	33
Network analysis.....	33
Data Availability .....	34
Results and Discussion .....	34
Protein quantification from purified cells.....	34
Evaluation of proteomics data quality.....	34
Comparison of two iTRAQ labeling strategies.....	35
Proteomic profiles of two TIV-vaccinated subjects .....	38
Differential analysis of proteins from two TIV-vaccinated subjects .....	42
Conclusions.....	49
Acknowledgements.....	49
References .....	50
III. QUANTITATIVE PROTEOMIC ANALYSIS OF HUMAN IMMUNE CELLS IN RESPONSE TO AS03-ADJUVANTED H5N1 VACCINATION.....	54
Introduction.....	54
Methods and Materials .....	57
Clinical study design .....	57

Immune cell purification .....	58
Immune serologic assays .....	58
Quantitative proteomic analysis .....	58
Quality Control of Protein Samples .....	59
Peptide and protein quantitation .....	60
Analysis datasets.....	61
Significant Proteins.....	62
Gene set enrichment analysis.....	62
Protein-protein interaction networks.....	63
Regularized logistic regression analysis .....	63
Results and Discussion .....	63
Protective antibody responses .....	63
Multiple baseline time points enhance sensitivity .....	67
AS03-modulated protein responses across time .....	70
AS03-induces antigen processing and presentation pathways.....	75
Antigen presentation and oxidative stress response proteins predict seroprotection status .....	76
Comparison of proteomic and transcriptomic data .....	77
Conclusion.....	79
Acknowledgements.....	80
References .....	81
IV. CONCLUSIONS AND PERSPECTIVES.....	86
Summary .....	86
Study Limitations .....	88
Future Directions .....	89
Protein Validation Studies.....	89
Metabolomics .....	90
AS03 Mechanism of Action.....	90
Conclusion.....	92
References .....	93
Appendix	
A. SUPPORTING INFORMATION: CHAPTER II .....	97
B. SUPPORTING INFORMATION: CHAPTER III .....	99
Supplemental Methods .....	99
Ethics statement .....	99
Study products.....	99
Analysis population.....	100
Reference Channel Selection .....	100
Normalization.....	100
Supplementary Results.....	101
Quality Control.....	101
Supplementary Figures and Tables .....	102
C. ASSESSMENT OF INSTRUMENT STABILITY .....	139
CURRICULUM VITAE .....	141

## LIST OF FIGURES

Figure 1.1 Influenza virus structure. <sup>3</sup> .....	1
Figure 1.2 Timeline and evolution of pandemic influenza viruses. <sup>8</sup> .....	2
Figure 1.3 Locations of confirmed human cases for avian influenza A (H5N1). <sup>14</sup> .....	3
Figure 1.4. Evolution of the H5 hemagglutinin protein. ....	4
Figure 1.5 Overview of the immune response timeline after a vaccine is given. ....	5
Figure 1.6 The principle of vaccine induced immunological memory as illustrated with a tetanus toxoid vaccine. ....	7
Figure 1.7 Peptide fragmentation locations. ....	15
Figure 1.8 Comparison of quantitative proteomic mass spectrometry methods. ....	16
Figure 1.9 iTRAQ labeling method. ....	18
Figure 2.1 Breakdown of the components in blood. ....	30
Figure 2.2 Flow cytometry analysis of immune cell types purified from human blood. ....	31
Figure 2.3 Adequate protein quantity is obtained from sorted immune cells for proteomics applications. ....	34
Figure 2.4 Proteomics quality control. ....	35
Figure 2.5 Two iTRAQ strategies for quantitative proteomic analysis of immune cells after vaccination. ....	36
Figure 2.6 Comparison of global proteome analysis for two iTRAQ strategies. ....	37
Figure 2.7 Circos representation of baseline proteomic profiles of PBMC and individual immune cell types. ....	38
Figure 2.8 Proteomic analysis of purified immune cells in subject HD31 after TIV vaccination. ..	39
Figure 2.9 Proteomic analysis of purified immune cells in subject HD30 after TIV vaccination. ..	40
Figure 2.10 Principal component analysis reveals poor correlation of proteomes between subjects. ....	41
Figure 2.11 Visualization of differentially expressed proteins in PBMC and individual immune cell types. ....	43
Figure 2.12 Unique modules of proteins are differentially expressed in each immune cell type after TIV vaccination. ....	44
Figure 2.13 Networks derived from DE proteins at d1 post-TIV vaccination. ....	46
Figure 2.14 Networks derived from DE proteins at d3 post-TIV vaccination. ....	47
Figure 2.15 Networks derived from DE proteins at d7 post-TIV vaccination. ....	48
Figure 3.1. AS03-adjuvanted H5N1 vaccination enhances the antibody response. ....	55
Figure 3.2 AS03-adjuvanted H5N1 vaccination induced a protective immune response relative to non-adjuvanted vaccine. ....	64
Figure 3.3 Experimental summary statistics by cell type. ....	65

Figure 3.4 Empirical cumulative distribution function plots of protein missingness across samples. ....	66
Figure 3.5 Baseline variability shown by PCA biplots. ....	67
Figure 3.6 Effect of multiple baseline timepoints. ....	69
Figure 3.7 Venn diagrams of differentially abundant proteins by cell type .....	71
Figure 3.8 Heatmaps of DA protein baseline log <sub>2</sub> fold changes for each cell type at each post-vaccination time point. ....	73
Figure 3.9 HLA Class I family time trends of mean log <sub>2</sub> fold changes from baseline by vaccine group. ....	74
Figure 3.10 Heatmap of enriched MSigDB Reactome pathways. ....	76
Figure 3.11 Monocyte day 3 protein-protein interaction network. ....	78
Figure 4.1 Overview of systems vaccinology methods. ....	92
Figure B-1 PCA plots identified outliers in data from each cell type. ....	102
Figure B-2 Boxplots of log <sub>2</sub> ICCS ratios before median normalization. ....	103
Figure B-3 Boxplots of log <sub>2</sub> ICCS ratios after median normalization. ....	104
Figure B-4 Heatmaps of DA protein baseline log <sub>2</sub> fold changes for B cells at each post-vaccination time point. ....	105
Figure B-5 Heatmaps of DA protein baseline log <sub>2</sub> fold changes for monocytes at each post-vaccination time point. ....	106
Figure B-6 Heatmaps of DA protein baseline log <sub>2</sub> fold changes for neutrophils at each post-vaccination time point. ....	107
Figure B-7 Heatmaps of DA protein baseline log <sub>2</sub> fold changes for NK cells at each post-vaccination time point. ....	108
Figure B-8 Heatmaps of DA protein baseline log <sub>2</sub> fold changes for T cells at each post-vaccination time point, ....	109
Figure B-9 Neutrophil experiments control chart. ....	110
Figure B-10 Boxplots assessing response of internal standard yeast proteins. ....	110
Figure B-11 Comparison of peptide normalization methods. ....	111
Figure C-1 Assessment of stability in LTQ. ....	139



## LIST OF TABLES

Table 2.1 Shared DE proteins.....	42
Table 2.2 Comparison of differentially expressed proteins in PBMC and individual immune cell types.....	43
Table 3.1 Proteomics samples for which no iTRAQ results were reported due to insufficient amounts of protein .....	59
Table 3.2 Outlying proteomics samples .....	61
Table 3.3 Proteins encoded by genes determined to be differentially expressed in a parallel RNA-Seq experiment.....	80
Table A-1 Normalized protein expression in human immune cells prior to and post-TIV vaccination.....	97
Table A-2 Normalized protein expression in human immune cells prior to and post-TIV vaccination filtered to remove zero values and contaminating keratins from subject HD30 .....	97
Table A-3 Normalized protein expression in human immune cells prior to and post-TIV vaccination filtered to remove zero values and contaminating keratins from subject HD31 .....	97
Table A-4 Top networks and pathways identified in TIV-vaccinated subjects.....	98
Table B-1 Differentially abundant proteins for B cells at Day 1.....	112
Table B-2 Differentially abundant proteins for B cells at Day 3.....	113
Table B-3 Differentially abundant proteins for B cells at Day 7.....	114
Table B-4 Differentially abundant proteins from B cells at Day 28.....	114
Table B-5 Differentially abundant proteins from monocytes cells at Day 1. ....	115
Table B-6 Differentially abundant proteins from monocytes cells at Day 3. ....	116
Table B-7 Differentially abundant proteins from monocytes at Day 7. ....	117
Table B-8 Differentially abundant proteins for monocytes at Day 28. ....	118
Table B-9 Differentially abundant proteins from neutrophils at Day 1.....	119
Table B-10 Differentially abundant proteins from neutrophils at Day 3.....	120
Table B-11 Differentially abundant proteins from neutrophils at Day 7.....	120
Table B-12 Differentially abundant proteins from neutrophils at Day 28.....	121
Table B-13 Differentially abundant proteins from NK cells at Day 1.....	122
Table B-14 Differentially abundant proteins from NK cells at Day 3.....	123
Table B-15 Differentially abundant proteins from NK cells at Day 7.....	123
Table B-16 Differentially abundant proteins from NK cells at Day 28.....	124
Table B-17 Differentially abundant proteins from T cells at Day 1.....	124
Table B-18 Differentially abundant proteins from T cells at Day 3.....	125
Table B-19 Differentially abundant proteins from T cells at Day 7.....	125

Table B-20 Differnetially abundant proteins from T cells at Day 28. ....	125
Table B-21 Significant protein family overlap between cell types. ....	126
Table B-22 Significantly enriched MSigDB Reactome Pathways for B cells at day 7.....	128
Table B-23 Significantly enriched MSigDB Reactome Pathways for B cells at day 28.....	128
Table B-24 Significantly enriched MSigDB Reactome Pathways for monocytes at day 3.....	129
Table B-25 Significantly enriched MSigDB Reactome Pathways for monocytes at day 7.....	131
Table B-26 Significantly enriched MSigDB Reactome Pathways for monocytes at day 28.....	132
Table B-27 Significantly enriched MSigDB Reactome Pathways for neutrophils at day 1.....	132
Table B-28 Significantly enriched MSigDB Reactome Pathways for neutrophils at day 3.....	133
Table B-29 Significantly enriched MSigDB Reactome Pathways for neutrophils at day 7.....	133
Table B-30 Significantly enriched MSigDB Reactome Pathways for neutrophils at day 28.....	134
Table B-31 Significantly enriched MSigDB Reactome Pathways for NK cells at day 3.....	134
Table B-32 Significantly enriched MSigDB Reactome Pathways for T cells at day 1.....	135
Table B-33 Significantly enriched MSigDB Reactome Pathways for T cells at day 7.....	135
Table B-34 Combination of protein families differentiating between seroprotection status for monocytes at day 1.....	136
Table B-35 Combination of protein families differentiating between seroprotection status for monocytes at day 3.....	136
Table B-36 Combination of protein families differentiating between seroprotection status for monocytes at day 7.....	137
Table B-37 Combination of protein families differentiating between seroprotection status for neutrophils at day 1. ....	138
Table C-1 Components of Pepmix Samples .....	139

## ABBREVIATIONS

2D-DIGE	2-diminesional difference gel electrophoresis
AQUA	Absolute quantitation
AS03	Adjuvant System 03
BCA	Bicinchoninic acid assay
CID	Collision induced dissociation
CV	Coefficient of variation
DA	Differentially abundant
DC	Dendritic cell
DE	Differentially expressed
ESI	Electrospray ionization
FACS	Fluorescence activated cell sorting
FDR	False discover rate
GMT	Geometric mean titer
GSK	GlaxoSmithKline
HA	Hemagglutinin
HAI	Hemagglutination inhibition
HCD	Higher-energy collisional dissociation
HLA	Human leukocyte antigen
HPAI	Highly pathogenic avian influenza
ICAT	Isotope-coded affinity tags
ICCS	Immune cell common standard
iTRAQ	Isobaric tags for relative and absolute quantitation
LC	Liquid chromatography
LAIV	Live attenuated influenza vaccine

LPS	Lipopolysaccharide
MACS	Magnetic activated cell sorting
MDCK	Madin-Darby canine kidney
MHC	Major histocompatibility complex
MMTS	Methyl methanethiosulfonate
MPL	Monophosphoryl lipid A
MRM	Multiple reaction monitoring
MS	Mass spectrometry
MudPIT	Multidimensional protein identification technology
NA	Neuraminidase
NK	Natural killer cell
Nt	Neutralization titers
PAMP	Pattern-associated molecular patterns
PBMC	Peripheral blood mononuclear cell
PBS	Phosphate buffered saline
PCA	Principal component analysis
PMN	Polymorphonuclear cell
PSME	Proteasome activator subunit
PRR	Pattern recognition receptor
SILAC	Stable isotope labeling with amino acids in cell culture
SV	Split virus
TCEP	Tris(2-carboxyethyl)phosphine
TLR	Toll-like receptor
TMT	Tandem mass tags
TIV	Trivalent inactivated influenza vaccine

# CHAPTER I

## INTRODUCTION

### Introduction to influenza

Influenza is one of the most well-known viruses and infectious diseases because of its global spread and seasonal patterns. Influenzas are enveloped viruses that contain 7-8 negative-sense, single-stranded RNA segments, which code for up to 14 different proteins (Figure 1.1). Based on immunologic and biologic properties, influenza viruses are divided into three main types: A, B, and C.<sup>1</sup> Influenza A, the major genera infecting humans, is further divided into subtypes and named based on the two major membrane glycoproteins: hemagglutinin (HA) and neuraminidase (NA). Eighteen HA and 11 NA subtypes have been identified thus far, however not all types cause human infection.<sup>2</sup>

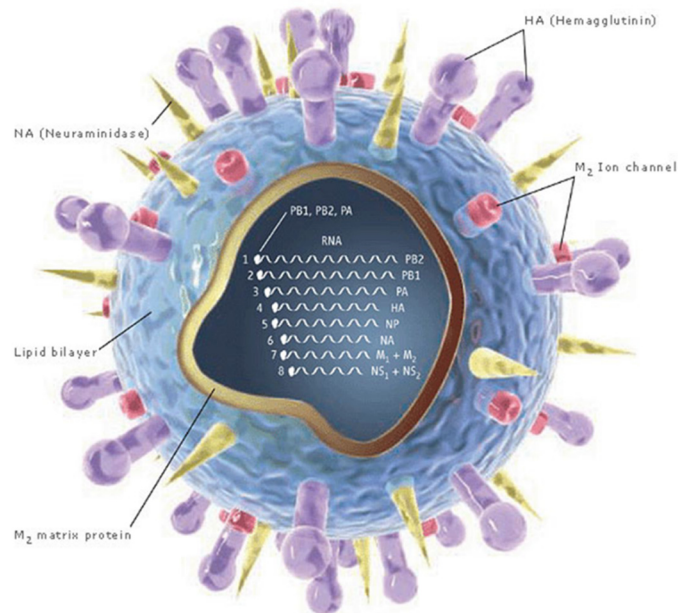


**Figure 1.1 Influenza virus structure.**<sup>3</sup> Reprinted with permission from AAAS.

Each year 3-5 million infections and 250,000-500,000 deaths associated with seasonal influenza outbreaks occur worldwide.<sup>4</sup> While there is a seasonal influenza vaccine, it has to be updated each year to match the strains circulating in the population.<sup>5</sup> Influenza viruses have no RNA polymerase proofreading activity, which yields an error rate of approximately one mutation per replicated genome.<sup>6</sup> As mutations build up (antigenic drift), the virus can escape immune surveillance and require a new vaccine. Additionally, the segmented nature of the RNA genome allows for major antigenic changes through reassortment of co-infecting viruses, typically in an intermediate host (antigenic shift).<sup>7</sup> This introduces new HA and/or NA subtypes into a naïve human population, which can lead to pandemics (Figure 1.2).

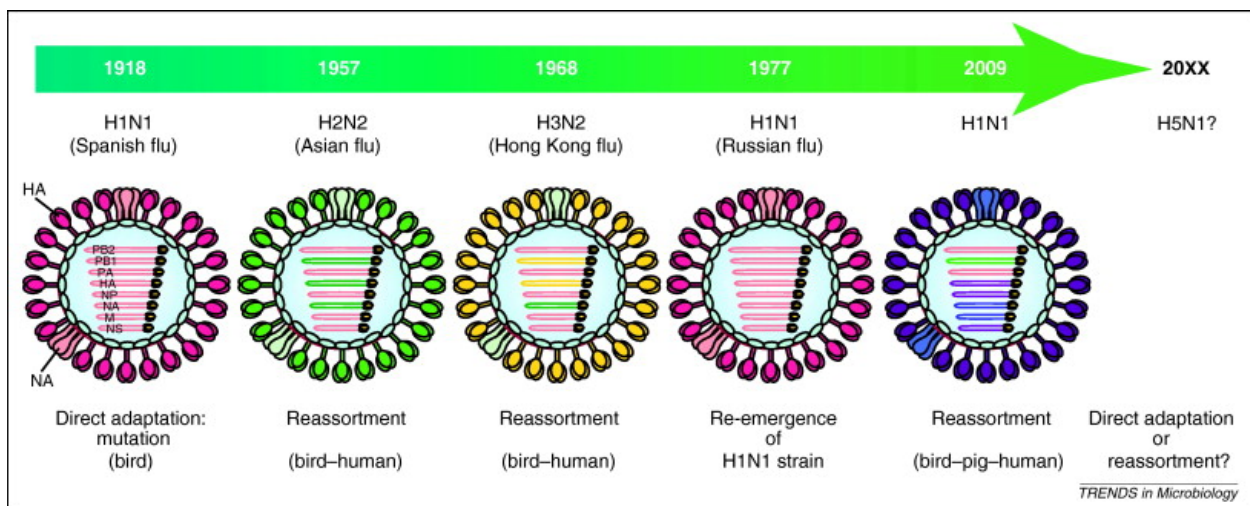


**Figure 1.2 Timeline and evolution of pandemic influenza viruses.**<sup>8</sup> Pandemics in the 20<sup>th</sup> century were caused by various reassortments with between birds, pigs, and humans. The color of the proteins and gene segments represent the originating species: pink = avian, green = human, yellow = human, blue = swine, purple = swine. Future pandemic viruses could emerge from antigenic drift, antigenic shift, or re-emergence of old strains. Reprinted from Trends in Microbiology, with permission from Elsevier.

The 1918 Spanish Influenza (H1N1) pandemic infected 20-40% of the world's population and killed approximately 50 million people, making it the worst influenza pandemic on record.<sup>9</sup> Three other influenza pandemics occurred in the 20<sup>th</sup> century and one in the 21<sup>st</sup> century. Fortunately, these pandemics have not been as catastrophic. All five of these pandemic influenza viruses had

some form of avian origin.<sup>10-12</sup> Today, the biggest potential pandemics are highly pathogenic avian influenza (HPAI) viruses. The first direct HPAI transmission from birds to humans occurred in 1997 in Hong Kong with H5N1.<sup>13</sup> Since then, there have been 856 confirmed human cases and a 53% mortality rate (Figure 1.3).<sup>14</sup> Almost all of the cases have occurred from direct bird-to-human transmission. The failure of the viruses to be readily transmitted from human to human has kept it from becoming a pandemic.

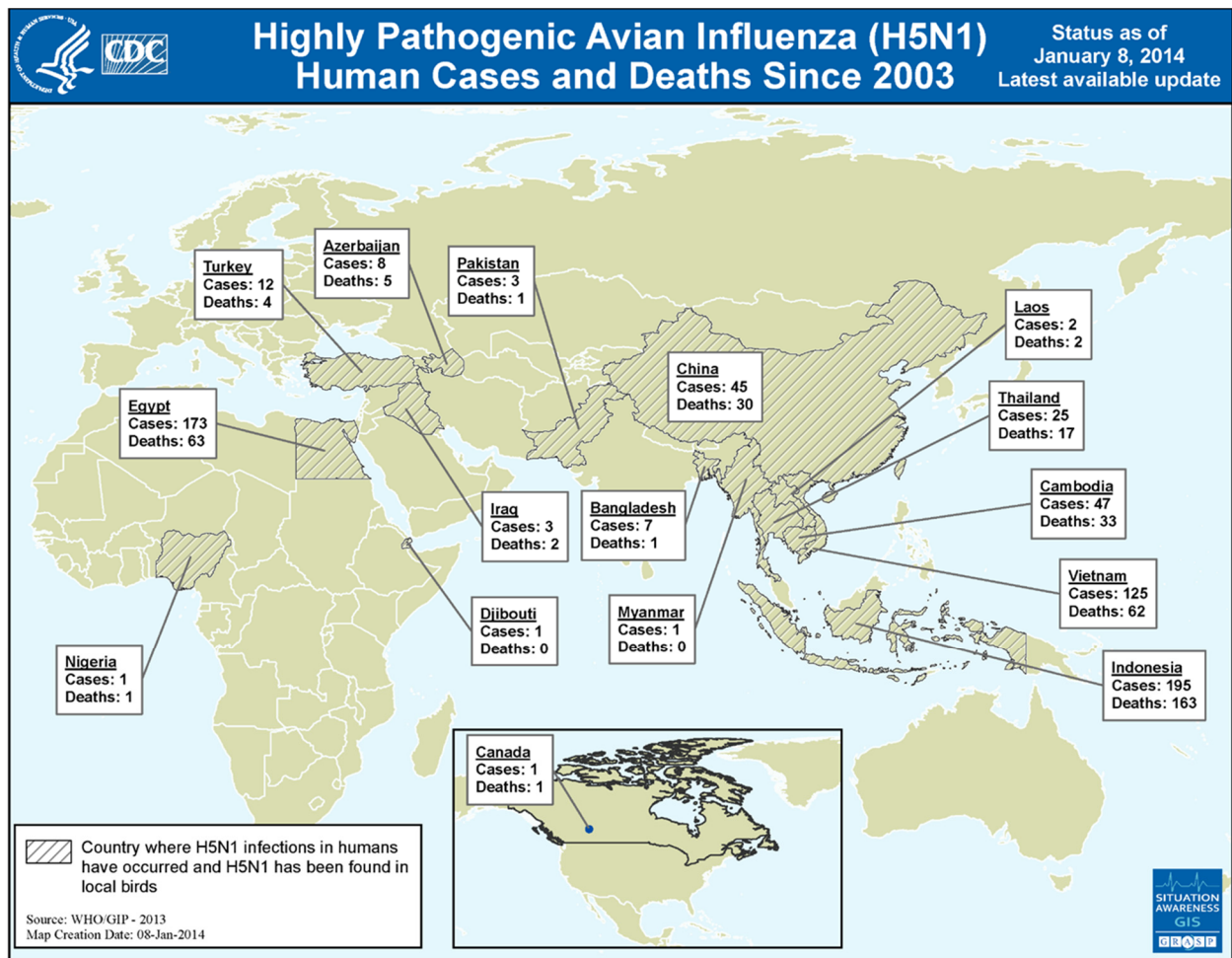
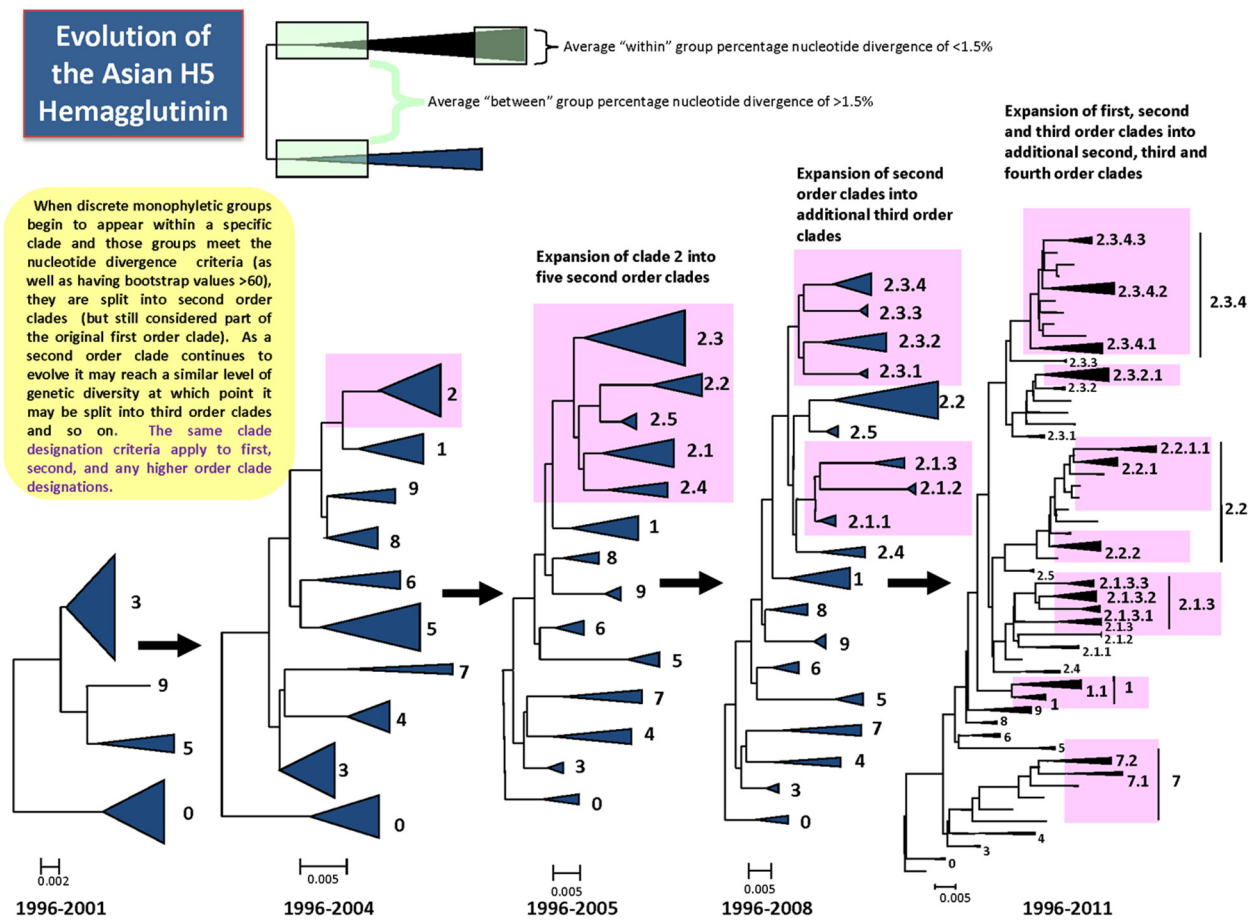


Figure 1.3 Locations of confirmed human cases for avian influenza A (H5N1).<sup>14</sup>

H5N1 is a very diverse avian influenza subtype. The World Health Organization (WHO) has created a unified nomenclature system for the many clades and sub-clades of H5N1 that is

continuously updated when clades diverge (Figure 1.4).<sup>15-16</sup> Given how quickly H5N1 has diversified in ten years, it is reasonable to worry about if the mutations acquired over time will eventually lead to human-to-human transmissibility in the near future. In fact, Herfst *et al.* showed that only five mutations were necessary for H5N1 to become airborne and transmissible between ferrets, an accepted model for human transmissibility.<sup>17</sup>



**Figure 1.4. Evolution of the H5 hemagglutinin protein.** Over time, the WHO has divided the clades into second order, third order, etc. clades based on nucleotide divergence in the H5 HA protein.<sup>15</sup>

### Immune responses to infections and vaccines

The human immune system is a complex collection of different organs, cell types, and effector molecules, that recognize, neutralize, and eliminate infectious microorganisms, such as the



influenza virus.<sup>18</sup> This complex system also recognizes and responds identically to microbial antigens in vaccines to produce immunological protection against the naturally occurring pathogenic organisms. The immune system is divided into two branches: the innate and adaptive systems. Both branches are defined by specialized cell types and functions (Figure 1.5)

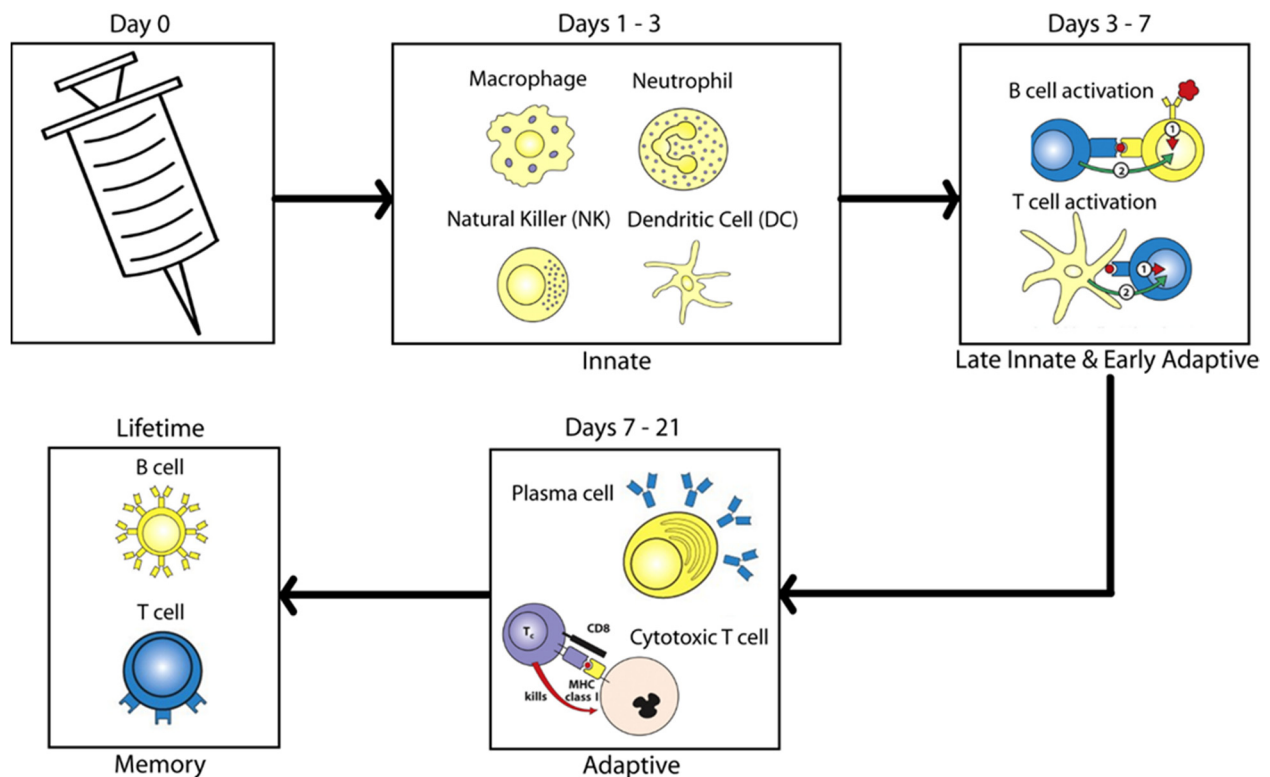


**Figure 1.5 Overview of the immune response timeline after a vaccine is given.** Cell icons reproduced from Janeway's Immunobiology by Murphy, Kenneth et al. with permission of Garland Sciences via Copyright Clearance Center.

The innate immune system acts as the first line of defense against infectious agents. It responds rapidly, but does not lead to long lasting, protective immunity against the pathogen. Innate cells, including neutrophils, macrophages, natural killer cells (NK), and dendritic cells (DC), rely on a limited number of receptors and secreted proteins to recognize and respond to common foreign antigenic features termed pathogen associated molecular patterns (PAMPs).<sup>18</sup> Microbial products including lipopolysaccharides, peptidoglycans, bacterial RNA and DNA, and lipoteichoic

acid are examples of PAMPs recognized by the host's innate pattern recognition receptors (PRRs). When pathogens are detected, they are phagocytized and degraded by the innate cells. The activated innate cells secrete numerous cytokines and chemokines that, in turn, activate and recruit other immune cells to the site of infection. NK cells, while innate in nature, are derived from the lymphoid lineage, while the other innate cell types differentiate from the myeloid lineage. A unique feature of NK cells is their ability to recognize stressed cells and directly induce apoptosis in cells that are missing key cell surface receptors.<sup>18</sup>

Macrophages and DCs, also called antigen-presenting cells, display peptides from the destroyed pathogen on their cell surface using the major histocompatibility complex (MHC) protein complex. The MHC is a group of cell surface proteins that controls a large portion of the immune system in all vertebrates. The MHC binds pathogen-derived peptide fragments and displays them on the host's cell surface for T cells to recognize.<sup>18</sup> In a healthy cell, the proteasome degrades intracellular proteins into short peptides and amino acids for recycling and building of new proteins. Some of these peptides are transported to the endoplasmic reticulum, where they are associated with MHC class I molecules and are presented on the cell's surface in the MHC complex, which indicates the cell is healthy.<sup>19</sup> MHC class II receptors display peptides derived from extracellular proteins that have been phagocytosed and digested in the lysosomes of the host cell. Antigen-presenting cells migrate to the lymph nodes where they present peptides in the context of MHC to naïve, antigen-specific T cells, thus activating them.<sup>18</sup>

Compared to the innate immune response, an adaptive immune response takes longer to generate, but is highly specific to the particular antigen and pathogen. Critically important, the adaptive immune system provides long-lasting protection against the pathogen, which is the ultimate goal of vaccination. There are two broad classes of adaptive responses. First, B lymphocytes are responsible for the humoral antibody response.<sup>18</sup> Each B cell has a unique B-cell receptor on its surface, which binds to one particular antigen. Naïve B cells whose receptors bind antigen and receive a secondary signal from a T-helper cell differentiate into either plasma

cells or memory B cells.<sup>18</sup> Plasma cells proliferate and secrete large amounts of antibodies that recognize the targeted pathogen, neutralize it, and mark it for destruction. Next, T lymphocytes are responsible for cell-mediated immunity, which recognizes and destroys infected host cells. Several subsets of T cells exist, each with a different function. T-helper cells assist other cells, such as B cells, macrophages, and cytotoxic T cells, in their functions. This type of T cell becomes activated from interaction with MHC class II complexes. Cytotoxic T cells destroy infected host cells by recognizing foreign antigens displayed in the context of the MHC class I receptor on the surface of the infected cell. Finally, regulatory T cells are critical for the maintenance of tolerance by shutting down cell-mediated immunity at the end of the infection. Long-lived memory B and T cells enable the immune system to rapidly respond to and neutralize secondary infections by pathogens that have previously been encountered (Figure 1.6).<sup>18</sup> The protective function of the memory adaptive immune response includes neutralizing the pathogens before they can enter host cells, as well as recognizing and destroying pathogen-infected cells before the pathogen can multiply. Vaccines mimic pathogenic infections by stimulating the immune system to respond and acquire immunological memory.

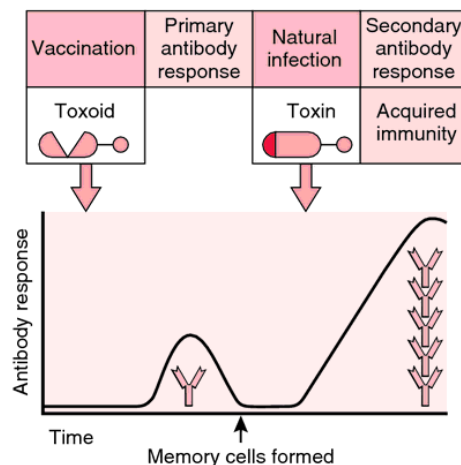


**Figure 1.6 The principle of vaccine induced immunological memory as illustrated with a tetanus toxoid vaccine.** Vaccination with a chemically modified tetanus toxin produces a toxoid, which has no toxicity, but retains its epitopes. A primary antibody response is formed against this toxoid. Later when a natural infection of tetanus toxin occurs, B cells are restimulated and produce a faster and more intense secondary antibody response to the original epitope. From Roitt et al. 2001.<sup>20</sup>

## **A brief history of influenza vaccines**

Vaccinating against the influenza virus is the primary approach for controlling the infection. As vaccines mimic natural pathogenic infections by stimulating the immune system to respond and acquire immunological memory, inactivated and live attenuated vaccines have been developed.<sup>21</sup> A live attenuated influenza vaccine (LAIV) was first developed in 1936,<sup>22-23</sup> followed by an inactivated influenza vaccine in the 1940s.<sup>24</sup> Live attenuated vaccines are passed through a foreign host to become less pathogenic, while inactivated vaccines use heat or formaldehyde to kill the pathogen.<sup>9</sup> Over time, whole-virus vaccines have been largely replaced with purified split virus and subunit vaccines in order to reduce reactogenicity. Split virus vaccines have the virus disrupted by a detergent, while subunit vaccines are further purified to include only the portion of the pathogen that stimulates the immune system, such as the HA protein of influenza viruses. Today, the main seasonal influenza vaccine available is an inactivated trivalent influenza vaccine (TIV), which includes representative strains for A/H1N1, A/H3N2, and B virus.<sup>21</sup> The specific strains are selected based on the surveillance of the circulating viruses from the previous year.<sup>25</sup> Quadrivalent vaccines, which contain both lineages of B virus, are also available, however these are not yet as widespread.<sup>26</sup>

Pandemic influenza vaccines historically have been developed using the same technology as the inactivated seasonal vaccines. The viruses are grown in the allantoic cavities of embryonated chicken eggs, harvested as liquid, undergo inactivation with formalin or  $\beta$ -propiolactone, and are further purified to remove unwanted proteins and other molecules.<sup>9</sup> However, vaccine development for avian influenzas has been hindered due to the virus being rapidly lethal to eggs, the system in which these viruses are grown.<sup>21</sup> Therefore, the product obtained is poorly immunogenic. An inactivated split-virus influenza A/Vietnam (H5N1) vaccine prepared by Sanofi Pasteur requires two 90  $\mu$ g doses given 28 days apart to stimulate an antibody response in 57% of young healthy adults.<sup>27</sup> For comparison, standard seasonal vaccines include just 15  $\mu$ g of HA protein per strain.

Research toward growing viruses for vaccines in continuous cell lines is ongoing in order to eliminate the need for eggs.<sup>28-30</sup> This would allow for increased reproducibility, reduced risk of animal-derived protein products in the vaccines, and allow individuals allergic to eggs to be vaccinated. Two cell lines are the main focus of research: African green monkey kidney cells (Vero) and Madin-Darby canine kidney cells (MDCK). A comparison study of these two cell lines infected with a human influenza virus identified 55 proteins and 32 proteins, respectively, which were shown to be differentially expressed through 2-dimensional difference gel electrophoresis (2D-DIGE) and nano-liquid chromatography (LC) - electrospray ionization (ESI)-MS/MS.<sup>29</sup> The Vero cells showed a stronger stress response to the virus, which may increase cell apoptosis early before enough product is generated. MDCK cells did not show stress responses. Vaccines produced from both cell lines have been in clinical trials showing similar immunogenicity and safety metrics to traditional egg manufacturing methods.<sup>31-34</sup> In 2012 the FDA approved the Flucelvax (Novartis) vaccine, which uses MDCK cells for manufacture. Further, in August 2016, the FDA approved the use of cell-based candidate vaccine viruses in the production of Flucelvax,<sup>35</sup> which could pave the way for avian influenza vaccines to be produced from these cells.

An additional benefit of producing pandemic avian influenza vaccine viruses in cell lines is that these methods may produce more immunogenic strains. Clinical trials of a Vero cell-derived whole virus H5N1 vaccine have shown that subjects showed protective responses after two 7.5 µg or 3.75 µg doses given 21 days apart.<sup>33-34</sup> However, it may be years before pandemic avian influenza vaccines produced using this method are licensed for widespread use. Therefore, other methods of enhancing the immunogenicity to vaccine antigens need to be developed.

### **Vaccine adjuvants**

Adjuvants are one approach to enhance the immunogenicity to vaccine antigens. Adjuvants are added to vaccines in order to increase the stimulation of the immune response by either

enhancing antigen presentation or providing costimulatory signals.<sup>36</sup> Adjuvants have been called the “dirty little secret” of vaccines by the scientific community due to how they were discovered.<sup>37</sup> In 1930, Glenny and colleagues noticed that after precipitating diphtheria toxoid with aluminum sulfate and injecting the “dirty” vaccine into guinea pigs, there was a much greater immune response than to the toxoid alone.<sup>38-39</sup> Using an adjuvant, the amount of antigen can be decreased (dose-sparing). In addition, adjuvanted vaccines can improve the immune response in populations who respond poorly to vaccines, such as elderly and immunocompromised individuals.<sup>36</sup>

Several types of immunologic adjuvants exist depending on the mechanism used to stimulate the immune response.<sup>40</sup> Inorganic aluminum salts, typically aluminum phosphate and aluminum hydroxide (termed alum), are the most widely used adjuvants in human vaccines.<sup>41</sup> Alum has been shown to activate complement<sup>42</sup> and the Nalp3 inflammasome,<sup>43</sup> but the precise mechanism behind the action of alum adjuvants is unknown. It has been hypothesized that the antigen adsorbs on the alum particles, which prolongs its availability to antigen presenting cells.<sup>41</sup> However, it has also been shown that alum causes inflammation at the injection site, resulting in antigen presenting cells being recruited to the area.<sup>41</sup>

In addition to alum, monophosphoryl lipid A (MPL) is an adjuvant used in licensed U.S. vaccines. MPL is derived from the lipopolysaccharide (LPS) of *Salmonella Minnesota* R595,<sup>44</sup> but has only ~0.1% of the toxicity of LPS.<sup>45-47</sup> MPL works by signaling through Toll-like receptor 4 (TLR4) to induce a balanced Th1/Th2 immune response.<sup>48</sup> MPL generally is used in combination with other compounds as an adjuvant system, rather than alone.<sup>47</sup> As AS04, MPL is adsorbed onto alum and is included in the licensed HPV vaccine Cervarix (GlaxoSmithKline).<sup>48</sup> Additionally, MPL is found with QS21, a plant saponin, in AS02 and AS01, where AS01 also contains liposomes.<sup>47, 49</sup> Most recently, the WHO announced that pilot projects of the Mosquirix (RTS,S/AS01) vaccine against malaria will be conducted in sub-Saharan African countries to assess the efficacy of the vaccine in the field, which may help it get licensed.<sup>50-51</sup>

Oil-in-water emulsion adjuvants are another class that are used, particularly in instances when alum adjuvants have proven insufficient. They are thought to increase the trafficking of DCs and macrophages to the lymph nodes.<sup>41</sup> In addition, they are thought to increase the release of cytokines and chemokines from innate cells at the injection site, thus recruiting B and T cells to the site. MF59 (Novartis), a squalene-based adjuvant, appeared for the first time in a U.S. seasonal flu vaccine (FLUAD) during the 2016-2017 season after being licensed in 2015.<sup>52</sup> Another oil-in-water emulsion adjuvant, AS03 (squalene +  $\alpha$ -tocopherol, GlaxoSmithKline), is included in an H5N1 vaccine in the U.S. National Stockpile in case of a pandemic.<sup>53</sup>

Many other types of adjuvants are being developed with the hope of being able to more finely tune the immune response for each pathogen. The saponin QS-21 has been shown to activate human monocyte-derived dendritic cells and promote expression of IL-1 $\beta$ .<sup>54</sup> Synthetic oligodeoxynucleotides containing unmethylated CpG motifs (CpG adjuvants) target TLR9 and enhance humoral immunity.<sup>55</sup> Cytokine mixtures,<sup>56</sup> bacterial endotoxins, D-tetrapeptide-based hydrogels,<sup>57</sup> and others have also been investigated to direct the immune response.<sup>58</sup>

### **Systems biology in the study of vaccines**

Historically, vaccines have been developed empirically using observational knowledge of natural infections and immunity classically illustrated by Edward Jenner's smallpox vaccine in 1798.<sup>59</sup> Jenner used moderately harmful cowpox to immunize against the much more dangerous smallpox (*Variola*) disease. Jenner obtained this idea through a combination of village folklore about milkmaids not becoming infected with smallpox because of previous exposure to cowpox and a conversation in 1763 with Dr. John Fewster who speculated that cowpox might protect against smallpox.<sup>60</sup> When this approach proved successful, more controlled, and scientific experiments were developed to lessen the pathogenicity of specific disease-causing vaccines.<sup>59</sup> Louis Pasteur first showed the attenuation of infectious pathogens by passage in tissue or cell cultures during the development of a chicken cholera vaccine in the late 1870s.<sup>59</sup> Since then, a

number of successful vaccines have been developed using attenuated pathogens or even just killed pathogens. However, due to the empirical nature of vaccine development, not much was understood about how these vaccines were conferring protection. Still, immunologists found methods to assess the efficacy of vaccines.

Correlates of protection, a measurable immune response that is statistically related and responsible for protection, were identified for each vaccine.<sup>61</sup> Antigen-specific antibody titers against the vaccine have been the gold standard for correlates of protection for most pathogens.<sup>61-62</sup> Vaccine-specific antibody levels are measured through standardized serological methods including ELISA to determine binding antibody titers, as well as neutralization and hemagglutination inhibition (HAI) assays. These methods result in a single value representing the full immune response. For example, following influenza vaccination, a serum HAI antibody level greater than 1:40 dilution against the hemagglutinin protein is considered protective.<sup>62</sup> However, a single value threshold may not be sufficient as a correlate of protection due to the natural variability of human biology. In addition, measuring antibody response may not always be the best or only correlate of protection. T cell response is another form of protection that is currently used for the varicella zoster<sup>63</sup> and Bacillus Calmette-Guerin (BCG)<sup>64</sup> vaccines. CD4+ T-cell proliferation assays are the correlate of protection for the zoster vaccine, while interferon levels produced by CD4+ T cells are measured after BCG vaccination.<sup>64</sup> Identifying correlates that are not based on antibodies tends to be more time consuming, expensive, and difficult to perform and interpret compared to antibody assays.

In response to such limitations and difficulties to identify and measure vaccine correlates of protection, current vaccine research has seen a large push toward systems biology studies to study global immune responses to vaccines. Systems biology is an interdisciplinary approach, typically combining multiple –omics fields, that aims to explain complex interactions between all components in biological systems.<sup>65</sup> This approach (termed systems vaccinology) allows for the mechanisms of vaccines to be better understood in order to develop better vaccines and to assess



the efficacy of current vaccines. One goal of systems vaccinology is to predict vaccine immunogenicity and efficacy without relying on the current correlates of protection that are not necessarily the best indicators of protection.<sup>65</sup>

It is hypothesized that dynamic blood transcriptomes and proteomes will show immune response events that correlate with traditional correlates of protection. The first vaccine to be studied this way was the yellow fever vaccine, YF-17D.<sup>66-67</sup> Considered one of the most successful vaccines ever developed, YF-17D provided a good model vaccine to determine the utility of applying systems approaches to vaccines.<sup>65</sup> Using RNA microarrays, Querec *et al.* identified translation initiation factor EIF2AK4 as being correlated with protective cell-mediated and antibody responses, thus providing a predictive signature.<sup>66</sup> Similar studies for TIV<sup>68-69</sup> and meningococcal conjugate vaccines<sup>70</sup> have also identified specific gene signatures correlated either positively or negatively with ultimate antibody responses. Any of these signatures could potentially be classified as correlates of protection if they pass validation. Most interestingly, very early gene expression patterns have been identified as being associated with later antibody responses.<sup>69, 71</sup> Bucasas *et al.*<sup>69</sup> and Nakaya *et al.*<sup>71</sup> identified interferon signaling and antigen presentation pathways up-regulated within the first 24 hours after vaccination. This is a very significant finding for the area of pandemic vaccines, where early determination of a person's ability to develop long-term protection is beneficial. These systems vaccinology studies have offered insights into how protective immunity is generated by investigating multiple immune system components, including mRNA transcripts, antibody responses, and proteins, to obtain a comprehensive assessment of the response to vaccines.<sup>65, 72</sup>

### **Proteomics in systems vaccinology**

While transcriptomic studies are currently expanding our knowledge base about the response to vaccines, systems vaccinology is largely ignoring the proteomics piece of the puzzle. Transcriptomics and proteomics are closely related in that they measure dynamic expression

patterns in response to stimuli. However, multiple studies demonstrate that mRNA and protein expression do not correlate at a given time or even over time.<sup>73-75</sup> By excluding proteomic data, important information about the immune response and possible correlates of protection are potentially missed.

Initial proteomic studies have taken an almost identical approach to RNA studies and used protein and peptide microarrays. Davies *et al.* printed the entire proteome of vaccinia virus on microarray chips and then probed the chips with serum from vaccinated individuals.<sup>76</sup> Antibodies in the serum bound to proteins on the chip were observed using fluorescent secondary antibodies to obtain a quantitative measurement. Price *et al.* found similar results using both whole protein and peptide microarrays for influenza. In addition, peptide-array reactivity significantly correlated with age and neutralization titer.<sup>77</sup> It also has been proposed that certain biomarkers present prior to vaccination can also predict later vaccine response. Using peptide microarrays, four viral influenza hemagglutinin peptides were identified with expression levels that correlated to the pre-vaccination HAI titer.<sup>78</sup> This allowed for a model that successfully identified “good” and “poor” responders to an influenza vaccine based on their baseline antibody repertoire. It is important to note, though, that these studies tested only the antibody repertoire, a small portion of the immune system’s proteome response, to vaccines.

### **Quantitative Proteomic Methods and iTRAQ**

Gel-based proteomic methods largely dominated the proteomics field until mass spectrometry (MS)-based methods were introduced.<sup>79</sup> MS allows for the high-throughput detection of ionized gas-phase analytes based on their mass-to-charge ratio ( $m/z$ ). Electrospray ionization (ESI) is one available method to ionize the analytes.<sup>80</sup> As ESI ionizes analytes from solution, it can easily be combined with liquid separation methods, such as liquid chromatography (LC).<sup>81-83</sup> This is especially beneficial for highly complex proteomics samples.<sup>84</sup> After ionization, analytes are manipulated by electric and/or magnetic fields in order to separate them by their  $m/z$  for detection.

Tandem mass spectrometry (MS/MS) can also be performed to obtain more structural information about the analytes.<sup>85</sup> In MS/MS, a precursor ion is selected, isolated, and fragmented into product ions, which are then detected. This can be done in time within one trapping analyzer or in space with hybrid instruments containing multiple analyzers in series. In the case of proteomics, the starting sample is typically a mix of peptides derived from enzyme digested proteins. When these peptides undergo MS/MS, sequence information can be extracted from their spectra because peptides fragment at predictable locations, with b- and y-ions being the most common (Figure 1.7).<sup>84</sup> Further, the peptides can then be mapped back onto the proteins from databases in order to determine which proteins were present in the original sample.<sup>86</sup>

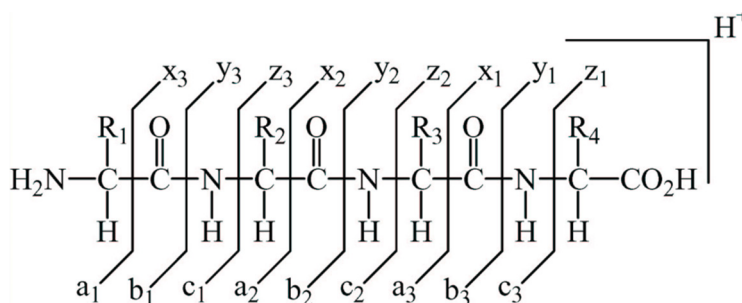


**Figure 1.7 Peptide fragmentation locations.**

Currently, proteomics methods are focused on quantitative studies rather than just protein identifications.<sup>87-88</sup> Multiple methods have been developed for quantitation of proteins using MS, each offering benefits and limitations (Figure 1.8).<sup>89</sup> Generally, these methods are divided between label-free and label-based methods. Label-free methods first allowed for the comparison of the same proteins across different experiments in their natural state. The area under the curve obtained as peptides elute or spectral counting are two methods for label-free quantitation,<sup>90</sup> however high reproducibility is required for the different samples to be compared.<sup>91</sup>

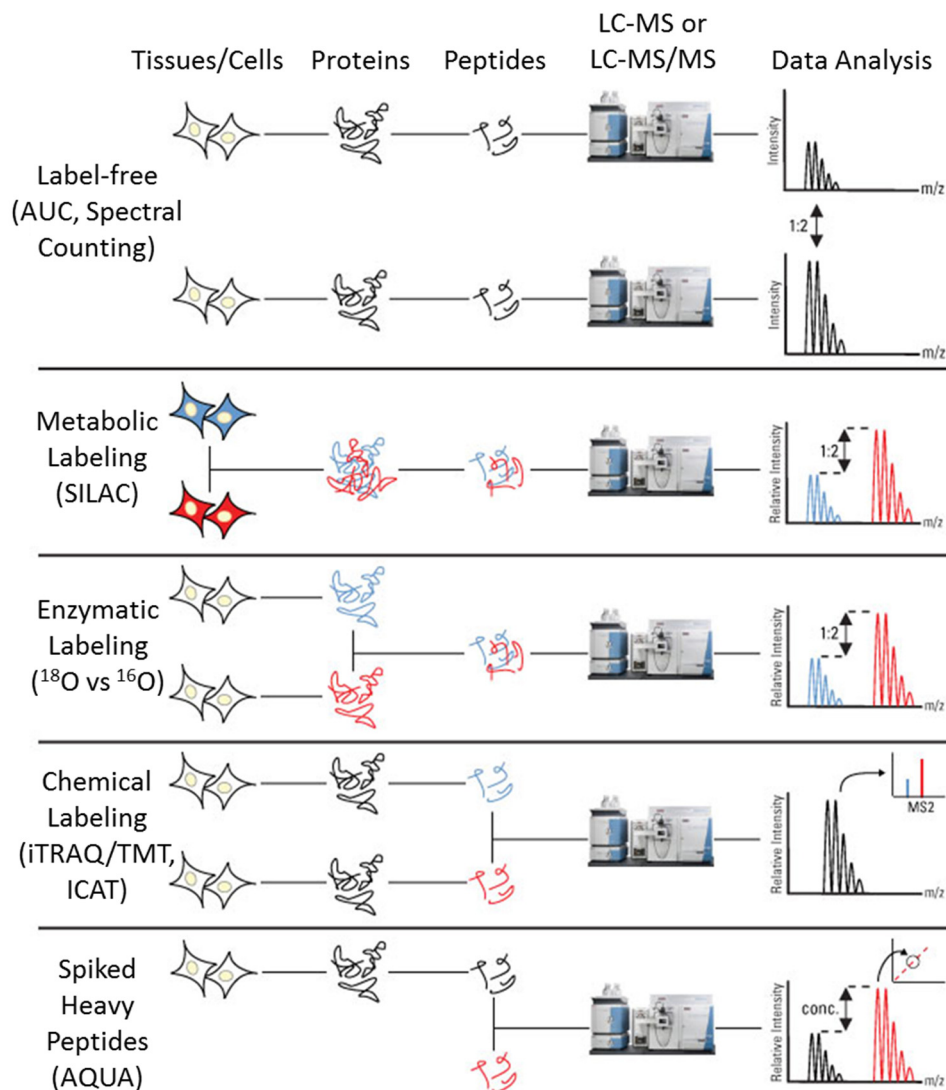


**Figure 1.8 Comparison of quantitative proteomic mass spectrometry methods.** Each method indicates when samples are labeled (shown by blue [light] and red [heavy]). The exception is label-free quantitation, which analyzes each sample individually and compares the data using AUC, spectral counting, etc. Samples are labeled *in vivo* in metabolic labeling, combined, and processed for analysis. In enzymatic and chemical labeling, protein extraction occurs prior to labeling. Enzymatic labeling adds the isotopes during digestion. With chemical labeling, the peptides are labeled after digestion. Isobaric tags, a subcategory of chemical labeling, requires LC-MS/MS to generate cleaved tag spectra in the MS<sup>2</sup> for quantitation. Known amounts of spiked heavy peptides are added to unlabeled samples, which allows for a standard curve to be made. This leads to absolute quantitation. Adapted from Thermo.<sup>92</sup>

Stable isotope-labeling methods were developed to overcome the label-free limitations and offer higher accuracy of measurements, but do require additional steps and higher cost. Label-based methods make use of stable heavy isotopes ( $^{13}\text{C}$ ,  $^{15}\text{N}$ ,  $^{18}\text{O}$ ) to produce mass shifts of peptide peaks in the mass spectrum, while maintaining the original isotope pattern.<sup>91</sup> These heavy

isotopes largely do not affect the behavior of the peptides and proteins during chromatography or in the mass spectrometer. Therefore, the relative-abundance ratios (peak intensities) of peptides can be compared between the different labeled samples to obtain quantitative information.

The simplest labeling method involves the spike-in of isotope labeled standards, which allows for absolute quantitation (AQUA). However, heavy-labeled peptides have to be synthesized for each peptide being quantified, which can be costly.<sup>93</sup> Isotope labels can also be covalently linked to the proteins and peptides. In this case, the isotope labels are introduced metabolically, enzymatically, or chemically.<sup>82</sup> Stable isotope labeling by amino acids in cell culture (SILAC) is the most common method for metabolically labeling proteins.<sup>94</sup> SILAC uses  $^{13}\text{C}_6$ -Lys and  $^{13}\text{C}_6$ - and  $^{15}\text{N}_4$ -Arg containing cell media to label proteins *in vivo*. While this reduces the variability by introducing the labels early on, this method is only possible with experiments involving growing cells.<sup>95</sup> Enzymatic labeling introduces either  $^{18}\text{O}$  or  $^{16}\text{O}$  into peptides during proteolysis, so no additional steps are needed.<sup>96</sup> However, these labels lead to small mass shifts, so high-resolution instruments are required. Chemical labeling, however, is the most common approach for label-based proteomics methods, due to the fact that any sample can be labeled.<sup>91</sup> This method involves the derivatization of peptides with isotopically labeled tags. ICAT (isotope-coded affinity tags)<sup>97</sup>, TMT (tandem mass tags)<sup>98</sup>, and iTRAQ (isobaric tags for relative and absolute quantitation)<sup>99</sup> are all different methods that utilize chemical labeling for quantitation and each allow for different multiplexing capabilities. Weaknesses associated with chemical labeling include incomplete labeling reactions and potential for side reactions.<sup>95</sup>

The iTRAQ method is advantageous because it allows for the simultaneous analysis of up to eight different samples within one experiment.<sup>99-100</sup> Each reagent contains a peptide reactive group, balance group, and reporter group (Figure 1.9A), but overall each reagent has the same molecular weight and produce identical mass shifts. The N-hydroxysuccinimide ester portion of the peptide reactive group reacts with primary amines to label peptides with an isobaric tag. Each sample is labeled with a different reagent, containing different distributions of heavy isotopes in

the reporter group, and mixed. Tagged peptides with identical sequences co-elute and are detected as a single precursor ion (Figure 1.9B). Upon fragmentation of a tagged peptide ion, the reporter ions are measured in the  $m/z$  113-121 range of the MS/MS spectrum. The relative intensities of these reporter ions are proportional to the relative abundances of the labeled peptide between the different samples.

The various MS-based quantitative proteomics methods allow for a higher throughput assessment of a system's proteome than previous quantitation methods. By applying an iTRAQ strategy in systems vaccinology studies, a more global and quantitative view of the immune response can be achieved.

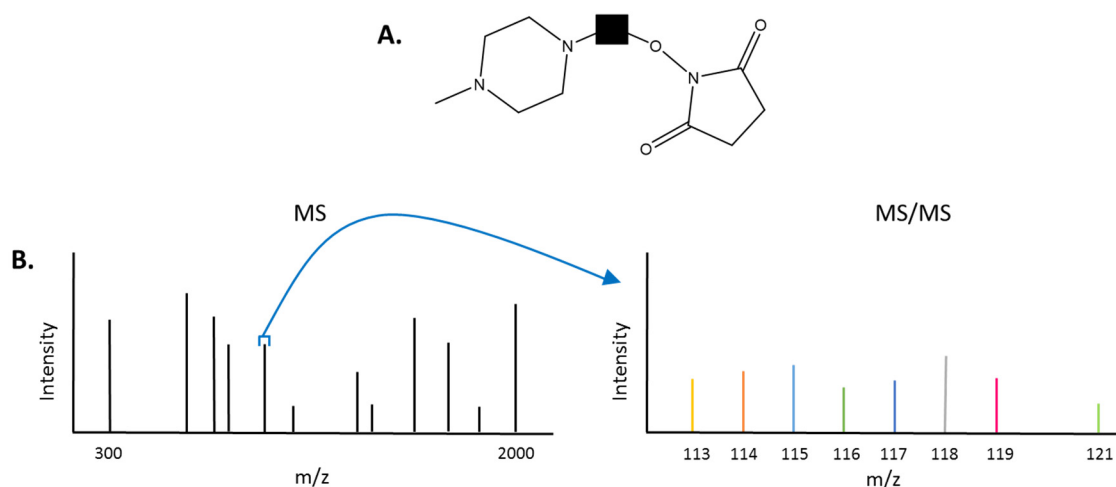


**Figure 1.9 iTRAQ labeling method.** (A) General structure of the individual iTRAQ reagents includes the peptide reactive group (right), balance group (middle), and reporter group. (B) Identical labeled peptides co-elute and are detected as one precursor peak in the MS spectrum. After fragmentation, reporter ions are detected in the low mass range of the MS/MS spectrum, which allows for the quantitative information to be extracted.

### Scope of this work

The goal of this dissertation is to develop and optimize a method for assessing the proteomic response in individual immune cells following vaccination and then apply that method to an adjuvanted influenza vaccine clinical trial in order to better understand the mechanism of action of the adjuvant. Chapter II describes the development and optimization of the quantitative

proteomic method to investigate the immune response in purified immune cells across time. The optimized method multiplexed the same cell type at various time points together using 8-plex iTRAQ. This also serves as a proof-of-concept study showing that by analyzing individual immune cell types, more proteins are identified compared to traditional whole blood or PBMC samples, allowing for a more complete picture of the immune response to be obtained. Chapter III discusses the proteomic results obtained from the AS03-adjuvanted H5N1 clinical trial, which used the optimized method developed in Chapter II. A comparison of these proteomic results to results from a transcriptomics study conducted in parallel is also included. These chapters showcase one of the first times quantitative shotgun proteomics has been used to assess the immune response to a vaccine. By doing so, a more complete understanding of the immune response and vaccine mechanism can be obtained.

### Acknowledgements

Large portions of the this chapter were adapted with permission from A. C. Galassie and A. J. Link, Proteomic contributions to our understanding of vaccine and immune responses. *Proteomics Clinical Applications* 2015, 9, 972-989.

### References

1. Nayak, D.; Shivakoti, S.; Balogun, R. A.; Lee, G.; Zhou, Z. H., Structure, disassembly, assembly, and budding of influenza viruses. In *Textbook of Influenza*, Webster, R. G.; Monto, A. S.; Braciale, T. J.; Lamb, R. A., Eds. John Wiley & Sons, Ltd: Chichester, West Sussex, UK, 2013; pp 37-56.
2. Centers for Disease Control and Prevention Influenza Type A Viruses. <http://www.cdc.gov/flu/avianflu/influenza-a-virus-subtypes.htm> (accessed November 11, 2016).
3. Kaiser, J., A One-Size-Fits-All Flu Vaccine? *Science* **2006**, 312, 380-382.
4. Kreijtz, J. H. C. M.; Fouchier, R. A. M.; Rimmelzwaan, G. F., Immune responses to influenza virus infection. *Virus Res* **2011**, 162, 19-30.
5. Crowe, J. E., Universal Flu Vaccines: Primum non nocere. *Science Translational Medicine* **2013**, 5, 200fs34-200fs34.

6. Boivin, S.; Cusack, S.; Ruigrok, R. W.; Hart, D. J., Influenza A virus polymerase: structural insights into replication and host adaptation mechanisms. *The Journal of biological chemistry* **2010**, *285* (37), 28411-7.
7. Donatelli, I.; Castrucci, M. R.; De Marco, M. A.; Delogu, M.; Webster, R. G., Human-Animal Interface: The Case for Influenza Interspecies Transmission. *Advances in experimental medicine and biology* **2016**, 1-17.
8. Watanabe, Y.; Ibrahim, M. S.; Suzuki, Y.; Ikuta, K., The changing nature of avian influenza A virus (H5N1). *Trends in microbiology* **2012**, *20* (1), 11-20.
9. Bridges, C. B.; Katz, J. M.; Levandrowski, R. A.; Cox, N. J., Inactivated Influenza Vaccines. In *Vaccines, Expert Consult*, 5th ed.; Elsevier, Inc: China, 2008; pp 259-290.
10. Kawaoka, Y.; Krauss, S.; Webster, R. G., Avian-to-human transmission of the PB1 gene of Influenza A viruses in the 1957 and 1968 pandemics. *Journal of Virology* **1989**, *63* (11), 4603-4608.
11. Taubenberger, J. K.; Reid, A. H.; Lourens, R. M.; Wang, R.; Jin, G.; Fanning, T. G., Characterization of the 1918 influenza virus polymerase genes. *Nature* **2005**, *437* (7060), 889-93.
12. Smith, G. J.; Vijaykrishna, D.; Bahl, J.; Lycett, S. J.; Worobey, M.; Pybus, O. G.; Ma, S. K.; Cheung, C. L.; Raghvani, J.; Bhatt, S.; Peiris, J. S.; Guan, Y.; Rambaut, A., Origins and evolutionary genomics of the 2009 swine-origin H1N1 influenza A epidemic. *Nature* **2009**, *459* (7250), 1122-5.
13. Baz, M.; Luke, C. J.; Cheng, X.; Jin, H.; Subbarao, K., H5N1 vaccines in humans. *Virus Research* **2013**, *178* (1), 78-98.
14. World Health Organization *Cumulative number of confirmed human cases for avian influenza A(H5N1) reported to WHO, 2003-2016*; 2016.
15. World Health Organization (WHO) /OIE/FAO, Toward a Unified Nomenclature System for Highly Pathogenic Avian Influenza Virus (H5N1). *Emerging Infectious Diseases* **2008**, *14*, e1-e1.
16. WHO/OIE/FAO H5N1 Evolution Working Group, Continued evolution of highly pathogenic avian influenza A (H5N1): updated nomenclature. *Influenza and Other Respiratory Viruses* **2012**, *6*, 1-5.
17. Herfst, S.; Schrauwen, E. J. A.; Linster, M.; Chutinimitkul, S.; de Wit, E.; Munster, V. J.; Sorrell, E. M.; Bestebroer, T. M.; Burke, D. F.; Smith, D. J.; Rimmelzwaan, G. F.; Osterhaus, A. D. M. E.; Fouchier, R. A. M., Airborne transmission of influenza A/H5N1 virus between ferrets. *Science* **2012**, *336*, 1534-41.
18. Murphy, K., *Janeway's Immunobiology*. 8th ed.; Garland Science: London, 2012.
19. Shoshan, S. H.; Admon, A., MHC-bound antigens and proteomics for novel target discovery. *Future Med* **2004**, *5* (7), 845-859.



20. Miller-Keane Encyclopedia and Dictionary of Medicine, N., and Allied Health, Vaccination. <http://medical-dictionary.thefreedictionary.com/vaccination> (accessed December 10 2016).
21. Keitel, W. A.; Neuzil, K. M.; Treanor, J. J., Immunogenicity, efficacy of inactivated/live virus seasonal and pandemic vaccines. In *Textbook of Influenza*, Webster, R. G.; Monto, A. S.; Braciale, T. J.; Lamb, R. A., Eds. John Wiley & Sons, Ltd: Chichester, West Sussex, UK, 2013; pp 313-326.
22. Smorodintsev, A. A.; Tushinsky, M. D.; Drobyshevskaya, A. I.; Korovin, A. A., Investigation on volunteers infected with the influenza virus. *Am J Med Sci* **1937**, *194*, 159-170.
23. Stokes, J.; Chenoweth, A. D.; Waltz, A. D.; Gladen, R. G.; Shaw, D., Results of Immunization by Means of Active Virus of Human Influenza. *The Journal of clinical investigation* **1937**, *16* (2), 237-43.
24. Salk, J. E.; Lavin, G. I.; Francis, T., The antigenic potency of epidemic influenza virus following inactivation by ultraviolet radiation. *Journal of Experimental Medicine* **1940**, *72* (6), 729-745.
25. Centers for Disease Control and Prevention Selecting viruses for the seasonal influenza vaccine. <https://www.cdc.gov/flu/about/season/vaccine-selection.htm> (accessed Jan. 16, 2017).
26. Centers for Disease Control and Prevention Quadrivalent Influenza Vaccine. <http://www.cdc.gov/flu/protect/vaccine/quadrivalent.htm> (accessed December 2, 2016).
27. Treanor, J. J.; Campbell, J. D.; Zangwill, K. M.; Rowe, T.; Wolff, M., Safety and immunogenicity of an inactivated subvirion influenza A (H5N1) vaccine. *N Engl J Med* **2006**, *354*, 1343-1351.
28. Genzel, Y.; Reichl, U., Continuous cell lines as a production system for influenza vaccines. *Expert Rev Vaccines* **2009**, *8* (12), 1681-1692.
29. Vester, D.; Rapp, E.; Kluge, S.; Genzel, Y.; Reichl, U., Virus–host cell interactions in vaccine production cell lines infected with different human influenza A virus variants: A proteomic approach. *J Proteomics* **2010**, *73*, 1656-1669.
30. Hegde, N. R., Cell culture-based influenza vaccines: A necessary and indispensable investment for the future. *Human vaccines & immunotherapeutics* **2015**, *11* (5), 1223-34.
31. Palache, A. M.; Brands, R.; van Scharrenburg, G. J. M., Immunogenicity and reactogenicity of influenza subunit vaccines produced in MDCK cells or fertilized chicken eggs. *The Journal of infectious diseases* **1997**, *176* (Suppl 1), S20-S23.
32. Halperin, S. A.; Nestruck, A. C.; Eastwood, B. J., Safety and immunogenicity of a new influenza vaccine grown in mammalian cell culture. *Vaccine* **1998**, *16* (13), 1331-1335.
33. Tambyah, P. A.; Wilder-Smith, A.; Pavlova, B. G.; Barrett, P. N.; Oh, H. M.; Hui, D. S.; Yuen, K. Y.; Fritsch, S.; Aichinger, G.; Loew-Baselli, A.; van der Velden, M.; Maritsch, F.; Kistner, O.; Ehrlich, H. J., Safety and immunogenicity of two different doses of a Vero cell-

- derived, whole virus clade 2 H5N1 (A/Indonesia/05/2005) influenza vaccine. *Vaccine* **2012**, 30 (2), 329-35.
34. van der Velden, M. V.; Aichinger, G.; Pollabauer, E. M.; Low-Baselli, A.; Fritsch, S.; Benamara, K.; Kistner, O.; Muller, M.; Zeitlinger, M.; Kollaritsch, H.; Vesikari, T.; Ehrlich, H. J.; Barrett, P. N., Cell culture (Vero cell) derived whole-virus non-adjuvanted H5N1 influenza vaccine induces long-lasting cross-reactive memory immune response: homologous or heterologous booster response following two dose or single dose priming. *Vaccine* **2012**, 30 (43), 6127-35.
  35. Centers for Disease Control and Prevention Cell-based flu vaccines. (accessed January 17, 2017).
  36. Coffman, R. L.; Sher, A.; Seder, R. A., Vaccine Adjuvants: Putting Innate Immunity to Work. *Immunity* **2010**, 33, 492-503.
  37. Travis, K., Deciphering Immunology's Dirty Secret. *The Scientist* January 1, 2007, pp 46-51.
  38. Glenny, A., Insoluble precipitates in diphtheria and tetanus immunization. *Br Med J* **1930**, 2 (3632), 244-245.
  39. de Veer, M., New developments in vaccine research -- unveiling the secret of vaccine adjuvants. *Discov Med* **2011**, 12 (64), 195-204.
  40. Sayers, S.; Ulysse, G.; Xiang, Z.; He, Y., Vaxjo: a web-based vaccine adjuvant database and its application for analysis of vaccine adjuvants and their uses in vaccine development. *Journal of biomedicine & biotechnology* **2012**, 2012, 831486.
  41. Ribeiro, C. M. S.; Schijns, V. E. J. C., Immunology of Vaccine Adjuvants. In *Vaccine Adjuvants*, Davies, G., Ed. Humana Press: New York, 2010; pp 1-14.
  42. Ramanathan, V. D.; Badenoch-Jones, P.; Turk, J. L., Complement activation by aluminum and zirconium compounds. *Immunology* **1979**, 37 (4), 881-888.
  43. Eisenbarth, S. C.; Colegio, O. R.; O'Connor, W.; Sutterwala, F. S.; Flavell, R. A., Crucial role for the Nalp3 inflammasome in the immunostimulatory properties of aluminium adjuvants. *Nature* **2008**, 453 (7198), 1122-6.
  44. Qureshi, N.; Takayama, K., Purification and structural determination of nontoxic lipid A obtained from the lipopolysaccharide of *Salmonella Typhimurium*. *The Journal of biological chemistry* **1982**, 257 (19), 11808-11815.
  45. Mata-Haro, V.; Cekic, C.; Martin, M.; Chilton, P. M.; Casella, C. R.; Mitchell, T. C., The vaccine adjuvant monophosphoryl lipid A as a TRIF-biased agonist of TLR4. *Science* **2007**, 316 (5831), 1628-1632.
  46. Okemoto, K.; Kawasaki, K.; Hanada, K.; Miura, M.; Nishijima, M., A Potent Adjuvant Monophosphoryl Lipid A Triggers Various Immune Responses, but Not Secretion of IL-1 or Activation of Caspase-1. *The Journal of Immunology* **2006**, 176 (2), 1203-1208.

47. Casella, C. R.; Mitchell, T. C., Putting endotoxin to work for us: monophosphoryl lipid A as a safe and effective vaccine adjuvant. *Cellular and molecular life sciences : CMLS* **2008**, *65* (20), 3231-40.
48. Baldridge, J. R.; McGowan, P.; Evans, J. T.; Cluff, C.; Mossman, S.; Johnson, D.; Persing, D., Taking a Toll on human disease: Toll-like receptor 4 agonists as vaccine adjuvants and monotherapeutic agents. *Expert Opin Biol Ther* **2004**, *4* (7), 1129-38.
49. Didierlaurent, A. M.; Laupeze, B.; Di Pasquale, A.; Hergli, N.; Collignon, C.; Garcon, N., Adjuvant system AS01: helping to overcome the challenges of modern vaccines. *Expert Rev Vaccines* **2017**, *16* (1), 55-63.
50. World Health Organization *SAGE/MPAC evidence to recommendations table on the use of malaria vaccines*; 2016; pp 1-11.
51. Gosling, R.; von Seidlein, L., The Future of the RTS,S/AS01 Malaria Vaccine: An Alternative Development Plan. *PLoS medicine* **2016**, *13* (4), e1001994.
52. Centers for Disease Control and Prevention FLUAD flu vaccine with adjuvant. <https://www.cdc.gov/flu/protect/vaccine/adjuvant.htm> (accessed January 17, 2017).
53. Food and Drug Administration FDA approves first adjuvanted vaccine for prevention of H5N1 avian influenza. (accessed January 17, 2017).
54. Welsby, I.; Detienne, S.; N’Kuli, F.; Thomas, S.; Wouters, S.; Bechtold, V.; De Wit, D.; Gineste, R.; Reinheckel, T.; Elouahabi, A.; Courtoy, P. J.; Didierlaurent, A. M.; Goriely, S., Lysosome-Dependent Activation of Human Dendritic Cells by the Vaccine Adjuvant QS-21. *Frontiers in immunology* **2017**, *7*, 663.
55. Bode, C.; Zhao, G.; Steinhagen, F.; Kinjo, T.; Klinman, D. M., CpG DNA as a vaccine adjuvant. *Expert Rev Vaccines* **2011**, *10* (4), 499-511.
56. Tovey, M. G.; Lallemand, C., Adjuvant activity of cytokines. *Methods Mol Biol* **2010**, *626*, 287-309.
57. Luo, Z.; Wu, Q.; Yang, C.; Wang, H.; He, T.; Wang, Y.; Wang, Z.; Chen, H.; Li, X.; Gong, C.; Yang, Z., A Powerful CD8+ T-Cell Stimulating D-Tetra-Peptide Hydrogel as a Very Promising Vaccine Adjuvant. *Adv Mater* **2016**, 1-9.
58. Vogel, F. R.; Hem, S. L., Immunologic Adjuvants. In *Vaccines, Expert Consult*, 5th ed.; El: China, 2008; pp 59-71.
59. Plotkin, S. L.; Plotkin, S. A., A Short History of Vaccination. In *Vaccines*, 5th ed.; Plotkin, S. A.; Orenstein, W. A.; Offit, P. A., Eds. Elsevier: China, 2008; pp 1-16.
60. Jesty, R.; Williams, G., Who invented vaccination? *Malta Medical Journal* **2011**, *23* (2), 29-32.
61. Plotkin, S. A., Correlates of Vaccine-Induced Immunity. *Clinical Infectious Diseases* **2008**, *47*, 401-409.

62. Plotkin, S. A., Correlates of Protection Induced by Vaccination. *Clin Vaccine Immunol* **2010**, *17*, 1055-1065.
63. Weinberg, A.; Zhang, J. H.; Oxman, M. N.; Johnson, G. R.; Hayward, A. R.; Caulfield, M. J.; Irwin, M. R.; Clair, J.; Smith, J. G.; Stanley, H.; Marchese, R. D.; Harbecke, R.; Williams, H. M.; Chan, I. S. F.; Arbeit, R. D.; Gershon, A. A.; Schödel, F.; Morrison, V. A.; Kauffman, C. A.; Straus, S. E.; Schmader, K. E.; Davis, L. E.; Levin, M. J., Varicella-Zoster Virus-Specific Immune Responses to Herpes Zoster in Elderly Participants in a Trial of a Clinically Effective Zoster Vaccine. *The Journal of infectious diseases* **2009**, *200*, 1068-1077.
64. Fletcher, H., Correlates of Immune Protection from Tuberculosis. *Curr Mold Med* **2007**, *7*, 319-325.
65. Pulendran, B.; Li, S.; Nakaya, H. I., Systems vaccinology. *Immunity* **2010**, *33*, 516-529.
66. Querec, T. D.; Akondy, R. S.; Lee, E. K.; Cao, W.; Nakaya, H. I.; Teuwen, D.; Pirani, A.; Gernert, K.; Deng, J.; Marzolf, B.; Kennedy, K.; Wu, H.; Bennouna, S.; Oluoch, H.; Miller, J.; Vencio, R. Z.; Mulligan, M.; Aderem, A.; Ahmed, R.; Pulendran, B., Systems biology approach predicts immunogenicity of the yellow fever vaccine in humans. *Nat Immunol* **2009**, *10*, 116-125.
67. Gaucher, D.; Therrien, R.; Kettaf, N.; Angermann, B. R.; Boucher, G.; Filali-Mouhim, A.; Moser, J. M.; Mehta, R. S.; Drake, D. R.; Castro, E.; Akondy, R.; Rinfret, A.; Yassine-Diab, B.; Said, E. A.; Chouikh, Y.; Cameron, M. J.; Clum, R.; Kelvin, D.; Somogyi, R.; Greller, L. D.; Balderas, R. S.; Wilkinson, P.; Pantaleo, G.; Tartaglia, J.; Haddad, E. K.; Sékaly, R.-P., Yellow fever vaccine induces integrated multilineage and polyfunctional immune responses. *J Exp Med* **2008**, *205*, 3119-3131.
68. Nakaya, H. I.; Wrammert, J.; Lee, E. K.; Racioppi, L.; Marie-Kunze, S.; Haining, W. N.; Means, A. R.; Kasturi, S. P.; Khan, N.; Li, G.-M.; McCausland, M.; Kanchan, V.; Kokko, K. E.; Li, S.; Elbein, R.; Mehta, A. K.; Aderem, A.; Subbarao, K.; Ahmed, R.; Pulendran, B., Systems biology of vaccination for seasonal influenza in humans. *Nat Immunol* **2011**, *12*, 786-795.
69. Bucasas, K. L.; Franco, L. M.; Shaw, C. A.; Bray, M. S.; Wells, J. M.; Niño, D.; Arden, N.; Quarles, J. M.; Couch, R. B.; Belmont, J. W., Early Patterns of Gene Expression Correlate With the Humoral Immune Response to Influenza Vaccination in Humans. *The Journal of infectious diseases* **2011**, *203*, 921-929.
70. Li, S.; Roupheal, N.; Duraisingham, S.; Romero-Steiner, S.; Presnell, S.; Davis, C.; Schmidt, D. S.; Johnson, S. E.; Milton, A.; Rajam, G.; Kasturi, S.; Carlone, G. M.; Quinn, C.; Chaussabel, D.; Palucka, A. K.; Mulligan, M. J.; Ahmed, R.; Stephens, D. S.; Nakaya, H. I.; Pulendran, B., Molecular signatures of antibody responses derived from a systems biology study of five human vaccines. *Nat Immunol* **2014**, *15*, 195-204.
71. Nakaya, H. I.; Hagan, T.; Duraisingham, S. S.; Lee, E. K.; Kwissa, M.; Roupheal, N.; Frasca, D.; Gersten, M.; Mehta, A. K.; Gaujoux, R.; Li, G. M.; Gupta, S.; Ahmed, R.; Mulligan, M. J.; Shen-Orr, S.; Blomberg, B. B.; Subramaniam, S.; Pulendran, B., Systems Analysis of Immunity to Influenza Vaccination across Multiple Years and in Diverse Populations Reveals Shared Molecular Signatures. *Immunity* **2015**, *43* (6), 1186-98.

72. D'Argenio, D. A.; Wilson, C. B., A Decade of Vaccines: Integrating Immunology and Vaccinology for Rational Vaccine Design. *Immunity* **2010**, *33*, 437-440.
73. Yeung, E. S., Genome-wide correlation between mRNA and protein in a single cell. *Angew Chem Int Ed Engl* **2011**, *50*, 583-585.
74. Anderson, L.; Silhamer, J., A comparison of selected mRNA and protein abundances in human liver. *Electrophoresis* **1997**, *18* (3-4), 533-537.
75. Greenbaum, D.; Colangelo, C.; Williams, K.; Mark, G., Comparing protein abundance and mRNA expression levels on a genomic scale. *Genome Biol* **2003**, *4* (9), 117.1-117.18.
76. Davies, D. H.; Molina, D. M.; Wrammert, J.; Miller, J.; Hirst, S.; Mu, Y.; Pablo, J.; Unal, B.; Nakajima-Sasaki, R.; Liang, X.; Crotty, S.; Karem, K. L.; Damon, I. K.; Ahmed, R.; Villarreal, L.; Felgner, P. L., Proteome-wide analysis of the serological response to vaccinia and smallpox. *Proteomics* **2007**, *7*, 1678-1686.
77. Price, J. V.; Jarrell, J. A.; Furman, D.; Kattah, N. H.; Newell, E.; Dekker, C. L.; Davis, M. M.; Utz, P. J., Characterization of Influenza Vaccine Immunogenicity Using Influenza Antigen Microarrays. *PLoS One* **2013**, *8*, e64555.
78. Furman, D.; Jovic, V.; Kidd, B.; Shen-Orr, S.; Price, J.; Jarrell, J.; Tse, T.; Huang, H.; Lund, P.; Maecker, H. T.; Utz, P. J.; Dekker, C. L.; Koller, D.; Davis, M. M., Apoptosis and other immune biomarkers predict influenza vaccine responsiveness. *Mol Syst Biol* **2013**, *9*, 659.
79. Oudenhove, L. V.; Devreese, B., A review on recent developments in mass spectrometry instrumentation and quantitative tools advancing bacterial proteomics. *Appl Microbio Biotechnol* **2013**, *97*, 4749-4762.
80. Fenn, J. B.; Mann, M.; Meng, C. K.; Wong, S. F.; Whitehouse, C. M., Electrospray ionization for mass spectrometry of large biomolecules. *Science* **1989**, *246*, 64-71.
81. Aebersold, R.; Mann, M., Mass spectrometry-based proteomics. *Nature* **2003**, *422*, 198-207.
82. Yates, J. R.; Ruse, C. I.; Nakorchevsky, A., Proteomics by Mass Spectrometry: Approaches, Advances, and Applications. *Annu Rev Biomed Eng* **2009**, *11*, 49-79.
83. Rudnick, P. A.; Clauser, K. R.; Kilpatrick, L. E.; Tchekhovskoi, D. V.; Neta, P.; Blonder, N.; Billheimer, D. D.; Blackman, R. K.; Bunk, D. M.; Cardasis, H. L.; Ham, A.-J. L.; Jaffe, J. D.; Kinsinger, C. R.; Mesri, M.; Neubert, T. A.; Schilling, B.; Tabb, D. L.; Tegeler, T. T.; Vega-Montoto, L.; Variyath, A. M.; Wang, M.; Wang, P.; Whiteaker, J. R.; Zimmerman, L. J.; Carr, S. A.; Fisher, S. J.; Gibson, B. W.; Paulovich, A. G.; Regnier, F. E.; Rodriguez, H.; Spiegelman, C.; Tempst, P.; Liebler, D. C.; Stein, S. E., Performance metrics for liquid chromatography-tandem mass spectrometry systems in proteomics analysis. *Molecular & cellular proteomics : MCP* **2010**, *9* (2), 225-241.
84. Hunt, D. F.; Yates, J. R., 3rd; Shabanowitz, J.; Winston, S.; Hauer, C. R., Protein sequencing by tandem mass spectrometry. *Proceedings of the National Academy of Sciences of the United States of America* **1986**, *83*, 6233-6237.

85. McLafferty, F. W., Tandem mass spectrometry. *Science* **1981**, *214* (4518), 280-287.
86. Eng, J. K.; McCormack, A. L.; Yates, J. R., An approach to correlate tandem mass spectral data of peptides with amino acid sequences in a protein database. *J Am Soc Mass Spectrom* **1994**, *5*, 976-989.
87. Bantscheff, M.; Lemeer, S.; Savitski, M. M.; Kuster, B., Quantitative mass spectrometry in proteomics: critical review update from 2007 to the present. *Anal Bioanal Chem* **2012**, *404* (4), 939-65.
88. Bantscheff, M.; Schirle, M.; Sweetman, G.; Rick, J.; Kuster, B., Quantitative mass spectrometry in proteomics: a critical review. *Anal Bioanal Chem* **2007**, *389* (4), 1017-31.
89. Bakalarski, C. E.; Kirkpatrick, D. S., A biologist's field guide to multiplexed quantitative proteomics. *Molecular & cellular proteomics : MCP* **2016**, *15* (5), 1489-1497.
90. Neilson, K. A.; Ali, N. A.; Muralidharan, S.; Mirzaei, M.; Mariani, M.; Assadourian, G.; Lee, A.; van Sluyter, S. C.; Haynes, P. A., Less label, more free: approaches in label-free quantitative mass spectrometry. *PROTEOMICS* **2011**, *11* (4), 535-53.
91. Nikolov, M.; Schmidt, C.; Urlaub, H., Quantitative Mass Spectrometry-Based Proteomics: An Overview. In *Quantitative Methods in Proteomics*, Marcus, K., Ed. Humana Press: New York, 2012; pp 85-100.
92. Thermo Fisher Scientific Quantitative Proteomics. <https://www.thermofisher.com/us/en/home/life-science/protein-biology/protein-biology-learning-center/protein-biology-resource-library/pierce-protein-methods/quantitative-proteomics.html> (accessed January 18, 2017).
93. Kirkpatrick, D. S.; Gerber, S. A.; Gygi, S. P., The absolute quantification strategy: a general procedure for the quantification of proteins and post-translational modifications. *Methods* **2005**, *35* (3), 265-73.
94. Ong, S. E.; Blagoev, B.; Kratchmarova, I.; Kristensen, D. B.; Steen, H.; Pandey, A.; Mann, M., Stable isotope labeling by amino acids in cell culture, SILAC, as a simple and accurate approach to expression proteomics. *Molecular & Cellular Proteomics* **2002**, *1*, 376-386.
95. Ludwig, C.; Bensimon, A., Isotope labeled standards in Skyline. **2015**.
96. Mirgorodskaya, O. A.; Kozmin, Y. P.; Titov, M. I.; Korner, R.; Sonksen, C. P.; Roepstorff, P., Quantitation of peptides and proteins by matrix-assisted laser desorption/ionization mass spectrometry using <sup>18</sup>O-labeled internal standards. *Rapid communications in mass spectrometry : RCM* **2000**, *14*, 1226-1232.
97. Gygi, S. P.; Rist, B.; Gerber, S. A.; Turecek, F.; Gelb, M. H.; Aebersold, R., Quantitative analysis of complex protein mixtures using isotope-coded affinity tags. *Nat Biotechnol* **1999**, *17*, 994-999.
98. Thompson, A.; Schafer, J.; Kuhn, K.; Kienle, S.; Schwarz, J.; Schmidt, G.; Neumann, T.; Hamon, C., Tandem mass tags: a novel quantification strategy for comparative analysis of complex proteins mixtures by MS/MS. *Analytical Chemistry* **2003**, *75*, 1895-1904.

99. Ross, P. L.; Huang, Y. N.; Marchese, J. N.; Williamson, B.; Parker, K.; Hattan, S.; Khainovski, N.; Pillai, S.; Dey, S.; Daniels, S.; Purkayastha, S.; Juhasz, P.; Martin, S.; Bartlet-Jones, M.; He, F.; Jacobson, A.; Pappin, D. J., Multiplexed Protein Quantitation in *Saccharomyces cerevisiae* Using Amine-reactive Isobaric Tagging Reagents. *Molecular & cellular proteomics : MCP* **2004**, 3, 1154-1169.
100. Applied Biosystems, Multiplex protein quantitation using iTRAQ reagents - 8 plex. In *Multiplex protein quantitation using iTRAQ reagents - 8 plex*, Applied Biosystems, Ed.

## CHAPTER II

### A CELL-BASED SYSTEMS BIOLOGY ASSESSMENT OF HUMAN BLOOD TO MONITOR PROTEOMIC IMMUNE RESPONSES AFTER INFLUENZA VACCINATION

#### Introduction

Systems biology is a comprehensive approach to describe complex interactions between multiple components in a biological system.<sup>1</sup> Using high-dimensional molecular approaches, systems biology identifies changes caused by perturbations such as infection or vaccination, combined with extensive computation analysis to model and predict responses.<sup>1</sup> In the context of vaccinology, systems biology offers an approach to dissect the human immune response after immunization by correlating changes in the transcriptome or proteome with antibody or cell-mediated immune responses, in order to make predictions about vaccine efficacy and potentially adverse events, such as pain, headache, fever, and fatigue.<sup>2-3</sup>

Systems biology studies with influenza vaccines have identified modules of genes that positively correlated with protective immune responses.<sup>4-5</sup> For example, interferon-responsive genes that were up-regulated at early time points after TIV positively correlated with robust HAI titers.<sup>4-5</sup> Nakaya *et al.* found that an elevated antibody response to TIV, but not LAIV, correlated with up-regulation of B cell-specific transcripts, including immunoglobulins and the TNFRSF17 surface receptor.<sup>6</sup> Using the Nakaya dataset, Tan *et al.* identified immunoglobulin and complement genes as well as proliferation-associated genes to be predictors of protective antibody production in response to TIV.<sup>7</sup> They concluded that enrichment of these gene sets at 7 days post-TIV vaccination was likely due to an increase of proliferating plasmablasts in subjects with elevated antibody response.<sup>7</sup>

In addition to studying post-vaccination responses, predictive correlates identified prior to vaccination have also been studied. Tsang *et al.* showed that baseline proportions of 126 immune



cell sub-populations in the blood could predict influenza vaccine-induced antibody responses.<sup>8</sup> Furman *et al.* identified several additional baseline predictors of protective immunity, including the frequency of CD8+ T cells and NK cells, as well as multiple differentially expressed gene modules.<sup>9</sup> These included genes associated with: 1) apoptotic pathways; 2) cell survival and proliferation; 3) cell-to-cell signaling; 4) RNA post-transcriptional modification; and 5) carbohydrate metabolism.<sup>9</sup>

Despite insights to the global human immune responses to influenza vaccines obtained from these and other studies, the majority of systems biology studies are limited in scope to total RNA from whole blood or peripheral blood mononuclear cells (PBMC).<sup>4,7-11</sup> Blood is comprised of many hematopoietic cell types that are present in varying proportions (Figure 2.1) and therefore, responses elicited from under-represented cell types are likely masked by those of predominant cells.<sup>12</sup> Nakaya *et al.* observed this when transcription factor XBP-1 was upregulated in sorted B cells, but not PBMC, after TIV vaccination.<sup>6</sup> XBP-1 is necessary for the terminal differentiation of antibody-forming plasma cells, and therefore an important factor for developing protective immunity.<sup>6</sup> Additionally, when utilizing PMBC to monitor the immune response, the contributions of polymorphonuclear (PMN) cells – the prime contributors to innate immunity – are ignored, as these cells are separated out. Furthermore, an immune response represents a highly coordinated effort from multiple hematopoietic cell types – each with their own inherent programming.<sup>13</sup> Therefore, it is vitally important to analyze and model individual immune cell types in response to vaccination.

To develop a comprehensive systems biology model for studying immune responses following vaccination, we developed an efficient protocol to quantitatively analyze five purified immune cell types from human blood that contribute to both innate and adaptive immune responses: T cells, B cells, NK cells, monocytes, and neutrophils. Unlike previous systems vaccinology studies, my protocol uses quantitative proteomics to monitor changes in protein expression prior to and after TIV vaccination. My results reveal that protein expression profiles from each sorted cell type differ

significantly from the profile obtained from PBMC. Comparison of differentially expressed proteins after vaccination with 2011-2012 seasonal TIV further shows considerable differences between PBMC and sorted cells. Together, my data suggest that important cell type-specific information is gained when purified cells rather than PBMC or whole blood are sampled in systems studies.

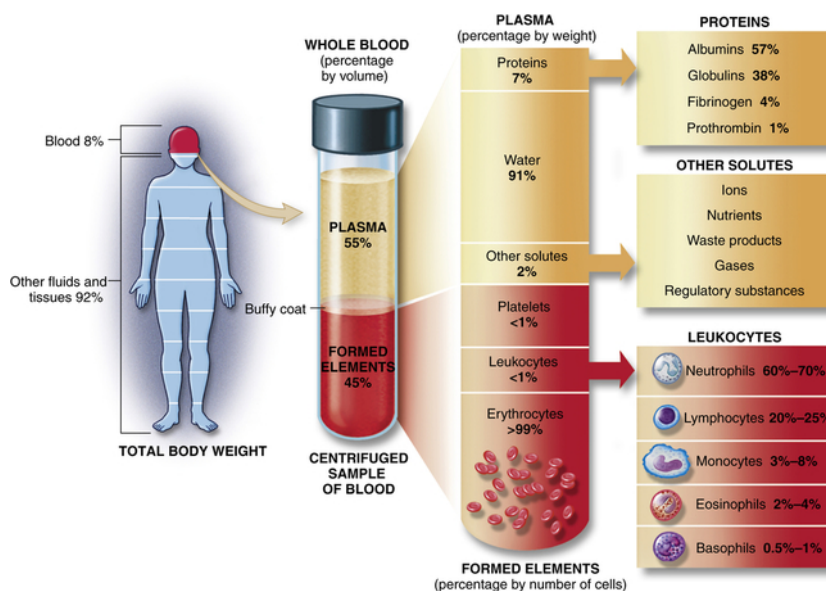


**Figure 2.1 Breakdown of the components in blood.** Immune cells, found in the leukocytes category represent a very small portion of a blood sample. Additionally, these immune cells have different concentrations compared to one another.<sup>14</sup>

## Methods and Materials

### *Seasonal TIV vaccination of human volunteers and blood collection*

Volunteer recruitment and vaccination protocols for this study were approved by the Vanderbilt Institutional Review Board (IRB#111030 “CLR-03 2011-Immune Cells and Soluble Factors from Healthy Donor”). After obtaining written informed consent, two subjects were vaccinated with a single dose of 2011-2012 seasonal trivalent inactivated influenza vaccine (TIV) (strains included: A/California/7/09 (H1N1), A/Perth/16/2009 (H3N2), and B/Brisbane/60/2008). Blood samples (90 mL) from the two vaccinated subjects were processed prior to vaccination (day 0) and at days 1, 3, and 7 post-vaccination for downstream quantitative proteomic analysis.

### Immune cell isolation

Freshly collected whole blood was fractionated into PBMCs and PMNs over a Ficoll density gradient (GE Healthcare, Marlborough, MA). PBMC and PMN fractions were then subjected to magnetic-activated cell sorting (MACS) to positively select CD3+ T cells, CD14+ monocytes, CD15+ neutrophils, CD19+ B cells or negatively enrich for CD3-CD14-CD15-CD19- NK and mDC (Figure 2.2). MACS-enriched cells were further subjected to fluorescence-activated cell sorting (FACS) to achieve  $\geq 98\%$  purity (Figure 2.2). Recovery of sorted mDC cells was insufficient for proteomic analysis ( $1 \times 10^6$  cells needed) and therefore proteomic analysis was not performed on this cell type.

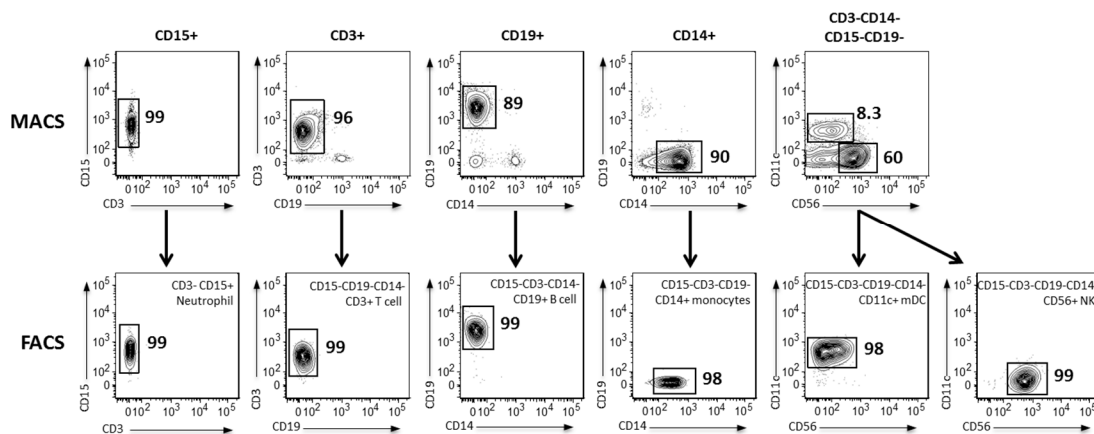


**Figure 2.2 Flow cytometry analysis of immune cell types purified from human blood.** PMN and PBMC cell fractions from a single representative subject were subjected to CD15+, CD3+, CD19+, and CD14+ positive selection or CD19-CD15-Cd14-CD3- enrichment (top panels) via magnetic sorting (MACS). MACS-enriched cells were stained with a cocktail of antibodies and subjected to FACS (bottom panels) to obtain highly purified neutrophil, T cell, B cell, monocyte, and NK populations for systems analysis.

### iTRAQ experiment preparation

Protein extracts from PBMC and sorted immune cells ( $1 \times 10^6$  cells) from two vaccinated human subjects were prepared by ultrasonating cells in lysis buffer (50% trifluoroethanol 50 mM HEPES). The protein amounts were quantified using a BCA assay. An immune cell common standard (ICCS) control sample composed of protein extracts from PBMC and CD15+ cells (80%

and 20%, respectively, by protein weight) was included in duplicate in all 8-plex iTRAQ experiments. Ten micrograms of protein per sample was reduced by 50 mM tris(2-carboxyethyl)phosphine (TCEP), cysteine blocked by 200 mM methyl methanethiosulfonate (MMTS), and digested with trypsin (1:50 trypsin:protein) overnight.<sup>15-18</sup> The peptides were desalted through solid phase extraction with a reverse phase microtrap column (Michrom BioResources, Auburn, CA). The peptides were resolubilized in 7  $\mu$ L 500 mM triethylammonium bicarbonate. Twelve microliters of iTRAQ reagent (AB Sciex, Framingham, MA) were added to the peptide samples. The labeling reactions were incubated with shaking for 2 h, pooled together, frozen, and lyophilized. The iTRAQ labeled samples were resolubilized in buffer A (5% acetonitrile/0.1% formic acid in water) to 0.5  $\mu$ g/ $\mu$ L and analyzed by MudPIT using an Eksigent 2-D nanoLC pump coupled to a nanoESI-LTQ-Orbitrap XL mass spectrometer (Thermo Scientific, Waltham, MA). The precursor ions were analyzed in the Orbitrap followed by 4 CID fragment ion scans in the ion trap to identify the peptides. The precursor ions were then fragmented by HCD to measure reporter ion intensities in the Orbitrap.<sup>19-21</sup>

#### *Quantitative proteomic analysis*

For each precursor ion, the CID and HCD spectra were merged using *Proteome Discoverer v1.3* (Thermo Scientific, Waltham, MA). The merged fragmentation spectra were searched against a forward and reverse concatenated human Ensembl protein and common contaminants database (gene model 74) using the *Sequest* database search engine running under *Proteome Discoverer*.<sup>22-23</sup> Precursor mass tolerance was set to 20 ppm and fragment mass tolerance to 0.8 Da. iTRAQ modification of N-terminus and  $\epsilon$ -amine of lysines and  $\beta$ -methylthiolation of cysteines were used as static/constant modifications of the peptides. Oxidation of methionine and tryptophan and deamidation of asparagine and glutamine were used as dynamic/variable modifications of the peptides. Protein assembly, reporter ion quantitation, and statistical analysis

were performed with a 5% peptide and protein FDR using *ProteoIQ* v2.61 (Premier Biosoft, Palo Alto, CA).

#### *Comparative and differential analysis*

Prior to differential analysis, missing values and contaminating keratin proteins were removed from the protein lists. A  $\geq 1.25$  fold change (calculated in *ProteoIQ*) in expression between pairwise comparisons (days 0-1, 0-3, and 0-7) was considered significant. Comparative analysis of the proteomic profiles between cell types was performed using Spearman correlation coefficients. Principal component analysis (PCA) was performed in *R* and plotted using the *rgl* package.<sup>24</sup> Hierarchical clustering analysis, dendograms, and heatmaps were generated using *Cluster3.0* and *Java Treeview*, respectively.<sup>25-26</sup> A Unix bash shell command was used to identify differentially expressed proteins shared between individuals and cell types, as well as to create lists of proteins for heat maps.

#### *Visualization of proteins across the human genome*

Genome-wide visualization of relative protein expression from PBMC and each purified immune cell type was generated using the open-source *Circos* software package.<sup>27</sup> The genome location for individual protein data points was mapped using *BioMart*.<sup>28</sup>

#### *Network analysis*

Differentially expressed proteins identified in both subjects after vaccination were imported into *Ingenuity Pathway Analysis* (Qiagen, Alameda, CA) to identify the most significantly affected unique canonical pathways, biological functions, and networks between time points.

## Data Availability

The raw proteomics data and unfiltered database search results are available via the ProteomeXchange Consortium (<http://proteomecentral.proteomexchange.org>) with the dataset identifier PXD001657 and DOI 10.6019/PXD001657.

## Results and Discussion

### Protein quantification from purified cells

Prior to performing quantitative proteomics, protein lysates from PBMC and sorted cells were quantified. The different cell types ( $1 \times 10^6$  cells) generated between 30-80  $\mu\text{g}$  protein/sample (Figure 2.3). Neutrophils contained the highest amount of protein, followed by monocytes, while lymphocytes contained the least. As monocytes and neutrophils are much larger than lymphocytes,<sup>29</sup> it is reasonable to see higher protein amounts from these cell types since the assays were performed based on cell number and not cell volume. Lundberg *et al.* previously showed a correlation between cell size and protein expression levels.<sup>30</sup> To remove this bias from later analyses, experiments were done on normalized protein weights rather than cell number.

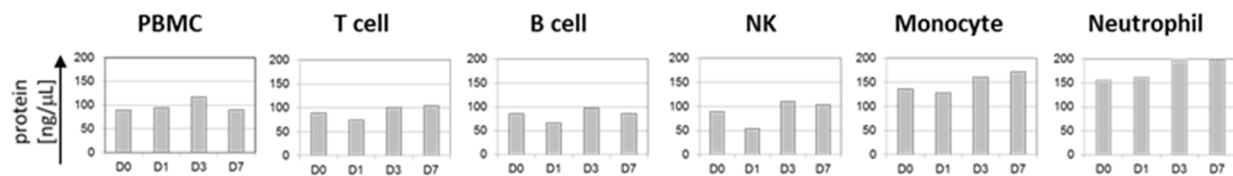


**Figure 2.3 Adequate protein quantity is obtained from sorted immune cells for proteomics applications.** Total protein isolated from sorted immune cells ( $1 \times 10^6$  each cell type) from a single vaccinated subject was quantified.

### Evaluation of proteomics data quality

A slope of the regression line  $>0.8$  between the technical replicates of the common control (ICCS) based upon pseudospectral counts was required as a quality control threshold (Figure 2.4A). A plot of  $\log_2$  fold changes against pseudospectral counts was used to assess the effect of

sampling over the observed fold changes. The symmetric distribution of  $\log_2$  fold changes versus pseudospectral counts suggests the differential expression analysis was unbiased by protein abundances (Figure 2.4B). Distribution of relative expression across different samples was visualized using cluster dot plots to see if obvious differences occurred between samples (Figure 2.4C). The ICCS iTRAQ channels showed a wider range of expression values (last two columns) compared to the purified cell types, likely due to being a compilation of cell types. Experiments where the purified cell types showed similar protein expression distributions were considered in compliance.

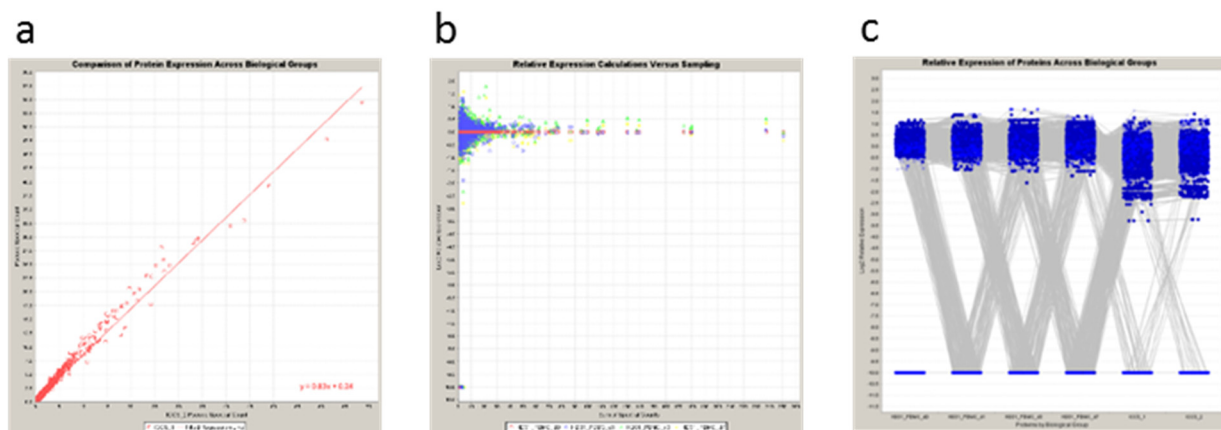


**Figure 2.4 Proteomics quality control.** (a) Scatter plot showing the protein abundances measured in two technical replicates of the ICCS common control. Each dot represents an individual protein. X-axis represents the protein abundances measured in replicate 2. Y-axis represents the protein abundances in replicate 1. (b) Scatter plot showing the distribution of fold changes of proteins with respect to their abundances. Each dot represents an individual protein. X-axis represents protein abundance. Y-axis represents fold changes. (c) Cluster dot plot showing the distribution of fold changes in different iTRAQ channels. Each dot represents an individual protein and the lines represent patterns of expression change.

### *Comparison of two iTRAQ labeling strategies*

Two iTRAQ labeling strategies were tested to determine the optimal pooling strategy for detecting proteomic changes after vaccination (Figure 2.5). In strategy 1, all six cell types at a single time point were multiplexed into one experiment. In strategy 2, all four time points from a single cell type were multiplexed into an experiment. Strategy 1 is advantageous because the

technical experimental variation between cell types at each time point would be minimized. However, since the MS/MS method selects peptides for fragmentation and therefore identification and quantitation based upon their abundance in the sample proteins present in higher amounts across the samples would be preferentially quantified. Thus, differentially changing proteins with low expression from a single cell-type might not be quantified. Further, by increasing the complexity of the sample pool through multiplexing lysates from six different cell types, co-fragmentation of co-eluting peptides might cause an increase in iTRAQ signal interference, and therefore possibly negate the effects of purifying the cells. In contrast, strategy 2 does not have the potential signal interference problems because the sample complexity is reduced due to similar proteomes being pooled together. This would also ensure quantitation of a larger fraction of cell type-specific proteins. However, strategy 2 may detect artifacts due to technical experimental variation.

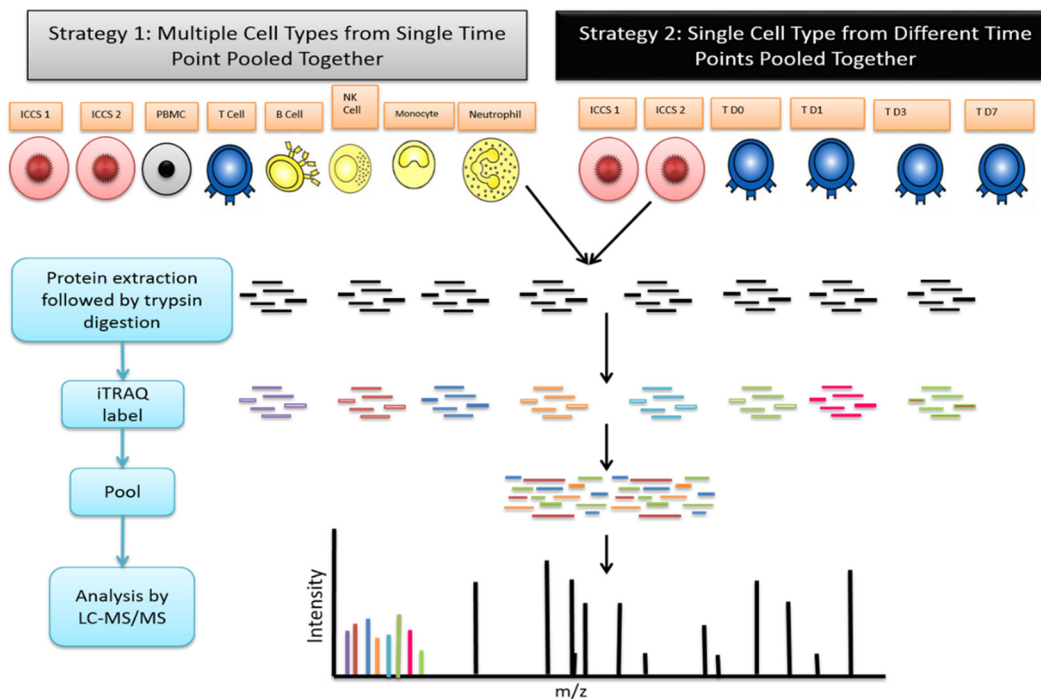


**Figure 2.5 Two iTRAQ strategies for quantitative proteomic analysis of immune cells after vaccination.** Experimental design. In strategy 1, multiple immune cell types from one time point were multiplexed together in the experiment. In strategy 2, different time points from the same immune cell type were multiplexed together. An immune cell common standard (ICCS) was used to normalize reporter ion intensities across the experiments.



The two strategies were compared with both unsupervised hierarchical clustering and PCA (Figure 2.6). In strategy 1, the cell types did not completely cluster together in the unsupervised hierarchical clustering analysis. However, the cell types in strategy 2 did cluster together. Additionally, the heatmap shows distinct protein expression patterns for the different cell types in strategy 2, while strategy 1 has very similar patterns for the cells derived from the PBMC fraction (monocytes, NK cells, B cells, and T cells). The neutrophil samples show a relatively different clustering compared to the other cell types, as they originate from the PMN blood fraction. This is also observed in the PCA plots (Figure 2.6B). There is poor clustering of the cell types in strategy 1 and the different cell types fail to separate. In contrast, strategy 2's PCA plot shows distinct clustering of the cell types (Figure 2.6B). The neutrophil samples clustering the furthest away indicating their different protein expression. The possibility of these results being caused by batch effects was discounted as the samples from each individual iTRAQ experiment using strategy 1 did not cluster together by either hierarchical clustering or PCA. Overall, strategy 2 produced cell-type specific clustering and protein expression patterns by both methods, while strategy 1 did not. Therefore, strategy 2 was considered the optimal approach and employed for the remaining proteomic analysis.

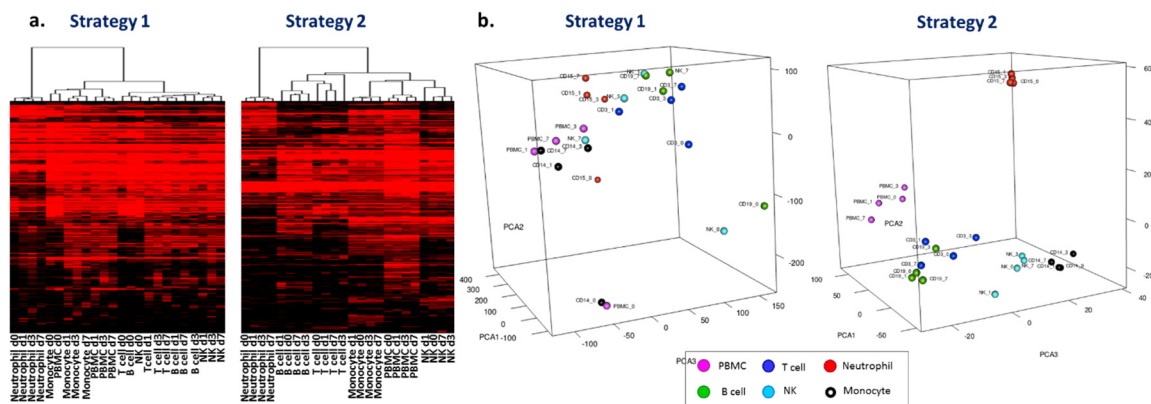


**Figure 2.6 Comparison of global proteome analysis for two iTRAQ strategies.**(a) Unsupervised hierarchical clustering analysis and (b) PCA of pseudo-spectral counts from one subject generated using strategy 1 (left panels; 5,676 proteins, filtered to remove zero values and contaminating keratins) or strategy 2 (right panels, 3,852 proteins, filtered to remove zero values and contaminating keratins) reveals that cell-types cluster together and display distinct cell-type specific patterns of protein expression using strategy 2, but not with strategy 1.

### *Proteomic profiles of two TIV-vaccinated subjects*

The proteomes of PBMC and five purified immune cell types from two subjects before (day 0) and after TIV vaccination (days 1, 3, and 7) were analyzed by MS to identify changes in the immune response. Approximately 7000 proteins were identified in 44 protein samples (Table A-1). After removing zero values (identified but not quantified proteins) and contaminating keratins, approximately 4000 proteins from each subject were retained for further analysis (Table A-2 - Table A-3). The PBMC and purified immune cell baseline (day 0) proteomes from one vaccinated subject (HD31) plotted over the length of the human genome showed activity across the majority of the genome indicating unbiased genome coverage (Figure 2.7). This plot also showed distinct proteomic profiles between the different cell types at baseline. The results agreed with the observations made during the iTRAQ pooling strategies experiments.

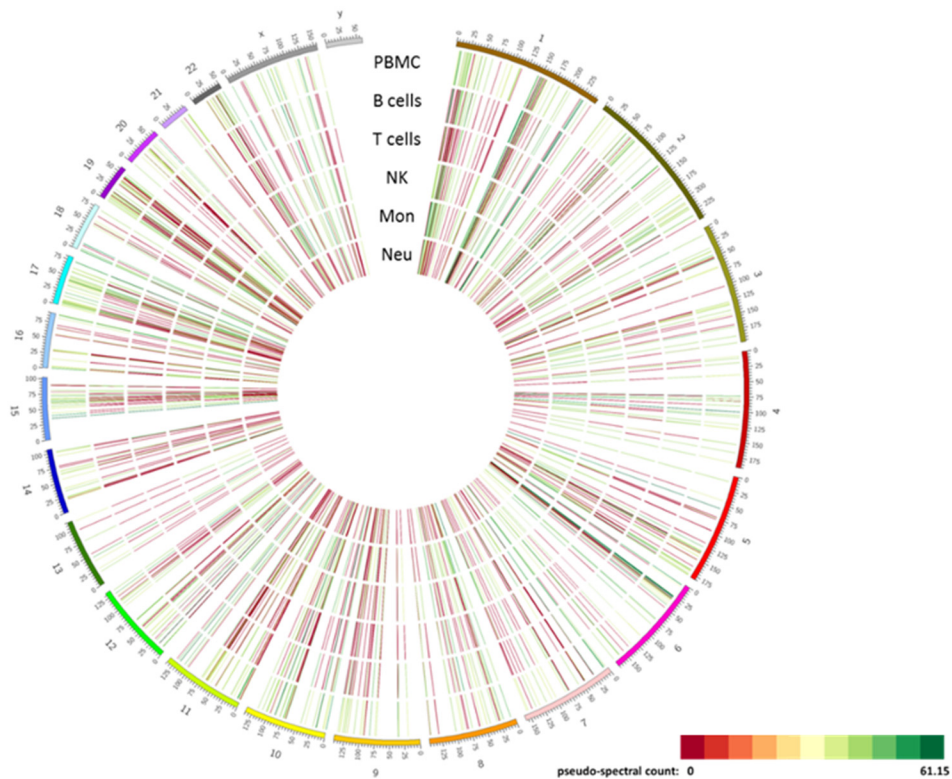


**Figure 2.7** Circos representation of baseline proteomic profiles of PBMC and individual immune cell types. Bars on the outside of the circle represent individual chromosomes. The heat-map color scaling parameter was set to “scale\_log\_base = 10” to allow for optimal color space.

Pair-wise comparisons of baseline proteomic data (day 0) from one subject showed poor correlation between PBMC and sorted cells (Figure 2.8A). The highest correlation was observed between monocytes and PBMC. However a Spearman correlation coefficient of 0.72 suggests a poor correlation. PCA revealed that all cell types clustered distinctly from each other (Figure 2.8B). Semi-supervised hierarchical clustering analysis of identified proteins showed that each cell type displayed a distinct protein expression profile that differed from both PBMC and the other cell types (Figure 2.8C). This indicates that the immune cell purification strategy employed allowed for the identification of proteins that are masked in the PBMC sample. As current vaccine studies use either whole blood or PBMCs to assess the vaccine response, these low abundant proteins would be missed in the analyses and therefore a full picture of the response to vaccines would not yet been synthesized.

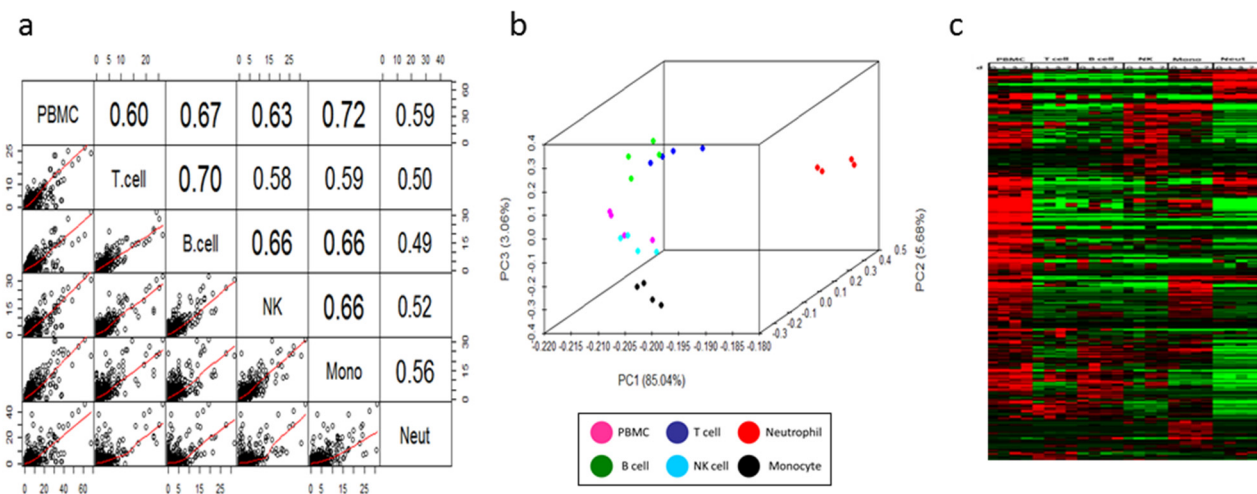


**Figure 2.8 Proteomic analysis of purified immune cells in subject HD31 after TIV vaccination. (a)** Pair-wise comparison of day 0 protein profiles (3,852 proteins, filtered to remove zero values and contaminating keratins) from subject HD31 shows that proteomes of sorted cells correlate poorly with PBMC. **(b)** PCA of protein profiles from subject HD31 at four time points shows that purified immune cell types cluster into distinct groups. **(c)** Semi-supervised hierarchical clustering analysis of relative protein expression from a vaccinated individual reveals that purified immune cells have distinct proteomic expression profiles compared to PBMC. Data was centered across protein and cell type; red = up, black = no change, green = down.

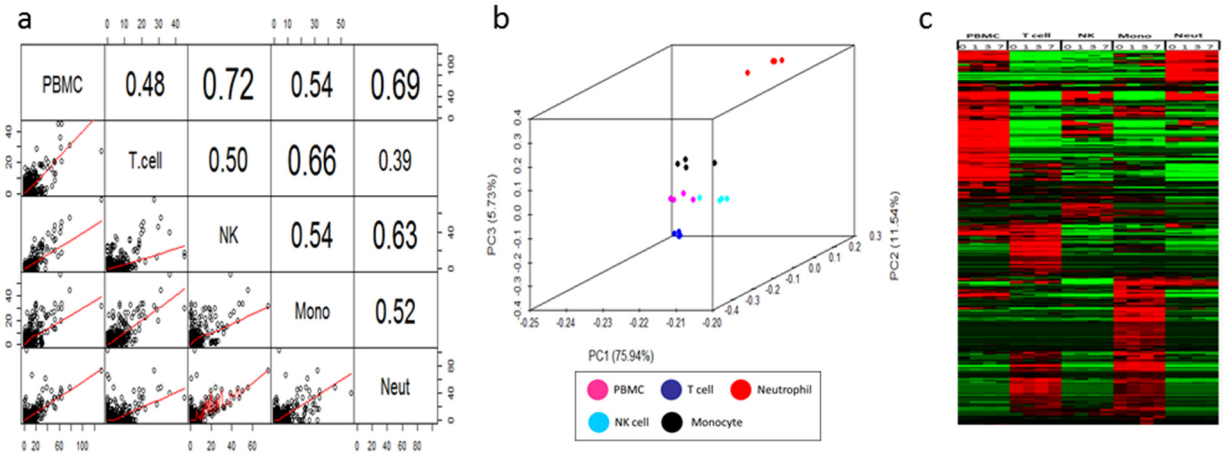


**Figure 2.9 Proteomic analysis of purified immune cells in subject HD30 after TIV vaccination. (a)** Pair-wise comparison of day 0 protein profiles from subject HD30 shows that proteomes of sorted cells correlate poorly with PBMC. **(b)** PCA of protein profiles from subject HD30 at four time points shows that purified immune cell types cluster into distinct groups. **(c)** Semi-supervised hierarchical clustering analysis of relative protein expression from a vaccinated individual reveals that purified immune cells have distinct proteomic expression profiles compared to PBMC. Data was centered across protein and cell type; red = up, black = no change, green = down.

The proteome of the second vaccinated subject (HD30) also showed distinct protein expression profiles among the different cell types and a lack of correlation between the different cell types (Figure 2.9). However, PCA of the proteomics data for both subjects showed that while the cell types at all time points clustered similarly on a per-subject basis, the cells from the two subjects did not cluster together (Figure 2.10). Overall, intra-individual variability in the cell type responses from subject HD31 is smaller than the intra-individual variability in subject HD30 and the inter-individual variability between the two. This indicates that either different subsamples of the proteome were identified from each subject or the same subsample of identified proteins were identified in both subjects but were responding at different levels. Either possibility is likely due to biological variability between the proteomes of the two subjects. It has been estimated that 20-40% of immune variation is due to heritable factors and 5% to intrinsic factors,<sup>31</sup> leaving a large portion of immune variation due to environmental and other factors.<sup>32</sup> While these estimates are based on leukocyte population subsets and function, it can be extrapolated that this variation also occurs on the protein level as the proteins do the work in the cell.

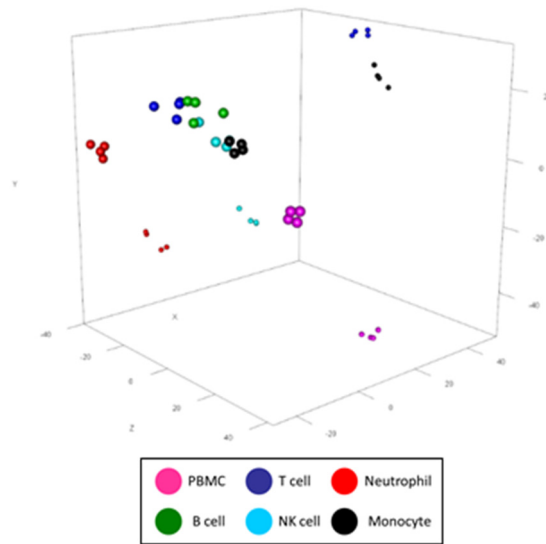


**Figure 2.10 Principal component analysis reveals poor correlation of proteomes between subjects.** Proteins (5,304 total proteins, filtered to remove zero values and contaminating keratins) from subject 1 (HD31; large circles) and subject 2 (HD30; small circles) were clustered in the same experiment. PC1 = 77.19%, PC2 = 6.99%, PC3 = 5.23%.

Previous studies investigating inter-individual proteome variability in various biological matrices showed protein abundance variance ranging between 10% and 148%.<sup>31-33</sup> While none of these studies investigated the variability of purified cell populations, one study measured the mean variation to be 28% in the PBMC proteome of 24 individuals.<sup>31</sup> Our study of two subjects showed average CV values ranging between 43-57% for the pseudospectral counts of individual immune cell types at day 0. These higher CV values are likely due to a small sample size. However, the maximum protein CV for the cell types was 133%, which is in agreement with previous reported values.<sup>31-33</sup> This high variability may pose a challenge when identifying shared protein responses. Indeed, less than 20% of differentially expressed (DE) proteins responding in the same direction were shared between both subjects for most cell types and time points (Table 2.1). The proof-of-concept study showed additional unique protein identifications on a cell-type level obtained from purifying immune cells for proteomic vaccine studies. With only two subjects, the statistical power is not sufficient to allow for biological conclusions, only observations. A larger sample size would be needed to extract specific biological information.

**Table 2.1 Shared DE proteins.**

Cell type	Time point	HD30		HD31		Shared	
		Up	Down	Up	Down	Up	Down
<b>PBMC</b>	d0-1	292	200	369	216	9	13
	d0-3	375	171	340	523	79	27
	d0-7	254	323	499	366	51	25
<b>T cell</b>	d0-1	347	220	116	806	1	93
	d0-3	419	48	248	837	19	1
	d0-7	665	37	24	661	0	3
<b>B cell</b>	d0-1	N/A	N/A	227	505	N/A	N/A
	d0-3	N/A	N/A	265	517	N/A	N/A
	d0-7	N/A	N/A	170	442	N/A	N/A
<b>NK</b>	d0-1	216	255	455	249	8	11
	d0-3	176	193	157	642	7	38
	d0-7	256	376	231	467	8	26
<b>Monocyte</b>	d0-1	529	547	127	399	4	35
	d0-3	310	952	262	390	16	97
	d0-7	374	581	200	334	14	44
<b>Neutrophil</b>	d0-1	118	151	172	119	0	5
	d0-3	109	120	119	206	11	8
	d0-7	128	77	84	238	6	12

*Differential analysis of proteins from two TIV-vaccinated subjects*

For comparison of proteomic changes in PBMC and sorted immune cells, DE proteins  $\geq 1.25$  fold after vaccination were investigated. While standard methods for determining fold change typically use a 2x fold change threshold, this level failed to identify significant numbers of shared DE proteins between both subjects. I hypothesize that this is likely due to iTRAQ under-reporting fold changes that has been previously reported.<sup>34</sup> By choosing the 1.25 threshold, comprehensive lists of DE proteins from each cell type that were shared between both subjects at each time point were obtained. There was little correlation between PBMC and purified immune cell types when comparing DE proteins (Table 2.2). The greatest overlap occurred between monocytes and PBMC at day 3 with 25% of the proteins being shared. This is expected as monocytes and PBMCs had high Spearman correlation coefficients as discussed earlier. Interestingly, this comparison also indicates a time trend in the number of DE proteins identified, with the most identified at day 3 in all cell types.

**Table 2.2 Comparison of differentially expressed proteins in PBMC and individual immune cell types.**

	Day 0-1		Day 0-3		Day 0-7	
	# proteins identified *	# (%) shared with PBMC	# proteins identified *	# (%) shared with PBMC	# proteins identified *	# (%) shared with PBMC
<b>PBMC</b>	585	-	863	-	865	-
<b>T cell</b>	922	41 (7.0%)	1085	132 (15.3%)	685	74 (8.6%)
<b>B cell</b>	732	75 (12.8%)	782	40 (4.6%)	612	89 (10.3%)
<b>NK</b>	704	71 (12.1%)	799	141 (16.3%)	698	129 (14.9%)
<b>Monocyte</b>	526	36 (6.2%)	652	222 (25.7%)	534	163 (18.8%)
<b>Neutrophil</b>	291	48 (8.2%)	325	84 (9.7%)	322	42 (4.9%)

Circos was used to plot DE proteins over the length of the human genome and to visualize overlap of DE proteins at three time points after TIV vaccination (Figure 2.11). The plots showed a lack of substantial overlap in DE proteins between PBMC and each cell type at each time point, as indicated by there being more grey lines than red.

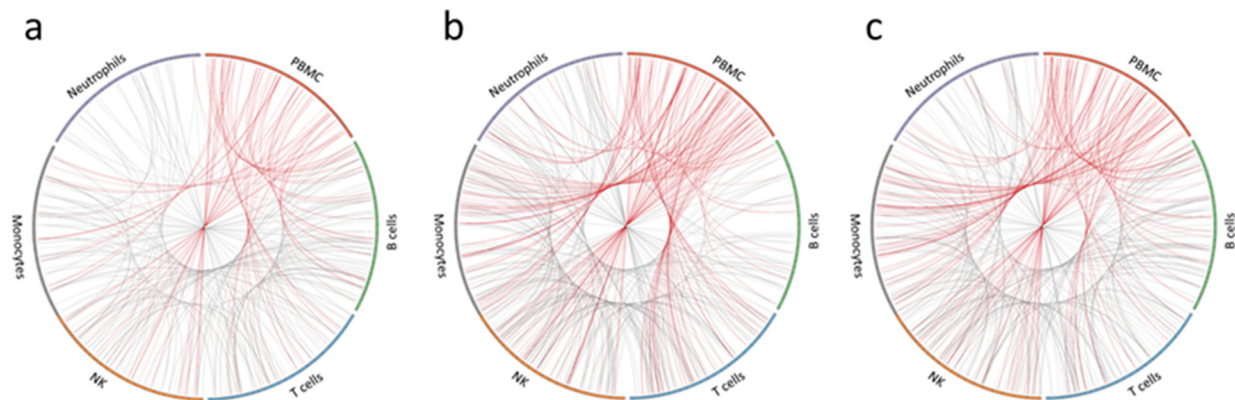


**Figure 2.11 Visualization of differentially expressed proteins in PBMC and individual immune cell types.** Circos plots of DE proteins from a vaccinated subject at (a) day 1, (b) day 3, and (c) day 7 post-TIV vaccination. For each cell type, the colored bar on the outer circle represents the entire human genome; segments within the bars divide the genomes into chromosomes. Red lines indicate DE proteins that are shared between PBMC and purified immune cell types. Grey lines indicate DE proteins that are shared between the purified immune cell types.

Finally, semi-supervised hierarchical clustering revealed little overlap in the shared DE proteins from each cell type at each time point (Figure 2.12). This analysis suggest variability between the two subjects' innate immune cell proteomes. This is most noticeable in NK cells at day 7, where a subset of proteins are up-regulated in one donor while down-regulated in the second donor (Figure 2.12C). However, the majority of the shared DE proteins are responding in the same direction just at different intensities when comparing between donors. Histone proteins are one example of this, as they are largely up-regulated in the majority of the cell types for both donors. This is expected because histones have been observed to increase circulation in response to stress, infection, and inflammation.<sup>35</sup>

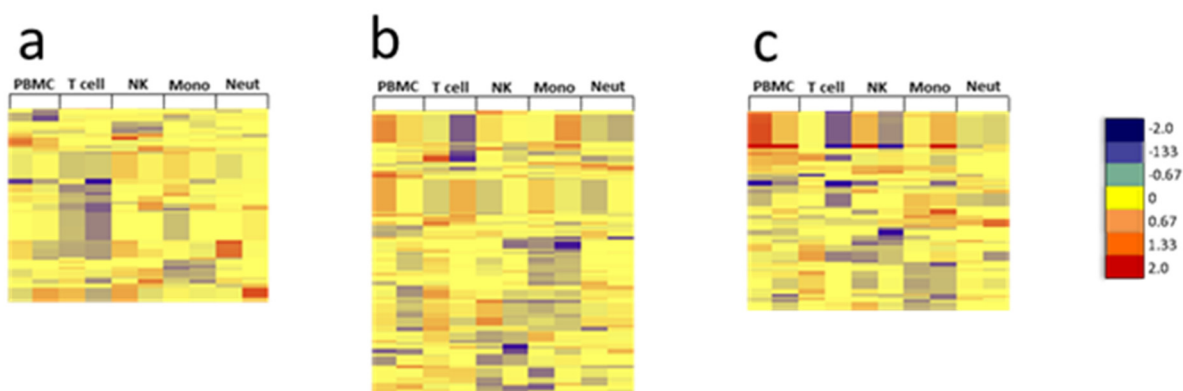


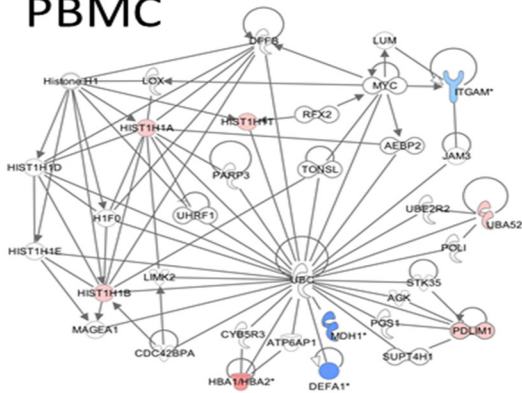
**Figure 2.12 Unique modules of proteins are differentially expressed in each immune cell type after TIV vaccination.** Log<sub>2</sub> fold change values of shared DE proteins in each cell type from both subjects were clustered at (a) day 1 (196 proteins), (b) day 3 (263 proteins), and (c) day 7 (199) proteins post-vaccination. Very little overlap of differentially expressed proteins is observed between cell types; red = up, yellow = no change, blue = down. B cell data was derived from only one subject due to insufficient recovery of B cells from the second subject.

Lists of significant DE proteins were functionally analyzed using Ingenuity Pathway Analysis (IPA) to identify the most significant biological interactions following vaccination. The top network identified showed unique biological networks induced in each cell type and time point. These results support the observed different responses from these purified immune cells (Figure 2.13- Figure 2.15). The network annotations and the top canonical pathways identified from each cell type and time point were determined (Table A-4). Each cell type had different function annotations



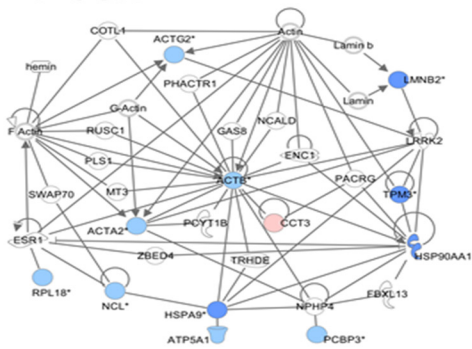
derived from the networks. Most of these were generic functions, such as cellular assembly, cell cycle, and cellular movement. However, inflammatory response and immune cell trafficking were identified for monocytes at day 1 and NK cells at day 3, respectively, showing that proteome analysis of the immune response of individual immune cell populations can identify important immune responses.

### PBMC



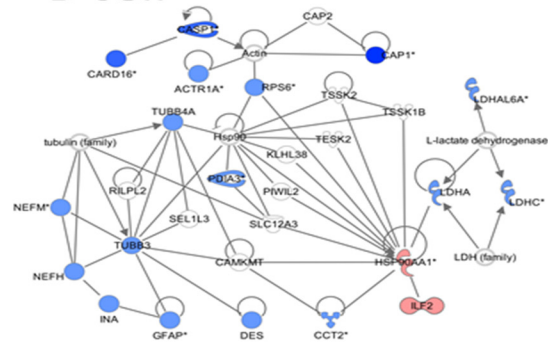
© 2000-2014 Ingenuity Systems, Inc. All rights reserved.

### T cell



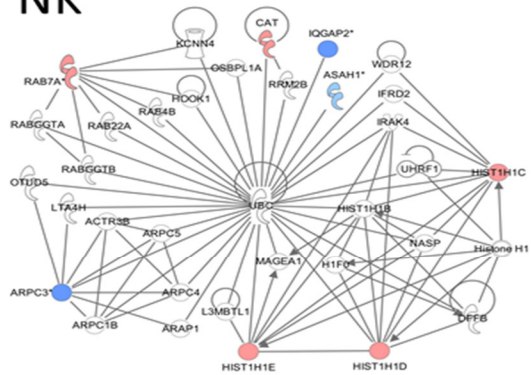
© 2000-2014 Ingenuity Systems, Inc. All rights reserved.

### B cell



© 2000-2014 Ingenuity Systems, Inc. All rights reserved.

### NK



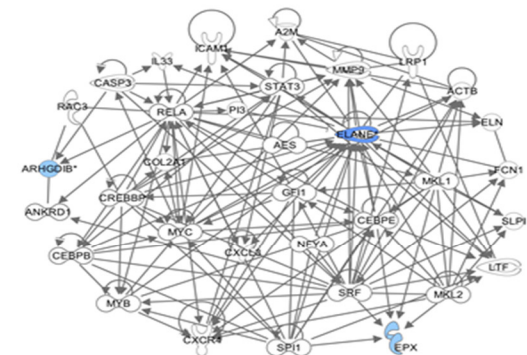
© 2000-2014 Ingenuity Systems, Inc. All rights reserved.

### Monocyte



© 2000-2014 Ingenuity Systems, Inc. All rights reserved.

### Neutrophil

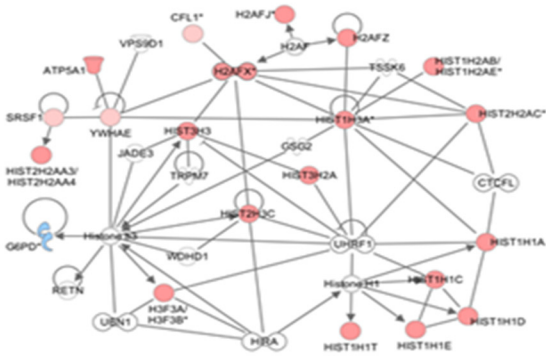


© 2000-2014 Ingenuity Systems, Inc. All rights reserved.



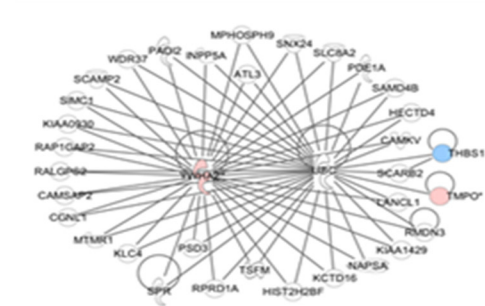
**Figure 2.13 Networks derived from DE proteins at d1 post-TIV vaccination.** DE proteins identified in both subjects at day 1 post-vaccination were imported into IPA, and the top network identified in each cell type is displayed (\*multiple ENSPs mapped to these proteins). Very little overlap of individual proteins or biological networks that are activated is observed between cell types. B cell data was derived from only one subject due to insufficient B cell recovery from the second subject.

## PBMC



© 2000-2014 Ingenuity Systems, Inc. All rights reserved.

## T cell



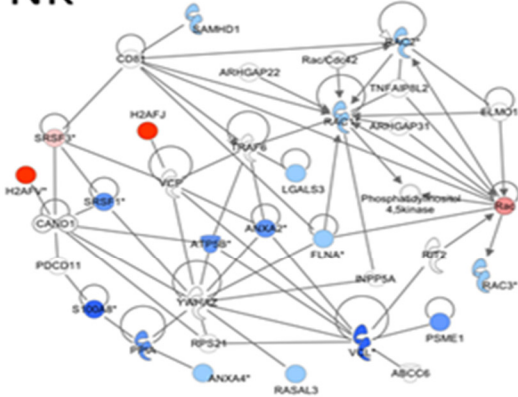
© 2000-2014 Ingenuity Systems, Inc. All rights reserved.

## B cell



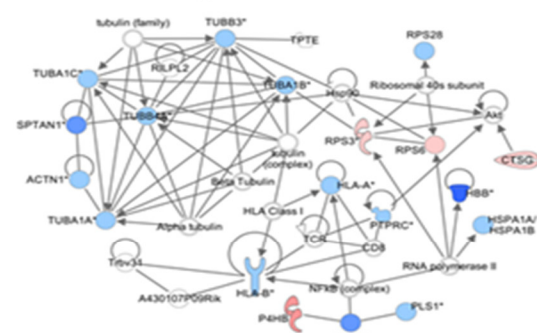
© 2000-2014 Ingenuity Systems, Inc. All rights reserved.

## NK



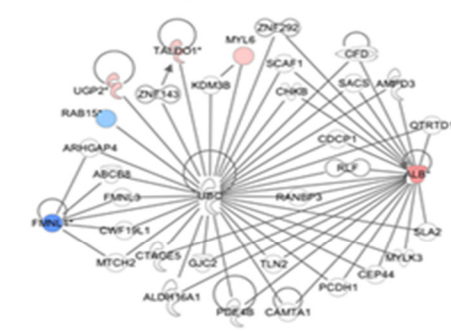
© 2000-2014 Ingenuity Systems, Inc. All rights reserved.

## Monocyte



© 2000-2014 Ingenuity Systems, Inc. All rights reserved.

## Neutrophil

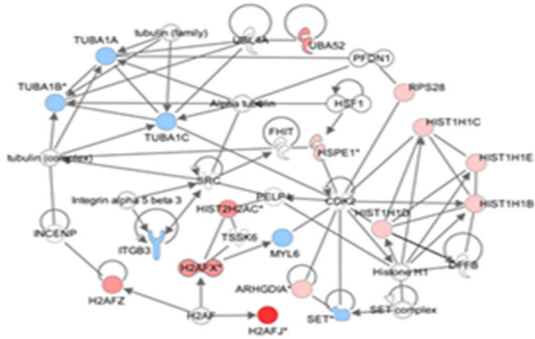


© 2000-2014 Ingenuity Systems, Inc. All rights reserved.



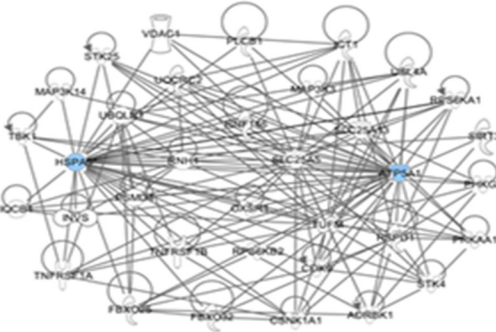
**Figure 2.14 Networks derived from DE proteins at d3 post-TIV vaccination.** DE proteins identified in both subjects at day 3 post-vaccination were imported into IPA, and the top network identified in each cell type is displayed (\*multiple ENSPs mapped to these proteins). Very little overlap of individual proteins or biological networks that are activated is observed between cell types. B cell data was derived from only one subject due to insufficient B cell recovery from the second subject

## PBMC



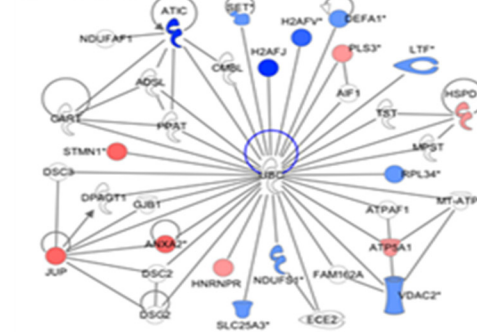
© 2000-2014 Ingenuity Systems, Inc. All rights reserved.

## T cell



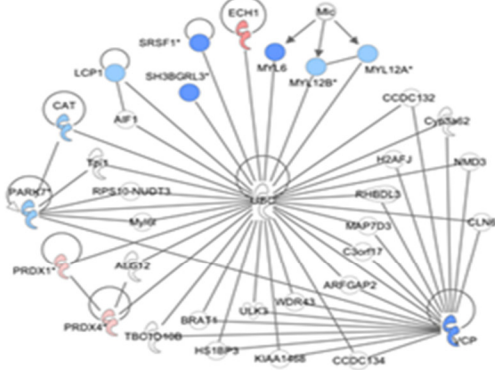
© 2000-2014 Ingenuity Systems, Inc. All rights reserved.

## B cell



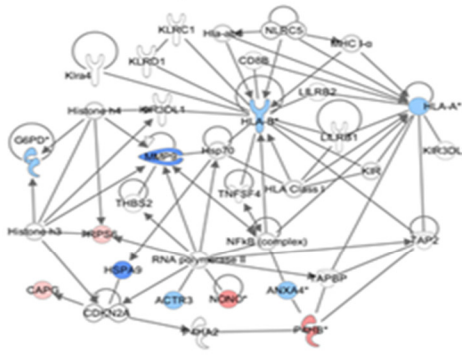
© 2000-2014 Ingenuity Systems, Inc. All rights reserved.

## NK



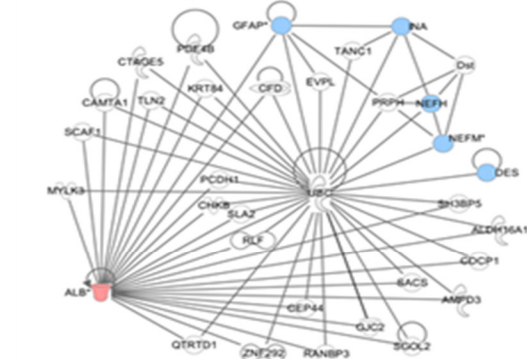
© 2000-2014 Ingenuity Systems, Inc. All rights reserved.

## Monocyte



© 2000-2014 Ingenuity Systems, Inc. All rights reserved.

## Neutrophil



© 2000-2014 Ingenuity Systems, Inc. All rights reserved.



**Figure 2.15 Networks derived from DE proteins at d7 post-TIV vaccination.** DE proteins identified in both subjects at day 1 post-vaccination were imported into IPA, and the top network identified in each cell type is displayed (\*multiple ENSPs mapped to these proteins). Very little overlap of individual proteins or biological networks that are activated is observed between cell types. B cell data was derived from only one subject due to insufficient B cell recovery from the second subject.

## **Conclusions**

The goal of this study was to develop methods and establish protocols that can be used in future systems vaccinology studies. By utilizing an efficient cell-sorting protocol, sufficient numbers of five immune cell types purified from freshly collected human whole blood were obtained for quantitative proteomic analysis. Additionally, this study optimized the strategy to generate and analyze the quantitative proteomics data. Differential analysis for each human primary immune cell type revealed unique proteomic expression profiles as well as changing biological networks during the early response after vaccination. The methods and strategies developed in this project provided a unique and important opportunity to investigate the quantitative and qualitative differences between human PBMC and individual immune cell types. Only a small fraction of DE proteins identified in the purified immune cell types were also identified in the PBMC fraction. Thus, by analyzing each cell type individually, cell-specific proteomic contributions to the immune response following vaccination were identified. This cell type-specific information, coupled with unbiased systems biology approaches, provides a more comprehensive and robust approach to monitor and eventually model vaccine and infectious disease responses. The approach developed in this pilot project will help guide future systems biology studies aimed at modeling and predicting complex responses to vaccines and vaccine components involving interactions between multiple cell types.

## **Acknowledgements**

Large portions of the this chapter were adapted with permission from K.L. Hoek, P. Samir, L.M. Howard, X. Niu, N. Prasad, A.C. Galassie, Q. Liu, T.M. Allos, K.A. Floyd, Y. Guo, Y. Shyr, S.E. Levy, S. Joyce, K.M. Edwards, and A.J. Link, A Cell-Based Systems Biology Assessment of Human Blood to Monitor Immune Responses after Influenza Vaccination. Plos One 2015 Feb. 23; 10(2):e0118528. doi: 10.1371/journal.pone.0118528.

This work was conducted in part using the resources of the Advanced Computing Center for Research and Education at Vanderbilt University, Nashville, Tennessee. Flow Cytometry experiments were performed in the VMC Flow Cytometry Shared Resource. The VMC Flow Cytometry Shared Resource is supported by the Vanderbilt Ingram Cancer Center (P30 CA68485) and the Vanderbilt Digestive Disease Research Center (DK058404). We thank Attila Csordas and the PRIDE team for assistance uploading the proteomics data sets to the ProteomXchange consortium PRIDE database.

This project was funded in part with Federal funds from the National Institutes of Allergy and Infectious Disease, National Institutes of Health, Department of Health and Human Services, under Contract No. 272200800007C, CTSA award No. UL1TR000445 from the National Center for Advancing Translational Sciences, the Childhood Infections Research Program grant T32-AI095202-01, the Immunobiology of Blood and Vascular Systems training grant 5 T32 HL69765-12, and NIH grant GM064779. The contents of this manuscript are solely the responsibility of the authors and do not necessarily represent official views of the National Center for Advancing Translational Sciences or the National Institutes of Health. The funders had no role in the study design, data collection and analysis, decision to publish, or preparation of the manuscript.

## References

1. Ideker, T.; Galitski, T.; Hood, L., A new approach to decoding life: systems biology. *Annual Review Genomics and Human Genetics* **2001**, *2*, 343-372.
2. Pulendran, B.; Li, S.; Nakaya, H. I., Systems vaccinology. *Immunity* **2010**, *33*, 516-529.
3. Trautmann, L.; Sekaly, R.-P., Solving vaccine mysteries: a systems biology perspective. *Nature Immunology* **2011**, *12*, 729-731.
4. Bucasas, K. L.; Franco, L. M.; Shaw, C. A.; Bray, M. S.; Wells, J. M.; Niño, D.; Arden, N.; Quarles, J. M.; Couch, R. B.; Belmont, J. W., Early Patterns of Gene Expression Correlate With the Humoral Immune Response to Influenza Vaccination in Humans. *The Journal of infectious diseases* **2011**, *203*, 921-929.
5. Obermoser, G.; Presnell, S.; Domico, K.; Xu, H.; Wang, Y.; Anguiano, E.; Thompson-Snipes, L.; Ranganathan, R.; Zeitner, B.; Bjork, A.; Anderson, D.; Speake, C.; Ruchaud,

- E.; Skinner, J.; Alsina, L.; Sharma, M.; Dutartre, H.; Cepika, A.; Israelsson, E.; Nguyen, P.; Nguyen, Q.-A.; Harrod, A. C.; Zurawski, S. M.; Pascual, V.; Ueno, H.; Nepom, G. T.; Quinn, C.; Blankenship, D.; Palucka, K.; Banchereau, J.; Chaussabel, D., Systems Scale Interactive Exploration Reveals Quantitative and Qualitative Differences in Response to Influenza and Pneumococcal Vaccines. *Immunity* **2013**, *38*, 831-844.
6. Nakaya, H. I.; Wrammert, J.; Lee, E. K.; Racioppi, L.; Marie-Kunze, S.; Haining, W. N.; Means, A. R.; Kasturi, S. P.; Khan, N.; Li, G.-M.; McCausland, M.; Kanchan, V.; Kokko, K. E.; Li, S.; Elbein, R.; Mehta, A. K.; Aderem, A.; Subbarao, K.; Ahmed, R.; Pulendran, B., Systems biology of vaccination for seasonal influenza in humans. *Nat Immunol* **2011**, *12*, 786-795.
  7. Tan, Y.; Tamayo, P.; Nakaya, H.; Pulendran, B.; Mesirov, J. P.; Haining, W. N., Gene signatures related to B-cell proliferation predict influenza vaccine-induced antibody response. *European Journal of Immunology* **2014**, *44*, 285-295.
  8. Tsang, J. S.; Schwartzberg, P. L.; Kotliarov, Y.; Biancotto, A.; Xie, Z.; Germain, R. N.; Wang, E.; Olnes, M. J.; Narayanan, M.; Golding, H.; Moir, S.; Dickler, H. B.; Perl, S.; Cheung, F.; Obermoser, G.; Chaussabel, D.; Palucka, K.; Chen, J.; Fuchs, J. C.; Ho, J.; Khurana, S.; King, L. R.; Langweiler, M.; Liu, H.; Manischewitz, J.; Pos, Z.; Posada, J. G.; Schum, P.; Shi, R.; Valdez, J.; Wang, W.; Zhou, H.; Kastner, D. L.; Marincola, F. M.; McCoy, J. P.; Trinchieri, G.; Young, N. S., Global Analyses of Human Immune Variation Reveal Baseline Predictors of Postvaccination Responses. *Cell* **2014**, *157*, 499-513.
  9. Furman, D.; Jovic, V.; Kidd, B.; Shen-Orr, S.; Price, J.; Jarrell, J.; Tse, T.; Huang, H.; Lund, P.; Maecker, H. T.; Utz, P. J.; Dekker, C. L.; Koller, D.; Davis, M. M., Apoptosis and other immune biomarkers predict influenza vaccine responsiveness. *Mol Syst Biol* **2013**, *9*, 659.
  10. Gaucher, D.; Therrien, R.; Kettaf, N.; Angermann, B. R.; Boucher, G.; Filali-Mouhim, A.; Moser, J. M.; Mehta, R. S.; Drake, D. R.; Castro, E.; Akondy, R.; Rinfret, A.; Yassine-Diab, B.; Said, E. A.; Chouikh, Y.; Cameron, M. J.; Clum, R.; Kelvin, D.; Somogyi, R.; Greller, L. D.; Balderas, R. S.; Wilkinson, P.; Pantaleo, G.; Tartaglia, J.; Haddad, E. K.; Sékaly, R.-P., Yellow fever vaccine induces integrated multilineage and polyfunctional immune responses. *J Exp Med* **2008**, *205*, 3119-3131.
  11. Querec, T. D.; Akondy, R. S.; Lee, E. K.; Cao, W.; Nakaya, H. I.; Teuwen, D.; Pirani, A.; Gernert, K.; Deng, J.; Marzolf, B.; Kennedy, K.; Wu, H.; Bennouna, S.; Oluoch, H.; Miller, J.; Vencio, R. Z.; Mulligan, M.; Aderem, A.; Ahmed, R.; Pulendran, B., Systems biology approach predicts immunogenicity of the yellow fever vaccine in humans. *Nat Immunol* **2009**, *10*, 116-125.
  12. Alberts, B.; Johnson, A.; Lewis, J.; Raff, M.; Roberts, K.; Walter, P., *Molecular Biology of the Cell*. 5th edition ed.; Garland Science: New York, NY, 2007.
  13. Murphy, K., *Janeway's Immunobiology*. 8th ed.; Garland Science: London, 2012.
  14. Patton, K. T.; Thibodeau, G. A., *Anatomy and Physiology*. 8th ed.; Elsevier: 2013.
  15. Applied Biosystems, Multiplex protein quantitation using iTRAQ reagents - 8 plex. In *Multiplex protein quantitation using iTRAQ reagents - 8 plex*, Applied Biosystems, Ed.

16. Applied Biosystems, Multiplex Protein Quantitation using iTRAQ Reagents - 8plex. In *Multiplex Protein Quantitation using iTRAQ Reagents - 8plex*, Applied Biosystems, Ed.
17. Pappin, D. J., An iTRAQ Primer. In *An iTRAQ Primer*, US HUPO News.
18. Ross, P. L.; Huang, Y. N.; Marchese, J. N.; Williamson, B.; Parker, K.; Hattan, S.; Khainovski, N.; Pillai, S.; Dey, S.; Daniels, S.; Purkayastha, S.; Juhasz, P.; Martin, S.; Bartlett-Jones, M.; He, F.; Jacobson, A.; Pappin, D. J., Multiplexed Protein Quantitation in *Saccharomyces cerevisiae* Using Amine-reactive Isobaric Tagging Reagents. *Molecular & cellular proteomics : MCP* **2004**, *3*, 1154-1169.
19. Hu, Q.; Noll, R. J.; Li, H.; Makarov, A.; Hardman, M.; Graham Cooks, R., The Orbitrap: a new mass spectrometer. *Journal of mass spectrometry : JMS* **2005**, *40* (4), 430-43.
20. Scigelova, M.; Makarov, A., Orbitrap Mass Analyzer – Overview and Applications in Proteomics. *PROTEOMICS* **2006**, *6*, 16–21.
21. Zubarev, R. A.; Makarov, A., Orbitrap Mass Spectrometry. *Analytica* **2013**, *85*, 5288-5296.
22. Eng, J. K.; Fischer, B.; Grossman, J.; MacCoss, M. J., A fast SEQUEST cross correlation algorithm. *J Proteome Res* **2008**, *7*, 4598-4602.
23. Eng, J. K.; McCormack, A. L.; Yates, J. R., An approach to correlate tandem mass spectral data of peptides with amino acid sequences in a protein database. *J Am Soc Mass Spectrom* **1994**, *5*, 976-989.
24. R Core Team R: A Language and Environment for Statistical Computing. <http://www.R-project.org>.
25. Eisen, M. B.; Spellman, P. T.; Brown, P. O.; Botstein, D., Cluster analysis and display of genome-wide expression patterns. *PNAS* **1998**, *95*, 14863-14868.
26. Saldanha, A. J., Java Treeview--extensible visualization of microarray data. *Bioinformatics* **2004**, *20* (17), 3246-8.
27. Krzywinski, M.; Schein, J.; Birol, I.; Connors, J.; Gascoyne, R.; Horsman, D.; Jones, S. J.; Marra, M. A., Circos: an information aesthetic for comparative genomics. *Genome research* **2009**, *19* (9), 1639-45.
28. Kasprzyk, A., BioMart: driving a paradigm change in biological data management. *Database* **2011**, *2011*, bar049.
29. Rubbelke, D. L. Tissues of the Human Body: An Introduction. [http://www.mhhe.com/biosci/ap/histology\\_mh/tismodov.html#overview](http://www.mhhe.com/biosci/ap/histology_mh/tismodov.html#overview) (accessed January 19, 2017).
30. Lundberg, E.; Gry, M.; Oksvold, P.; Kononen, J.; Andersson-Svahn, H.; Ponten, F.; Uhlen, M.; Asplund, A., The correlation between cellular size and protein expression levels--normalization for global protein profiling. *J Proteomics* **2008**, *71* (4), 448-60.



31. Maes, E.; Landuyt, B.; Mertens, I.; Schoofs, L., Interindividual variation in the proteome of human peripheral blood mononuclear cells. *PLoS ONE* **2013**, *8* (4), e61933.
32. Yamakawa, K.; Yoshida, K.; Nishikawa, H.; Kato, T.; Iwamoto, T., Comparative analysis of interindividual variations in the seminal plasma proteome of fertile men with identification of potential markers for azoospermia in infertile patients. *Journal of andrology* **2007**, *28* (6), 858-65.
33. Corzett, T. H.; Fodor, I. K.; Choi, M. W.; Walsworth, V. L.; Turteltaub, K. W.; McCutchen-Maloney, S. L.; Chromy, B. A., Statistical analysis of variation in the human plasma proteome. *Journal of biomedicine & biotechnology* **2010**, *2010*, 258494.
34. Ow, S. Y.; Salim, M.; Noirel, J.; Evans, C.; Rehman, I.; Wright, P. C., iTRAQ underestimation in simple and complex mixtures: "the good, the bad, and the ugly". *J Proteome Res* **2009**, *8*, 5347-5355.
35. Chen, R.; Kang, R.; Fan, X. G.; Tang, D., Release and activity of histone in diseases. *Cell death & disease* **2014**, *5*, e1370.

## CHAPTER III

# QUANTITATIVE PROTEOMIC ANALYSIS OF HUMAN IMMUNE CELLS IN RESPONSE TO AS03-ADJUVANTED H5N1 VACCINATION

### Introduction

Developing vaccines against highly pathogenic avian influenza H5N1 is a critically important public health priority due to the high morbidity and mortality associated with influenza infection.<sup>1</sup> However, vaccine development has been hindered by the poor immunogenicity of the H5N1 HA protein when compared with seasonal influenza vaccines.<sup>2</sup> Oil-in-water emulsion adjuvants have demonstrated great promise in enhancing antibody responses at low antigen doses.<sup>3-4</sup> Adjuvant system 03 (AS03)<sup>5-6</sup>, an  $\alpha$ -tocopherol-based oil-in-water emulsion adjuvant, is one such adjuvant. Alpha-tocopherol, an isoform of vitamin E, is a fat soluble antioxidant that works in the glutathione peroxidase pathway to disable the production of free radicals in tissues.<sup>7</sup> Dietary vitamin E supplementation has been shown to aid the immune response, particularly with earlier antibody production to certain pathogens and neutrophil and macrophage phagocytosis and chemotaxis.<sup>8-</sup>  
<sup>11</sup> However, little is known about the benefits of vitamin E as an injectable. The other main ingredients in AS03 are squalene and polysorbate 80 (polyoxyethylene sorbitan-20 monooleate).<sup>5</sup> Squalene is a triterpene collected from shark liver, but also is produced in human liver. It is an essential molecule used for the synthesis of cholesterol, vitamin D, and other steroid hormones and is commonly used in many cosmetics, medications, and other adjuvants.<sup>3</sup> Finally, polysorbate 80 is an emulsifier used in the pharmaceutical and food industries to stabilize aqueous formations.<sup>3</sup>

AS03 has been shown to markedly enhance antibody responses.<sup>3-4</sup> HAI and neutralizing (Nt) antibody titers were significantly increased following two doses of an AS03-adjuvanted H5N1 inactivated, split-virion vaccine, including when dose-sparing vaccines were used (Figure 3.1).<sup>3-4</sup>

The geometric mean titers (GMTs) showed that an adjuvant effect was observed after both doses, but especially after the second. Overall, the addition of the adjuvant allowed for lower amounts of antigen per dose and more protection while being generally well tolerated, with few severe reactions and adverse events.<sup>4-5, 12-17</sup>

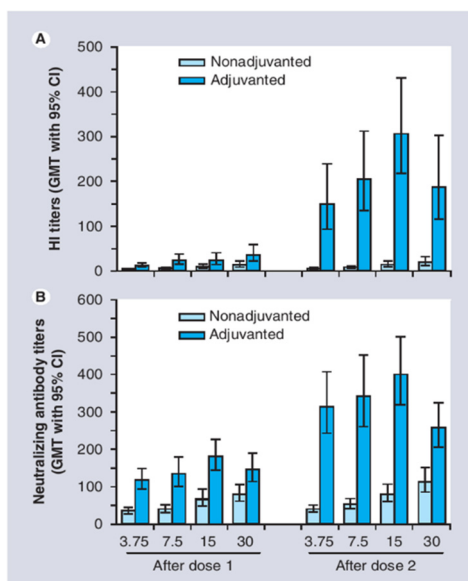


**Figure 3.1. AS03-adjuvanted H5N1 vaccination enhances the antibody response.** (A) Homologous Hemagglutination-inhibiting and (B) neutralizing antibody titers in human volunteers after two administrations of a nonadjuvanted or an AS03-adjuvanted H5N1 vaccine. Different doses of influenza antigen were used (from 3.75 to 30 µg).<sup>3</sup>

AS03 has also been shown to increase the frequency of H5N1-specific memory B cells and CD4+ T cell responses, and to induce both cross-reactive antibody and CD4+ T cell responses when administered with H5N1 vaccine.<sup>16</sup> In mouse models, AS03 increased production of monocyte- and neutrophil-recruiting chemokines, promoted the migration of antigen presenting cells to the draining lymph nodes, and enhanced antigen uptake by monocytes.<sup>15</sup> Recently, it was reported that injection of AS03 in rabbits induced a transient inflammatory response as measured by an increase in neutrophil number in the blood.<sup>17</sup> Additionally, early changes in cytokine and chemokine levels after AS03-adjuvanted H1N1 vaccination were attributed to mouse

monocytes.<sup>18</sup> While AS03 enhances the immune response to H5N1 vaccine antigens, the underlying molecular mechanisms are still poorly understood.

One of the concerns regarding the H5N1 vaccines is safety since higher doses are required to elicit a protective response. AS03-adjuvanted vaccines are well tolerated in the healthy adult population, although there are more incidences of local and systemic reactogenicity, such as injection site pain, muscle ache, headache, and fatigue.<sup>3</sup> A concerning discovery, however, was an increased incidence of narcolepsy in patients aged 4-19 after receiving Pandemrix™, a monovalent H1N1 vaccine adjuvanted with AS03 licensed in Europe for the 2009-2010 influenza season.<sup>19-20</sup> Epidemiologic studies indicated a 6 - 13-fold increased risk among the vaccinated, compared to nonvaccinated adolescents.<sup>21</sup> However, a recent study implicates antibodies to the influenza nucleoprotein as the narcolepsy cause, due to their cross-reactivity with human neural hypocretin receptor 2.<sup>22</sup> However, the possible contribution of adjuvants to autoimmune diseases and general safety of adjuvants remain a concern.<sup>23</sup> These findings demonstrate the necessity in comprehensively understanding the mechanisms of action of AS03.

Systems vaccinology allows the human immune response to be comprehensively studied by combining –omics analysis with humoral and cell-mediated immune responses to increase our understanding of the mechanisms by which vaccines and adjuvants confer protection.<sup>24-28</sup> Such studies typically focus only on transcriptome analysis. However, a comprehensive systems vaccinology approach that understands both transcriptomics and proteomics could enhance the understanding of vaccine responses.

We developed a systems biology approach to study the transient immune response following vaccination with a seasonal, inactivated influenza vaccine (trivalent) at the individual primary immune cell type-level.<sup>29</sup> This cell-based approach provided a more comprehensive understanding of the human immune response to vaccination compared to using PBMCs.<sup>29</sup> Additionally, we analyzed both transcriptomic and proteomic responses to a seasonal influenza vaccine.<sup>29</sup> Using the same immune cell-based approach, a randomized, double-blinded,

controlled, Phase I prospective clinical trial to assess the molecular immune responses of an intramuscular split-virus (SV), influenza A/H5N1 (A/Indonesia/05/2005) vaccine given with or without AS03 adjuvant was conducted. Here the changes in the immune cell proteome in responses to these well tolerated vaccines are assessed.

## Methods and Materials

### *Clinical study design*

Twenty healthy adult volunteers aged 19 – 39 years were enrolled in a randomized, double-blinded, controlled Phase I clinical trial designed to determine safety, reactogenicity, and immunogenicity of an inactivated subvirion monovalent influenza A/H5N1 (A/Indonesia/05/2005) vaccine given with or without the AS03 adjuvant. Each subject received two 0.5 mL intramuscular injection doses of 3.75 µg HA per dose with either PBS (SV-PBS) or AS03 adjuvant (4.86 mg polysorbate 80, 11.86 mg α-tocopherol, and 10.69 mg squalene) (SV-AS03) 28 days apart (vaccine product description in **APPENDIX B**). Permuted block randomization with random block sizes of 2 and 4 were applied to improve balance between the vaccine groups. All protocols and consent forms were approved by the Vanderbilt University Institutional Review Board (IRB# 120404 "VTEU 02-2011- A Randomized, Double-Blinded, Controlled, Phase I Study in Healthy Adults to Assess the Safety, Reactogenicity, and Immunogenicity of Intramuscular Subvirion Inactivated Monovalent Influenza A/H5N1 Virus Vaccine Administered With and Without AS03 Adjuvant: Standard and Systems Biology Analyses (DMID 10-0074)").

Peripheral blood samples (100 mL) were collected on days -28, -14, and 0, prior to the first vaccine dose for baseline assessment, and days 1, 3, 7, and 28 post-vaccination for serology, RNA-seq,<sup>30</sup> and proteomics analysis. A final blood sample was collected on Day 56 (28 days after the second vaccine dose) for serological analysis only (see **APPENDIX B**).

### *Immune cell purification*

Purified immune cell populations were isolated from whole blood samples as previously described in Chapter II and published protocols.<sup>29</sup> Briefly, PBMC and PMN fractions were isolated using a Ficoll-paque PLUS (GE Healthcare) separation. These fractions were subjected to magnetic bead separation followed by FACS on a BD FACSAriaIII flow cytometry to acquire  $\geq 98\%$  pure cell populations of neutrophils, monocytes, NK cells, B cells, and T cells for proteomic analysis.

### *Immune serologic assays*

H5-specific HAI and Nt assays were performed at Days 0 (prior to first vaccination), 1, 3, 7, and 28 (prior to the second vaccination) after the initial vaccine dose and 28 days (Day 56) after the second vaccine dose.<sup>31</sup> Titers below the limit of detection (1:10) were given a value of 1:5 prior to statistical analysis. The proportion of subjects achieving serum HAI and Nt antibody titers of 1:40 or greater, and a 4-fold or greater increase in antibodies were calculated for each time point.

### *Quantitative proteomic analysis*

Quantitative mass spectrometry was performed on protein extracts from sorted immune cells as previously described.<sup>29</sup> Briefly, protein extracts were obtained using a modified lysis buffer (50% trifluoroethanol 50 mM HEPES)<sup>32</sup> and quantified by BCA analysis.<sup>33</sup> Due to insufficient amount of collected protein, 17 samples were removed from analysis at this stage (Table 3.1). An immune cell common standard (ICCS) control sample was prepared using 80% PBMC and 20% neutrophil protein extracts (by weight) and included in all iTRAQ experiments as a reference channel. For each subject and cell type, 10  $\mu\text{g}$  of reduced, alkylated, and trypsinized protein extracts were labeled with 8plex iTRAQ tags (AB Sciex), pooled, and analyzed by MudPIT using an Eksigent 2-D nanoLC pump coupled to a nanoESI-LTQ-Orbitrap XL mass spectrometer

(Thermo Scientific).<sup>29</sup> Precursor ions were analyzed in the Orbitrap followed by 4 CID fragment ion scans in the ion trap for peptide identification. The precursor ions were then fragmented by HCD to measure the reporter ion intensities in the Orbitrap.<sup>29</sup>

**Table 3.1 Proteomics samples for which no iTRAQ results were reported due to insufficient amounts of protein**

<b>Subject ID</b>	<b>Cell Type</b>	<b>Study Day</b>
<b>A</b>	B cells	Day -14
<b>A</b>	T cell	Day 3
<b>F</b>	B cells	Day 3
<b>H</b>	B cells	Day -28
<b>H</b>	B cells	Day 0
<b>H</b>	B cells	Day 28
<b>I</b>	B cells	Day -28
<b>I</b>	NK cells	Day 0
<b>I</b>	NK cells	Day 1
<b>I</b>	NK cells	Day 3
<b>L</b>	Monocytes	Day 3
<b>L</b>	T cells	Day 7
<b>N</b>	NK cells	Day 28
<b>O</b>	B cells	Day -14
<b>O</b>	T cells	Day -14
<b>Q</b>	NK cells	Day 1

#### *Quality Control of Protein Samples*

Two *S. cerevisiae* proteins (enolase and alcohol dehydrogenase) were added to each sample prior to digestion to act as markers for errors in digestion and iTRAQ labeling. Prior to iTRAQ labeling, 1 µg of each the trypsin-digested protein samples was combined with 0.100 fmol glu-1-fibrinopeptide B (glufib) and run on an LTQ mass spectrometer (Thermo Scientific) as quality control. Previously, the stability of the instrument was assessed for its ability to handle the number of samples (**APPENDIX C**). The raw files were converted to mzxml files and searched against the human protein database using *X!Tandem* within the *Global Proteome Machine* (GPM).<sup>34</sup> Samples where the internal standards were identified and showed similar protein numbers to the ICCS control samples were deemed sufficient for iTRAQ labeling and further analysis. Samples that

were outside of the acceptable limits were checked by visual inspection, re-quantified by BCA, re-digested, and re-checked for compliance.

Each iTRAQ experiment was assessed for consistency as well. The reporter ion intensities for all identified peptides of the two yeast proteins were compared within each subject level experiment. Additionally, the pseudo-spectral counts for yeast proteins as a whole were compared across all 20 experiments for each cell type. Samples that showed values inconsistent with others of the same cell type were checked statistically to determine if they were true outliers and re-analyzed if there was enough material.

### *Peptide and protein quantitation*

The CID and HCD spectra were merged for each precursor ion, using *Proteome Discoverer v1.3* (Thermo Scientific). The merged spectra were searched against a forward and reverse concatenated human Ensembl protein database containing 169,816 sequences (gene model 74) using the *Sequest* database search engine within *Proteome Discoverer*.<sup>35-36</sup> The precursor mass tolerance and fragment mass tolerance were set to 20 ppm and 0.8 Da, respectively. Static modifications of the peptides were set to iTRAQ modification of N-terminus and  $\epsilon$ -amines of lysines and  $\beta$ -methylthiolation of cysteines. Additionally, oxidation of methionine and tryptophan and deamidation of asparagine and glutamine were used as dynamic modifications.

Protein assembly, reporter ion quantitation and statistical analysis were performed with a 5% peptide and protein FDR using *ProteoIQ v2.61* (Premier Biosoft). Peptide intensities within each 8-plex iTRAQ experiment were normalized so that the sum of reporter ion intensities was the same across all channels within the experiment. For each 8-plex iTRAQ experiment, protein level quantifications were calculated for each experimental channel by calculating the median of the  $\log_2$  ratios (experimental channel intensity divided by the ICCS reference channel intensity) for all assigned peptides. The ICCS channel was chosen as reference after comparing the number of quantitative values obtained when it was used as a reference versus Day 0 as a reference (see



**APPENDIX B).** Peptides with missing experimental or reference reporter ion intensities or with intensities below the threshold (intensity < 10) were not included in the median calculations. Indistinguishable proteins with identical median ratios across all subjects and time points were collapsed into one representative Ensembl protein ID with the longest protein sequence.

### *Analysis datasets*

PCA and 1-Spearman correlation distance were used to identify outlying samples (Figure B-1). Seventeen samples, including 4 baseline samples, were flagged as strong outliers based on their placement compared to other cell type samples (Table 3.2). Among these outliers, 7 (41%) were attributable to one neutrophil iTRAQ experiment.

**Table 3.2 Outlying proteomics samples**

<b>Subject ID</b>	<b>Experiment ID</b>	<b>Cell type</b>	<b>Study Visit Day</b>
<b>A</b>	A_NK_3	NK-cells	Day 3
<b>B</b>	B_Neu_5	Neutrophils	Day 28
<b>C</b>	C_Neu_4	Neutrophils	Day 7
<b>H</b>	H_B_2	B-cells	Day 1
<b>I</b>	I_Neu_A	Neutrophils	Day -28
<b>I</b>	I_Neu_B	Neutrophils	Day -14
<b>I</b>	I_Neu_1	Neutrophils	Day 0
<b>I</b>	I_Neu_2	Neutrophils	Day 1
<b>I</b>	I_Neu_3	Neutrophils	Day 3
<b>I</b>	I_Neu_4	Neutrophils	Day 7
<b>I</b>	I_Neu_5	Neutrophils	Day 28
<b>L</b>	L_B_1	B-cells	Day 0
<b>L</b>	L_B_3	B-cells	Day 3
<b>L</b>	L_B_5	B-cells	Day 28
<b>N</b>	N_Neu_4	Neutrophils	Day 7
<b>R</b>	R_B_5	B-cells	Day 28
<b>R</b>	R_Mono_2	Monocytes	Day 1

Protein ratio distributions across samples were median-normalized within the cell type group to reduce systematic variability between the iTRAQ experiments (see **APPENDIX B**) (Figure B-2

- Figure B-3). For multivariate data visualization, missing protein ratios within cell type were imputed using the k-nearest neighbors algorithm (k=5) using the *impute* package in R (version 1.34.0). Proteins identified in at least 75% of samples within each cell type were considered and only samples for which at least 20% of proteins were non-missing were included in the imputation step. Resulting imputed per-cell type data matrices were also merged to generate a combined set (all cell types together) using zero log<sub>2</sub> ratios to align disparate proteins between cell types.

The Ensembl protein database (Ensemble Version 74) was clustered using CD-HIT software (Version 4.6.1, 08/27/2012) to derive a set of protein families based on 50% protein sequence identity. One representative Ensembl protein ID with the longest protein sequence was selected as the protein family name.

### *Significant Proteins*

Differentially abundant (DA) proteins were identified through the use of an exact two-sided 2-sample permutation test of the mean difference (*coin* R package, version 1.0.23) for each post-vaccination day and cell type combination, if proteins had at least 3 non-missing fold changes for each treatment group. Proteins were considered significant if  $p \leq 0.05$  and the mean treatment fold changes differed by 1.2 fold. Significantly DA proteins and subjects were clustered by their baseline log<sub>2</sub> fold change values using pairwise uncentered Pearson correlation distances and complete linkage clustering. Proteins missing from individual samples were given a value of 0.

### *Gene set enrichment analysis*

Protein accessions were mapped to their corresponding Ensembl Gene IDs. Gene sets and databases were obtained from the KEGG database (version 70.0) and MSigDB (Version 4.0). The *goseq* package in R (version 1.12.0) was used to evaluate gene set enrichment using the hypergeometric distribution to assess significance with the Benjamini-Hochberg correction

applied to adjust for multiple testing.<sup>37</sup> Gene sets with a FDR of  $\leq 0.05$  that contained genes encoding for at least two significant protein families were considered significantly enriched.

#### *Protein-protein interaction networks*

Uniprot IDs and gene symbols for the DA proteins were obtained using the Uniprot retrieve/ID mapping tool. Known human-human and human-influenza A protein-protein interactions were extracted from the IntAct database. The list of interactions was filtered for nodes with a distance of 1 to significantly DA proteins and the networks were visualized using *Cytoscape* (version 3.1.1).

#### *Regularized logistic regression analysis*

A regularized logistic regression model was fit for monocytes (day 1, 3, 7, and 28) and neutrophils (day 1 and 3) to identify protein responses that are correlated with seroprotection (HAI  $\geq 1:40$ ) at any post-vaccination day using the *gimnet* R package (version 2.0-2). Only these cell types were included because they had a sufficiently large number of protein families with non-missing values for at least 9 of the subjects in each treatment group. An elastic net regularization step (combination of L1 Lasso and L2 ridge penalization,  $\alpha=0.5$ ) was included to avoid overfitting. Leave-one-out cross validation was used to determine the optimum parameters which minimized the mean misclassification error between seroprotection response groups.

## **Results and Discussion**

#### *Protective antibody responses*

HAI and Nt antibody titers were determined in order to assess the protective response obtained from each vaccine. Titers did not increase from baseline during the first 7 days after vaccination in either SV-AS03 or SV-PBS groups (Figure 3.2A). At day 28, there was no significant difference in the mean HAI GMT between groups, with no subjects showing an HAI response in the PBS group, while one subject in the SV-AS03 group exhibited an HAI titer  $\geq 1:40$  and a  $>4$ -fold rise in

titer (Figure 3.2B). By day 56, 9 subjects in the SV-AS03 group achieved seroconversion and seroprotection for HAI titers, while none of the SV-PBS group subjects reached seroprotection titers, resulting in a significant difference between the two groups ( $p < 0.001$ ). For the Nt assay, at days 28 and 56, the SV-AS03 group showed significantly higher GMT titers compared to SV-PBS ( $p = 0.015$  and  $p < 0.001$ , respectively). All subjects within the SV-AS03 group showed seroconversion and seroprotection at day 56, contrasting to the 3 subjects in the SV-PBS group. As the vaccines used in this study were identical in composition to those used in previous studies, these results were anticipated. Overall, this indicates that the SV-AS03 vaccine is eliciting protective immune responses, while the SV-PBS vaccine failed to produce a significant response.

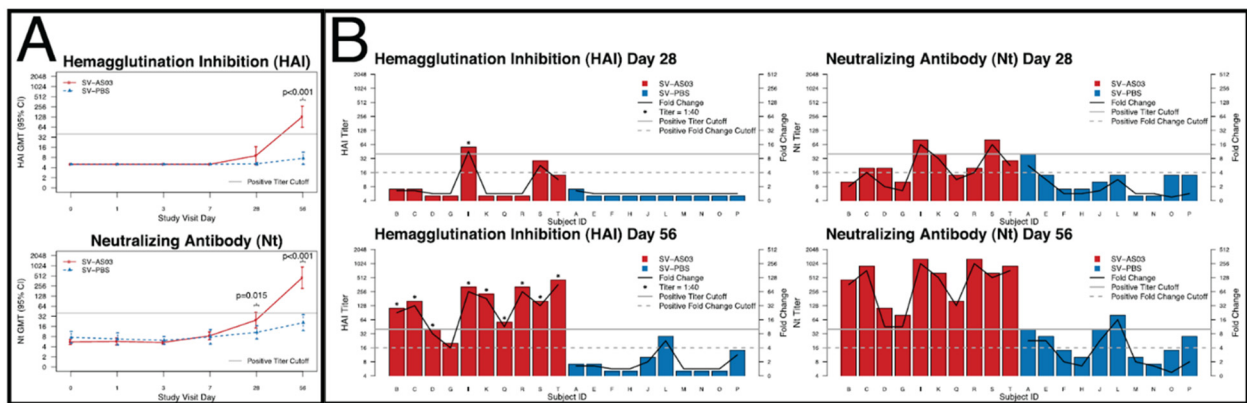


**Figure 3.2 AS03-adjuvanted H5N1 vaccination induced a protective immune response relative to non-adjuvanted vaccine.** (A) HAI and Nt antibody GMT and 95% CI at each time point by vaccine group; p-values are based on two-sided t-test on the log scale adjusting for unequal variances if necessary. No multiple testing adjustment was carried out. (B) HAI and Nt titers in individual subjects at days 28 and 56 by vaccine group; titer is represented by bar height (left y-axis) while fold change from baseline is shown as a connected black line (right y-axis), cut-offs are indicated by grey lines (solid: 1:40 titer, dashed: 4-fold change).<sup>30</sup>

### iTRAQ experiments

In order to identify the molecular mechanisms responsible for the differences seen in antibody responses between the SV-AS03 and SV-PBS vaccine groups, quantitative proteomic analysis was performed. An average of 2,900 proteins from 450 protein groups were identified in each 8-plex iTRAQ experiment. While identified proteins in each cell type did not largely differ in physical

properties (Figure 3.3), the number of identified proteins was higher in monocytes compared to the other immune cell types. This is consistent with previous reports suggesting that monocytes play an important role in responding to AS03.<sup>15, 18</sup>

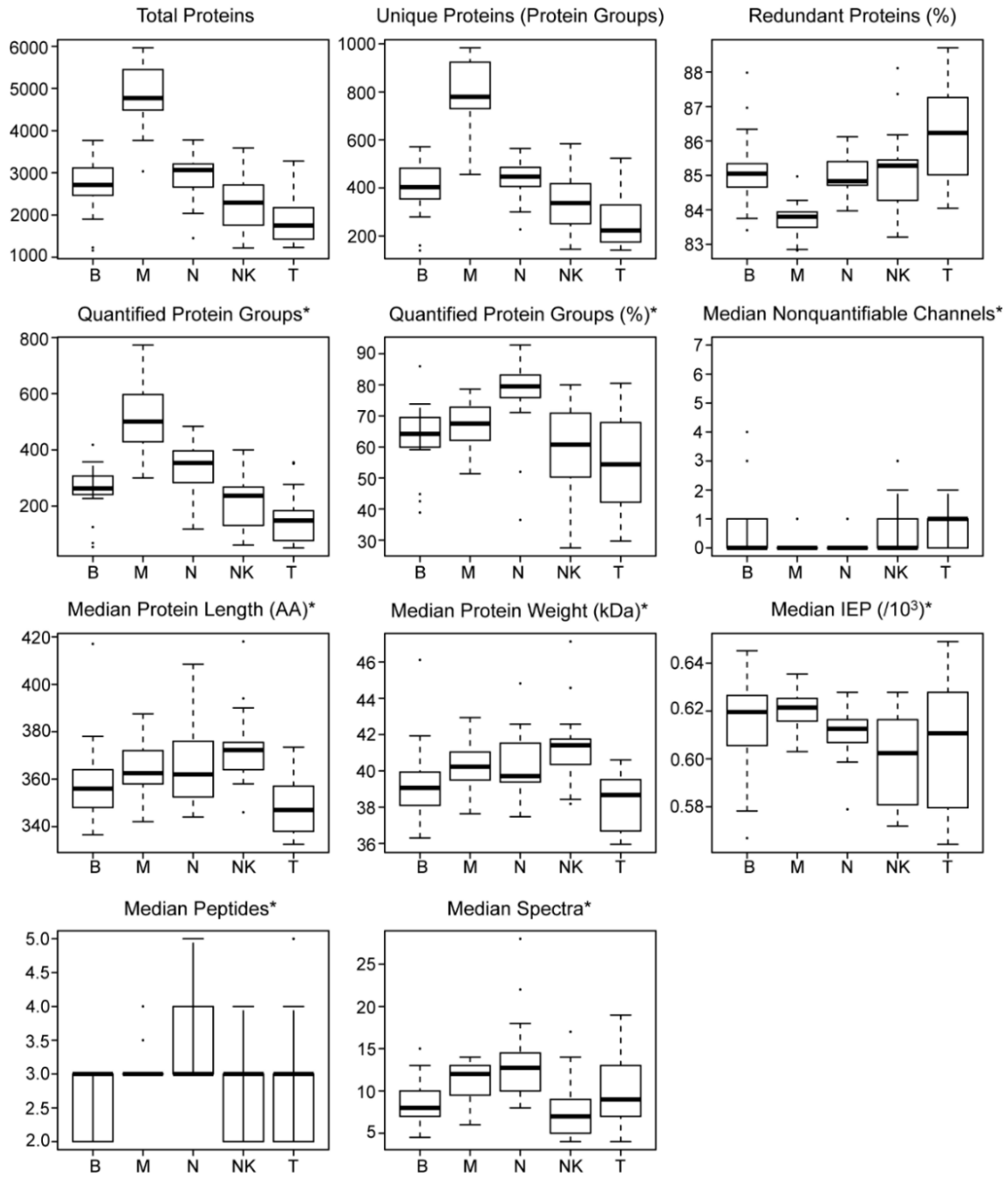


**Figure 3.3 Experimental summary statistics by cell type.** \*: restricted to the representative protein in a protein group for which at least one of the 7 iTRAQ channels was quantified. Cell types across the bottom: B cells, Monocytes, Neutrophils, NK cells, T cells.

Using the top hit per protein group, the main analysis set was comprised of quantifications for 3,247 proteins (1,580 protein families based on 50% sequence identity) compared to the immune cell common standard. Broken down by cell type, 533 (T cells), 665 (NK cells), 813 (B cells), 860 (neutrophils), and 1,252 (monocytes) protein families were identified. Many proteins were only quantifiable in a subset of samples and we observed different levels of quantification sensitivity for the five cell types (Figure 3.4). For example, while 17.1% and 10.4% of monocyte and neutrophil proteins were quantified in at least 90% (126 out of 140) of their respective samples, the percentage ranged from 1.1-2.5% for the other cell types, indicating lower proteome coverage for those cell types (Figure 3.4). This could be due to the prevalence of highly abundant proteins diluting the low abundant signals, variability between subjects, different proteins being identified at different time points, or the common phenomenon of missing peptides in iTRAQ experiments.<sup>38-</sup>  
<sup>39</sup> Additionally, pooling the identified proteins from all cell types and time points showed higher levels of missing samples, indicating that disparate protein sets were identified across cell types. This is generally expected as the five immune cell types have different functions and timelines in the immune response.

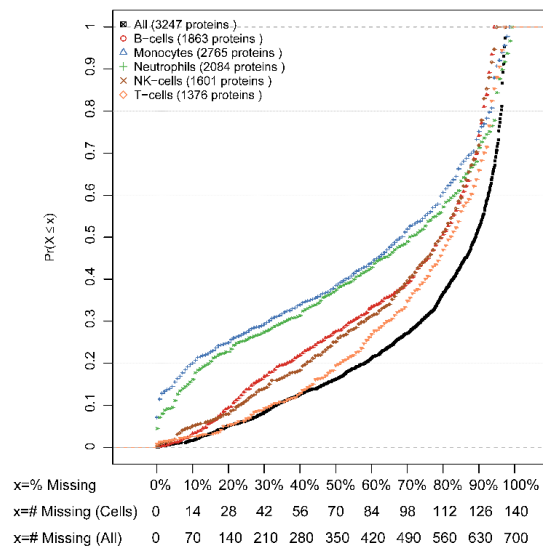


**Figure 3.4 Empirical cumulative distribution function plots of protein missingness across samples.** Table on bottom indicates the number of samples that could be missing corresponding to the percentages.

### Multiple baseline time points enhance sensitivity

Vaccine studies traditionally use only one collected sample prior to vaccination as the baseline measurement. While this reduces sample numbers and costs to both researchers and volunteers, this practice may be allowing more inconsistency into the study because of the inherent variability of human biology. Variation in the three pre-vaccination time points was largely due to the immune cell type, similar to the variation in all time points (Figure 3.5).

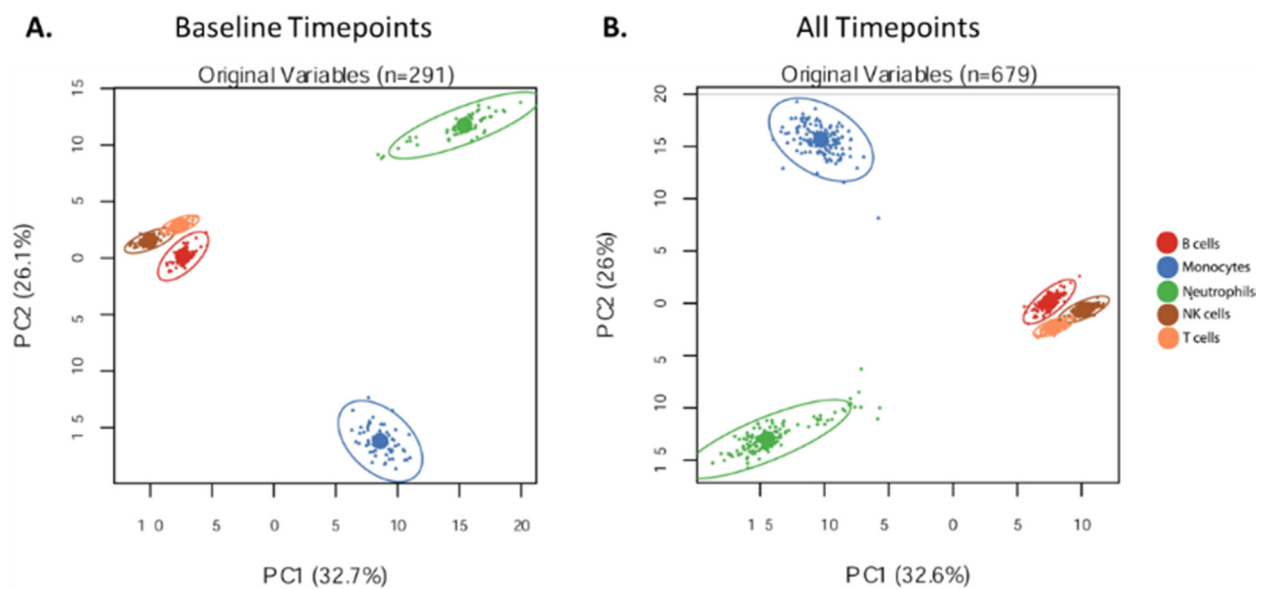


**Figure 3.5 Baseline variability shown by PCA biplots.** Variation at (A) pre-vaccination time points and (B) all time points is driven by cell type.

To assess the impact of using multiple baseline time points on the number of proteins identified, the results from all three baseline measures (day -28, -14, and 0) were compared to one (day 0), and two (day -14 and day 0) baseline measures for monocytes and neutrophils, as these cell types had the most proteins identified. With each additional baseline measurement included, the sensitivity of the protein identifications increased, as shown by the height of the bars (Figure 3.6). In almost all cases, including two baseline measures had at least 80% protein identification overlap with the three baseline measure dataset. Additionally, including more baseline measures

reduces the number of false positives in the data sets as the FDR is consistently higher when fewer baseline measurements are used (Figure 3.6). Monocytes at day 3 is the most striking example of the loss in sensitivity that occurs when fewer baseline measurements are collected. With fold change of  $>1.2$ , which this study used as a threshold, the sensitivity decreased from approximately 0.95 down to 0.45 when the number of baseline measures was reduced from two to one. Overall, the difference in sensitivity between using three and two baseline measures is relatively small. While increasing the number of baseline measurements also increases both the time and money costs for these studies, it gives more confidence in the results as well as potentially more identified proteins. Here, all three baseline measurements were averaged and used for the remaining analysis.



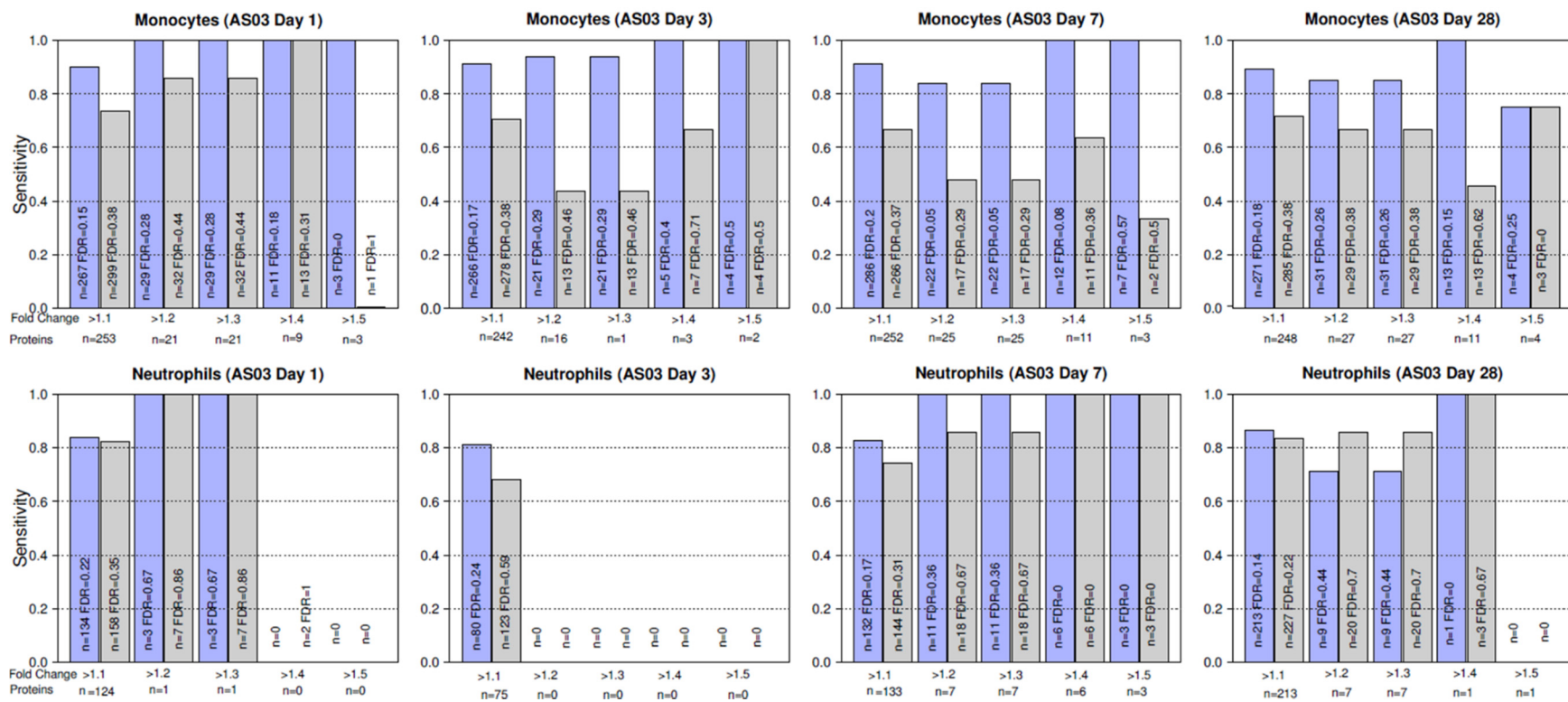


**Figure 3.6 Effect of multiple baseline timepoints.** Protein identification sensitivity for experiments using one (grey) or two (blue) baseline measures were compared to using all three for multiple fold change cutoffs. The FDR was also calculated for each case and is shown inside the bars. Different possible fold change cutoffs are across the bottom. The number of proteins identified at each fold change cutoff is shown by the n value either below the plots (three baseline time points) or inside the bars (one and two baseline time points)

### *AS03-modulated protein responses across time*

To compare the protein log<sub>2</sub> fold changes from baseline between the SV-AS03 and control SV-PBS vaccine groups, significant DA proteins were determined using a per-protein permutation test ( $p \leq 0.05$ ) and treatment fold change cutoff of  $\geq 1.2$  fold for each cell type at days 1, 3, 7, and 28 post-vaccination. The number of DA proteins (protein families) identified between the two vaccine groups for each cell type was: T cells: 60 (28); NK cells: 80 (40); B cells: 109 (50); neutrophils: 100 (55); and monocytes: 172 (108) (Table B-1 – Table B-20). Little overlap of DA proteins between post-vaccination time points within the same cell type was observed (Figure 3.7).<sup>29</sup> Lee *et al.* showed a similar transient response in mice infected with *Brucella abortus*.<sup>40</sup> They observed more proteins at the individual time points rather than shared between time points, which supports our hypothesis that different subsets of proteins are being activated at different times and that our selected time points were too far apart to show the overlap.

Of the 188 unique DA protein families, 64 (34%) were reported for at least two cell types, with TUBB3 (tubulin, beta 3 class III) family-related proteins being differentially abundant in all five cell types (Table B-21). Additionally, proteins in the HLA (major histocompatibility complex, class I) family were significantly differentially abundant in all cell types, except T cells and pyruvate kinase members were found for all immune cells except NK cells.

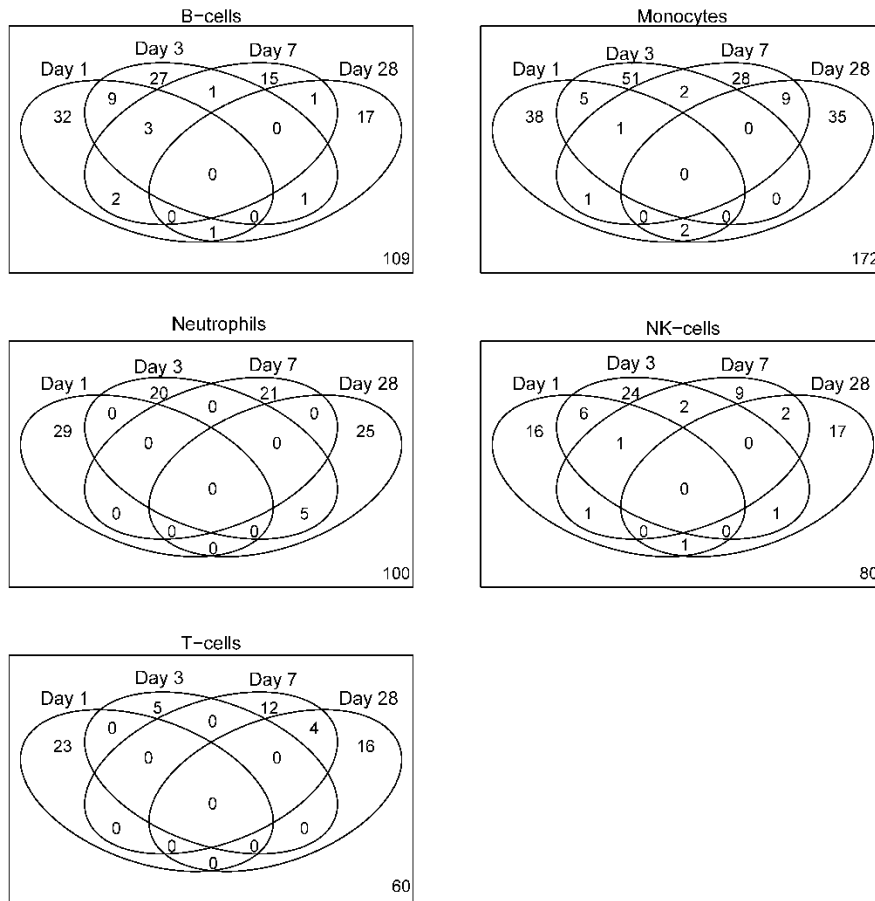


**Figure 3.7 Venn diagrams of differentially abundant proteins by cell type**

Overall, the observed vaccine effect between the SV-AS03 and SV-PBS groups was strongest for monocytes at day 1 and 3, both in terms of number (24 and 33) and percentage of protein families (77%) with higher responses in the SV-AS03 group (Figure 3.8). Additionally, differential protein responses in B cells at days 1 and 3 were primarily increased for the SV-AS03 group, which is likely associated with the B cells acting in their role as antigen presenting cells, as these time points are too early for the B cell antibody production. Finally, at day 1, neutrophils had a higher fraction of protein families that were elevated from baseline for the SV-AS03 group. The prevalence of increased proteomic responses in the SV-AS03 group for these time points suggests that AS03 induces early responses rather than bolstering the later responses.

Homologous proteins including many HLA-protein family members tended to cluster within their cell type based on their baseline fold changes (Figure 3.8). One exception was observed in NK cells at day 3, where HLA proteins clustered separately. Baseline response time trends for DA proteins from the HLA protein family showed that the mean response was higher in the SV-AS03 compared to the SV-PBS vaccine group in monocytes, neutrophils, and B cells (Figure 3.9). For all three cell types, an initial peak response was observed at day 3 for the SV-AS03 group with responses returning to near-baseline levels by day 7. In contrast to the other two cell types, neutrophils showed an additional increase in response for the SV-AS03 group at day 28, however there was an increase in unidentified proteins for a number of subjects at that time point. For NK cells, while HLA DA proteins showed consistent baseline trends with a peak at day 3, responses in the SV-PBS group were much more divergent with an overall higher mean response at day 1 compared to the SV-AS03 group, which could potentially be due to noise in those signals. Interestingly, there is an increase in HLA protein expression in the SV-PBS group from B cells, indicating that the unadjuvanted vaccine may be inducing HLA proteins in B cells only. This could be a possible mechanism for how a few of the subjects in the SV-PBS group showed seroconversion in their Nt titers, however this would need to be validated.

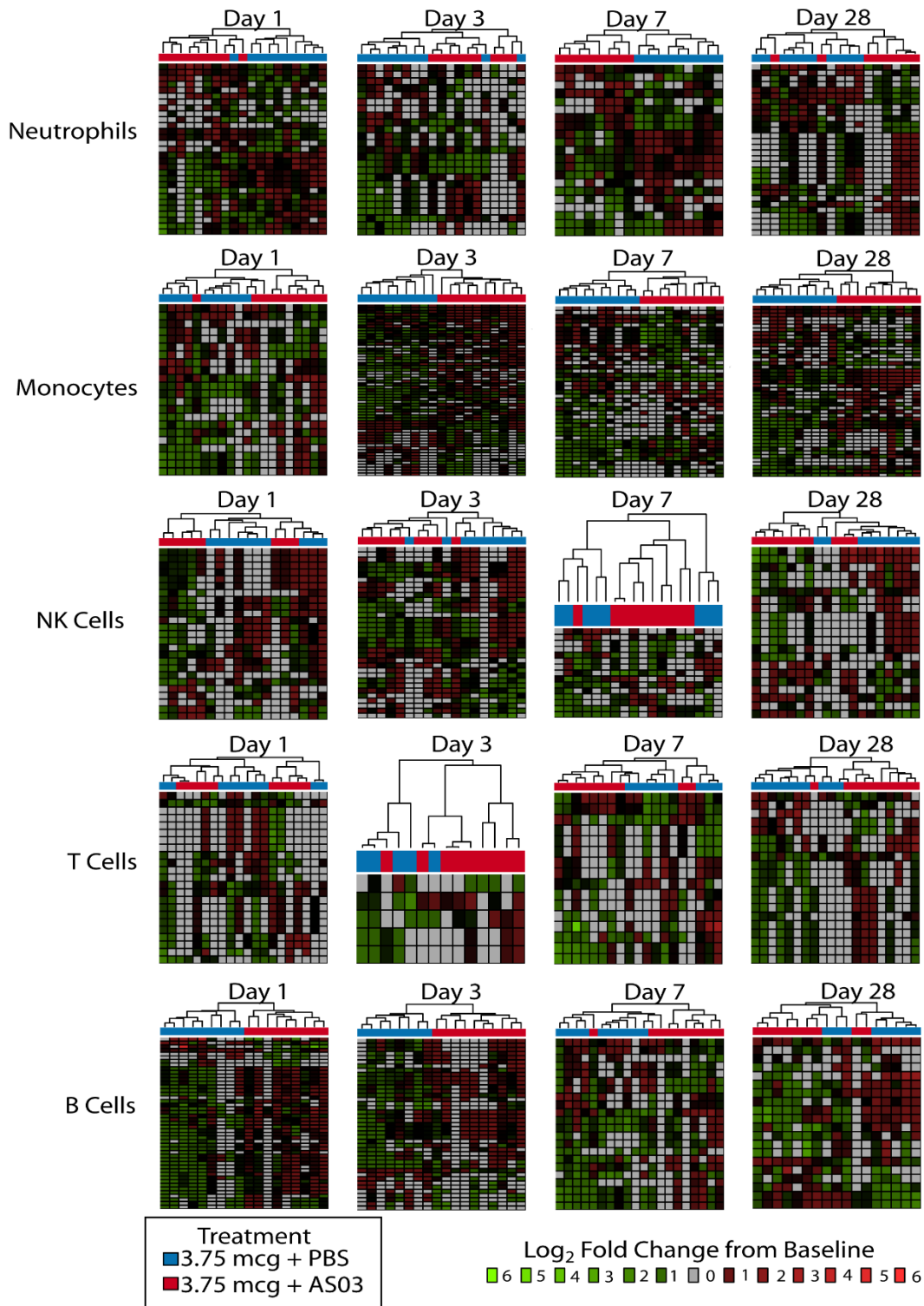


**Figure 3.8 Heatmaps of DA protein baseline  $\log_2$  fold changes for each cell type at each post-vaccination time point.** Dendrograms were obtained using complete linkage clustering of uncentered pairwise Pearson correlation distances between  $\log_2$  fold changes.  $\log_2$  fold changes of 0 were imputed for missing values. Protein cluster membership (50% sequence identity) is along the protein dendrogram on the left side; vaccine group membership is highlighted below the subject dendrogram at the top. Red: up-regulated from baseline; green: down-regulated from baseline; grey: missing observations. Larger versions of these heatmaps available in Appendix B

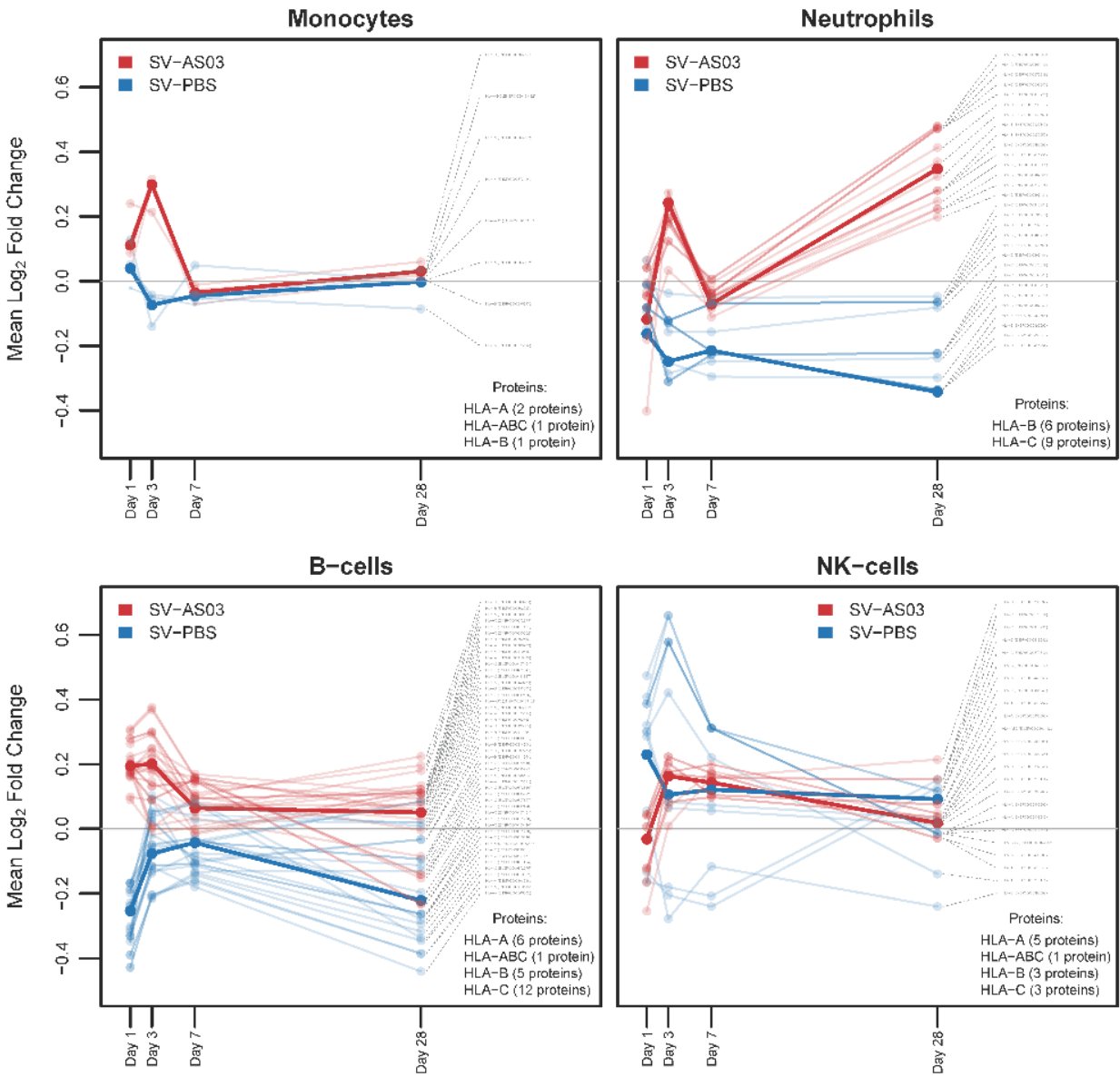


**Figure 3.9 HLA Class I family time trends of mean log<sub>2</sub> fold changes from baseline by vaccine group.** Data only includes cell types with differentially abundant HLA proteins. Individual HLA family protein time trends are plotted in lighter colors. The mean log<sub>2</sub> fold changes across all HLA protein family members are in bold.

### *AS03-induces antigen processing and presentation pathways*

Gene set enrichment analysis showed that genes encoding for DA proteins are involved in a range of biological processes including protein metabolism, tubulin folding, platelet activation, and immune system-related processes (Table B-22 -Table B-33). Antigen processing and presentation-related pathways were enriched in monocytes and neutrophils at day 3, including *Class I MHC-mediated antigen processing and presentation*, *Antigen processing and cross presentation*, and *ER phagosome* pathways (source: Reactome, Figure 3.10). This strongly suggests that SV-AS03 enhances antigen presentation at early time points, which is essential for the ultimate production of antibodies and activation of cytotoxic T-cells. Unexpectedly, *Antigen presentation folding assembly and peptide loading of class I MHC* was enriched for B cells at day 7, with the proteins being upregulated in the SV-AS03 group. While B cells are a professional APC, they usually present antigen to helper T cells via the MHC class II complex.<sup>41</sup> However, Hon *et al.* and others have shown that B cells are able to also participate in cross-presentation to present antigen to cytotoxic T cells via the MHC class I complex, which could be happening here.<sup>41-42</sup>

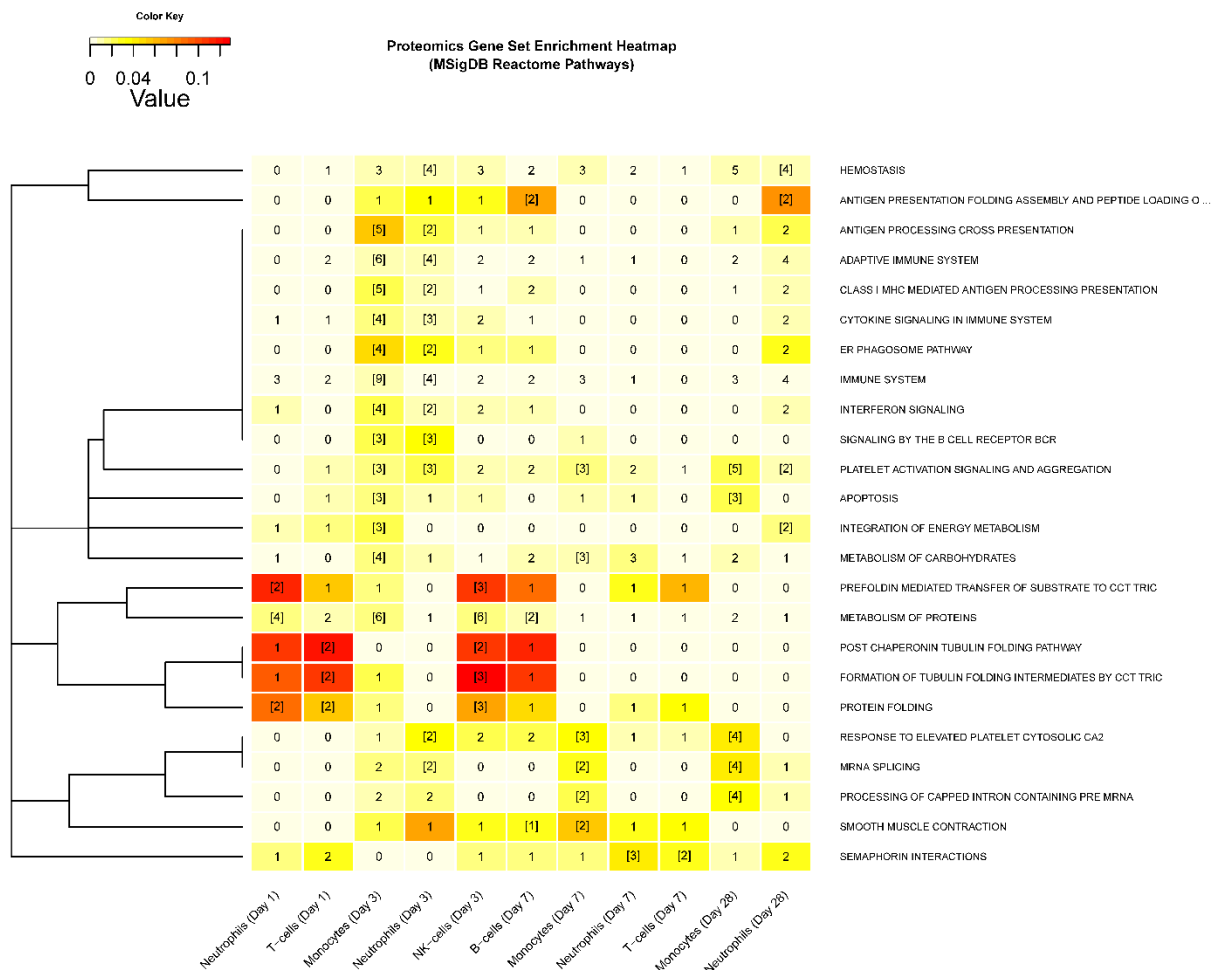


**Figure 3.10 Heatmap of enriched MSigDB Reactome pathways.** Gene sets significantly enriched in at least two conditions (cell type/time point combinations) are shown. Cells are color-coded by the Jaccard similarity index. Numbers in the cells represent the DA protein families in a set. Cells with protein family numbers in brackets indicate significantly enriched sets. Sets were clustered on the Jaccard distance between their binary enrichment pattern.

### *Antigen presentation and oxidative stress response proteins predict seroprotection status*

To identify AS03-modulated protein families that are predictive of seroprotection status (HAI titer  $\geq 1:40$ ) at day 56, regularized logistic regression analysis was performed using imputed protein family baseline responses as predictors (Table B-34 - Table B-37). To reduce the impact of missing observations on the imputation process, the analysis was performed on the most complete datasets (monocytes and neutrophils) and proteins with quantifications for 9 of 10 subjects in each vaccine group. MPO (myeloperoxidase) and SOD2 (superoxide dismutase 2) protein families, which are involved in inflammation and oxidative stress responses, were among



those identified as positive predictors of seroprotection in monocytes at day 1 (Table B-34). Surprisingly, while similar inflammation and oxidative stress-related protein families, including NCF4 (neutrophil cytosolic factor 4) and GZMB (granzyme B), were identified as predictors in neutrophils at day 1, they were negative predictors (Table B-37). In fact, the majority of the proteins included in the day 1 neutrophil model for seroprotection prediction were negative predictors, indicating that early time point neutrophils were potentially reducing the antibody response. Yang *et al.* previously reported that depletion of neutrophils following an adjuvanted vaccination actually increase the CD4+ T cell and antibody responses in mice.<sup>43</sup> While they were using neither AS03 nor H5N1 in their vaccinations, this could explain the negative association observed in the neutrophils.

Four of the 12 selected protein families identified as predictors of seroprotection in monocytes at day 3 were related to *Class I MHC-mediated antigen processing and presentation* including HLA (major histocompatibility complex, class I family), PSME 1 and PSME 2 (PA28 alpha/beta proteasome activator subunit families), as well as ITGB5 (integrin, beta 5 family) (Table B-35). For all these protein families, an increase in fold change from baseline resulted in an increased likelihood of seroprotection. Changes in PSME2 had the highest impact. The monocyte day 3 protein-protein interaction network (Figure 3.11) shows HLA and proteasome family proteins separated by two intermediate nodes indicating their close functional relationship. However, it remains unclear by what mechanism up-regulation of HLA class I molecules, proteasome activators, and other inflammation proteins enhance seroprotection.

### *Comparison of proteomic and transcriptomic data*

Differentially expressed (DE) genes (SV-AS03 vs. SV-PBS) identified in the transcriptomics study conducted in parallel<sup>30</sup> were compared to the proteomics results. Twenty-three DA protein families were associated with DE genes identified for any cell type-time point combination (Table 3.3). Interestingly, increased PSME1 and PSME2 proteomic responses for the SV-AS03 group in

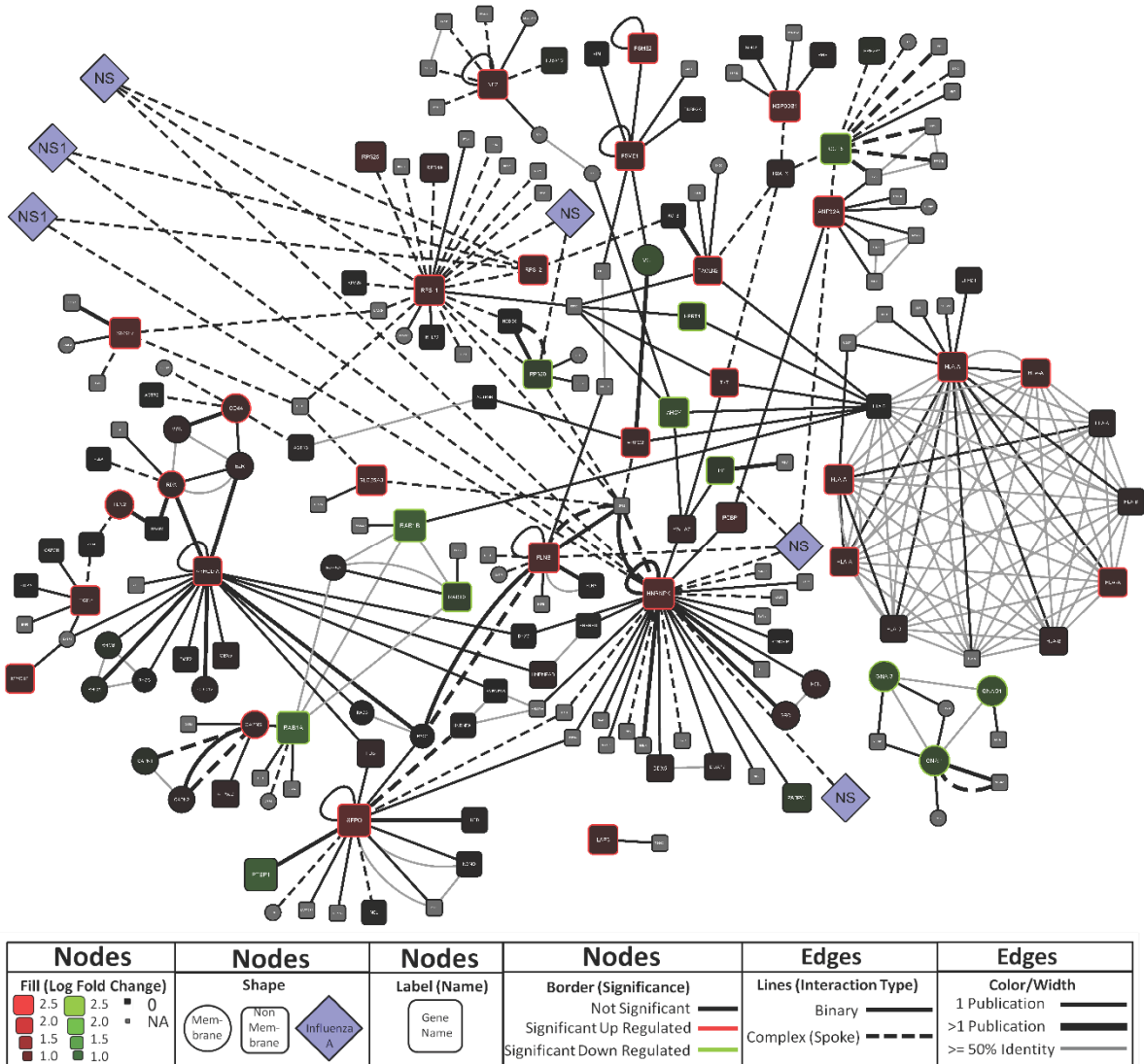


**Figure 3.11 Monocyte day 3 protein-protein interaction network.** Human-human and human-*Influenza A* experimental interactions for which at least one interacting partner was differentially abundant between vaccine groups are shown. The mean log<sub>2</sub> fold change between vaccine groups was used if multiple Ensembl protein IDs mapped to one UniProt ID.

monocytes at day 3 corresponded with increased transcriptomic changes in the genes encoding these proteins in monocytes at day 1. Change in PSME2 were significant in both the proteomic and transcriptomic studies. While HLA Class I protein encoding genes were slightly up-regulated but not significantly differentially expressed in the SV-AS03 group in monocytes, the *Class I MHC-mediated antigen processing and presentation* pathway was significantly enriched in DE genes

up-regulated in SV-AS03 group at day 1.<sup>30</sup> Together these findings imply a delayed Class I-related antigen presentation response on the protein level (day 3) following an initial transcriptomics response at 24h post-vaccination. A post-transcriptional regulation mechanism may be modulating the expression of antigen processing and presentation proteins in monocytes.<sup>44</sup>

As anticipated, very few of the differential protein families (12%, 23 of 188) were identified in the transcriptomics analysis for any cell type-time point combination. This lack of shared responses has been seen in previous comparison studies<sup>45-46</sup> and likely stems from translational control of gene expression, degradation of mRNA prior to translation, post-translational modifications of proteins, bias towards highly abundant proteins, small sample size, and general noise in the data.<sup>47</sup> Despite the lack of individual shared responses, the proteomic analysis on the pathway level confirmed the enrichment of the *Class I antigen processing and presentation* pathway at day 1 based on transcriptomics results for monocytes and neutrophils albeit two days later (day 3, Figure 3.10).

## Conclusion

The goal of this study was to investigate the changes in immune cell proteomes after H5N1 vaccination with or without AS03 in order to better understand the mechanisms by which AS03 enhances protection. Even with a small sample size, this study highlights the strengths of assessing proteomic responses of multiple individual immune cell types in parallel by demonstrating a transient response to the AS03-adjuvanted influenza vaccine shown by modifications of the immune cell's proteomic profiles across the entire immune response. Furthermore, this study identified a strong antigen processing and presentation response at early time points that could also predict later seroprotection. In summary, the application of a cell-based proteomics approach allows a more granular assessment of immune cell-specific responses that, compared with transcriptomics results, revealed additional aspects of the immune responses to AS03-adjuvanted influenza vaccine.

**Table 3.3 Proteins encoded by genes determined to be differentially expressed in a parallel RNA-Seq experiment.** Protein families that contained at least one differentially abundant protein and at least one protein that was encoded by a differentially expressed gene were included.

<b>Protein Family ID</b>	<b>Gene ID</b>	<b>Gene Name</b>	<b>Gene Description</b>
<b>ENSP00000346550</b>	ENSG00000138772	ANXA3	Annexin A3
<b>ENSP00000310219</b>	ENSG00000126803	HSPA2	Heat shock 70kDa protein 2
<b>ENSP00000363071</b>	ENSG00000026025	VIM	Vimentin
<b>ENSP00000357283</b>	ENSG00000113368	LMNB1	Lamin B1
<b>ENSP00000249750</b>	ENSG00000128918	ALDH1A2	Aldehyde dehydrogenase 1 family, member A2
<b>ENSP00000446252</b>	ENSG00000112096	SOD2	Superoxide dismutase 2, mitochondrial
<b>ENSP00000379038</b>	ENSG00000025708	TYMP	Thymidine phosphorylase
<b>ENSP00000468041</b>	ENSG00000126247	CAPNS1	Calpain, small subunit 1
<b>ENSP00000433138</b>	ENSG00000137752	CASP1	Caspase 1, apoptosis-related cysteine peptidase
<b>ENSP00000372155</b>	ENSG00000092010	PSME1	Proteasome (prosome, macropain) activator subunit 1 (PA28 alpha)
<b>ENSP00000216802</b>	ENSG00000100911	PSME2	Proteasome (prosome, macropain) activator subunit 2 (PA28 beta)
<b>ENSP00000226299</b>	ENSG00000002549	LAP3	Leucine aminopeptidase 3
<b>ENSP00000362409</b>	ENSG00000136830	FAM129B	Family with sequence similarity 129, member B
<b>ENSP00000345023</b>	ENSG00000065621	GSTO2	Glutathione S-transferase omega 2
<b>ENSP00000053867</b>	ENSG00000030582	GRN	Granulin
<b>ENSP00000378669</b>	ENSG00000109107	ALDOC	Aldolase C, fructose-bisphosphate
<b>ENSP00000221992</b>	ENSG00000007306	CEACAM7	Carcinoembryonic antigen-related cell adhesion molecule 7
<b>ENSP00000423563</b>	ENSG00000263521	HIST2H2AC	Histone cluster 2, H2ac
<b>ENSP00000386881</b>	ENSG00000135636	DYSF	Dysferlin
<b>ENSP00000222553</b>	ENSG00000105835	NAMPT	Nicotinamide phosphoribosyltransferase
<b>ENSP00000289473</b>	ENSG00000158517	NCF1	Neutrophil cytosolic factor 1
<b>ENSP00000394842</b>	ENSG00000115271	GCA	Grancalcin, EF-hand calcium binding protein
<b>ENSP00000357721</b>	ENSG00000143546	S100A8	S100 calcium binding protein A8

### Acknowledgements

Portions of the this chapter were adapted with permission from L.M. Howard, K.L. Hoek, J.B. Goll, P. Samir, A.C. Galassie, T.M. Allos, X. Niu, L.E. Gordy, C.B. Creech, N. Prasad, T.L. Jensen, H. Hill, S.E. Levy, S. Joyce, A.J. Link, and K.M. Edwards, Cell-based systems biology analysis of

human AS03-adjuvanted H5N1 avian influenza vaccine responses: A phase I randomized controlled trial. *PLoS ONE* 12(1): e0167488. Doi:10.1371/journal.pone.0167488.

The vaccine and adjuvant provided by the US Department of Health and Human Services Biomedical Advanced Research and Development Authority from the National Pre-pandemic Influenza Vaccine Stockpile and were manufactured by Sanofi Pasteur (H5N1 vaccine) and GlaxoSmithKline Biologicals (AS03 adjuvant). This project was funded in part with federal funds from the National Institutes of Allergy and Infectious Disease, National Institutes of Health, Department of Health and Human Services, under Contract Nos. 272200800007C and 2722001300023I and NIH RO1 Grant No. GM64779; the Vanderbilt Clinical and Translational Science Award grant NIH RR024975 (UL1TR000445); the Childhood Infectious Research Program grant T32-AI095202-01; the Vanderbilt Department of Pediatrics Turner-Hazinkski Award, VA Merit Award BX001444; and the Immunobiology of Blood and Vascular Systems training grant 5T32HL069765-12.

## References

1. World Health Organization *Cumulative number of confirmed human cases for avian influenza A(H5N1) reported to WHO, 2003-2016*; 2016.
2. Treanor, J. J.; Campbell, J. D.; Zangwill, K. M.; Rowe, T.; Wolff, M., Safety and immunogenicity of an inactivated subvirion influenza A (H5N1) vaccine. *N Engl J Med* **2006**, *354*, 1343-1351.
3. Garçon, N.; Vaughn, D. W.; Didierlaurent, A. M., Development and evaluation of AS03, an Adjuvant System containing  $\alpha$ -tocopherol and squalene in an oil-in-water emulsion. *Expert Rev Vaccines* **2012**, *11*, 349-366.
4. Leroux-Roels, I.; Borkowski, A.; Vanwolleghe, T.; Dramé, M.; Clement, F.; Hons, E.; Devaster, J.-M.; Leroux-Roels, G., Antigen sparing and cross-reactive immunity with an adjuvanted rH5N1 prototype pandemic influenza vaccine: a randomised controlled trial. *Lancet* **2007**, *370* (9587), 580-589.
5. Langley, J. M.; Frenette, L.; Ferguson, L.; Riff, D.; Sheldon, E.; Risi, G.; Johnson, C.; Li, P.; Kenney, R.; Innis, B.; Fries, L., Safety and cross-reactive immunogenicity of candidate AS03-adjuvanted prepandemic H5N1 influenza vaccines: a randomized controlled phase 1/2 trial in adults. *The Journal of infectious diseases* **2010**, *201*, 1644-1653.

6. Lasko, B.; Reich, D.; Madan, A.; Roman, F.; Li, P.; Vaughn, D., Rapid immunization against H5N1: a randomized trial evaluating homologous and cross-reactive immune responses to AS03A-adjuvanted vaccination in adults. *The Journal of infectious diseases* **2011**, *204*, 574-581.
7. Packer, L.; Weber, S. U.; Rimbach, G., Molecular aspects of alpha-tocotrienol antioxidant action and cell signalling. *The Journal of nutrition* **2001**, *131* (2), 369S-373S.
8. Devaraj, S.; Li, D.; Jialal, I., The effects of alpha tocopherol supplementation on monocyte function. *J. Clin. Invest.* **1996**, *98* (3), 756-763.
9. Bendich, A., Antioxidant vitamins and their functions in immune responses. In *Advances in experimental medicine and biology*, Bendich, A.; Phillips, M.; Tengerdy, R. P., Eds. Springer: 1990; Vol. 262, pp 35-55.
10. Hughes, D. A., Antioxidant vitamins and immune function. In *Nutrition and Immune Function: Frontiers in Nutritional Science, No. 1*, Calder, P. C.; Field, C. J.; Gill, H. S., Eds. CAB International: Wallingford, GB, 2002.
11. Meydani, S. N.; Beharka, A. A., Recent developments in vitamin E and immune response. *Nutrition Reviews* **1996**, *56* (1), S49-S58.
12. Leroux-Roels, G., Prepandemic H5N1 influenza vaccine adjuvanted with AS03: a review of the pre-clinical and clinical data. *Expert Opinion on Biological Therapy* **2009**, *9* (8), 1057-1071.
13. Chen, W. H.; Jackson, L. A.; Edwards, K. M.; Keitel, W. A.; Hill, H.; Noah, D. L.; Creech, C. B.; Patel, S. M.; Mangal, B.; Kotloff, K. L., Safety, Reactogenicity, and Immunogenicity of Inactivated Monovalent Influenza A(H5N1) Virus Vaccine Administered With or Without AS03 Adjuvant. *Open forum infectious diseases* **2014**, *1* (3), ofu091.
14. Godeaux, O.; Izurieta, P.; Madariaga, M.; Dramé, M.; Li, P.; Vaughn, D. W., Immunogenicity and safety of AS03A-adjuvanted H5N1 influenza vaccine prepared from bulk antigen after stockpiling for 4 years. *Vaccine* **2015**, *33*, 2189-2195.
15. Morel, S.; Didierlaurent, A.; Bourguignon, P.; Delhayé, S.; Baras, B.; Jacob, V.; Planty, C.; Elouahabi, A.; Harvengt, P.; Carlsen, H.; Kielland, A.; Chomez, P.; Garçon, N.; Van Mechelen, M., Adjuvant System AS03 containing  $\alpha$ -tocopherol modulates innate immune response and leads to improved adaptive immunity. *Vaccine* **2011**, *29*, 2461-2473.
16. Moris, P.; Most, R. v. d.; Leroux-Roels, I.; Clement, F.; Dramé, M.; Hanon, E.; Leroux-Roels, G. G.; Mechelen, M. V., H5N1 influenza vaccine formulated with AS03A induces strong cross-reactive and polyfunctional CD4 T-cell responses. *J Clin Immunol* **2011**, *31*, 443-454.
17. Segal, L.; Wouters, S.; Morelle, D.; Gautier, G.; Le Gal, J.; Martin, T.; Kuper, F.; Destexhe, E.; Didierlaurent, A. M.; Garçon, N., Non-clinical safety and biodistribution of AS03-adjuvanted inactivated pandemic influenza vaccines. *Journal of applied toxicology : JAT* **2015**, *35* (12), 1564-1576.

18. Sobolev, O.; Binda, E.; O'Farrell, S.; Lorenc, A.; Pradines, J.; Huang, Y.; Duffner, J.; Schulz, R.; Cason, J.; Zambon, M.; Malim, M. H.; Peakman, M.; Cope, A.; Capila, I.; Kaundinya, G. V.; Hayday, A. C., Adjuvanted influenza-H1N1 vaccination reveals lymphoid signatures of age-dependent early responses and of clinical adverse events. *Nat Immunol* **2016**, *17* (2), 204-213.
19. Ahmed, S. S.; Schur, P. H.; MacDonald, N. E.; Steinman, L., Narcolepsy, 2009 A(H1N1) pandemic influenza, and pandemic influenza vaccinations: what is known and unknown about the neurological disorder, the role for autoimmunity, and vaccine adjuvants. *J Autoimmun* **2014**, *50*, 1-11.
20. Miller, E.; Andrews, N.; Stellitano, L.; Stowe, J.; Winstone, A. M.; Shneerson, J.; Verity, C., Risk of Narcolepsy in Children and Young People Receiving AS03 Adjuvanted Pandemic A/H1N1 2009 Influenza Vaccine: Retrospective Analysis. *BMJ (Clinical Research ed.)* **2013**, *346*, f2375.
21. Nohynek, H.; Jokinen, J.; Partinen, M.; Vaarala, O.; Kirjavainen, T.; Sundman, J.; Himanen, S.; Hublin, C.; Julkunen, I.; Olsen, P.; Saarenpaa-Heikkila, O.; Kilpi, T., AS03 adjuvanted AH1N1 vaccine associated with an abrupt increase in the incidence of childhood narcolepsy in Finland. *PLoS ONE* **2012**, *7* (3), e33536.
22. Ahmed, S. S.; Volkmoth, W.; Duca, J.; Corti, L.; Pallaoro, M.; Pezzicoli, A.; Karle, A.; Rigat, F.; Rappuoli, R.; Narashimhan, V.; Julkunen, I.; Vuorela, A.; Vaarala, O.; Nohynek, H.; Pasini, F. L.; Montomoli, E.; Trombetta, C.; Adams, C. M.; Rothbard, J.; Steinman, L., Antibodies to influenza nucleoprotein cross-react with human hypocretin receptor 2. *Science Translational Medicine* **2015**, *7* (294), 29ra105.
23. Pellegrino, P.; Clementi, E.; Radice, S., On vaccine's adjuvants and autoimmunity: Current evidence and future perspectives. *Autoimmunity reviews* **2015**.
24. Pulendran, B.; Li, S.; Nakaya, H. I., Systems vaccinology. *Immunity* **2010**, *33*, 516-529.
25. Li, S.; Nakaya, H. I.; Kazmin, D. A.; Oh, J. Z.; Pulendran, B., Systems biological approaches to measure and understand vaccine immunity in humans. *Semin Immunol* **2013**, *25*, 209-218.
26. Nakaya, H. I.; Wrammert, J.; Lee, E. K.; Racioppi, L.; Marie-Kunze, S.; Haining, W. N.; Means, A. R.; Kasturi, S. P.; Khan, N.; Li, G.-M.; McCausland, M.; Kanchan, V.; Kokko, K. E.; Li, S.; Elbein, R.; Mehta, A. K.; Aderem, A.; Subbarao, K.; Ahmed, R.; Pulendran, B., Systems biology of vaccination for seasonal influenza in humans. *Nat Immunol* **2011**, *12*, 786-795.
27. Querec, T. D.; Akondy, R. S.; Lee, E. K.; Cao, W.; Nakaya, H. I.; Teuwen, D.; Pirani, A.; Gernert, K.; Deng, J.; Marzolf, B.; Kennedy, K.; Wu, H.; Bennouna, S.; Oluoch, H.; Miller, J.; Vencio, R. Z.; Mulligan, M.; Aderem, A.; Ahmed, R.; Pulendran, B., Systems biology approach predicts immunogenicity of the yellow fever vaccine in humans. *Nat Immunol* **2009**, *10*, 116-125.
28. Li, S.; Roupheal, N.; Duraisingham, S.; Romero-Steiner, S.; Presnell, S.; Davis, C.; Schmidt, D. S.; Johnson, S. E.; Milton, A.; Rajam, G.; Kasturi, S.; Carlone, G. M.; Quinn, C.; Chaussabel, D.; Palucka, A. K.; Mulligan, M. J.; Ahmed, R.; Stephens, D. S.; Nakaya,

- H. I.; Pulendran, B., Molecular signatures of antibody responses derived from a systems biology study of five human vaccines. *Nat Immunol* **2014**, *15*, 195-204.
29. Hoek, K. L.; Samir, P.; Howard, L. M.; Niu, X.; Prasad, N.; Galassie, A.; Liu, Q.; Allos, T. M.; Floyd, K. A.; Guo, Y.; Levy, S. E.; Joyce, S.; Edwards, K. M.; Link, A. J., A cell-based systems biology assessment of human blood to monitor immune responses after influenza vaccination. *PLoS One* **2015**, *10* (2), e0118528.
  30. Howard, L. M.; Hoek, K. L.; Goll, J. B.; Samir, P.; Galassie, A. C.; Allos, T. M.; Niu, X.; Gordy, L. E.; Creech, C. B.; Prasad, N.; Jensen, T. L.; Hill, H.; Levy, S. E.; Joyce, S.; Link, A. J.; Edwards, K. M., Cell-based systems biology analysis of human AS03-adjuvanted H5N1 avian influenza vaccine responses: a phase I randomized controlled trial. *PLoS ONE* **2017**, *12* (1), e0167488.
  31. Noah, D. L.; Hill, H.; Hines, D.; White, E. L.; Wolff, M. C., Qualification of the hemagglutination inhibition assay in support of pandemic influenza vaccine licensure. *Clin Vaccine Immunol* **2009**, *16* (4), 558-66.
  32. Wang, H.; Qian, W.-J.; Mottaz, H. M.; Clauss, T. R. W.; Anderson, D. J.; Moore, R. J.; Camp, D. G. I.; Khan, A. H.; Sforza, D. M.; Pallavicini, M.; Smith, D. J.; Smith, R. D., Development and evaluation of a micro- and nanoscale proteomic sample preparation method. *Journal of Proteome Research* **2005**, *4*, 2397-2403.
  33. Smith, P. K.; Krohn, R. I.; Hermanson, G. T.; Mallia, A. K.; Gartner, F. H.; Provenzano, M. D.; Fujimoto, E. K.; Goeke, N. M.; Olson, B. J.; Klenk, D. C., Measurement of protein using bicinchoninic acid. *Analytical Biochemistry* **1985**, *150*, 76-85.
  34. Fenyo, D.; Eriksson, J.; Beavis, R., Mass spectrometric protein identification using the global proteome machine. *Methods Mol Biol* **2010**, *673*, 189-202.
  35. Eng, J. K.; Fischer, B.; Grossman, J.; MacCoss, M. J., A fast SEQUEST cross correlation algorithm. *J Proteome Res* **2008**, *7*, 4598-4602.
  36. Eng, J. K.; McCormack, A. L.; Yates, J. R., An approach to correlate tandem mass spectral data of peptides with amino acid sequences in a protein database. *J Am Soc Mass Spectrom* **1994**, *5*, 976-989.
  37. Benjamini, Y.; Hochberg, Y., Controlling the false discovery rate: A practical and powerful approach to multiple testing. *Journal of the Royal Statistical Society. Series B (Methodological)* **1995**, *57* (1), 289-300.
  38. Luo, R.; Colangelo, C. M.; Sessa, W. C.; Zhao, H., Bayesian analysis of iTRAQ data with nonrandom missingness: identification of differentially expressed proteins. *Statistics in biosciences* **2009**, *1* (2), 228-245.
  39. Luo, R.; Zhao, H., Protein quantitation using iTRAQ: review on the sources of variations and analysis of nonrandom missingness. *Stat Interface* **2012**, *5* (1), 99-107.
  40. Lee, J. J.; Simborio, H. L.; Reyes, A. W.; Kim, D. G.; Hop, H. T.; Min, W.; Her, M.; Jung, S. C.; Yoo, H. S.; Kim, S., Proteomic analyses of the time course responses of mice



- infected with *Brucella abortus* 544 reveal immunogenic antigens. *FEMS microbiology letters* **2014**, 357 (2), 164-74.
41. Ackerman, A. L.; Cresswell, P., Cellular mechanisms governing cross-presentation of exogenous antigens. *Nat Immunol* **2004**, 5 (7), 678-84.
  42. Hon, H.; Oran, A.; Brocker, T.; Jacob, J., B Lymphocytes Participate in Cross-Presentation of Antigen following Gene Gun Vaccination. *The Journal of Immunology* **2005**, 174 (9), 5233-5242.
  43. Yang, C. W.; Strong, B. S.; Miller, M. J.; Unanue, E. R., Neutrophils influence the level of antigen presentation during the immune response to protein antigens in adjuvants. *J Immunol* **2010**, 185 (5), 2927-34.
  44. Piccirillo, C. A.; Bjur, E.; Topisirovic, I.; Sonenberg, N.; Larsson, O., Translational control of immune responses: from transcripts to translomes. *Nat Immunol* **2014**, 15 (6), 503-11.
  45. Yeung, E. S., Genome-wide correlation between mRNA and protein in a single cell. *Angew Chem Int Ed Engl* **2011**, 50, 583-585.
  46. Anderson, L.; Silhaver, J., A comparison of selected mRNA and protein abundances in human liver. *Electrophoresis* **1997**, 18 (3-4), 533-537.
  47. Vogel, C.; Marcotte, E. M., Insights into the regulation of protein abundance from proteomic and transcriptomic analyses. *Nature reviews. Genetics* **2012**, 13 (4), 227-32.

## CHAPTER IV

### CONCLUSIONS AND PERSPECTIVES

#### Summary

Vaccines have significantly reduced world-wide mortality caused by infectious diseases by producing long-term immunological memory.<sup>1</sup> As a result, vaccines have been one of the most cost-effective advancements in medicine, particularly with influenza. Seasonal influenza outbreaks cause 3-5 million infections worldwide and the associated vaccines are typically 70-80% effective.<sup>2-3</sup> However, pandemic influenza vaccines, particularly avian influenzas, tend to not be particularly effective for unknown reasons.<sup>3</sup> Therefore, vaccine manufacturers have started using adjuvants to enhance the protective response from the vaccine and to help reduce the amount of antigen required.<sup>4</sup> While this approach has worked with moderate success for such adjuvants like monophosphoryl lipid A in the HPV vaccine and MF59 in one seasonal influenza vaccine,<sup>5</sup> the adjuvant AS03 has shown slower success due to initial safety issues.<sup>6-7</sup> By being associated with an increased risk of narcolepsy in children, even when more recent reports have implicated other causes,<sup>8-10</sup> AS03 has yet to be approved for the general public.

Studies examining how AS03 and its components work have largely been conducted using animal models.<sup>11-12</sup> However, they are not necessarily a good analogy for human studies.<sup>13-15</sup> Therefore, we sought to investigate the molecular mechanisms of AS03 on a cell-population level using a human cohort. First, cell purification and protein quantitation multiplexing strategies needed for a large study were developed, as described in Chapter II. Using both MACS and FACS, highly purified immune cell populations were collected for proteomics analysis, along with the standard PBMC fraction for comparison. By comparing two competing iTRAQ multiplexing strategies, it was shown that pooling together the same cell types at different time points was superior to pooling different cell types at the same time point, in terms of identifying cell-type

specific protein responses. Further, the fraction of shared differentially expressed proteins from each immune cell population with the unpurified immune cells was very small, indicating a more complete data set was obtained from the purified cells.

Chapter II introduced one of the first examples of using quantitative shotgun proteomic analysis in a systems vaccinology study. The majority of systems vaccinology reviews have discussed the benefit of including proteomics data, but fail to provide any such example.<sup>16-18</sup> Instead, they describe numerous studies utilizing transcriptomics and antibody responses.<sup>19-24</sup> Genomics, transcriptomics, and proteomics complement each other.<sup>25</sup> While the genome is static, transcriptomics and proteomics dynamically respond to environmental changes. Even so, the correlation between transcriptomics and proteomics can be low due to post-transcriptional regulatory mechanisms.<sup>26</sup> By including proteomics data, we can obtain a more comprehensive picture of the immune response following vaccination.

Building on the methods developed in Chapter II, Chapter III reported the results from a Phase I prospective clinical trial assessing the molecular immune responses of an H5N1 vaccine given with or without AS03 adjuvant. This trial represents the first instance of AS03 being investigated in humans by systems biology methods. Distinct responses were observed in all cell types, but monocytes demonstrated the strongest differential signal, followed by neutrophils. Antigen processing and presentation pathways were shown to be enriched in these cell types at early time points for both proteomic and transcriptomic analysis. Prediction models identified inflammation and oxidative stress proteins at day 1, as well as immunoproteasome subunits at day 3, as predictors of later seroprotective antibody responses. However, the correlation of these proteins to seroprotective antibody responses needs to be validated in a larger study. Once confirmed, this set of proteins could potentially be used to assess the effectiveness of the AS03-H5N1 vaccine. This would be especially important during a pandemic outbreak to determine if a person would ultimately achieve protection or if the dose would be better going to someone else.

## Study Limitations

Although the research described here identified many proteome changes in the immune response to influenza vaccines, some limitations were unavoidable. First, the small sample size of 2 subjects in Chapter II and 10 subjects per group in Chapter III limits the generalizability of our results. However, these studies demonstrate the strengths of analyzing proteomic responses in systems vaccinology studies. By including proteomics, additional aspects of the immune response were identified as compared to transcriptomics and serological analysis conducted alone, allowing for a more comprehensive picture of the immune response. Second, since this pilot study and clinical trial was conceptualized, designed, and conducted, new mass spectrometry methods using MS3<sup>27</sup> and MultiNotch MS3<sup>28</sup> for iTRAQ analysis have been published. These methods show a reduction in the ratio distortion seen in iTRAQ experiments and allow for more proteins to be quantified overall. While we were unable to adopt the newer methods in these studies, due to the limitations on altering protocols after they are approved and the trial begins, future systems vaccinology studies will greatly benefit from these enhancements. This, however, does not discredit the observations made here; it just suggests that additional information could have been obtained. Finally, the immune cells used in these studies were purified from venous whole blood, rather than a combination of venous blood, lymphoid tissues, and muscle tissue at the site of injection. After APCs come in contact with a pathogen, they migrate to the lymph nodes in order to activate the adaptive immune response.<sup>29</sup> By sampling only blood, “fresh” immune cells are likely being sampled more than any activated ones over time, leading to important signals being diluted. Blood is a relatively quick and easy sample to collect and it was not possible to collect lymphoid and muscle tissue from healthy human subjects. Even with using only blood, models of protein combinations that could predict later seroprotection status were identified. It is reasonable to hypothesize that these models, based on blood, may be useful in the case of a H5N1 pandemic outbreak in order to quickly identify those who will achieve protection from the vaccine.

## Future Directions

### *Protein Validation Studies*

The clinical trial described in Chapter III identified hundreds of proteins that were differentially expressed between subjects who received AS03-H5N1 and those who received the control PBS-H5N1 vaccine. A small subset of these proteins were further selected in prediction models for seroprotection. However, in order for these proteins and models to be fully applied as correlates of protection, they must be validated and confirmed. The Link lab is currently working on methods to validate both the proteomics and transcriptomics results using a human monocyte THP-1 cell line.

Western blotting has historically been considered the gold standard for validating protein quantitation, however the field is moving more toward multiple reaction monitoring (MRM) for validation, as it is more reliable, reproducible, and accurate.<sup>30</sup> MRM is a targeted mass spectrometry approach that measures only the precursor and fragment ions of analytes of interest as transitions.<sup>31</sup> During MRM method development, a list of proteins of interest are imported into Skyline,<sup>32</sup> where the program fragments the proteins *in silico* and provides lists of possible transitions based on spectral libraries. This list is then narrowed down to pick at least three proteotypic peptides per protein and at least three transitions per peptide for scouting runs. Scouting runs test the detectability, stability, and reproducibility of the transitions. The MRM transition list is then reduced further iteratively until a final method is produced. Finally, synthetic peptides corresponding to the proteins of interest are used as internal standards to obtain the quantitative information. Currently, the initial transition list for the scouting runs has been made for validation of the monocyte data. However, there are a number of steps to be completed before the method will be usable for the validation of the clinical trial proteins. Further, this process will need to be completed for the neutrophil results, if not all the remaining cell types.

### *Metabolomics*

Metabolomics is considered the “final frontier” in systems biology.<sup>17, 33</sup> Therefore, investigating the metabolomic response to an AS03-adjuvanted H5N1 vaccine is a logical step for further understanding how it works. Metabolomics is the method of measuring and identifying small molecules, typically under 2000 Da. As the components of AS03 are all small molecules, it is possible to hypothesize that the degradation products could be measured throughout the immune response allowing for a better understanding of both the immune response and the pharmacokinetics of the adjuvant. Million Tegenge and Robert Mitkus created a physiologically based pharmacokinetic model which predicted that  $\alpha$ -tocopherol would peak in serum at 8 hours, rapidly transfer to draining lymph nodes, and be stored in adipose tissue.<sup>34</sup> However, their model was based on data collected from studies conducted in sheep and required a number of informed assumptions regarding human biology. By using metabolomics, the components of AS03 could be followed after vaccination to fully understand how they work, rather than relying on assumptions.

Further, the AS03-adjuvant degradation products could also be stimulating the immune response themselves, as metabolites can regulate signal transduction and regulate immune functions.<sup>17, 35</sup> The application of metabolomics to studying vaccines is relatively new, however one study identified sets of metabolites that differentiated between vaccinated and unvaccinated cows.<sup>36</sup> Similar to our proteomics analysis, the metabolites identified would also need to be validated.

### *AS03 Mechanism of Action*

Understanding the exact mechanism of how AS03 works is vitally important for it to be licensed for general use. The best way to investigate this would be to compare the response of AS03 alone to the response of the AS03-H5N1 vaccine and the response of an unadjuvanted H5N1 vaccine. This three-way comparison would help identify which signals stem from AS03, rather than the

normal response to an antigen. Ethical concerns prohibit the use of AS03 alone without a vaccine in humans, as it has not been assessed for safety in that manner. Therefore, these experiment will have be carried out in cell culture and animal models. While the methods outlined in Chapters II-III can and should be applied to these experiments, the data obtained will not be fully comparable to the human results.

In order to get the most complete understanding of the AS03 mechanism of action, all of the omics data from the human clinical trial and any cell culture/animal model experiments would need to be compared and integrated. This is the area where systems vaccinology faces the most challenges ahead. Individual omics studies generate enormous amounts of data and systems vaccinology aims to integrate many different types of omics studies (Figure 4.1). Effectively combining multiple omics datasets requires understanding each one individually statistically and biologically, as they all come with their own background and experimental noise, complexity, and format.<sup>37-38</sup> While there are tools to aid in the integration of multiple data types, they mainly are derived from methods for analyzing one data type and therefore do not completely bridge the gap.<sup>38</sup> Furthermore, these methods are mathematically complex to both operate and understand. Until a tool that will effectively combine all omics data types is developed, it will be difficult to produce a complete mechanism of action for AS03 or any other adjuvant.

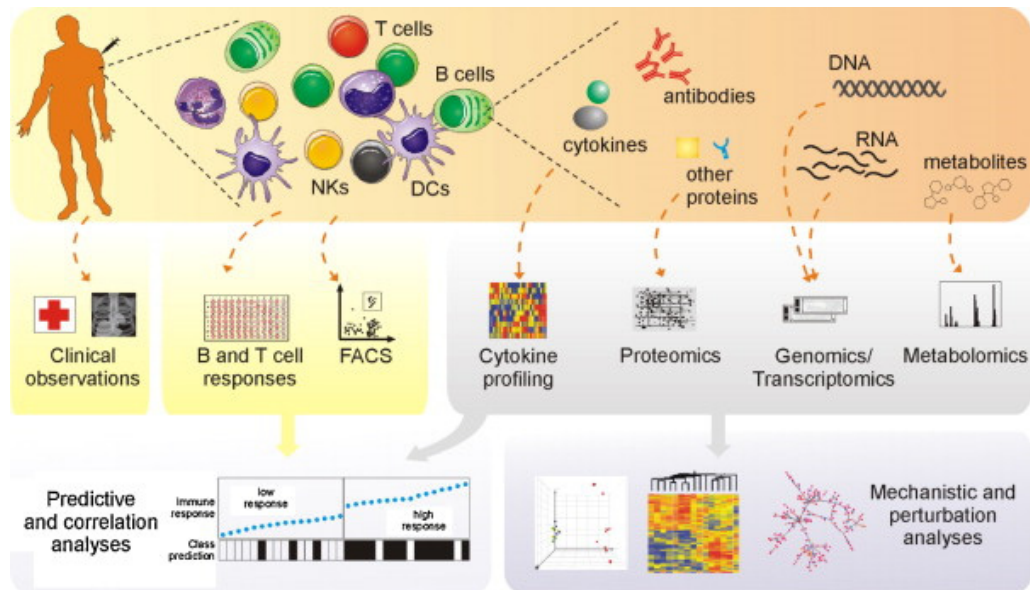


**Figure 4.1 Overview of systems vaccinology methods.** Systems vaccinology aims to collect and integrate data from all components of the immune response. A combination of standardized immune serologic assays with the high-throughput transcriptomic, proteomic, and metabolomic measurements will provide the opportunity to predict immunologic protection from vaccines.<sup>17</sup> Reprinted from Seminars in Immunology, with permission from Elsevier.

## Conclusion

Applying quantitative proteomics to the field of systems vaccinology represents a step forward for understanding the immune response to vaccines on a granular level. Overall, the methods in this dissertation outline the benefit of both separating the individual immune cell populations and using quantitative proteomics to study the immune response to vaccines. Many differences were observed when the responses from purified individual immune cell types were compared to PBMC after a seasonal influenza vaccine. Each individual immune cell type showed unique biological networks associated with their differential proteins. Further, when the developed methods were applied during a clinical trial of an AS03-adjuvanted H5N1 vaccine, monocytes and neutrophils showed significant upregulation of antigen processing and presentation proteins, which corresponded to similar results observed at the transcriptomics level. The approaches outlined here can guide future systems biology studies aimed at modeling and predicting complex responses to vaccines, vaccine adjuvants, or even natural infections between multiple cell types.



## References

1. Germain, R. N., Vaccines and the Future of Human Immunology. *Immunity* **2010**, 33, 441-450.
2. Kreijtz, J. H. C. M.; Fouchier, R. A. M.; Rimmelzwaan, G. F., Immune responses to influenza virus infection. *Virus Res* **2011**, 162, 19-30.
3. Gottlieb, T.; Ben-Yedidia, T., Epitope-based approaches to a universal influenza vaccine. *J Autoimmun* **2014**, 54, 15-20.
4. Vogel, F. R.; Hem, S. L., Immunologic Adjuvants. In *Vaccines, Expert Consult*, 5th ed.; El: China, 2008; pp 59-71.
5. Centers for Disease Control and Prevention Vaccine Adjuvants. <https://www.cdc.gov/vaccinesafety/concerns/adjuvants.html> (accessed December 12, 2016).
6. Nohynek, H.; Jokinen, J.; Partinen, M.; Vaarala, O.; Kirjavainen, T.; Sundman, J.; Himanen, S.; Hublin, C.; Julkunen, I.; Olsen, P.; Saarenpaa-Heikkila, O.; Kilpi, T., AS03 adjuvanted AH1N1 vaccine associated with an abrupt increase in the incidence of childhood narcolepsy in Finland. *PLoS ONE* **2012**, 7 (3), e33536.
7. Ahmed, S. S.; Schur, P. H.; MacDonald, N. E.; Steinman, L., Narcolepsy, 2009 A(H1N1) pandemic influenza, and pandemic influenza vaccinations: what is known and unknown about the neurological disorder, the role for autoimmunity, and vaccine adjuvants. *J Autoimmun* **2014**, 50, 1-11.
8. Vaarala, O.; Vuorela, A.; Partinen, M.; Baumann, M.; Freitag, T. L.; Meri, S.; Saavalainen, P.; Jauhiainen, M.; Soliymani, R.; Kirjavainen, T.; Olsen, P.; Saarenpaa-Heikkila, O.; Rouvinen, J.; Roivainen, M.; Nohynek, H.; Jokinen, J.; Julkunen, I.; Kilpi, T., Antigenic Differences between AS03 Adjuvanted Influenza A (H1N1) Pandemic Vaccines: Implications for Pandemrix-Associated Narcolepsy Risk. *PLoS ONE* **2014**, 9 (12), e114361.
9. Ahmed, S. S.; Volkmoth, W.; Duca, J.; Corti, L.; Pallaoro, M.; Pezzicoli, A.; Karle, A.; Rigat, F.; Rappuoli, R.; Narashimhan, V.; Julkunen, I.; Vuorela, A.; Vaarala, O.; Nohynek, H.; Pasini, F. L.; Montomoli, E.; Trombetta, C.; Adams, C. M.; Rothbard, J.; Steinman, L., Antibodies to influenza nucleoprotein cross-react with human hypocretin receptor 2. *Science Translational Medicine* **2015**, 7 (294), 29ra105.
10. Ambati, A.; Poiret, T.; Svahn, B. M.; Valentini, D.; Khademi, M.; Kockum, I.; Lima, I.; Arnheim-Dahlstrom, L.; Lamb, F.; Fink, K.; Meng, Q.; Kumar, A.; Rane, L.; Olsson, T.; Maeurer, M., Increased beta-haemolytic group A streptococcal M6 serotype and streptodornase B-specific cellular immune responses in Swedish narcolepsy cases. *Journal of internal medicine* **2015**, 278 (3), 264-276.
11. Morel, S.; Didierlaurent, A.; Bourguignon, P.; Delhay, S.; Baras, B.; Jacob, V.; Planty, C.; Elouahabi, A.; Harvengt, P.; Carlsen, H.; Kielland, A.; Chomez, P.; Garçon, N.; Van Mechelen, M., Adjuvant System AS03 containing  $\alpha$ -tocopherol modulates innate immune response and leads to improved adaptive immunity. *Vaccine* **2011**, 29, 2461-2473.

12. Segal, L.; Wouters, S.; Morelle, D.; Gautier, G.; Le Gal, J.; Martin, T.; Kuper, F.; Destexhe, E.; Didierlaurent, A. M.; Garçon, N., Non-clinical safety and biodistribution of AS03-  
adjuvanted inactivated pandemic influenza vaccines. *Journal of applied toxicology : JAT* **2015**, *35* (12), 1564-1576.
13. Mestas, J.; Hughes, C. C. W., Of Mice and Not Men: Differences between Mouse and  
Human Immunology. *J Immunol* **2004**, *172* (5), 2731-2738.
14. Su, L. F.; Han, A.; McGuire, H. M.; Furman, D.; Newell, E. W.; Davis, M. M., The promised  
land of human immunology. *Cold Spring Harbor symposia on quantitative biology* **2013**,  
*78*, 203-13.
15. Beura, L. K.; Hamilton, S. E.; Bi, K.; Schenkel, J. M.; Odumade, O. A.; Casey, K. A.;  
Thompson, E. A.; Fraser, K. A.; Rosato, P. C.; Filali-Mouhim, A.; Sekaly, R. P.; Jenkins,  
M. K.; Vezys, V.; Haining, W. N.; Jameson, S. C.; Masopust, D., Normalizing the  
environment recapitulates adult human immune traits in laboratory mice. *Nature* **2016**,  
*532* (7600), 512-6.
16. Pulendran, B.; Li, S.; Nakaya, H. I., Systems vaccinology. *Immunity* **2010**, *33*, 516-529.
17. Li, S.; Nakaya, H. I.; Kazmin, D. A.; Oh, J. Z.; Pulendran, B., Systems biological  
approaches to measure and understand vaccine immunity in humans. *Semin Immunol*  
**2013**, *25*, 209-218.
18. Buonaguro, L.; Wang, E.; Tornesello, M. L.; Buonaguro, F. M.; Marincola, F. M., Systems  
biology applied to vaccine and immunotherapy development. *BMC Systems Biology* **2011**,  
*5*, 146.
19. Li, S.; Roupheal, N.; Duraisingham, S.; Romero-Steiner, S.; Presnell, S.; Davis, C.;  
Schmidt, D. S.; Johnson, S. E.; Milton, A.; Rajam, G.; Kasturi, S.; Carlone, G. M.; Quinn,  
C.; Chaussabel, D.; Palucka, A. K.; Mulligan, M. J.; Ahmed, R.; Stephens, D. S.; Nakaya,  
H. I.; Pulendran, B., Molecular signatures of antibody responses derived from a systems  
biology study of five human vaccines. *Nat Immunol* **2014**, *15*, 195-204.
20. Nakaya, H. I.; Clutterbuck, E.; Kazmin, D.; Wang, L.; Cortese, M.; Bosinger, S. E.; Patel,  
N. B.; Zak, D. E.; Aderem, A.; Dong, T.; Del Giudice, G.; Rappuoli, R.; Cerundolo, V.;  
Pollard, A. J.; Pulendran, B.; Siegrist, C. A., Systems biology of immunity to MF59-  
adjuvanted versus nonadjuvanted trivalent seasonal influenza vaccines in early childhood.  
*Proceedings of the National Academy of Sciences of the United States of America* **2016**.
21. Nakaya, H. I.; Hagan, T.; Duraisingham, S. S.; Lee, E. K.; Kwissa, M.; Roupheal, N.;  
Frasca, D.; Gersten, M.; Mehta, A. K.; Gaujoux, R.; Li, G. M.; Gupta, S.; Ahmed, R.;  
Mulligan, M. J.; Shen-Orr, S.; Blomberg, B. B.; Subramaniam, S.; Pulendran, B., Systems  
Analysis of Immunity to Influenza Vaccination across Multiple Years and in Diverse  
Populations Reveals Shared Molecular Signatures. *Immunity* **2015**, *43* (6), 1186-98.
22. Nakaya, H. I.; Wrammert, J.; Lee, E. K.; Racioppi, L.; Marie-Kunze, S.; Haining, W. N.;  
Means, A. R.; Kasturi, S. P.; Khan, N.; Li, G.-M.; McCausland, M.; Kanchan, V.; Kokko, K.  
E.; Li, S.; Elbein, R.; Mehta, A. K.; Aderem, A.; Subbarao, K.; Ahmed, R.; Pulendran, B.,  
Systems biology of vaccination for seasonal influenza in humans. *Nat Immunol* **2011**, *12*,  
786-795.

23. Querec, T. D.; Akondy, R. S.; Lee, E. K.; Cao, W.; Nakaya, H. I.; Teuwen, D.; Pirani, A.; Gernert, K.; Deng, J.; Marzolf, B.; Kennedy, K.; Wu, H.; Bennouna, S.; Oluoch, H.; Miller, J.; Vencio, R. Z.; Mulligan, M.; Aderem, A.; Ahmed, R.; Pulendran, B., Systems biology approach predicts immunogenicity of the yellow fever vaccine in humans. *Nat Immunol* **2009**, *10*, 116-125.
24. Tan, Y.; Tamayo, P.; Nakaya, H.; Pulendran, B.; Mesirov, J. P.; Haining, W. N., Gene signatures related to B-cell proliferation predict influenza vaccine-induced antibody response. *European Journal of Immunology* **2014**, *44*, 285-295.
25. Adamczyk-Poplawska, M.; Markowicz, S.; Jagusztyn-Krynicka, E. K., Proteomics for development of vaccine. *J Proteomics* **2011**, *74*, 2596-2616.
26. Vogel, C.; Marcotte, E. M., Insights into the regulation of protein abundance from proteomic and transcriptomic analyses. *Nature reviews. Genetics* **2012**, *13* (4), 227-32.
27. Ting, L.; Rad, R.; Gygi, S. P.; Haas, W., MS3 eliminates ratio distortion in isobaric multiplexed quantitative proteomics. *Nat Methods* **2011**, *8* (11), 937-40.
28. McAlister, G. C.; Nusinow, D. P.; Jedrychowski, M. P.; Wuhr, M.; Huttlin, E. L.; Erickson, B. K.; Rad, R.; Haas, W.; Gygi, S. P., MultiNotch MS3 enables accurate, sensitive, and multiplexed detection of differential expression across cancer cell line proteomes. *Anal Chem* **2014**, *86* (14), 7150-8.
29. Murphy, K., *Janeway's Immunobiology*. 8th ed.; Garland Science: London, 2012.
30. Aebersold, R.; Burlingame, A. L.; Bradshaw, R. A., Western Blots versus Selected Reaction Monitoring Assays: Time to Turn the Tables? *Molecular & Cellular Proteomics* **2013**, *12*, 2381-2382.
31. Kitteringham, N. R.; Jenkins, R. E.; Lane, C. S.; Elliott, V. L.; Park, B. K., Multiple reaction monitoring for quantitative biomarker analysis in proteomics and metabolomics. *J Chromatogr B Biomed Sci Appl* **2009**, *877*, 1229-1239.
32. MacLean, B.; Tomazela, D. M.; Shulman, N.; Chambers, M.; Finney, G. L.; Frewen, B.; Kern, R.; Tabb, D. L.; Liebler, D. C.; MacCoss, M. J., Skyline: an open source document editor for creating and analyzing targeted proteomics experiments. *Bioinformatics* **2010**, *26* (7), 966-8.
33. Veenstra, T. D., Metabolomics: the final frontier? *Genome Medicine* **2012**, *4*, 40.
34. Tegenge, M. A.; Mitkus, R. J., A first-generation physiologically based pharmacokinetic (PBPK) model of alpha-tocopherol in human influenza vaccine adjuvant. *Regulatory toxicology and pharmacology : RTP* **2015**, *71* (3), 353-364.
35. Wellen, K. E.; Thompson, C. B., A two-way street: reciprocal regulation of metabolism and signalling. *Nature reviews. Molecular cell biology* **2012**, *13* (4), 270-6.
36. Gray, D. W.; Welsh, M. D.; Doherty, S.; Mansoor, F.; Chevallier, O. P.; Elliott, C. T.; Mooney, M. H., Identification of systemic immune response markers through metabolomic

- profiling of plasma from calves given an intra-nasally delivered respiratory vaccine. *Veterinary research* **2015**, 46, 7.
37. Buescher, J. M.; Driggers, E. M., Integration of omics: more than the sum of its parts. *Cancer & metabolism* **2016**, 4, 4.
  38. Gligorijevic, V.; Przulj, N., Methods for biological data integration: perspectives and challenges. *Journal of the Royal Society, Interface* **2015**, 12 (112).

## APPENDIX A

### SUPPORTING INFORMATION: CHAPTER II

The following three tables are too large to be included in this document, but can be accessed from the provided links. Each file reports normalized pseudospectral counts (NPSC) that were calculated in *ProteoIQ*. A value of zero indicates a protein was identified but not quantified, while an NA value indicates a protein was not identified in that sample at all.

**Table A-1 Normalized protein expression in human immune cells prior to and post-TIV vaccination.**

Link	<a href="https://drive.google.com/open?id=1GECKcX6pPg-NcgKJ9ixvdxThs1h-yxdOKNHVcOOyfgQ">https://drive.google.com/open?id=1GECKcX6pPg-NcgKJ9ixvdxThs1h-yxdOKNHVcOOyfgQ</a>
------	---

**Table A-2 Normalized protein expression in human immune cells prior to and post-TIV vaccination filtered to remove zero values and contaminating keratins from subject HD30**

Link	<a href="https://drive.google.com/open?id=18dUgJPractjufwTe88Spa1r0Am-fSa_dvHsrfQSbtys">https://drive.google.com/open?id=18dUgJPractjufwTe88Spa1r0Am-fSa_dvHsrfQSbtys</a>
------	---

**Table A-3 Normalized protein expression in human immune cells prior to and post-TIV vaccination filtered to remove zero values and contaminating keratins from subject HD31**

Link	<a href="https://drive.google.com/open?id=1AtnZoC1HHwfpq5oN74ww2MO_ZfAdm8r25oVOxadff-0">https://drive.google.com/open?id=1AtnZoC1HHwfpq5oN74ww2MO_ZfAdm8r25oVOxadff-0</a>
------	---

**Table A-4 Top networks and pathways identified in TIV-vaccinated subjects**

	Top Network Description	Top Canonical Pathway
<b>d0-1</b>		
<b>PBMC</b>	Hematological disease, reproductive system development and function, cellular assembly and organization	Granzyme A signaling
<b>T cell</b>	Endocrine system development and function, molecular transport, small molecule biochemistry	Mechanisms of viral exit from host cells
<b>B cell</b>	Cellular assembly and organization, cellular function and maintenance, nervous system development and function	Pyruvate fermentation to lactate
<b>NK</b>	Cellular assembly and organization, DNA replication, recombination and repair, post-translational modification	Granzyme A signaling
<b>Monocyte</b>	Dermatological disease and conditions, antimicrobial response, inflammatory response	Methylglyoxal degradation III
<b>Neutrophil</b>	Hematological system development and function, tissue morphology, cellular development	RhoGDI signaling
<b>d0-3</b>		
<b>PBMC</b>	Cellular assembly and organization, DNA replication, recombination and repair, connective tissue development and function	Granzyme A signaling
<b>T cell</b>	Hereditary disorder, metabolic disease, neurological disorder	Inhibition of angiogenesis by TSP1
<b>B cell</b>	Protein synthesis, RNA post-transcriptional modification, molecular transport	Lipid antigen presentation by CD1
<b>NK</b>	Cellular movement, hematological system development and function, immune cell trafficking	Actin cytoskeleton signaling
<b>Monocyte</b>	Cancer, endocrine system disorders, hematological disease	Sertoli cell-sertoli cell junction signaling
<b>Neutrophil</b>	Cell morphology, hereditary disorder, nervous system development and function	Pentose phosphate pathway (non-oxidative)
<b>d0-7</b>		
<b>PBMC</b>	Cellular assembly and organization, DNA replication, recombination and repair, cell cycle	Granzyme A signaling
<b>T cell</b>	Cell death and survival, embryonic development, post translational modification	Oxidative phosphorylation
<b>B cell</b>	Nucleic acid metabolism, cardiac arrhythmia, cardiovascular disease	Mitochondrial dysfunction
<b>NK</b>	Free radical scavenging, molecular transport, cellular assembly and organization	Regulation of actin-based motility by Rho
<b>Monocyte</b>	Cell death and survival, cellular compromise, protein trafficking	Neuroprotective role of THOP1 in Alzheimer's disease
<b>Neutrophil</b>	Cellular assembly and organization, cellular function and maintenance, neurological disease	Amyotrophic lateral sclerosis signaling

## APPENDIX B

### SUPPORTING INFORMATION: CHAPTER III

#### **Supplemental Methods**

##### *Ethics statement*

This study was approved by the Vanderbilt University Institutional Review Board, and the study was conducted in accordance with Good Clinical Practice, the Declaration of Helsinki, the US Code of Federal Regulations for the Protection of Human Subjects, and the Department of Health and Human Services Belmont Report. The study is registered on ClinicalTrials.gov (No. NCT01573312). All subjects provided written informed consent prior to initiation of study procedures. Subjects were assigned de-identified code numbers and their privacy strictly held in trust by study personnel, sponsors, and their agents. This confidentiality extends to cover testing of biological samples, in addition to the clinical information related to participants.

##### *Study products*

Inactivated monovalent influenza A/Indonesia/05/2005 H5N1 split-virus vaccine at a dosage of 3.75 mcg and phosphate buffered saline (PBS) diluent were both manufactured by Sanofi Pasteur. The AS03 adjuvant was manufactured by GlaxoSmithKline (GSK) and contained 4.86 mg polysorbate 80, 11.86 mg  $\alpha$ -tocopherol, and 10.69 mg squalene in an oil-in-water emulsion. The vaccine and adjuvant were provided by the US Department of Health and Human Services Biomedical Advanced Research and Development Authority from the National Pre-pandemic Influenza Vaccine Stockpile.

### *Analysis population*

The systems biology analysis population included all subjects who met all inclusion and exclusion criteria, who contributed at least one pre-vaccination blood sample (at Day -28, -14, or 0) and at least one post-vaccination blood sample (at Day 1, 3, 7, or 28) for which valid results were reported. The analyses included subjects by study product actually received. This population included 20 subjects (10 for each treatment group) including a subject in the SV-AS03 vaccine group, who received the second vaccination (Day 28) out-of-window. Time points with outlying measurements were identified separately for each assay.

### *Reference Channel Selection*

In order to determine the most advantageous method for normalizing the data within ProteoIQ, randomly selected donors and cell type data were analyzed first using Day 0 as the reference channel and second with ICCS as the reference channel. The  $\log_2$  ratios were exported for each method and plotted against each other in R (Figure B-11A). While both methods showed moderate correlation for peptides quantitated in both experiments (Figure B-11B), the experiment using ICCS as the reference channel showed more quantitated peptides overall. Further, a Bland-Altman plot showing the agreement between the two methods (Figure B-11C) showed a slight bias towards higher quantitation values in the method using ICCS as the reference, however with a value of 0.03122, the bias was small enough to not be considered. Therefore, the remaining analyses were performed using ICCS selected as the reference channel.

### *Normalization*

To account for systematic differences in the protein ratio distributions between iTRAQ experiments for the same cell type, protein ratios were normalized within cell type on the  $\log_2$  scale to align the medians of the protein ratio distributions across cell type samples. The following steps were taken for each cell type:



- (1) For each sample (140 per cell type), the median of the protein ratio distribution was determined using the quantifications obtained from the reference (top) protein within a protein group
- (2) The median of all the sample medians calculated in (1) was obtained
- (3) A sample specific scaling factor was then calculated as the difference between the cell type-specific median obtained in (2) and the sample-specific median obtained in (1)
- (4) The protein ratio distribution for each sample was then normalized by adding the scaling factor determined in (3).

Subject specific  $\log_2$  protein fold changes from baseline were calculated for each subject and post-vaccination day by subtracting the mean of the normalized  $\log_2$  baseline ratios from each of the subject's post-vaccination day ratios.

## **Supplementary Results**

### *Quality Control*

Due to the large number of experiments, samples were checked for consistency at different times during analysis. After digestion, the number of peptides and proteins identified helped determine if there were losses during the desalting step by solid phase extraction or if the original quantitation of protein was incorrect (Figure B-9). After each iTRAQ experiment, the two yeast proteins were used to determine if there was inconsistency within the experiment (Figure B-10A,B), indicating errors in labeling efficiency. The yeast proteins were also used after all 20 experiments of the same cell type were run to determine if any experiments appeared as outliers (Figure B-10C,D).



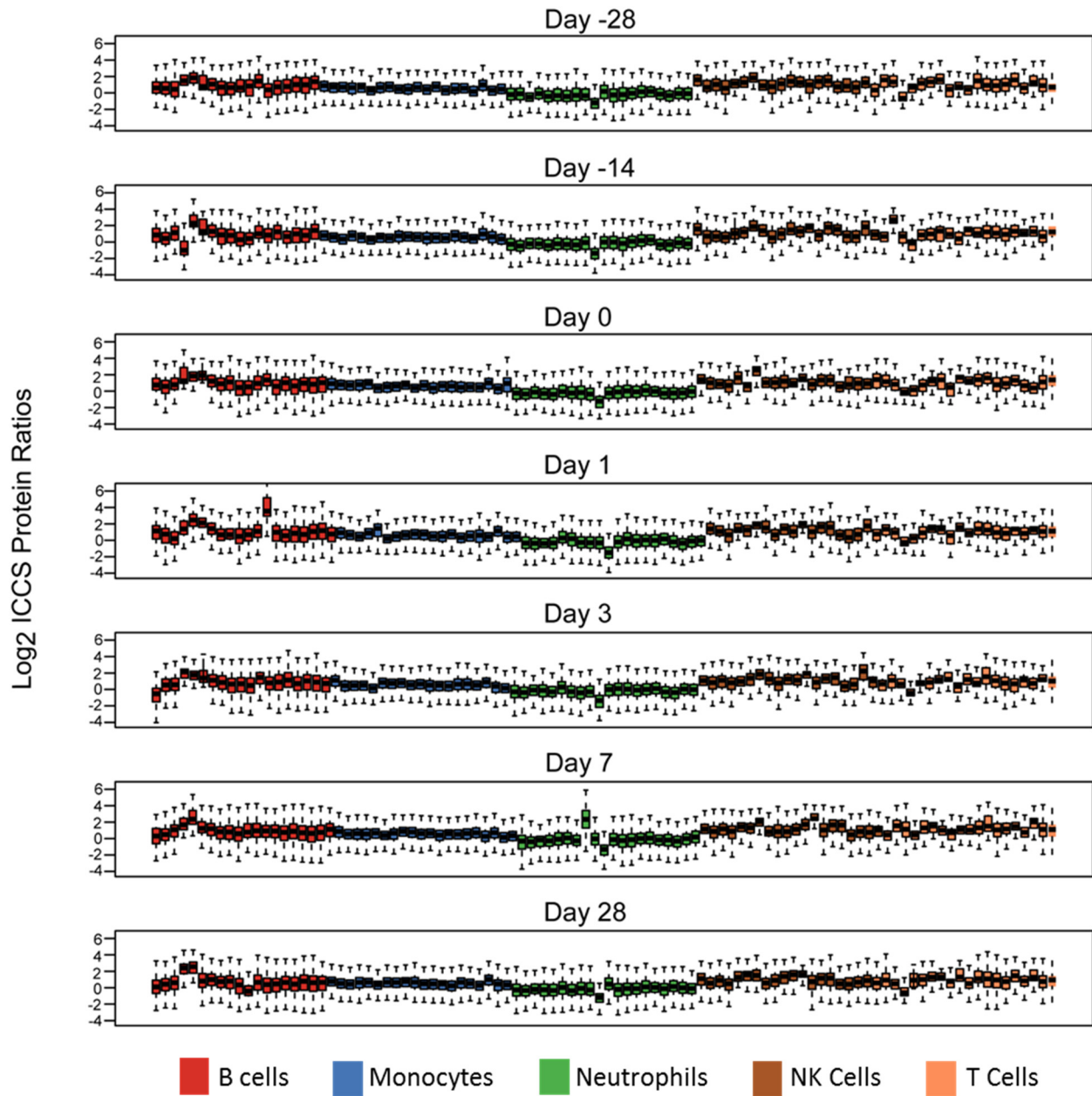
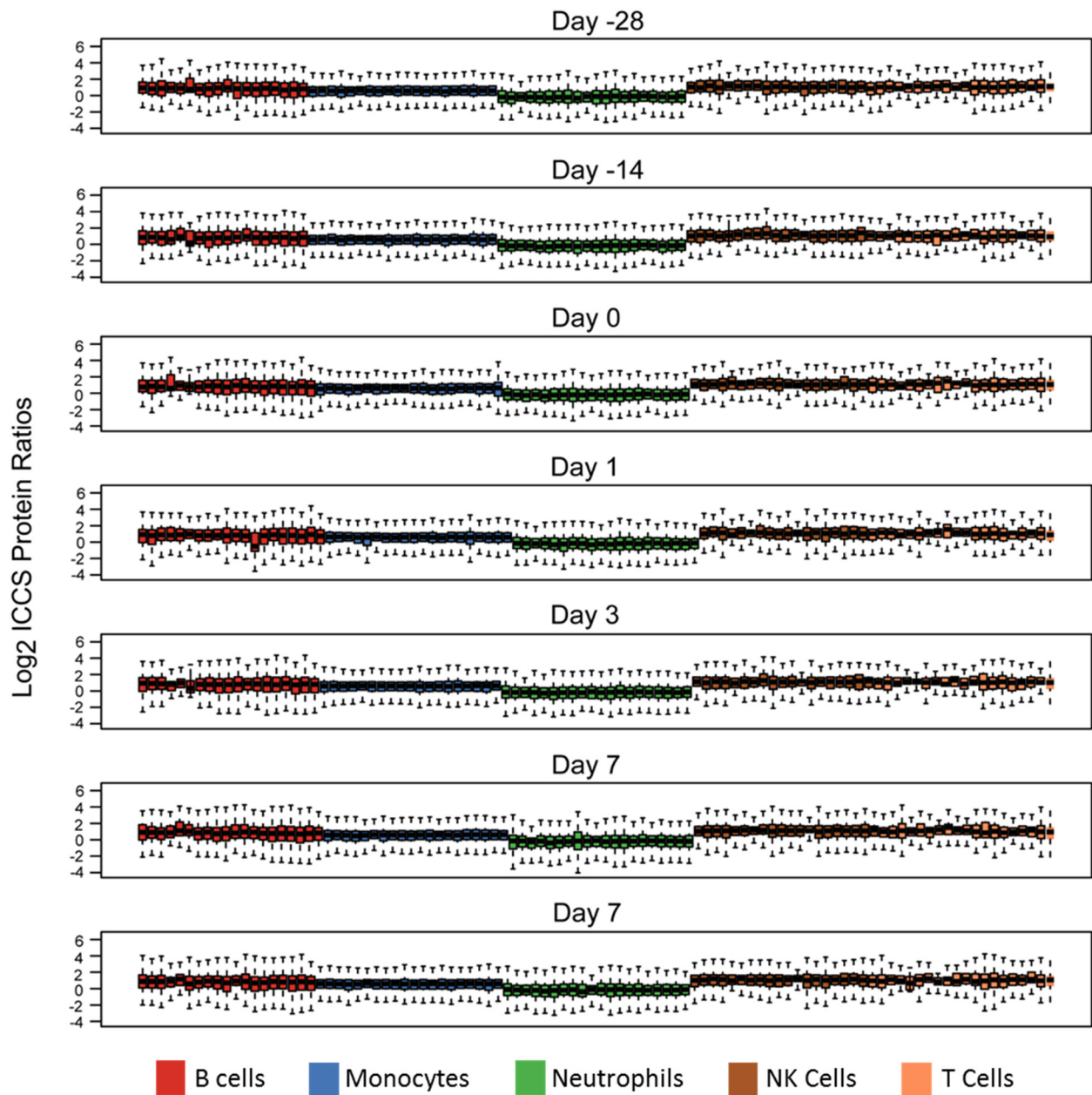
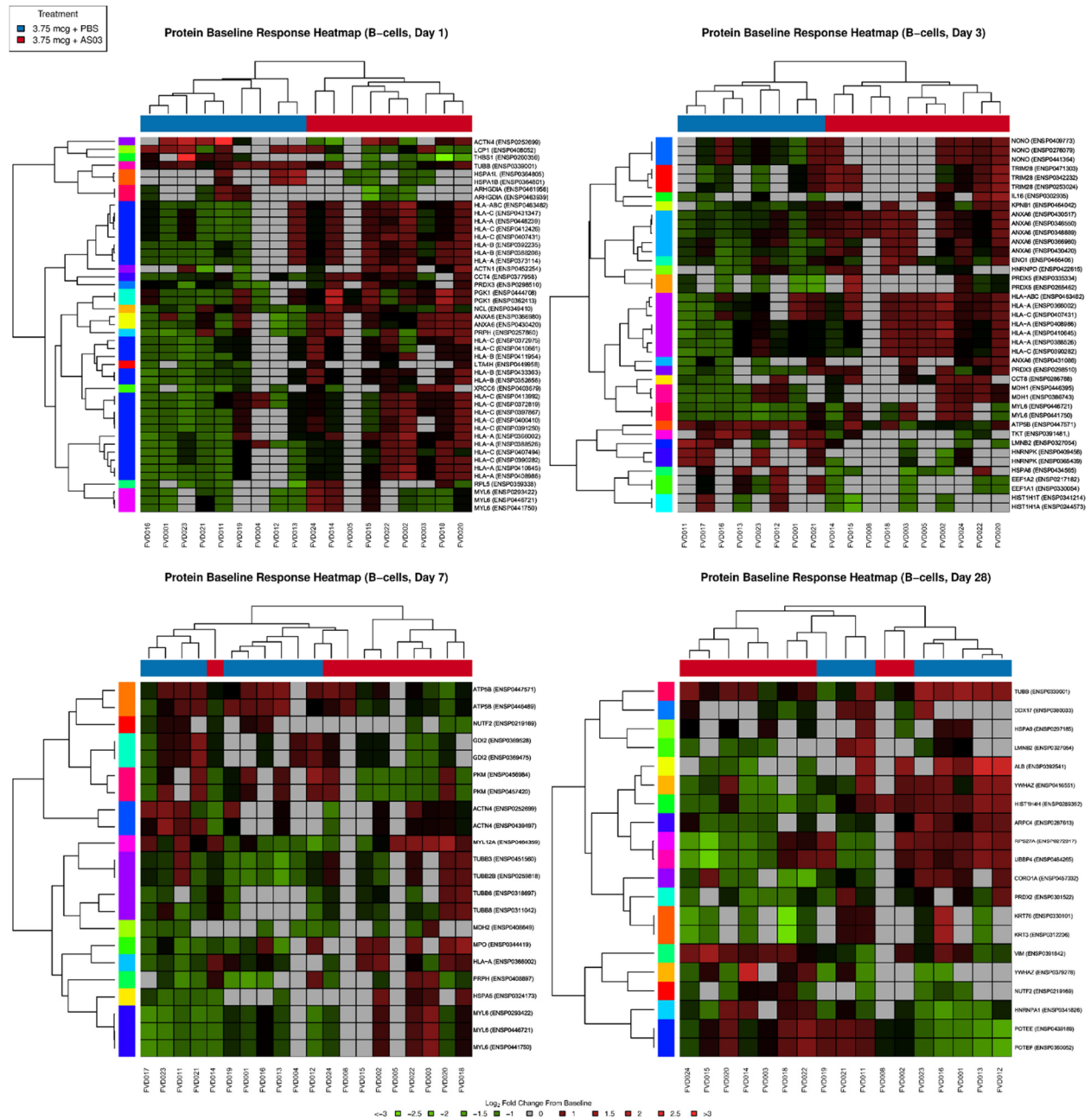


Figure B-2 Boxplots of  $\log_2$  ICCS ratios before median normalization. Outliers are omitted for clarity.



**Figure B-3** Boxplots of  $\log_2$  ICCS ratios after median normalization. Median normalization within cell type aligned protein ratio distributions, while retaining cell-type median centers. Outliers are omitted for clarity.



**Figure B-4 Heatmaps of DA protein baseline log<sub>2</sub> fold changes for B cells at each post-vaccination time point.** Dendrograms were obtained using complete linkage clustering of uncentered pairwise Pearson correlation distances between log<sub>2</sub> fold changes. Llog<sub>2</sub> fold changes of 0 were imputed for missing values. Protein cluster membership (50% sequence identity) is along the protein dendrogram on the left side; vaccine group membership is highlighted below the subject dendrogram at the top. Red: up-regulated from baseline; green: down-regulated from baseline; grey: missing observations.

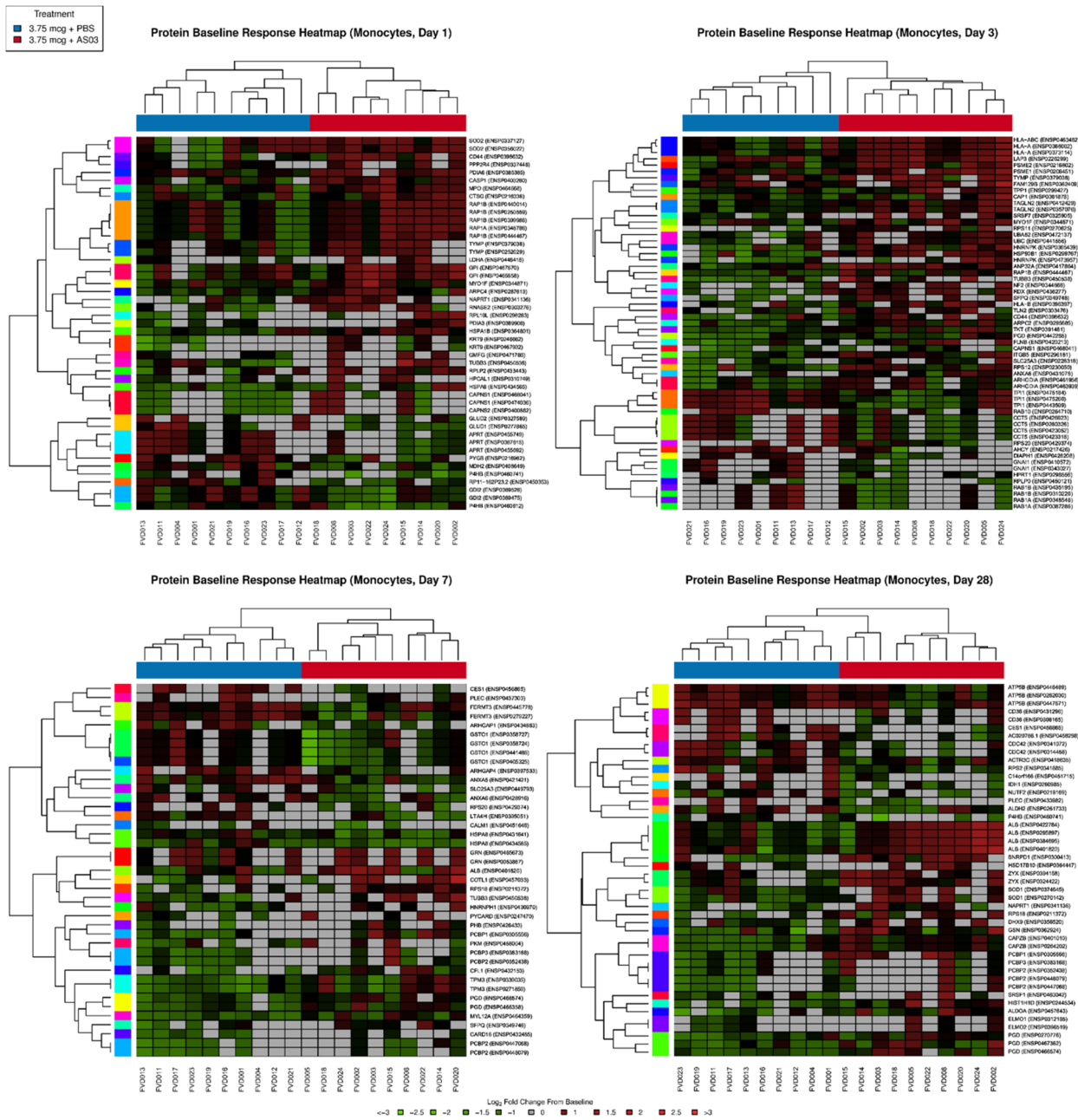


**Figure B-5 Heatmaps of DA protein baseline log<sub>2</sub> fold changes for monocytes at each post-vaccination time point.** Dendrograms were obtained using complete linkage clustering of uncentered pairwise Pearson correlation distances between log<sub>2</sub> fold changes. Log<sub>2</sub> fold changes of 0 were imputed for missing values. Protein cluster membership (50% sequence identity) is along the protein dendrogram on the left side; vaccine group membership is highlighted below the subject dendrogram at the top. Red: up-regulated from baseline; green: down-regulated from baseline; grey: missing observations

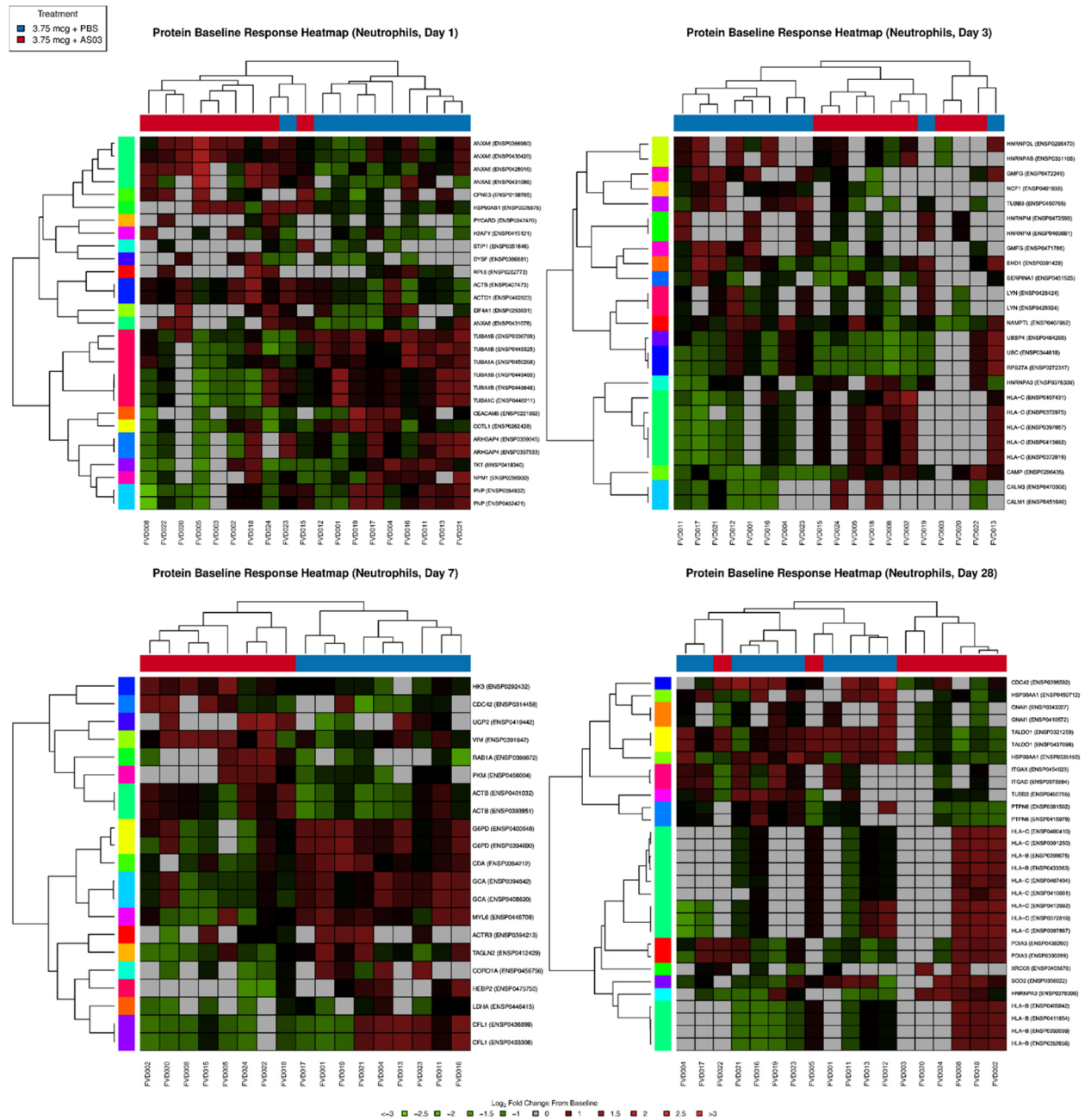


**Figure B-6 Heatmaps of DA protein baseline log<sub>2</sub> fold changes for neutrophils at each post-vaccination time point.** Dendrograms were obtained using complete linkage clustering of uncentered pairwise Pearson correlation distances between log<sub>2</sub> fold changes. Log<sub>2</sub> fold changes of 0 were imputed for missing values. Protein cluster membership (50% sequence identity) is along the protein dendrogram on the left side; vaccine group membership is highlighted below the subject dendrogram at the top. Red: up-regulated from baseline; green: down-regulated from baseline; grey: missing observations

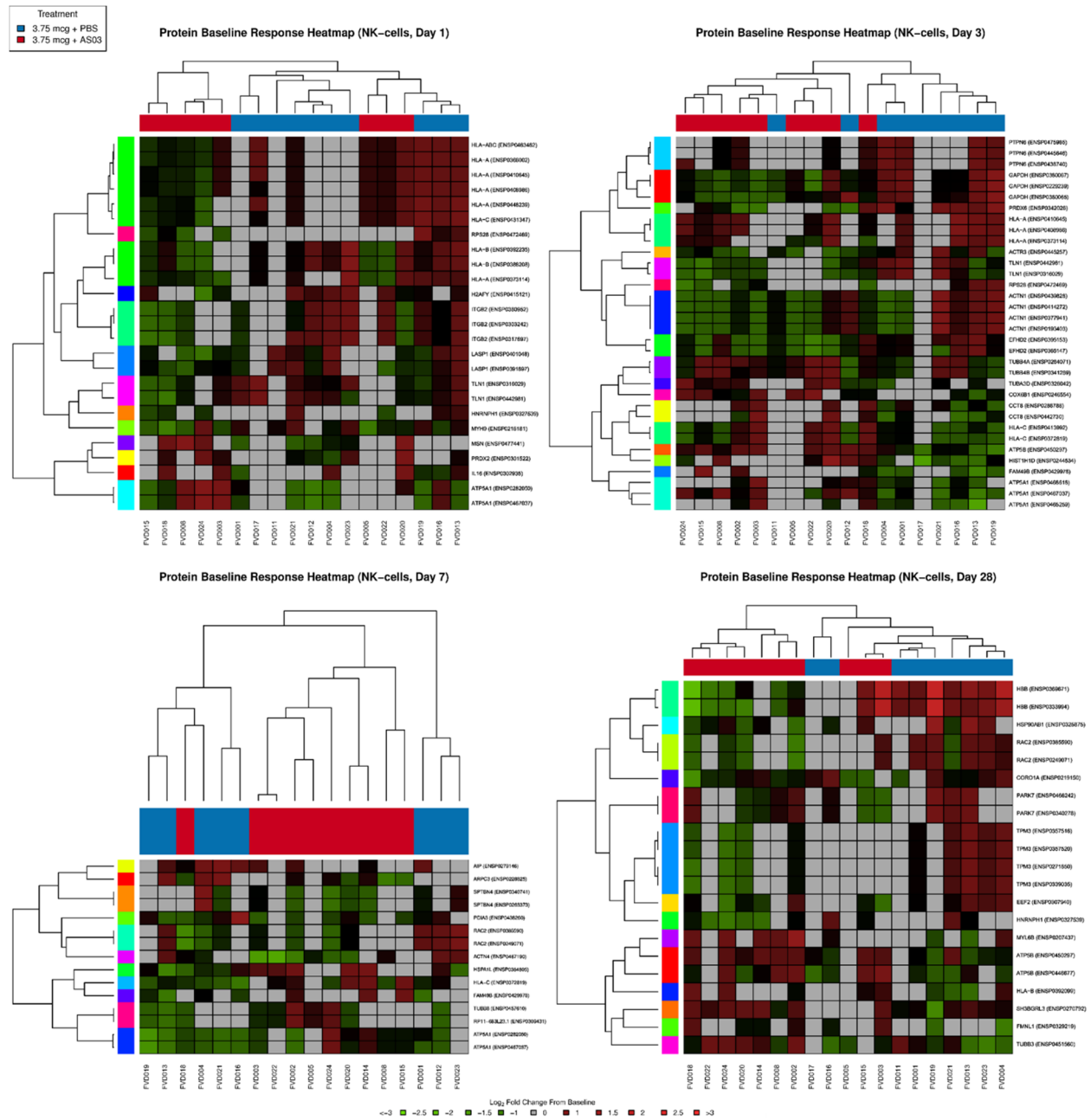


**Figure B-7 Heatmaps of DA protein baseline  $\log_2$  fold changes for NK cells at each post-vaccination time point.** Dendrograms were obtained using complete linkage clustering of uncentered pairwise Pearson correlation distances between  $\log_2$  fold changes.  $\log_2$  fold changes of 0 were imputed for missing values. Protein cluster membership (50% sequence identity) is along the protein dendrogram on the left side; vaccine group membership is highlighted below the subject dendrogram at the top. Red: up-regulated from baseline; green: down-regulated from baseline; grey: missing observations



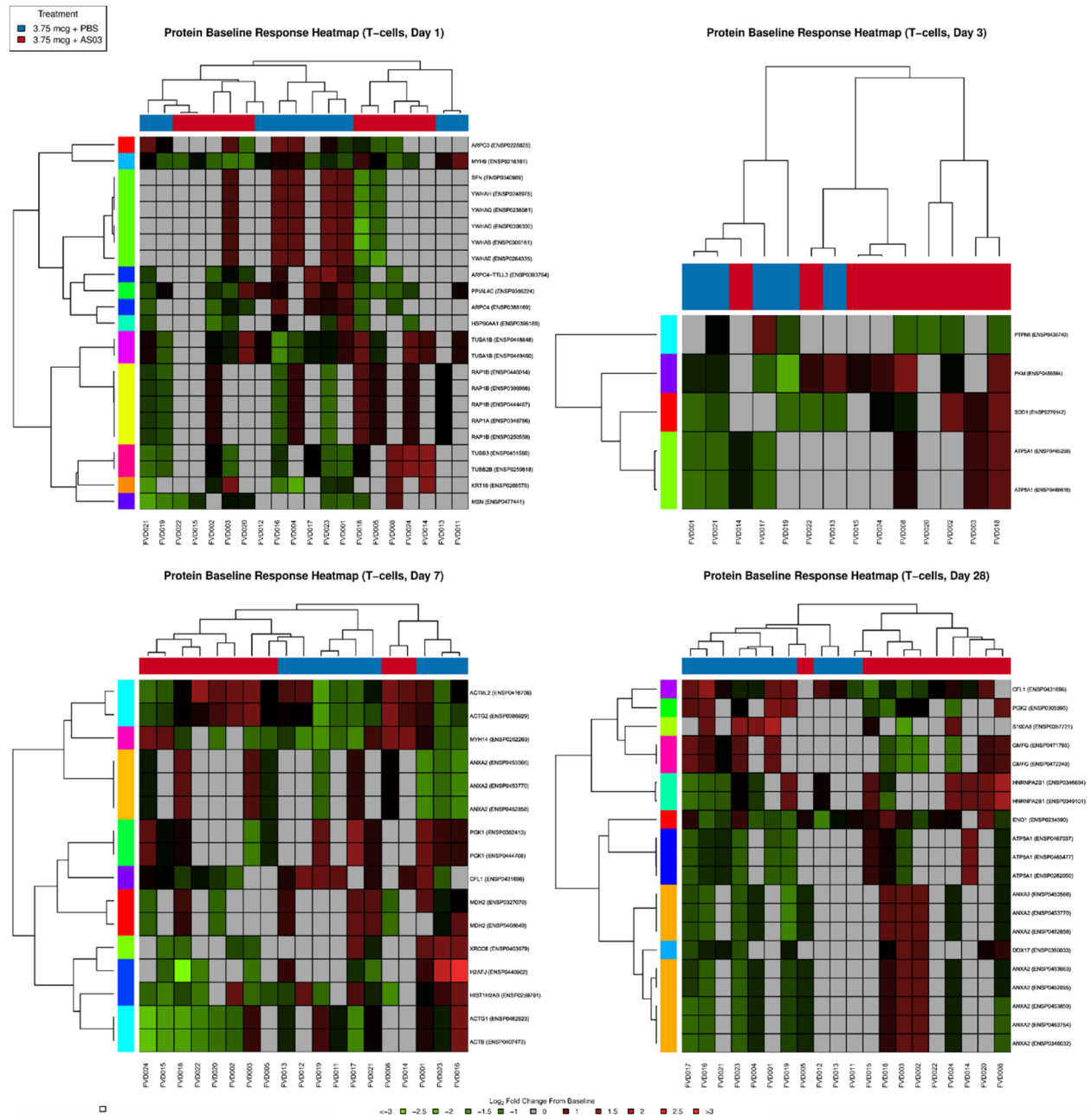


**Figure B-8 Heatmaps of DA protein baseline  $\log_2$  fold changes for T cells at each post-vaccination time point.** Dendrograms were obtained using complete linkage clustering of uncentered pairwise Pearson correlation distances between  $\log_2$  fold changes.  $\log_2$  fold changes of 0 were imputed for missing values. Protein cluster membership (50% sequence identity) is along the protein dendrogram on the left side; vaccine group membership is highlighted below the subject dendrogram at the top. Red: up-regulated from baseline; green: down-regulated from baseline; grey: missing observations

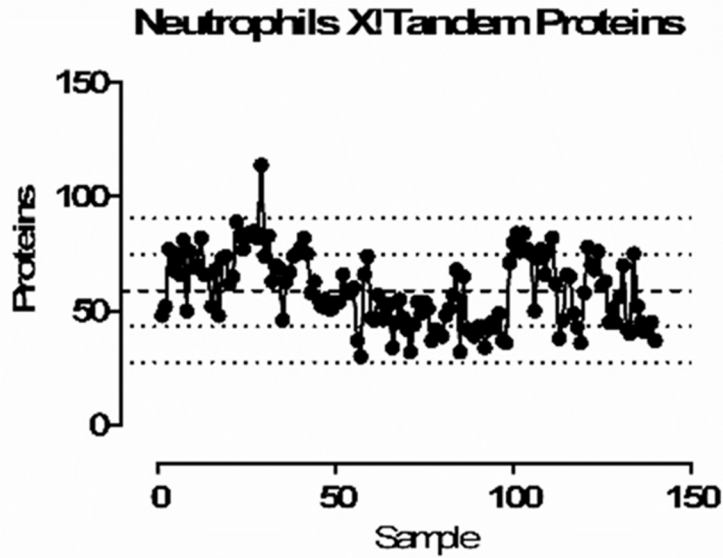


**Figure B-9 Neutrophil experiments control chart.** The number of proteins identified in each sample (from X!Tandem) were plotted over time. The middle bold dashed line indicates the average number of proteins identified across all neutrophil samples. The other lines indicate the 1<sup>st</sup> and 2<sup>nd</sup> standard deviation control limits in each direction

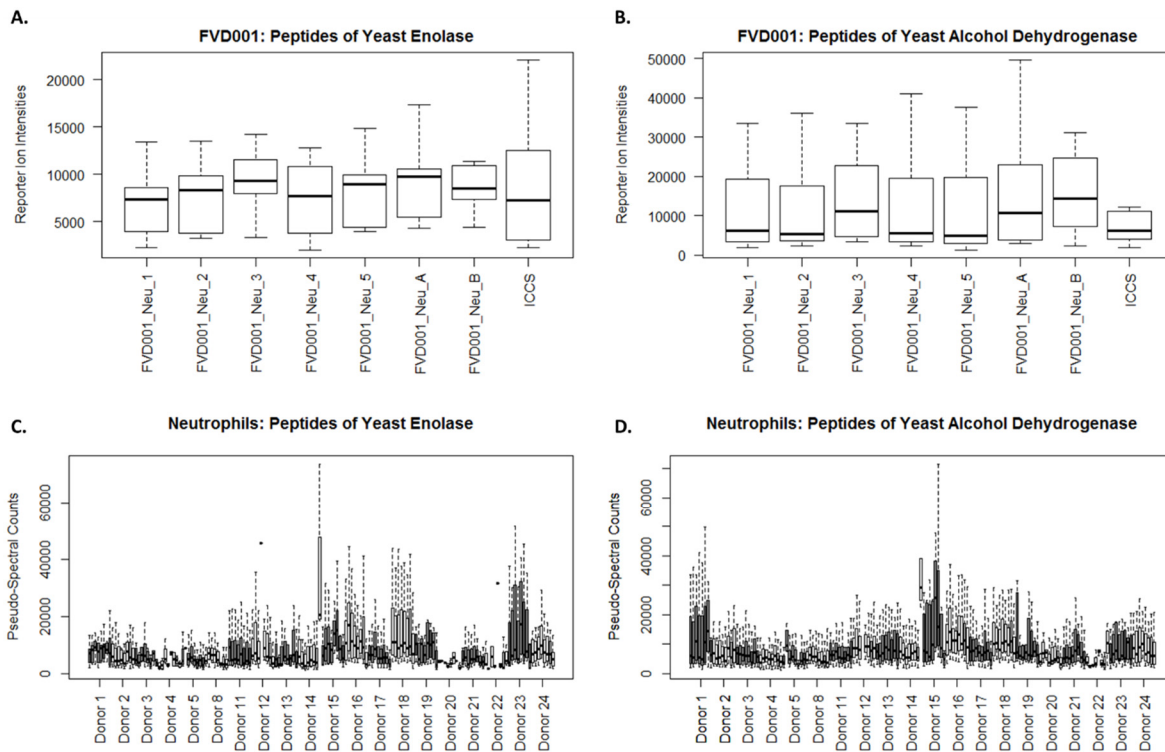


**Figure B-10 Boxplots assessing response of internal standard yeast proteins.** The reporter ion intensities of the individual peptides of (A) yeast enolase and (B) yeast alcohol dehydrogenase were plotted for each individual sample. Similarly, the pseudo-spectral counts on the protein level of (C) yeast enolase and (D) yeast alcohol dehydrogenase were compared to identify any inconsistent experiments or samples

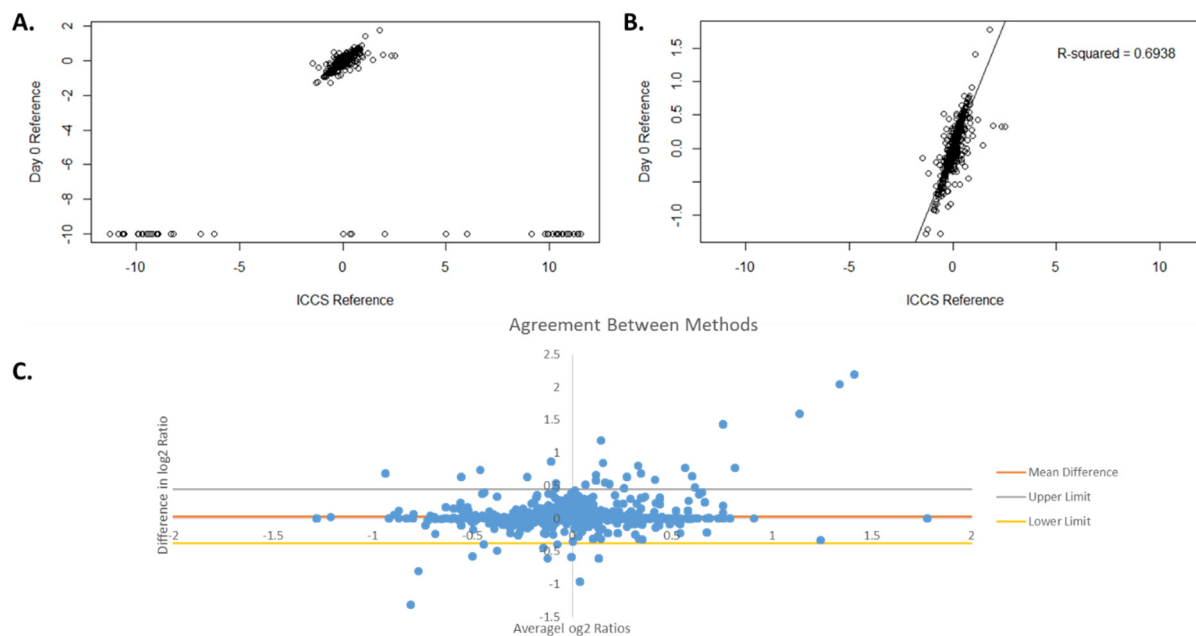


**Figure B-11 Comparison of peptide normalization methods.** (A) Exported log<sub>2</sub> ratios from an experiment using Day 0 as reference versus ICCS as reference showing that there were more peptides quantified when ICCS was the reference. ProteoIQ uses values of -10 when quantifications cannot be made. (B) Zoomed in plot of the cluster from (A) with a linear regression showing the moderate correlation between the methods. (C) Bland-Altman plot assessing the agreement between the two methods. Each point represents a protein. The mean value (bias) was slightly increased from 0. The upper and lower limits were defined as the second standard deviations from the mean of the difference between methods.

**Table B-1 Differentially abundant proteins for B cells at Day 1.** Proteins with the same ICCS-ratio were grouped together and represented by the longest protein in the group. \*mean baseline log<sub>2</sub> fold change.

Protein ID	Gene ID	Gene Name	Log2 Fold Change	z-statistic	P	Mean [N] (AS03)*	Mean [N] (PBS)*
ENSP00000408986	ENSG00000231834	HLA-A	0.7073	2.78929	0.0008	0.28 [8]	-0.43 [7]
ENSP00000410645	ENSG00000223980	HLA-A	0.7073	2.78929	0.0008	0.28 [8]	-0.43 [7]
ENSP00000390282	ENSG00000237022	HLA-C	0.5543	2.76956	0.003	0.16 [8]	-0.39 [7]
ENSP00000433363	ENSG00000206450	HLA-B	0.5601	2.70912	0.0006	0.21 [7]	-0.35 [7]
ENSP00000411954	ENSG00000206450	HLA-B	0.4905	2.67166	0.0006	0.17 [7]	-0.32 [7]
ENSP00000388526	ENSG00000235657	HLA-A	0.5056	2.64343	0.0053	0.2 [8]	-0.3 [9]
ENSP00000352656	ENSG00000206450	HLA-B	0.5395	2.63203	0.0006	0.19 [7]	-0.35 [7]
ENSP00000373114	ENSG00000206505	HLA-A	0.4218	2.61053	0.0065	0.22 [8]	-0.2 [7]
ENSP00000407494	ENSG00000237022	HLA-C	0.4886	2.57666	0.0061	0.1 [8]	-0.39 [7]
ENSP00000430420	ENSG00000197043	ANXA6	0.575	2.53443	0.0048	0.26 [8]	-0.32 [8]
ENSP00000397867	ENSG00000228299	HLA-C	0.5173	2.52548	0.0059	0.19 [8]	-0.33 [7]
ENSP00000391250	ENSG00000228299	HLA-C	0.5311	2.46462	0.0076	0.2 [7]	-0.33 [7]
ENSP00000400410	ENSG00000204525	HLA-C	0.5311	2.46462	0.0076	0.2 [7]	-0.33 [7]
ENSP00000366002	ENSG00000206503	HLA-A	0.6111	2.43126	0.004	0.3 [8]	-0.31 [7]
ENSP00000377958	ENSG00000115484	CCT4	0.3217	2.42337	0.0087	0.12 [8]	-0.21 [8]
ENSP00000403679	ENSG00000196419	XRCC6	0.7217	2.37822	0.0108	0.17 [6]	-0.56 [6]
ENSP00000392235	ENSG00000232126	HLA-B	0.3697	2.34576	0.0154	0.2 [8]	-0.17 [7]
ENSP00000463482	ENSG00000265434	HLA-ABC	0.5358	2.32412	0.0095	0.31 [8]	-0.23 [7]
ENSP00000407431	ENSG00000225691	HLA-C	0.4304	2.31709	0.0159	0.26 [8]	-0.17 [7]
ENSP00000449958	ENSG00000111144	LTA4H	0.4526	2.30571	0.0179	0.08 [3]	-0.37 [5]
ENSP00000388208	ENSG00000232126	HLA-B	0.3517	2.29162	0.0183	0.18 [8]	-0.17 [7]
ENSP00000364805	ENSG00000204390	HSPA1L	-1.3723	-2.27956	0.0286	-0.46 [4]	0.92 [3]
ENSP00000366980	ENSG00000197043	ANXA6	0.537	2.27011	0.0112	0.28 [8]	-0.26 [8]
ENSP00000359338	ENSG00000122406	RPL5	0.8482	2.25378	0.0159	0.1 [5]	-0.75 [5]
ENSP00000339001	ENSG00000196230	TUBB	-0.3182	-2.2245	0.0199	-0.03 [8]	0.29 [9]
ENSP00000372819	ENSG00000204525	HLA-C	0.4097	2.20802	0.023	0.17 [8]	-0.24 [9]
ENSP00000413992	ENSG00000233841	HLA-C	0.4097	2.20802	0.023	0.17 [8]	-0.24 [9]
ENSP00000372975	ENSG00000206435	HLA-C	0.4153	2.20053	0.0163	0.16 [8]	-0.26 [7]
ENSP00000293422	ENSG00000092841	MYL6	0.5224	2.19505	0.0169	0.01 [7]	-0.51 [6]
ENSP00000408052	ENSG00000136167	LCP1	-0.7035	-2.16541	0.0269	-0.1 [8]	0.6 [7]
ENSP00000298510	ENSG00000165672	PRDX3	0.4812	2.14585	0.0204	0.1 [7]	-0.38 [7]
ENSP00000252699	ENSG00000130402	ACTN4	-1.539	-2.12455	0.0265	-0.11 [7]	1.43 [5]
ENSP00000364801	ENSG00000204388	HSPA1B	-1.2342	-2.11092	0.0286	-0.44 [4]	0.79 [3]
ENSP00000257860	ENSG00000135406	PRPH	0.6258	2.06843	0.0362	0.23 [8]	-0.39 [8]
ENSP00000412426	ENSG00000225691	HLA-C	0.3325	2.05225	0.037	0.16 [8]	-0.17 [7]
ENSP00000431347	ENSG00000237022	HLA-C	0.3824	2.03957	0.0354	0.19 [8]	-0.19 [7]
ENSP00000362413	ENSG00000102144	PGK1	0.6227	2.00961	0.0305	0.46 [9]	-0.16 [8]
ENSP00000444708	ENSG00000102144	PGK1	0.6227	2.00961	0.0305	0.46 [9]	-0.16 [8]
ENSP00000349410	ENSG00000115053	NCL	0.3556	1.99868	0.0407	0.15 [9]	-0.21 [9]
ENSP00000410661	ENSG00000206452	HLA-C	0.3461	1.99458	0.0268	0.09 [7]	-0.26 [7]
ENSP00000260356	ENSG00000137801	THBS1	-2.3392	-1.98503	0.0022	-1.35 [6]	0.99 [5]
ENSP00000452254	ENSG00000072110	ACTN1	1.0923	1.9814	0.0357	0.35 [6]	-0.75 [3]
ENSP00000448239	ENSG00000229215	HLA-A	0.3681	1.97925	0.0421	0.18 [8]	-0.19 [7]
ENSP00000441750	ENSG00000092841	MYL6	0.4542	1.95809	0.0385	0.01 [7]	-0.44 [6]
ENSP00000446721	ENSG00000092841	MYL6	0.4542	1.95809	0.0385	0.01 [7]	-0.44 [6]
ENSP00000463939	ENSG00000141522	ARHGDI A	-1.0176	-1.87746	0.0286	-0.92 [3]	0.09 [4]
ENSP00000461956	ENSG00000141522	ARHGDI A	-1.0176	-1.87746	0.0286	-0.92 [3]	0.09 [4]

**Table B-2 Differentially abundant proteins for B cells at Day 3.** Proteins with the same ICCS-ratio were grouped together and represented by the longest protein in the group. \*mean baseline log<sub>2</sub> fold change.

Protein ID	Gene ID	Gene Name	Log2 Fold Change	z-statistic	P	Mean [N] (AS03)*	Mean [N] (PBS)*
ENSP00000346550	ENSG00000197043	ANXA6	0.4065	3.11319	0.0005	0.29 [9]	-0.12 [8]
ENSP00000430517	ENSG00000197043	ANXA6	0.4065	3.11319	0.0005	0.29 [9]	-0.12 [8]
ENSP00000348889	ENSG00000197043	ANXA6	0.3741	2.93086	0.0014	0.29 [9]	-0.09 [8]
ENSP00000430420	ENSG00000197043	ANXA6	0.412	2.89567	0.0006	0.19 [8]	-0.22 [8]
ENSP00000366980	ENSG00000197043	ANXA6	0.3427	2.46452	0.0107	0.2 [8]	-0.14 [8]
ENSP00000410645	ENSG00000223980	HLA-A	0.5046	2.44955	0.006	0.3 [9]	-0.21 [8]
ENSP00000388526	ENSG00000235657	HLA-A	0.344	2.44792	0.0094	0.21 [9]	-0.14 [8]
ENSP00000408986	ENSG00000231834	HLA-A	0.5039	2.44749	0.006	0.3 [9]	-0.2 [8]
ENSP00000330054	ENSG00000156508	EEF1A1	-0.755	-2.36715	0.0159	-0.59 [4]	0.17 [5]
ENSP00000217182	ENSG00000101210	EEF1A2	-0.755	-2.36715	0.0159	-0.59 [4]	0.17 [5]
ENSP00000390282	ENSG00000237022	HLA-C	0.4061	2.27519	0.0158	0.19 [9]	-0.22 [8]
ENSP00000447571	ENSG00000110955	ATP5B	-0.3447	-2.27181	0.0194	0.02 [10]	0.36 [8]
ENSP00000253024	ENSG00000130726	TRIM28	0.5507	2.25803	0.013	0.48 [6]	-0.08 [5]
ENSP00000298510	ENSG00000165672	PRDX3	0.3486	2.23207	0.0221	0.13 [7]	-0.22 [7]
ENSP00000365439	ENSG00000165119	HNRNPK	-0.8702	-2.22366	0.0286	-0.33 [4]	0.54 [4]
ENSP00000386743	ENSG00000014641	MDH1	0.4307	2.19144	0.0265	0.2 [5]	-0.24 [7]
ENSP00000446395	ENSG00000014641	MDH1	0.3984	2.17818	0.0278	0.2 [5]	-0.2 [7]
ENSP00000366002	ENSG00000206503	HLA-A	0.4861	2.1777	0.0216	0.37 [9]	-0.12 [7]
ENSP00000276079	ENSG00000147140	NONO	0.3883	2.11647	0.0316	0.39 [5]	0 [7]
ENSP00000409773	ENSG00000147140	NONO	0.3883	2.11647	0.0316	0.39 [5]	0 [7]
ENSP00000441364	ENSG00000147140	NONO	0.3883	2.11647	0.0316	0.39 [5]	0 [7]
ENSP00000464042	ENSG00000108424	KPNB1	0.2955	2.11637	0.0309	0.12 [7]	-0.17 [7]
ENSP00000327054	ENSG00000176619	LMNB2	-0.8584	-2.09801	0.0286	-0.3 [4]	0.56 [6]
ENSP00000431086	ENSG00000197043	ANXA6	0.5696	2.09283	0.0397	0.3 [4]	-0.27 [5]
ENSP00000391481	ENSG00000163931	TKT	-0.5798	-2.06549	0.0286	-0.17 [4]	0.4 [6]
ENSP00000286788	ENSG00000156261	CCT8	0.4101	2.0442	0.0364	0.25 [7]	-0.16 [4]
ENSP00000302935	ENSG00000172349	IL16	0.8634	2.03361	0.0286	0.58 [4]	-0.28 [4]
ENSP00000441750	ENSG00000092841	MYL6	0.4417	2.01354	0.0392	0.03 [7]	-0.41 [8]
ENSP00000446721	ENSG00000092841	MYL6	0.4417	2.01354	0.0392	0.03 [7]	-0.41 [8]
ENSP00000265462	ENSG00000126432	PRDX5	0.9914	2.00997	0.0238	0.27 [4]	-0.72 [5]
ENSP00000335334	ENSG00000126432	PRDX5	0.9914	2.00997	0.0238	0.27 [4]	-0.72 [5]
ENSP00000342232	ENSG00000130726	TRIM28	0.5497	2.00585	0.0411	0.39 [6]	-0.16 [5]
ENSP00000471303	ENSG00000130726	TRIM28	0.5497	2.00585	0.0411	0.39 [6]	-0.16 [5]
ENSP00000422615	ENSG00000138668	HNRNPD	0.3642	2.00538	0.0325	0.16 [5]	-0.2 [6]
ENSP00000463482	ENSG00000265434	HLA-ABC	0.3945	1.97131	0.0393	0.38 [9]	-0.02 [7]
ENSP00000409456	ENSG00000165119	HNRNPK	-0.9247	-1.95257	0.0286	-0.39 [3]	0.54 [4]
ENSP00000407431	ENSG00000225691	HLA-C	0.3412	1.92161	0.0477	0.29 [9]	-0.05 [7]
ENSP00000466406	ENSG00000074800	ENO1	0.3226	1.91022	0.0497	0.12 [9]	-0.2 [8]
ENSP00000434565	ENSG00000109971	HSPA8	-0.9648	-1.903	0.0476	-0.52 [6]	0.44 [3]
ENSP00000244573	ENSG00000124610	HIST1H1A	-0.906	-1.82175	0.0286	-0.83 [4]	0.07 [3]
ENSP00000341214	ENSG00000187475	HIST1H1T	-0.906	-1.82175	0.0286	-0.83 [4]	0.07 [3]

**Table B-3 Differentially abundant proteins for B cells at Day 7.** Proteins with the same ICCS-ratio were grouped together and represented by the longest protein in the group. \*mean baseline log<sub>2</sub> fold change.

Protein ID	Gene ID	Gene Name	Log2 Fold Change	z-statistic	P	Mean [N] (AS03)*	Mean [N] (PBS)*
ENSP00000344419	ENSG00000005381	MPO	0.8393	2.56217	0.0054	0.51 [6]	-0.33 [9]
ENSP00000446489	ENSG00000110955	ATP5B	-0.3238	-2.36343	0.0124	-0.06 [9]	0.26 [9]
ENSP00000219169	ENSG00000102898	NUTF2	-0.3975	-2.27857	0.0238	-0.33 [4]	0.07 [5]
ENSP00000293422	ENSG00000092841	MYL6	0.5626	2.17634	0.0228	0.06 [7]	-0.5 [9]
ENSP00000318697	ENSG00000176014	TUBB6	0.3592	2.16016	0.0177	0.05 [7]	-0.31 [5]
ENSP00000366002	ENSG00000206503	HLA-A	0.3386	2.13432	0.0297	0.16 [8]	-0.18 [8]
ENSP00000457420	ENSG00000067225	PKM	-0.4576	-2.1284	0.0313	-0.28 [9]	0.18 [7]
ENSP00000456984	ENSG00000067225	PKM	-0.5331	-2.11319	0.0274	-0.27 [9]	0.26 [7]
ENSP00000464359	ENSG00000101608	MYL12A	0.6255	2.10308	0.0306	0.42 [9]	-0.2 [10]
ENSP00000441750	ENSG00000092841	MYL6	0.5171	2.10227	0.0267	0.06 [7]	-0.46 [9]
ENSP00000446721	ENSG00000092841	MYL6	0.5171	2.10227	0.0267	0.06 [7]	-0.46 [9]
ENSP00000311042	ENSG00000173876	TUBB8	0.3636	2.08068	0.03	0.02 [8]	-0.34 [6]
ENSP00000451560	ENSG00000198211	TUBB3	0.4552	2.04531	0.0324	0.08 [7]	-0.37 [10]
ENSP00000408897	ENSG00000135406	PRPH	0.6509	1.98579	0.0455	-0.03 [7]	-0.69 [7]
ENSP00000447571	ENSG00000110955	ATP5B	-0.3097	-1.98236	0.0438	0.01 [9]	0.32 [9]
ENSP00000259818	ENSG00000137285	TUBB2B	0.4318	1.98137	0.0392	0.06 [7]	-0.37 [10]
ENSP00000252699	ENSG00000130402	ACTN4	-0.5388	-1.97812	0.0455	-0.17 [7]	0.37 [6]
ENSP00000324173	ENSG00000044574	HSPA5	0.5063	1.96433	0.0476	0.13 [5]	-0.38 [5]
ENSP00000439497	ENSG00000130402	ACTN4	-0.4252	-1.89806	0.0286	-0.12 [7]	0.3 [6]
ENSP00000369475	ENSG00000057608	GD12	-0.3427	-1.89183	0.046	-0.16 [7]	0.19 [7]
ENSP00000369528	ENSG00000057608	GD12	-0.3427	-1.89183	0.046	-0.16 [7]	0.19 [7]
ENSP00000408649	ENSG00000146701	MDH2	0.3102	1.88932	0.0381	-0.17 [4]	-0.48 [6]

**Table B-4 Differentially abundant proteins from B cells at Day 28.** Proteins with the same ICCS-ratio were grouped together and represented by the longest protein in the group. \*mean baseline log<sub>2</sub> fold change.

Protein ID	Gene ID	Gene Name	Log2 Fold Change	z-statistic	P	Mean [N] (AS03)*	Mean [N] (PBS)*
ENSP00000391842	ENSG00000026025	VIM	0.5545	2.33097	0.0054	0.44 [8]	-0.12 [8]
ENSP00000392541	ENSG00000163631	ALB	-1.619	-2.3264	0.0238	-0.18 [5]	1.44 [5]
ENSP00000341826	ENSG00000135486	HNRNPA1	0.6443	2.28261	0.0176	0.08 [7]	-0.57 [8]
ENSP00000287613	ENSG00000241553	ARPC4	-0.4291	-2.27666	0.0117	-0.18 [7]	0.25 [7]
ENSP00000416551	ENSG00000164924	YWHAZ	-0.7209	-2.24514	0.0211	-0.31 [7]	0.41 [8]
ENSP00000301522	ENSG00000167815	PRDX2	-0.4627	-2.20657	0.0256	-0.42 [7]	0.04 [7]
ENSP00000380033	ENSG00000100201	DDX17	-0.6019	-2.10303	0.0179	-0.13 [5]	0.47 [3]
ENSP00000219169	ENSG00000102898	NUTF2	0.4392	2.07719	0.0333	-0.1 [6]	-0.54 [4]
ENSP00000339001	ENSG00000196230	TUBB	-0.5617	-2.07438	0.0353	0.17 [9]	0.73 [8]
ENSP00000439189	ENSG00000188219	POTEE	0.6508	2.06758	0.0344	0.16 [9]	-0.49 [8]
ENSP00000350052	ENSG00000196604	POTEF	0.6473	2.05982	0.035	0.15 [9]	-0.5 [8]
ENSP00000464265	ENSG00000263563	UBBP4	-0.8152	-1.97507	0.0384	-0.57 [8]	0.24 [8]
ENSP00000272317	ENSG00000143947	RPS27A	-0.7723	-1.95436	0.0435	-0.52 [8]	0.25 [8]
ENSP00000379278	ENSG00000164924	YWHAZ	1.1055	1.95041	0.0303	0.26 [6]	-0.85 [5]
ENSP00000289352	ENSG00000158406	HIST1H4H	-0.5368	-1.95034	0.0486	-0.24 [9]	0.3 [8]
ENSP00000327054	ENSG00000176619	LMNB2	-0.6382	-1.93765	0.0159	-0.35 [4]	0.29 [5]
ENSP00000297185	ENSG00000113013	HSPA9	-0.3109	-1.93733	0.0179	-0.05 [5]	0.27 [3]
ENSP00000312206	ENSG00000186442	KRT3	-1.2285	-1.91181	0.0397	-1.08 [5]	0.15 [5]
ENSP00000330101	ENSG00000185069	KRT76	-1.2285	-1.91181	0.0397	-1.08 [5]	0.15 [5]
ENSP00000457332	ENSG00000102879	CORO1A	-0.6441	-1.90263	0.0495	-0.51 [7]	0.13 [7]

**Table B-5 Differentially abundant proteins from monocytes cells at Day 1.** Proteins with the same ICCS-ratio were grouped together and represented by the longest protein in the group. \*mean baseline log<sub>2</sub> fold change.

Protein ID	Gene ID	Gene Name	Log2 Fold Change	z-statistic	P	Mean [N] (AS03)*	Mean [N] (PBS)*
ENSP00000444467	ENSG00000127314	RAP1B	0.3222	2.73613	0.002	0.21 [9]	-0.11 [10]
ENSP00000385385	ENSG00000143870	PDIA6	0.2653	2.6592	0.0048	0.31 [8]	0.05 [10]
ENSP00000399986	ENSG00000127314	RAP1B	0.3307	2.5679	0.0064	0.27 [9]	-0.06 [10]
ENSP00000250559	ENSG00000127314	RAP1B	0.3303	2.56548	0.0065	0.27 [9]	-0.06 [10]
ENSP00000440014	ENSG00000127314	RAP1B	0.3303	2.56548	0.0065	0.27 [9]	-0.06 [10]
ENSP00000450353	ENSG00000257767	RP11-162P23.2	-0.2933	-2.46851	0.0104	-0.17 [7]	0.12 [8]
ENSP00000364801	ENSG00000204388	HSPA1B	0.284	2.39722	0.0123	0.14 [9]	-0.14 [10]
ENSP00000450538	ENSG00000258947	TUBB3	0.8022	2.35603	0.0098	0.57 [4]	-0.23 [9]
ENSP00000471786	ENSG00000130755	GMFG	0.3332	2.34175	0.0179	0.28 [3]	-0.05 [5]
ENSP00000310749	ENSG00000115756	HPCAL1	0.4947	2.33916	0.0179	0.35 [3]	-0.15 [5]
ENSP00000464668	ENSG00000005381	MPO	0.3105	2.33496	0.0138	0.24 [9]	-0.07 [10]
ENSP00000348786	ENSG00000116473	RAP1A	0.3204	2.32094	0.0166	0.27 [9]	-0.05 [10]
ENSP00000367615	ENSG00000198931	APRT	-0.3788	-2.30383	0.0114	-0.19 [5]	0.19 [7]
ENSP00000467932	ENSG00000171403	KRT9	0.9348	2.29994	0.0179	-0.06 [5]	-0.99 [3]
ENSP00000216962	ENSG00000100994	PYGB	-0.3854	-2.2957	0.0175	-0.17 [7]	0.22 [7]
ENSP00000455692	ENSG00000198931	APRT	-0.3741	-2.29467	0.0114	-0.19 [5]	0.18 [7]
ENSP00000460612	ENSG00000185624	P4HB	-0.3925	-2.27504	0.0145	-0.41 [9]	-0.02 [10]
ENSP00000455749	ENSG00000198931	APRT	-0.2876	-2.26845	0.0212	-0.1 [4]	0.18 [7]
ENSP00000356022	ENSG00000112096	SOD2	0.3923	2.23937	0.0174	0.32 [9]	-0.07 [9]
ENSP00000434565	ENSG00000109971	HSPA8	0.3659	2.23833	0.0203	0.05 [8]	-0.32 [10]
ENSP00000460741	ENSG00000185624	P4HB	-0.6968	-2.23562	0.0022	-0.65 [5]	0.05 [6]
ENSP00000337127	ENSG00000112096	SOD2	0.3804	2.22951	0.0179	0.37 [9]	-0.01 [9]
ENSP00000252029	ENSG00000025708	TYMP	0.2988	2.20491	0.0202	0.21 [7]	-0.09 [8]
ENSP00000298283	ENSG00000165496	RPL10L	0.8138	2.2031	0.0286	0.42 [4]	-0.39 [4]
ENSP00000327589	ENSG00000182890	GLUD2	-0.472	-2.17842	0.0238	-0.18 [5]	0.29 [4]
ENSP00000379038	ENSG00000025708	TYMP	0.2924	2.16845	0.0242	0.23 [7]	-0.06 [8]
ENSP00000287613	ENSG00000241553	ARPC4	0.3063	2.16014	0.0264	0.15 [9]	-0.15 [10]
ENSP00000398632	ENSG00000026508	CD44	0.4384	2.15912	0.0233	0.29 [8]	-0.15 [8]
ENSP00000216336	ENSG00000100448	CTSG	0.3307	2.15593	0.0241	0.25 [9]	-0.09 [10]
ENSP00000341136	ENSG00000147813	NAPRT1	0.4505	2.14563	0.0238	0.28 [6]	-0.17 [6]
ENSP00000246662	ENSG00000171403	KRT9	0.7412	2.1023	0.0238	-0.02 [5]	-0.76 [4]
ENSP00000277865	ENSG00000148672	GLUD1	-0.4252	-2.07638	0.028	-0.26 [6]	0.16 [7]
ENSP00000369475	ENSG00000057608	GDI2	-0.3286	-2.06098	0.0269	-0.26 [9]	0.07 [10]
ENSP00000369528	ENSG00000057608	GDI2	-0.3286	-2.06098	0.0269	-0.26 [9]	0.07 [10]
ENSP00000400882	ENSG00000256812	CAPNS2	0.5975	2.03693	0.0333	0.1 [4]	-0.5 [6]
ENSP00000403260	ENSG00000137752	CASP1	0.3021	2.03152	0.0339	0.23 [9]	-0.07 [8]
ENSP00000408649	ENSG00000146701	MDH2	-0.3035	-2.02767	0.037	-0.19 [8]	0.12 [10]
ENSP00000468041	ENSG00000126247	CAPNS1	0.5156	2.0266	0.0433	0.02 [5]	-0.5 [6]
ENSP00000344871	ENSG00000142347	MYO1F	0.3072	2.01814	0.0199	0.23 [9]	-0.08 [10]
ENSP00000474036	ENSG00000126247	CAPNS1	0.5785	2.00258	0.0333	0.1 [4]	-0.48 [6]
ENSP00000303276	ENSG00000169385	RNASE2	0.3807	1.98863	0.0449	0.16 [7]	-0.22 [6]
ENSP00000467670	ENSG00000105220	GPI	0.401	1.98392	0.0444	0.42 [9]	0.02 [9]
ENSP00000465858	ENSG00000105220	GPI	0.3872	1.97961	0.0454	0.41 [9]	0.02 [9]
ENSP00000337448	ENSG00000119383	PPP2R4	0.3159	1.97603	0.0366	0.23 [5]	-0.08 [7]
ENSP00000446415	ENSG00000134333	LDHA	0.3857	1.97198	0.0286	0.32 [3]	-0.07 [4]
ENSP00000433443	ENSG00000177600	RPLP2	0.4295	1.96727	0.0338	0.26 [7]	-0.17 [7]
ENSP00000389906	ENSG00000167004	PDIA3	0.4767	1.71624	0.0238	0.2 [4]	-0.27 [5]

**Table B-6 Differentially abundant proteins from monocytes cells at Day 3.** Proteins with the same ICCS-ratio were grouped together and represented by the longest protein in the group. \*mean baseline log<sub>2</sub> fold change.

Protein ID	Gene ID	Gene Name	Log2 Fold Change	z-statistic	P	Mean [N] (AS03)*	Mean [N] (PBS)*
ENSP00000373114	ENSG00000206505	HLA-A	0.3723	2.77873	0.0014	0.32 [10]	-0.06 [9]
ENSP00000349748	ENSG00000116560	SFPQ	0.5827	2.76377	0.0048	0.2 [6]	-0.39 [4]
ENSP00000475260	ENSG00000268548	TPH1	-0.3991	-2.6657	0.0037	-0.16 [10]	0.24 [9]
ENSP00000228318	ENSG00000075415	SLC25A3	0.4227	2.60471	0.0041	0.08 [7]	-0.35 [6]
ENSP00000206451	ENSG00000092010	PSME1	0.4581	2.60047	0.0028	0.39 [9]	-0.07 [9]
ENSP00000450538	ENSG00000258947	TUBB3	0.8854	2.58245	0.0023	0.44 [5]	-0.45 [8]
ENSP00000412429	ENSG00000158710	TAGLN2	0.3133	2.5787	0.0049	0.21 [10]	-0.11 [9]
ENSP00000216802	ENSG00000100911	PSME2	0.4113	2.56524	0.0071	0.3 [10]	-0.11 [9]
ENSP00000436277	ENSG00000137710	RDX	0.3872	2.53423	0.0087	0.17 [8]	-0.22 [6]
ENSP00000357076	ENSG00000158710	TAGLN2	0.307	2.50769	0.0073	0.2 [10]	-0.11 [9]
ENSP00000444467	ENSG00000127314	RAP1B	0.3021	2.47581	0.0081	0.13 [10]	-0.18 [9]
ENSP00000391481	ENSG00000163931	TKT	0.2951	2.4581	0.0091	0.07 [10]	-0.22 [9]
ENSP00000417864	ENSG00000140350	ANP32A	0.4417	2.45402	0.0037	0.35 [10]	-0.09 [9]
ENSP00000295685	ENSG00000163466	ARPC2	0.3171	2.44811	0.0069	0.07 [10]	-0.25 [8]
ENSP00000443599	ENSG00000111669	TPH1	-0.3831	-2.43927	0.0097	-0.15 [10]	0.23 [9]
ENSP00000299767	ENSG00000166598	HSP90B1	0.4754	2.41857	0.0086	0.2 [9]	-0.27 [8]
ENSP00000296181	ENSG00000082781	ITGB5	0.3684	2.40465	0.0082	0.09 [10]	-0.28 [9]
ENSP00000280326	ENSG00000150753	CCT5	-0.4373	-2.37248	0.0117	-0.16 [8]	0.27 [6]
ENSP00000426923	ENSG00000150753	CCT5	-0.4373	-2.37248	0.0117	-0.16 [8]	0.27 [6]
ENSP00000423318	ENSG00000150753	CCT5	-0.4672	-2.3598	0.0123	-0.19 [8]	0.27 [6]
ENSP00000423052	ENSG00000150753	CCT5	-0.4672	-2.3598	0.0123	-0.19 [8]	0.27 [6]
ENSP00000365439	ENSG00000165119	HNRNPK	0.48	2.3596	0.0139	0.2 [10]	-0.28 [7]
ENSP00000366002	ENSG00000206503	HLA-A	0.3415	2.35591	0.0132	0.29 [10]	-0.05 [9]
ENSP00000463482	ENSG00000265434	HLA-ABC	0.3408	2.32685	0.0145	0.3 [10]	-0.04 [9]
ENSP00000441556	ENSG00000150991	UBC	0.2785	2.32602	0.0137	0.17 [8]	-0.11 [6]
ENSP00000325905	ENSG00000115875	SRSF7	0.4814	2.30605	0.0065	0.33 [5]	-0.15 [6]
ENSP00000344871	ENSG00000142347	MYO1F	0.3353	2.26809	0.0196	0.28 [10]	-0.05 [9]
ENSP00000475184	ENSG00000111669	TPH1	-0.3066	-2.25173	0.0175	-0.07 [10]	0.24 [9]
ENSP00000420213	ENSG00000136068	FLNB	0.4518	2.23644	0.0162	0.12 [7]	-0.33 [8]
ENSP00000343027	ENSG00000127955	GNAI1	-0.4598	-2.22209	0.0286	-0.26 [4]	0.2 [4]
ENSP00000429374	ENSG00000008988	RPS20	-0.3586	-2.1927	0.0303	-0.05 [8]	0.31 [3]
ENSP00000226299	ENSG00000002549	LAP3	0.3863	2.18813	0.0246	0.44 [10]	0.06 [9]
ENSP00000442285	ENSG00000142657	PGD	0.2683	2.18268	0.0248	-0.09 [10]	-0.36 [9]
ENSP00000473957	ENSG00000165119	HNRNPK	0.7156	2.17693	0.026	0.24 [5]	-0.48 [6]
ENSP00000450121	ENSG00000089157	RPLP0	-0.2953	-2.15646	0.0119	-0.43 [6]	-0.14 [3]
ENSP00000379038	ENSG00000025708	TYMP	0.3961	2.15537	0.026	0.44 [8]	-0.05 [8]
ENSP00000303476	ENSG00000171914	TLN2	0.3402	2.10115	0.022	0.15 [8]	-0.19 [6]
ENSP00000344666	ENSG00000186575	NF2	0.3768	2.10033	0.0381	0.25 [6]	-0.13 [4]
ENSP00000299427	ENSG00000166340	TPP1	0.3351	2.08515	0.0309	0.2 [9]	-0.14 [9]
ENSP00000410572	ENSG00000127955	GNAI1	-0.3953	-2.06718	0.0286	-0.2 [3]	0.2 [4]
ENSP00000398632	ENSG00000026508	CD44	0.3551	2.0612	0.0357	0.12 [8]	-0.23 [8]
ENSP00000270625	ENSG00000142534	RPS11	0.429	2.05523	0.025	0.14 [7]	-0.29 [3]
ENSP00000387286	ENSG00000138069	RAB1A	-0.5775	-2.04975	0.0357	-0.28 [6]	0.29 [3]
ENSP00000472137	ENSG00000221983	UBA52	0.4032	2.04864	0.0068	0.17 [8]	-0.24 [7]
ENSP00000428208	ENSG00000131504	DIAPH1	-0.3077	-2.03963	0.0238	-0.18 [6]	0.13 [5]
ENSP00000230050	ENSG00000112306	RPS12	0.3751	2.03733	0.0382	0.11 [10]	-0.27 [9]
ENSP00000310226	ENSG00000174903	RAB1B	-0.5708	-2.03638	0.0357	-0.28 [6]	0.29 [3]
ENSP00000264710	ENSG00000084733	RAB10	-0.3504	-2.02108	0.0364	0.02 [7]	0.37 [4]
ENSP00000348546	ENSG00000138069	RAB1A	-0.5717	-2.02072	0.0357	-0.28 [6]	0.29 [3]
ENSP00000435195	ENSG00000174903	RAB1B	-0.565	-2.00747	0.0357	-0.27 [6]	0.29 [3]
ENSP00000396397	ENSG00000228964	HLA-B	0.3539	1.98366	0.0429	0.21 [8]	-0.14 [7]
ENSP00000463939	ENSG00000141522	ARHGDI	0.2838	1.98314	0.0416	0.04 [8]	-0.24 [9]
ENSP00000461956	ENSG00000141522	ARHGDI	0.2838	1.98314	0.0416	0.04 [8]	-0.24 [9]
ENSP00000431078	ENSG00000197043	ANXA6	0.3794	1.95532	0.0322	0.03 [9]	-0.35 [4]
ENSP00000298556	ENSG00000165704	HPRT1	-0.2656	-1.95154	0.0476	-0.13 [6]	0.13 [4]
ENSP00000361878	ENSG00000131236	CAP1	0.3348	1.94592	0.0406	0.12 [9]	-0.22 [9]
ENSP00000468041	ENSG00000126247	CAPNS1	0.2712	1.80847	0.0476	-0.16 [6]	-0.43 [6]
ENSP00000362409	ENSG00000136830	FAM129B	0.3373	1.76892	0.0476	0.48 [7]	0.14 [8]
ENSP00000217426	ENSG00000101444	AHCY	-0.4336	-1.64293	0.0152	-0.16 [5]	0.27 [6]



**Table B-7 Differentially abundant proteins from monocytes at Day 7.** Proteins with the same ICCS-ratio were grouped together and represented by the longest protein in the group. \*mean baseline log<sub>2</sub> fold change.

Protein ID	Gene ID	Gene Name	Log2 Fold Change	z-statistic	P	Mean [N] (AS03)*	Mean [N] (PBS)*
ENSP00000466574	ENSG00000142657	PGD	0.281	2.74065	0.0017	0 [9]	-0.28 [9]
ENSP00000466358	ENSG00000142657	PGD	0.2984	2.68614	0.0029	0.01 [10]	-0.29 [9]
ENSP00000450538	ENSG00000258947	TUBB3	0.7249	2.66224	0.0016	0.45 [5]	-0.27 [8]
ENSP00000397533	ENSG00000089820	ARHGAP4	-0.419	-2.54128	0.0064	-0.1 [6]	0.31 [7]
ENSP00000434565	ENSG00000109971	HSPA8	-0.3093	-2.5307	0.008	-0.45 [10]	-0.15 [10]
ENSP00000464359	ENSG00000101608	MYL12A	0.2868	2.48336	0.0105	-0.11 [10]	-0.4 [10]
ENSP00000456865	ENSG00000198848	CES1	-0.4919	-2.48095	0.0119	-0.2 [3]	0.29 [6]
ENSP00000428916	ENSG00000197043	ANXA6	-0.31	-2.38291	0.0134	-0.17 [9]	0.14 [7]
ENSP00000279227	ENSG00000149781	FERMT3	-0.3926	-2.37424	0.0079	-0.18 [10]	0.21 [10]
ENSP00000447068	ENSG00000197111	PCBP2	0.4153	2.33786	0.0065	-0.17 [5]	-0.58 [6]
ENSP00000305556	ENSG00000169564	PCBP1	0.5279	2.2875	0.0134	0.18 [7]	-0.35 [7]
ENSP00000432153	ENSG00000172757	CFL1	0.3889	2.21989	0.0186	-0.04 [8]	-0.43 [5]
ENSP00000401820	ENSG00000163631	ALB	0.5148	2.19295	0.0261	0.45 [9]	-0.06 [10]
ENSP00000247470	ENSG00000103490	PYCARD	0.5167	2.17885	0.0357	0.36 [3]	-0.16 [5]
ENSP00000405325	ENSG00000148834	GSTO1	-0.5195	-2.17467	0.0022	-0.42 [9]	0.09 [8]
ENSP00000441488	ENSG00000148834	GSTO1	-0.5195	-2.17467	0.0022	-0.42 [9]	0.09 [8]
ENSP00000211372	ENSG00000096150	RPS18	0.2644	2.1405	0.0295	0.12 [8]	-0.14 [5]
ENSP00000421421	ENSG00000164111	ANXA5	-0.2789	-2.13557	0.0292	-0.1 [10]	0.18 [10]
ENSP00000434883	ENSG00000175220	ARHGAP1	-0.3312	-2.10934	0.028	-0.21 [6]	0.13 [7]
ENSP00000432485	ENSG00000204397	CARD16	0.2667	2.10501	0.0238	-0.08 [3]	-0.35 [6]
ENSP00000448079	ENSG00000197111	PCBP2	0.3552	2.09513	0.0286	-0.23 [4]	-0.58 [6]
ENSP00000053867	ENSG00000030582	GRN	0.2784	2.0642	0.0328	0.43 [5]	0.15 [7]
ENSP00000465673	ENSG00000030582	GRN	0.2784	2.0642	0.0328	0.43 [5]	0.15 [7]
ENSP00000451646	ENSG00000198668	CALM1	-0.6001	-2.05969	0.0286	-0.7 [3]	-0.1 [4]
ENSP00000431641	ENSG00000109971	HSPA8	-0.2736	-2.05108	0.0359	-0.32 [10]	-0.05 [10]
ENSP00000395051	ENSG00000111144	LTA4H	-0.3563	-2.04888	0.0321	-0.3 [6]	0.05 [7]
ENSP00000430970	ENSG00000169045	HNRNPH1	0.3406	2.04025	0.0343	0.17 [4]	-0.17 [8]
ENSP00000456004	ENSG00000067225	PKM	0.4444	2.01955	0.0485	0.17 [4]	-0.27 [7]
ENSP00000445778	ENSG00000149781	FERMT3	-0.3024	-2.01385	0.0364	-0.09 [10]	0.21 [10]
ENSP00000429374	ENSG00000089888	RPS20	-0.4147	-1.97847	0.0333	-0.3 [6]	0.12 [4]
ENSP00000339035	ENSG00000143549	TPM3	0.3558	1.97454	0.0459	-0.06 [10]	-0.42 [10]
ENSP00000271850	ENSG00000143549	TPM3	0.3512	1.96791	0.0468	-0.07 [10]	-0.42 [10]
ENSP00000449793	ENSG00000075415	SLC25A3	-0.3168	-1.95529	0.0498	-0.27 [6]	0.04 [6]
ENSP00000457033	ENSG00000103187	COTL1	0.7792	1.93028	0.0411	0.57 [6]	-0.21 [5]
ENSP00000437303	ENSG00000178209	PLEC	-0.3251	-1.89668	0.0357	-0.03 [5]	0.3 [3]
ENSP00000426433	ENSG00000167085	PHB	0.5472	1.87642	0.0179	0.12 [5]	-0.43 [3]
ENSP00000349748	ENSG00000116560	SFPQ	0.3409	1.86095	0.0325	0.05 [6]	-0.29 [5]
ENSP00000352438	ENSG00000197111	PCBP2	0.4035	1.85388	0.0215	0.02 [5]	-0.38 [7]
ENSP00000358724	ENSG00000148834	GSTO1	-0.4471	-1.83363	0.041	-0.36 [9]	0.09 [8]
ENSP00000358727	ENSG00000148834	GSTO1	-0.4471	-1.83363	0.041	-0.36 [9]	0.09 [8]
ENSP00000383168	ENSG00000183570	PCBP3	0.42	1.7368	0.0364	0.04 [4]	-0.38 [7]

**Table B-8 Differentially abundant proteins for monocytes at Day 28.** Proteins with the same ICCS-ratio were grouped together and represented by the longest protein in the group. \*mean baseline log<sub>2</sub> fold change.

Protein ID	Gene ID	Gene Name	Log2 Fold Change	z-statistic	P	Mean [N] (AS03)*	Mean [N] (PBS)*
ENSP00000264202	ENSG00000077549	CAPZB	0.3408	2.89576	0.0018	0.06 [10]	-0.29 [10]
ENSP00000401010	ENSG00000077549	CAPZB	0.3408	2.89576	0.0018	0.06 [10]	-0.29 [10]
ENSP00000466574	ENSG00000142657	PGD	0.3377	2.7541	0.0032	0.05 [9]	-0.29 [10]
ENSP00000300413	ENSG00000167088	SNRPD1	0.5412	2.73227	0.0038	0.33 [9]	-0.21 [6]
ENSP00000374645	ENSG00000142168	SOD1	0.4292	2.6406	0.0043	0.31 [5]	-0.12 [10]
ENSP00000270142	ENSG00000142168	SOD1	0.456	2.61662	0.0049	0.26 [7]	-0.19 [10]
ENSP00000324422	ENSG00000159840	ZYX	0.4148	2.56262	0.0075	0.33 [9]	-0.08 [7]
ENSP00000262030	ENSG00000110955	ATP5B	-0.264	-2.50866	0.0087	0 [10]	0.26 [10]
ENSP00000394158	ENSG00000159840	ZYX	0.3584	2.41756	0.0061	0.33 [8]	-0.03 [7]
ENSP00000446489	ENSG00000110955	ATP5B	-0.2912	-2.39216	0.0137	-0.01 [10]	0.28 [10]
ENSP00000308165	ENSG00000135218	CD36	-0.4322	-2.34777	0.0159	-0.07 [5]	0.36 [4]
ENSP00000456865	ENSG00000198848	CES1	-0.7407	-2.34157	0.0119	-0.3 [3]	0.45 [6]
ENSP00000384695	ENSG00000163631	ALB	0.5104	2.33281	0.0147	0.4 [10]	-0.11 [10]
ENSP00000356520	ENSG00000135829	DHX9	0.4609	2.30305	0.007	0.31 [5]	-0.15 [8]
ENSP00000295897	ENSG00000163631	ALB	0.5141	2.30152	0.0163	0.39 [10]	-0.12 [10]
ENSP00000422784	ENSG00000163631	ALB	0.5141	2.30152	0.0163	0.39 [10]	-0.12 [10]
ENSP00000341885	ENSG00000140988	RPS2	-0.4399	-2.29651	0.0057	-0.22 [9]	0.22 [8]
ENSP00000305556	ENSG00000169564	PCBP1	0.5755	2.25579	0.0175	0.31 [7]	-0.26 [7]
ENSP00000244534	ENSG00000124575	HIST1H1D	0.4037	2.24014	0.0132	0.07 [9]	-0.34 [7]
ENSP00000401820	ENSG00000163631	ALB	0.5658	2.23835	0.0143	0.49 [10]	-0.07 [10]
ENSP00000447571	ENSG00000110955	ATP5B	-0.3174	-2.22556	0.0221	0.07 [10]	0.39 [10]
ENSP00000260985	ENSG00000138413	IDH1	-0.4728	-2.18566	0.026	-0.33 [6]	0.14 [5]
ENSP00000433982	ENSG00000178209	PLEC	-0.6956	-2.17528	0.0286	-0.42 [4]	0.28 [3]
ENSP00000457643	ENSG00000149925	ALDOA	0.5378	2.17092	0.0228	0.04 [10]	-0.5 [7]
ENSP00000261733	ENSG00000111275	ALDH2	-0.3089	-2.1499	0.0296	-0.19 [10]	0.12 [8]
ENSP00000463042	ENSG00000136450	SRSF1	0.6112	2.12592	0.0242	0.38 [3]	-0.23 [8]
ENSP00000341072	ENSG00000070831	CDC42	-0.3646	-2.1149	0.0303	-0.13 [5]	0.24 [8]
ENSP00000270776	ENSG00000142657	PGD	0.267	2.10835	0.0324	-0.01 [10]	-0.28 [10]
ENSP00000458298	ENSG00000262617	AC020766.1	-0.5044	-2.10102	0.0354	-0.2 [5]	0.3 [7]
ENSP00000431296	ENSG00000135218	CD36	-0.4002	-2.09542	0.0238	-0.04 [5]	0.36 [4]
ENSP00000467362	ENSG00000142657	PGD	0.3442	2.09522	0.0304	0.05 [10]	-0.29 [10]
ENSP00000362924	ENSG00000148180	GSN	0.5966	2.09155	0.0317	0.19 [10]	-0.41 [9]
ENSP00000341136	ENSG00000147813	NAPRT1	0.377	2.08657	0.0286	0.1 [7]	-0.28 [6]
ENSP00000447068	ENSG00000197111	PCBP2	0.5079	2.07445	0.0333	0.05 [4]	-0.46 [6]
ENSP00000448079	ENSG00000197111	PCBP2	0.5079	2.07445	0.0333	0.05 [4]	-0.46 [6]
ENSP00000314458	ENSG00000070831	CDC42	-0.4172	-2.07371	0.0319	-0.21 [5]	0.2 [8]
ENSP00000418635	ENSG00000106526	ACTR3C	-0.2867	-2.05299	0.0318	-0.1 [10]	0.18 [9]
ENSP00000396519	ENSG00000062598	ELMO2	0.2839	2.04572	0.0286	0.14 [3]	-0.15 [4]
ENSP00000312185	ENSG00000155849	ELMO1	0.2839	2.04572	0.0286	0.14 [3]	-0.15 [4]
ENSP00000219169	ENSG00000102898	NUTF2	-0.3061	-2.03085	0.0403	-0.28 [6]	0.03 [8]
ENSP00000211372	ENSG00000096150	RPS18	0.3517	2.01219	0.0404	0.17 [8]	-0.19 [5]
ENSP00000451715	ENSG00000087302	C14orf166	-0.6742	-2.00162	0.0286	-0.24 [4]	0.44 [3]
ENSP00000352438	ENSG00000197111	PCBP2	0.51	1.98984	0.0424	0.17 [4]	-0.34 [7]
ENSP00000383168	ENSG00000183570	PCBP3	0.51	1.98984	0.0424	0.17 [4]	-0.34 [7]
ENSP00000364447	ENSG00000072506	HSD17B10	0.2779	1.9777	0.0476	0.32 [4]	0.04 [5]
ENSP00000460741	ENSG00000185624	P4HB	-0.5743	-1.67413	0.019	-0.64 [4]	-0.07 [6]

**Table B-9 Differentially abundant proteins from neutrophils at Day 1.** Proteins with the same ICCS-ratio were grouped together and represented by the longest protein in the group. \*mean baseline log<sub>2</sub> fold change.

Protein ID	Gene ID	Gene Name	Log2 Fold Change	z-statistic	P	Mean [N] (AS03)*	Mean [N] (PBS)*
ENSP00000448648	ENSG00000123416	TUBA1B	-0.5433	-2.4951	0.0055	-0.3 [8]	0.25 [10]
ENSP00000428916	ENSG00000197043	ANXA6	0.5892	2.49034	0.0025	0.46 [8]	-0.13 [10]
ENSP00000449460	ENSG00000123416	TUBA1B	-0.5419	-2.45127	0.007	-0.28 [8]	0.26 [10]
ENSP00000449325	ENSG00000123416	TUBA1B	-0.4971	-2.41131	0.006	-0.27 [8]	0.23 [10]
ENSP00000448211	ENSG00000167553	TUBA1C	-0.5147	-2.3802	0.0088	-0.28 [8]	0.23 [10]
ENSP00000336799	ENSG00000123416	TUBA1B	-0.3654	-2.19522	0.0243	-0.11 [9]	0.26 [10]
ENSP00000221992	ENSG00000105388	CEACAM5	-0.6216	-2.16941	0.016	-0.51 [5]	0.12 [9]
ENSP00000431078	ENSG00000197043	ANXA6	0.493	2.15348	0.029	0.23 [5]	-0.27 [9]
ENSP00000418340	ENSG00000163931	TKT	-0.4987	-2.11328	0.0308	-0.45 [7]	0.05 [10]
ENSP00000262428	ENSG00000103187	COTL1	-0.4324	-2.10136	0.03	-0.37 [8]	0.06 [10]
ENSP00000415121	ENSG00000113648	H2AFY	0.2843	2.08407	0.035	0.07 [5]	-0.22 [8]
ENSP00000354532	ENSG00000198805	PNP	-0.5383	-2.07644	0.011	-0.42 [8]	0.12 [10]
ENSP00000450268	ENSG00000167552	TUBA1A	-0.2643	-2.04036	0.0289	-0.08 [8]	0.18 [10]
ENSP00000366980	ENSG00000197043	ANXA6	0.3724	2.01243	0.0198	0.35 [9]	-0.03 [10]
ENSP00000359045	ENSG00000089820	ARHGAP4	-0.3974	-2.01016	0.0416	-0.26 [6]	0.14 [10]
ENSP00000397533	ENSG00000089820	ARHGAP4	-0.3877	-1.99861	0.0422	-0.26 [6]	0.13 [10]
ENSP00000293831	ENSG00000161960	EIF4A1	0.4683	1.93987	0.0485	0.43 [3]	-0.04 [8]
ENSP00000325875	ENSG00000096384	HSP90AB1	0.3163	1.92885	0.0476	0.28 [6]	-0.03 [9]
ENSP00000296930	ENSG00000181163	NPM1	-0.4135	-1.92042	0.0492	-0.32 [6]	0.09 [9]
ENSP00000202773	ENSG00000089009	RPL6	0.4596	1.91374	0.0357	0.46 [3]	0 [5]
ENSP00000462823	ENSG00000184009	ACTG1	0.2764	1.9073	0.0477	0.17 [9]	-0.11 [10]
ENSP00000386881	ENSG00000135636	DYSF	0.4526	1.89898	0.0476	0.08 [4]	-0.38 [6]
ENSP00000431086	ENSG00000197043	ANXA6	0.515	1.89626	0.0382	0.39 [7]	-0.13 [8]
ENSP00000247470	ENSG00000103490	PYCARD	0.3722	1.88754	0.0357	0.15 [3]	-0.22 [5]
ENSP00000407473	ENSG00000075624	ACTB	0.2903	1.88553	0.0469	0.18 [9]	-0.11 [10]
ENSP00000351646	ENSG00000168439	STIP1	0.3125	1.87325	0.0286	0.09 [3]	-0.22 [4]
ENSP00000452421	ENSG00000198805	PNP	-0.4844	-1.86253	0.0344	-0.39 [8]	0.09 [10]
ENSP00000198765	ENSG00000085719	CPNE3	0.5114	1.84918	0.0498	0.33 [6]	-0.18 [6]
ENSP00000430420	ENSG00000197043	ANXA6	0.3254	1.82926	0.029	0.31 [9]	-0.02 [10]

**Table B-10 Differentially abundant proteins from neutrophils at Day 3.** Proteins with the same ICCS-ratio were grouped together and represented by the longest protein in the group. \*mean baseline log<sub>2</sub> fold change.

Protein ID	Gene ID	Gene Name	Log2 Fold Change	z-statistic	P	Mean [N] (AS03)*	Mean [N] (PBS)*
ENSP00000296435	ENSG00000164047	CAMP	0.392	2.18181	0.0255	0.03 [8]	-0.36 [10]
ENSP00000450765	ENSG00000258947	TUBB3	-0.3835	-2.15157	0.0242	-0.25 [4]	0.14 [7]
ENSP00000472249	ENSG00000130755	GMFG	-0.5138	-2.14947	0.0182	-0.24 [4]	0.27 [7]
ENSP00000428424	ENSG00000254087	LYN	-0.2905	-2.12822	0.0242	-0.22 [4]	0.07 [7]
ENSP00000469681	ENSG00000099783	HNRNPM	-0.2876	-2.11376	0.0286	-0.06 [3]	0.23 [4]
ENSP00000472599	ENSG00000099783	HNRNPM	-0.2876	-2.11376	0.0286	-0.06 [3]	0.23 [4]
ENSP00000372819	ENSG00000204525	HLA-C	0.5043	2.11135	0.0265	0.19 [5]	-0.31 [7]
ENSP00000413992	ENSG00000233841	HLA-C	0.5043	2.11135	0.0265	0.19 [5]	-0.31 [7]
ENSP00000397867	ENSG00000228299	HLA-C	0.5043	2.11135	0.0265	0.19 [5]	-0.31 [7]
ENSP00000428924	ENSG00000254087	LYN	-0.2824	-2.0704	0.0303	-0.22 [4]	0.06 [7]
ENSP00000372975	ENSG00000206435	HLA-C	0.5249	2.05472	0.0281	0.24 [5]	-0.29 [6]
ENSP00000407952	ENSG00000229644	NAMPTL	-0.2966	-2.05414	0.0371	-0.2 [9]	0.09 [10]
ENSP00000471786	ENSG00000130755	GMFG	-0.4639	-2.04815	0.0238	-0.18 [4]	0.29 [6]
ENSP00000295470	ENSG00000152795	HNRNPDL	-0.3082	-2.03505	0.0281	-0.05 [6]	0.26 [6]
ENSP00000464265	ENSG00000263563	UBBP4	-0.3727	-2.03259	0.0339	-0.39 [7]	-0.01 [10]
ENSP00000272317	ENSG00000143947	RPS27A	-0.3696	-2.01993	0.0339	-0.42 [7]	-0.05 [10]
ENSP00000344818	ENSG00000150991	UBC	-0.3696	-2.01993	0.0339	-0.42 [7]	-0.05 [10]
ENSP00000351108	ENSG00000197451	HNRNPAB	-0.3518	-2.00787	0.0333	-0.03 [6]	0.32 [4]
ENSP00000391429	ENSG00000110047	EHD1	-0.3819	-1.96425	0.0461	-0.25 [7]	0.14 [10]
ENSP00000451525	ENSG00000197249	SERPINA1	-0.3583	-1.94923	0.0443	-0.39 [5]	-0.03 [8]
ENSP00000376309	ENSG00000170144	HNRNPA3	0.2944	1.94279	0.0486	0.07 [6]	-0.22 [8]
ENSP00000470308	ENSG00000160014	CALM3	0.5545	1.88653	0.0476	0.1 [3]	-0.45 [6]
ENSP00000451646	ENSG00000198668	CALM1	0.5467	1.88112	0.0476	0.1 [3]	-0.45 [6]
ENSP00000407431	ENSG00000225691	HLA-C	0.5257	1.85492	0.0417	0.27 [5]	-0.25 [7]
ENSP00000401935	ENSG00000158517	NCF1	-0.3206	-1.84147	0.0417	-0.29 [3]	0.03 [7]

**Table B-11 Differentially abundant proteins from neutrophils at Day 7.** Proteins with the same ICCS-ratio were grouped together and represented by the longest protein in the group. \*mean baseline log<sub>2</sub> fold change.

Protein ID	Gene ID	Gene Name	Log2 Fold Change	z-statistic	P	Mean [N] (AS03)*	Mean [N] (PBS)*
ENSP00000408620	ENSG00000115271	GCA	-0.325	-2.78446	0.0022	-0.12 [8]	0.2 [9]
ENSP00000394842	ENSG00000115271	GCA	-0.3051	-2.71992	0.0027	-0.1 [8]	0.21 [9]
ENSP00000394690	ENSG00000160211	G6PD	-0.3663	-2.52888	0.0056	-0.12 [7]	0.25 [9]
ENSP00000400648	ENSG00000160211	G6PD	-0.3069	-2.37242	0.0092	-0.07 [7]	0.23 [9]
ENSP00000364212	ENSG00000158825	CDA	-0.272	-2.32051	0.0091	-0.06 [7]	0.21 [9]
ENSP00000292432	ENSG00000160883	HK3	0.2864	2.30087	0.0044	0.21 [8]	-0.08 [8]
ENSP00000433308	ENSG00000172757	CFL1	-0.5067	-2.26392	0.0208	-0.39 [7]	0.12 [9]
ENSP00000436899	ENSG00000172757	CFL1	-0.5067	-2.26392	0.0208	-0.39 [7]	0.12 [9]
ENSP00000456004	ENSG00000067225	PKM	0.376	2.23529	0.0182	0.21 [4]	-0.17 [7]
ENSP00000446415	ENSG00000134333	LDHA	-0.3277	-2.22834	0.0202	-0.4 [5]	-0.08 [7]
ENSP00000446709	ENSG00000092841	MYL6	-0.3326	-2.21544	0.0232	-0.15 [8]	0.18 [9]
ENSP00000456756	ENSG00000102879	CORO1A	-0.5378	-2.15625	0.0317	-0.3 [5]	0.24 [5]
ENSP00000391842	ENSG00000026025	VIM	0.3401	2.15219	0.026	0.3 [8]	-0.04 [9]
ENSP00000475750	ENSG00000051620	HEBP2	-0.9247	-2.11205	0.0179	-0.75 [3]	0.17 [5]
ENSP00000393951	ENSG00000075624	ACTB	0.299	2.07269	0.03	0.06 [8]	-0.24 [9]
ENSP00000401032	ENSG00000075624	ACTB	0.299	2.07269	0.03	0.06 [8]	-0.24 [9]
ENSP00000419442	ENSG00000169764	UGP2	0.8591	2.00253	0.0397	0.71 [4]	-0.15 [5]
ENSP00000412429	ENSG00000158710	TAGLN2	-0.322	-1.96932	0.0453	-0.26 [8]	0.06 [9]
ENSP00000386672	ENSG00000138069	RAB1A	0.693	1.91019	0.0397	0.19 [5]	-0.51 [5]
ENSP00000314458	ENSG00000070831	CDC42	0.5174	1.85235	0.0495	0.19 [7]	-0.33 [6]
ENSP00000394213	ENSG00000115091	ACTR3	-0.5107	-1.8179	0.0397	-0.13 [5]	0.38 [4]

**Table B-12 Differentially abundant proteins from neutrophils at Day 28.** Proteins with the same ICCS-ratio were grouped together and represented by the longest protein in the group. \*mean baseline log<sub>2</sub> fold change.

Protein ID	Gene ID	Gene Name	Log2 Fold Change	z-statistic	P	Mean [N] (AS03)*	Mean [N] (PBS)*
ENSP00000391592	ENSG00000111679	PTPN6	-0.4089	-2.97017	0.0005	-0.35 [5]	0.06 [9]
ENSP00000415979	ENSG00000111679	PTPN6	-0.3472	-2.88239	0.0008	-0.32 [5]	0.03 [8]
ENSP00000400842	ENSG00000223532	HLA-B	0.6593	2.50607	0.0091	0.32 [4]	-0.33 [7]
ENSP00000335153	ENSG00000080824	HSP90AA1	-0.3714	-2.50434	0.0085	-0.15 [8]	0.22 [10]
ENSP00000352656	ENSG00000206450	HLA-B	0.6153	2.47877	0.0091	0.28 [4]	-0.33 [7]
ENSP00000392099	ENSG00000223532	HLA-B	0.6153	2.47877	0.0091	0.28 [4]	-0.33 [7]
ENSP00000411954	ENSG00000206450	HLA-B	0.6153	2.47877	0.0091	0.28 [4]	-0.33 [7]
ENSP00000450765	ENSG00000258947	TUBB3	-0.4258	-2.451	0.0038	-0.22 [5]	0.2 [7]
ENSP00000391250	ENSG00000228299	HLA-C	0.5432	2.3708	0.0079	0.48 [4]	-0.06 [5]
ENSP00000400410	ENSG00000204525	HLA-C	0.5432	2.3708	0.0079	0.48 [4]	-0.06 [5]
ENSP00000407494	ENSG00000237022	HLA-C	0.3056	2.36907	0.0079	0.22 [4]	-0.08 [5]
ENSP00000399675	ENSG00000223532	HLA-B	0.4773	2.35741	0.0079	0.41 [4]	-0.06 [5]
ENSP00000433363	ENSG00000206450	HLA-B	0.4333	2.31936	0.0079	0.37 [4]	-0.06 [5]
ENSP00000300289	ENSG00000167004	PDIA3	0.3823	2.20357	0.0246	0.23 [5]	-0.15 [10]
ENSP00000450712	ENSG00000080824	HSP90AA1	-0.4117	-2.19649	0.0171	-0.15 [5]	0.26 [8]
ENSP00000376309	ENSG00000170144	HNRNPA3	0.4374	2.15353	0.0266	0.14 [6]	-0.3 [8]
ENSP00000373854	ENSG00000156886	ITGAD	-0.4075	-2.13916	0.0242	-0.27 [3]	0.14 [8]
ENSP00000438260	ENSG00000167004	PDIA3	0.3467	2.12947	0.0286	0.23 [5]	-0.11 [10]
ENSP00000343027	ENSG00000127955	GNAI1	-0.3691	-2.11803	0.0095	-0.24 [4]	0.13 [6]
ENSP00000410572	ENSG00000127955	GNAI1	-0.3671	-2.08544	0.019	-0.24 [4]	0.13 [6]
ENSP00000410661	ENSG00000206452	HLA-C	0.2956	2.03351	0.0286	0.25 [4]	-0.05 [4]
ENSP00000398592	ENSG00000070831	CDC42	-0.5533	-2.02779	0.035	0.04 [7]	0.6 [8]
ENSP00000356022	ENSG00000112096	SOD2	0.3881	2.0131	0.0356	0.32 [5]	-0.07 [10]
ENSP00000454623	ENSG00000140678	ITGAX	-0.3569	-2.00162	0.0303	-0.22 [3]	0.14 [8]
ENSP00000403679	ENSG00000196419	XRCC6	0.4503	1.99906	0.0286	0.34 [3]	-0.11 [4]
ENSP00000437098	ENSG00000177156	TALDO1	-0.3494	-1.96447	0.0413	-0.12 [7]	0.23 [10]
ENSP00000321259	ENSG00000177156	TALDO1	-0.3459	-1.95059	0.0427	-0.12 [7]	0.23 [10]
ENSP00000372819	ENSG00000204525	HLA-C	0.6948	1.94256	0.0394	0.47 [4]	-0.22 [7]
ENSP00000413992	ENSG00000233841	HLA-C	0.6948	1.94256	0.0394	0.47 [4]	-0.22 [7]
ENSP00000397867	ENSG00000228299	HLA-C	0.6948	1.94256	0.0394	0.47 [4]	-0.22 [7]

**Table B-13 Differentially abundant proteins from NK cells at Day 1.** Proteins with the same ICCS-ratio were grouped together and represented by the longest protein in the group. \*mean baseline log<sub>2</sub> fold change.

Protein ID	Gene ID	Gene Name	Log2 Fold Change	z-statistic	P	Mean [N] (AS03)*	Mean [N] (PBS)*
ENSP00000477441	ENSG00000147065	MSN	0.9323	2.67964	0.0079	0.73 [4]	-0.2 [5]
ENSP00000366002	ENSG00000206503	HLA-A	-0.3471	-2.4673	0.0093	0.04 [8]	0.39 [5]
ENSP00000463482	ENSG00000265434	HLA-ABC	-0.3471	-2.4673	0.0093	0.04 [8]	0.39 [5]
ENSP00000410645	ENSG00000223980	HLA-A	-0.3429	-2.44613	0.0101	0.04 [8]	0.39 [5]
ENSP00000448239	ENSG00000229215	HLA-A	-0.4676	-2.38313	0.0114	0.01 [7]	0.47 [5]
ENSP00000327539	ENSG00000169045	HNRNPH1	-0.3935	-2.34234	0.0286	-0.18 [4]	0.21 [3]
ENSP00000373114	ENSG00000206505	HLA-A	-0.4266	-2.33118	0.007	-0.13 [8]	0.3 [6]
ENSP00000317697	ENSG00000160255	ITGB2	-0.5493	-2.32988	0.014	-0.27 [5]	0.28 [8]
ENSP00000391897	ENSG00000002834	LASP1	-0.2817	-2.32049	0.0155	-0.16 [7]	0.12 [8]
ENSP00000392235	ENSG00000232126	HLA-B	-0.424	-2.27137	0.0152	-0.12 [7]	0.3 [8]
ENSP00000388208	ENSG00000232126	HLA-B	-0.407	-2.2568	0.0148	-0.12 [7]	0.29 [8]
ENSP00000401048	ENSG00000002834	LASP1	-0.425	-2.15595	0.0264	-0.25 [5]	0.17 [8]
ENSP00000316029	ENSG00000137076	TLN1	-0.3292	-2.14624	0.022	-0.14 [5]	0.19 [9]
ENSP00000442981	ENSG00000137076	TLN1	-0.4176	-2.13977	0.0185	-0.24 [5]	0.18 [9]
ENSP00000467037	ENSG00000152234	ATP5A1	0.7353	2.13443	0.0278	0.36 [5]	-0.37 [7]
ENSP00000303242	ENSG00000160255	ITGB2	-0.4429	-2.12891	0.0295	-0.2 [5]	0.24 [8]
ENSP00000380952	ENSG00000160255	ITGB2	-0.4429	-2.12891	0.0295	-0.2 [5]	0.24 [8]
ENSP00000282050	ENSG00000152234	ATP5A1	0.6672	2.12268	0.0303	0.32 [6]	-0.34 [7]
ENSP00000302935	ENSG00000172349	IL16	0.5059	2.05091	0.0357	0.48 [3]	-0.03 [5]
ENSP00000431347	ENSG00000237022	HLA-C	-0.4015	-2.04946	0.0379	0.01 [7]	0.41 [5]
ENSP00000408986	ENSG00000231834	HLA-A	-0.2768	-2.00183	0.0427	0.04 [8]	0.32 [5]
ENSP00000216181	ENSG00000100345	MYH9	-0.3616	-1.98636	0.0389	-0.28 [8]	0.08 [8]
ENSP00000472469	ENSG00000233927	RPS28	-0.5729	-1.97626	0.0286	-0.21 [4]	0.36 [3]
ENSP00000301522	ENSG00000167815	PRDX2	0.4264	1.92593	0.0397	0.41 [4]	-0.02 [5]
ENSP00000415121	ENSG00000113648	H2AFY	-0.3794	-1.69394	0.0476	-0.11 [5]	0.26 [6]

**Table B-14 Differentially abundant proteins from NK cells at Day 3.** Proteins with the same ICCS-ratio were grouped together and represented by the longest protein in the group. \*mean baseline log<sub>2</sub> fold change.

Protein ID	Gene ID	Gene Name	Log2 Fold Change	z-statistic	P	Mean [N] (AS03)*	Mean [N] (PBS)*
ENSP00000380065	ENSG00000111640	GAPDH	-0.505	-2.60099	0.0041	-0.15 [9]	0.36 [8]
ENSP00000438740	ENSG00000111679	PTPN6	-0.3582	-2.46857	0.0079	0.11 [5]	0.47 [4]
ENSP00000286788	ENSG00000156261	CCT8	0.4326	2.41856	0.0143	0.31 [4]	-0.13 [6]
ENSP00000395153	ENSG00000142634	EFHD2	-0.4273	-2.41211	0.0097	-0.31 [9]	0.12 [8]
ENSP00000445646	ENSG00000111679	PTPN6	-0.3924	-2.40175	0.0286	0.08 [4]	0.47 [4]
ENSP00000475985	ENSG00000268954	PTPN6	-0.3924	-2.40175	0.0286	0.08 [4]	0.47 [4]
ENSP00000450297	ENSG00000110955	ATP5B	0.4671	2.35779	0.0096	0.27 [8]	-0.2 [8]
ENSP00000442981	ENSG00000137076	TLN1	-0.477	-2.32866	0.0146	-0.29 [7]	0.18 [7]
ENSP00000264071	ENSG00000104833	TUBB4A	0.3226	2.29112	0.0183	0.27 [9]	-0.05 [8]
ENSP00000193403	ENSG00000072110	ACTN1	-0.4345	-2.27265	0.0161	-0.23 [9]	0.2 [8]
ENSP00000377941	ENSG00000072110	ACTN1	-0.4345	-2.27265	0.0161	-0.23 [9]	0.2 [8]
ENSP00000414272	ENSG00000072110	ACTN1	-0.4345	-2.27265	0.0161	-0.23 [9]	0.2 [8]
ENSP00000439828	ENSG00000072110	ACTN1	-0.4345	-2.27265	0.0161	-0.23 [9]	0.2 [8]
ENSP00000316029	ENSG00000137076	TLN1	-0.4574	-2.24918	0.014	-0.31 [7]	0.15 [7]
ENSP00000229239	ENSG00000111640	GAPDH	-0.4418	-2.24004	0.0188	-0.15 [9]	0.29 [8]
ENSP00000380067	ENSG00000111640	GAPDH	-0.4418	-2.24004	0.0188	-0.15 [9]	0.29 [8]
ENSP00000372819	ENSG00000204525	HLA-C	0.3762	2.22815	0.0238	0.17 [8]	-0.21 [7]
ENSP00000341289	ENSG00000188229	TUBB4B	0.3009	2.15077	0.028	0.25 [9]	-0.05 [8]
ENSP00000472469	ENSG00000233927	RPS28	-0.6694	-2.1255	0.0357	-0.36 [5]	0.31 [3]
ENSP00000413992	ENSG00000233841	HLA-C	0.3516	2.11551	0.0337	0.17 [8]	-0.18 [7]
ENSP00000445257	ENSG00000115091	ACTR3	-0.3052	-2.08108	0.0267	-0.24 [7]	0.06 [8]
ENSP00000408986	ENSG00000231834	HLA-A	-0.3543	-2.07277	0.0333	0.22 [7]	0.58 [4]
ENSP00000410645	ENSG00000223980	HLA-A	-0.3543	-2.07277	0.0333	0.22 [7]	0.58 [4]
ENSP00000442730	ENSG00000156261	CCT8	0.6711	2.06649	0.0397	0.34 [4]	-0.33 [5]
ENSP00000429978	ENSG00000153310	FAM49B	0.7826	2.02824	0.0179	0.33 [3]	-0.46 [5]
ENSP00000246554	ENSG00000126267	COX6B1	0.3945	2.01799	0.0283	0.26 [8]	-0.13 [4]
ENSP00000326042	ENSG00000075886	TUBA3D	0.3605	1.99826	0.0394	0.23 [7]	-0.13 [4]
ENSP00000342026	ENSG00000117592	PRDX6	-0.6719	-1.98867	0.0449	-0.28 [6]	0.39 [7]
ENSP00000373114	ENSG00000206505	HLA-A	-0.3559	-1.98248	0.0424	0.06 [7]	0.42 [4]
ENSP00000365147	ENSG00000142634	EFHD2	-0.3486	-1.9663	0.0449	-0.31 [9]	0.04 [8]
ENSP00000467037	ENSG00000152234	ATP5A1	0.4339	1.95642	0.0454	0.17 [8]	-0.26 [7]
ENSP00000244534	ENSG00000124575	HIST1H1D	0.6862	1.86118	0.0455	0.33 [5]	-0.36 [7]
ENSP00000468618	ENSG00000152234	ATP5A1	0.3769	1.80027	0.0429	0.22 [4]	-0.16 [6]
ENSP00000465259	ENSG00000152234	ATP5A1	0.6805	1.78399	0.0397	0.15 [4]	-0.53 [5]

**Table B-15 Differentially abundant proteins from NK cells at Day 7.** Proteins with the same ICCS-ratio were grouped together and represented by the longest protein in the group. \*mean baseline log<sub>2</sub> fold change.

Protein ID	Gene ID	Gene Name	Log2 Fold Change	z-statistic	P	Mean [N] (AS03)*	Mean [N] (PBS)*
ENSP00000228825	ENSG00000111229	ARPC3	-0.8939	-2.45638	0.0083	-0.23 [7]	0.66 [3]
ENSP00000467037	ENSG00000152234	ATP5A1	0.4979	2.28467	0.0095	-0.05 [8]	-0.54 [7]
ENSP00000279146	ENSG00000110711	AIP	-0.4026	-2.18037	0.0159	0.12 [4]	0.53 [5]
ENSP00000429978	ENSG00000153310	FAM49B	0.7391	2.13204	0.0357	0.4 [3]	-0.34 [5]
ENSP00000282050	ENSG00000152234	ATP5A1	0.4737	2.1284	0.0218	-0.03 [8]	-0.51 [7]
ENSP00000372819	ENSG00000204525	HLA-C	0.3972	2.09329	0.0317	0.16 [8]	-0.24 [7]
ENSP00000309431	ENSG00000173213	RP11-683L23.1	0.5046	2.04368	0.0333	0.05 [7]	-0.45 [3]
ENSP00000457610	ENSG00000261456	TUBB8	0.5046	2.04368	0.0333	0.05 [7]	-0.45 [3]
ENSP00000467190	ENSG00000130402	ACTN4	-0.8218	-2.03613	0.0343	-0.58 [8]	0.24 [4]
ENSP00000364805	ENSG00000204390	HSPA1L	0.5643	2.01564	0.0373	0.35 [6]	-0.21 [7]
ENSP00000249071	ENSG00000128340	RAC2	-0.5895	-1.96068	0.0368	-0.35 [5]	0.24 [6]
ENSP00000385590	ENSG00000128340	RAC2	-0.5895	-1.96068	0.0368	-0.35 [5]	0.24 [6]
ENSP00000263373	ENSG00000160460	SPTBN4	-0.4784	-1.73174	0.0476	-0.3 [5]	0.17 [4]
ENSP00000340741	ENSG00000160460	SPTBN4	-0.4784	-1.73174	0.0476	-0.3 [5]	0.17 [4]
ENSP00000438260	ENSG00000167004	PDIA3	-0.3385	-1.67852	0.0425	-0.2 [7]	0.14 [7]

**Table B-16 Differentially abundant proteins from NK cells at Day 28.** Proteins with the same ICCS-ratio were grouped together and represented by the longest protein in the group. \*mean baseline log<sub>2</sub> fold change.

Protein ID	Gene ID	Gene Name	Log2 Fold Change	z-statistic	P	Mean [N] (AS03)*	Mean [N] (PBS)*
ENSP00000450297	ENSG00000110955	ATP5B	0.3247	2.92022	0.0019	0.27 [8]	-0.05 [8]
ENSP00000446677	ENSG00000110955	ATP5B	0.4898	2.5298	0.0076	0.29 [8]	-0.2 [7]
ENSP00000339035	ENSG00000143549	TPM3	-0.7335	-2.36213	0.0079	-0.4 [4]	0.33 [5]
ENSP00000271850	ENSG00000143549	TPM3	-0.7335	-2.36213	0.0079	-0.4 [4]	0.33 [5]
ENSP00000357520	ENSG00000143549	TPM3	-0.6285	-2.3076	0.0159	-0.3 [4]	0.33 [5]
ENSP00000357516	ENSG00000143549	TPM3	-0.6285	-2.3076	0.0159	-0.3 [4]	0.33 [5]
ENSP00000207437	ENSG00000196465	MYL6B	0.7145	2.24612	0.0079	0.61 [5]	-0.1 [4]
ENSP00000340278	ENSG00000116288	PARK7	-0.4908	-2.17162	0.0273	-0.05 [7]	0.44 [4]
ENSP00000466242	ENSG00000116288	PARK7	-0.4908	-2.17162	0.0273	-0.05 [7]	0.44 [4]
ENSP00000329671	ENSG00000244734	HBB	-1.1892	-2.15378	0.0246	-0.14 [8]	1.05 [7]
ENSP00000327539	ENSG00000169045	HNRNPH1	-0.6008	-2.12921	0.0333	-0.37 [7]	0.23 [3]
ENSP00000249071	ENSG00000128340	RAC2	-0.5127	-2.12691	0.0281	-0.29 [5]	0.22 [6]
ENSP00000385590	ENSG00000128340	RAC2	-0.5127	-2.12691	0.0281	-0.29 [5]	0.22 [6]
ENSP00000329219	ENSG00000184922	FMNL1	0.5882	2.072	0.0179	0.11 [5]	-0.48 [3]
ENSP00000451560	ENSG00000198211	TUBB3	0.4275	2.05253	0.0366	0.18 [9]	-0.25 [8]
ENSP00000219150	ENSG00000102879	CORO1A	-0.3549	-2.04649	0.0195	-0.24 [9]	0.12 [8]
ENSP00000333994	ENSG00000244734	HBB	-1.1241	-2.03948	0.0375	-0.24 [8]	0.88 [7]
ENSP00000392099	ENSG00000223532	HLA-B	0.4542	1.96558	0.0476	0.21 [5]	-0.24 [4]
ENSP00000325875	ENSG00000096384	HSP90AB1	-0.5839	-1.93384	0.0429	-0.11 [7]	0.47 [5]
ENSP00000307940	ENSG00000167658	EEF2	-0.3722	-1.9202	0.0404	-0.2 [7]	0.17 [5]
ENSP00000270792	ENSG00000142669	SH3BGL3	0.3552	1.85843	0.0148	0.28 [8]	-0.07 [7]

**Table B-17 Differentially abundant proteins from T cells at Day 1.** Proteins with the same ICCS-ratio were grouped together and represented by the longest protein in the group. \*mean baseline log<sub>2</sub> fold change.

Protein ID	Gene ID	Gene Name	Log2 Fold Change	z-statistic	P	Mean [N] (AS03)*	Mean [N] (PBS)*
ENSP00000358224	ENSG00000198161	PPIAL4C	-0.3172	-2.2544	0.02	-0.22 [7]	0.1 [8]
ENSP00000269576	ENSG00000186395	KRT10	1.3023	2.1991	0.0317	0.52 [4]	-0.78 [5]
ENSP00000393764	ENSG00000250151	ARPC4-TTLL3	-0.5793	-2.18368	0.0238	-0.28 [5]	0.3 [5]
ENSP00000259818	ENSG00000137285	TUBB2B	0.6902	2.14351	0.0238	0.4 [6]	-0.29 [6]
ENSP00000451560	ENSG00000198211	TUBB3	0.6902	2.14351	0.0238	0.4 [6]	-0.29 [6]
ENSP00000388169	ENSG00000241553	ARPC4	-0.3506	-2.08212	0.0317	-0.27 [5]	0.08 [5]
ENSP00000216181	ENSG00000100345	MYH9	-0.306	-2.04984	0.0366	-0.34 [9]	-0.04 [10]
ENSP00000440014	ENSG00000127314	RAP1B	0.3568	2.02429	0.0381	0.15 [4]	-0.2 [6]
ENSP00000228825	ENSG00000111229	ARPC3	-0.4459	-2.01633	0.0411	-0.24 [5]	0.21 [6]
ENSP00000250559	ENSG00000127314	RAP1B	0.3413	1.99781	0.0333	0.15 [4]	-0.19 [6]
ENSP00000348786	ENSG00000116473	RAP1A	0.3413	1.99781	0.0333	0.15 [4]	-0.19 [6]
ENSP00000444467	ENSG00000127314	RAP1B	0.3413	1.99781	0.0333	0.15 [4]	-0.19 [6]
ENSP00000399986	ENSG00000127314	RAP1B	0.3413	1.99781	0.0333	0.15 [4]	-0.19 [6]
ENSP00000477441	ENSG00000147065	MSN	0.6398	1.91843	0.0429	-0.16 [6]	-0.8 [4]
ENSP00000264335	ENSG00000108953	YWHAE	-1.1652	-1.91077	0.0286	-0.74 [3]	0.42 [4]
ENSP00000248975	ENSG00000128245	YWHAH	-0.8436	-1.87684	0.0286	-0.45 [3]	0.4 [4]
ENSP00000340989	ENSG00000175793	SFN	-0.8436	-1.87684	0.0286	-0.45 [3]	0.4 [4]
ENSP00000238081	ENSG00000134308	YWHAQ	-0.8436	-1.87684	0.0286	-0.45 [3]	0.4 [4]
ENSP00000396189	ENSG00000080824	HSP90AA1	-0.4531	-1.85351	0.0286	-0.44 [4]	0.02 [4]
ENSP00000449460	ENSG00000123416	TUBA1B	0.35	1.84981	0.0471	0.2 [7]	-0.15 [9]
ENSP00000448648	ENSG00000123416	TUBA1B	0.35	1.84981	0.0471	0.2 [7]	-0.15 [9]
ENSP00000306330	ENSG00000170027	YWHAQ	-1.0967	-1.72571	0.0286	-0.69 [3]	0.41 [4]
ENSP00000300161	ENSG00000166913	YWHAH	-1.0814	-1.71639	0.0286	-0.69 [3]	0.4 [4]



**Table B-18 Differentially abundant proteins from T cells at Day 3.** Proteins with the same ICCS-ratio were grouped together and represented by the longest protein in the group. \*mean baseline log<sub>2</sub> fold change.

Protein ID	Gene ID	Gene Name	Log2 Fold Change	z-statistic	P	Mean [N] (AS03)*	Mean [N] (PBS)*
ENSP00000468618	ENSG00000152234	ATP5A1	0.6825	2.24065	0.0286	0.15 [4]	-0.53 [3]
ENSP00000465259	ENSG00000152234	ATP5A1	0.5901	2.23147	0.0286	0.14 [4]	-0.45 [3]
ENSP00000270142	ENSG00000142168	SOD1	0.512	1.96036	0.0429	0.1 [6]	-0.41 [4]
ENSP00000438740	ENSG00000111679	PTPN6	-0.4706	-1.86121	0.0286	-0.41 [4]	0.06 [3]
ENSP00000455584	ENSG00000067225	PKM	0.6226	1.70431	0.0346	0.26 [6]	-0.36 [5]

**Table B-19 Differentially abundant proteins from T cells at Day 7.** Proteins with the same ICCS-ratio were grouped together and represented by the longest protein in the group. \*mean baseline log<sub>2</sub> fold change.

Protein ID	Gene ID	Gene Name	Log2 Fold Change	z-statistic	P	Mean [N] (AS03)*	Mean [N] (PBS)*
ENSP00000403679	ENSG00000196419	XRCC6	-0.8634	-2.41711	0.0159	-0.4 [4]	0.46 [5]
ENSP00000386929	ENSG00000163017	ACTG2	0.523	2.38555	0.0061	0.21 [10]	-0.31 [9]
ENSP00000407473	ENSG00000075624	ACTB	-0.94	-2.36984	0.0126	-0.96 [7]	-0.02 [8]
ENSP00000462823	ENSG00000184009	ACTG1	-0.94	-2.36984	0.0126	-0.96 [7]	-0.02 [8]
ENSP00000408649	ENSG00000146701	MDH2	-0.5929	-2.19489	0.0317	-0.35 [4]	0.24 [5]
ENSP00000259791	ENSG00000137259	HIST1H2AB	-0.5639	-2.15511	0.0275	-0.48 [8]	0.09 [8]
ENSP00000452858	ENSG00000182718	ANXA2	0.672	2.14546	0.0317	0.08 [5]	-0.59 [5]
ENSP00000453770	ENSG00000182718	ANXA2	0.672	2.14546	0.0317	0.08 [5]	-0.59 [5]
ENSP00000453566	ENSG00000182718	ANXA2	0.672	2.14546	0.0317	0.08 [5]	-0.59 [5]
ENSP00000327070	ENSG00000146701	MDH2	-0.4244	-2.14219	0.0286	-0.27 [4]	0.15 [6]
ENSP00000431696	ENSG00000172757	CFL1	-0.3807	-2.13111	0.0291	-0.09 [7]	0.29 [7]
ENSP00000416706	ENSG00000169067	ACTBL2	0.5229	1.95735	0.0445	0.3 [10]	-0.22 [9]
ENSP00000262269	ENSG00000105357	MYH14	0.5881	1.95017	0.0494	0.1 [8]	-0.49 [9]
ENSP00000440902	ENSG00000246705	H2AFJ	-2.2355	-1.90964	0.0238	-1.53 [4]	0.7 [6]
ENSP00000362413	ENSG00000102144	PGK1	-0.5424	-1.86222	0.0368	-0.12 [5]	0.42 [6]
ENSP00000444708	ENSG00000102144	PGK1	-0.5503	-1.85639	0.0346	-0.13 [5]	0.42 [6]

**Table B-20 Differentially abundant proteins from T cells at Day 28.** Proteins with the same ICCS-ratio were grouped together and represented by the longest protein in the group. \*mean baseline log<sub>2</sub> fold change.

Protein ID	Gene ID	Gene Name	Log2 Fold Change	z-statistic	P	Mean [N] (AS03)*	Mean [N] (PBS)*
ENSP00000380033	ENSG00000100201	DDX17	0.3259	2.44908	0.0079	0.18 [5]	-0.15 [5]
ENSP00000452858	ENSG00000182718	ANXA2	0.5248	2.2103	0.0065	0.13 [6]	-0.39 [5]
ENSP00000453770	ENSG00000182718	ANXA2	0.5248	2.2103	0.0065	0.13 [6]	-0.39 [5]
ENSP00000453566	ENSG00000182718	ANXA2	0.5248	2.2103	0.0065	0.13 [6]	-0.39 [5]
ENSP00000452895	ENSG00000182718	ANXA2	0.3523	2.20641	0.0173	0.1 [6]	-0.25 [5]
ENSP00000453663	ENSG00000182718	ANXA2	0.3523	2.20641	0.0173	0.1 [6]	-0.25 [5]
ENSP00000346694	ENSG00000122566	HNRNPA2B1	0.6735	2.18942	0.0169	0.54 [6]	-0.14 [7]
ENSP00000346032	ENSG00000182718	ANXA2	0.3959	2.10576	0.0281	0.07 [6]	-0.33 [5]
ENSP00000453754	ENSG00000182718	ANXA2	0.3959	2.10576	0.0281	0.07 [6]	-0.33 [5]
ENSP00000453859	ENSG00000182718	ANXA2	0.3959	2.10576	0.0281	0.07 [6]	-0.33 [5]
ENSP00000305995	ENSG00000170950	PGK2	-0.6084	-2.09987	0.0368	-0.13 [6]	0.48 [5]
ENSP00000472249	ENSG00000130755	GMFG	-0.6483	-2.08625	0.0368	-0.37 [6]	0.28 [5]
ENSP00000471786	ENSG00000130755	GMFG	-0.6483	-2.08625	0.0368	-0.37 [6]	0.28 [5]
ENSP00000282050	ENSG00000152234	ATP5A1	0.4032	2.05407	0.0108	0.11 [5]	-0.29 [6]
ENSP00000465477	ENSG00000152234	ATP5A1	0.4032	2.05407	0.0108	0.11 [5]	-0.29 [6]
ENSP00000234590	ENSG00000074800	ENO1	0.2925	2.05008	0.0301	0.08 [9]	-0.21 [10]
ENSP00000467037	ENSG00000152234	ATP5A1	0.3905	2.01856	0.0108	0.11 [5]	-0.28 [6]
ENSP00000431696	ENSG00000172757	CFL1	-0.3909	-2.00154	0.0357	-0.13 [8]	0.26 [10]
ENSP00000349101	ENSG00000122566	HNRNPA2B1	0.6114	1.90079	0.0466	0.48 [6]	-0.14 [7]
ENSP00000357721	ENSG00000143546	S100A8	-1.3285	-1.82553	0.0286	-0.31 [3]	1.02 [4]

**Table B-21 Significant protein family overlap between cell types.** Proteins are ordered by the number of different cell types they are shared between

Protein ID	Gene ID	Gene Name	B-cells	Monocytes	Neutrophils	NK-cells	T-cells
ENSP00000451560	ENSG00000198211	TUBB3	Day 1,7,28	Day 1,3,7	Day 3,28	Day 3,7,28	Day 1
ENSP00000373123	ENSG00000206509	HLA-F	Day 1,3,7	Day 3	Day 3,28	Day 1,3,7,28	0
ENSP00000459921	ENSG00000262785	PKLR	Day 7	Day 7	Day 7		Day 3
ENSP00000346550	ENSG00000197043	ANXA6	Day 1,3	Day 3,7	Day 1		
ENSP00000353192	ENSG00000196419	XRCC6	Day 1		Day 28		Day 7
ENSP00000310219	ENSG00000173110	HSPA6	Day 1,3	Day 1,7		Day 7	
ENSP00000441750	ENSG00000092841	MYL6	Day 1,3,7		Day 7	Day 28	
ENSP00000451920	ENSG00000197045	GMFB		Day 1	Day 3		Day 28
ENSP00000388169	ENSG00000241553	ARPC4	Day 28	Day 1			Day 1
ENSP00000327070	ENSG00000146701	MDH2	Day 7	Day 1			Day 7
ENSP00000300289	ENSG00000167004	PDIA3		Day 1	Day 28	Day 7	
ENSP00000443475	ENSG00000167553	TUBA1C			Day 1	Day 3	Day 1
ENSP00000391481	ENSG00000163931	TKT	Day 3	Day 3	Day 1		
ENSP00000423563	ENSG00000113648	H2AFY			Day 1	Day 1	Day 7
ENSP00000335153	ENSG00000080824	HSP90AA1			Day 1,28	Day 28	Day 1
ENSP00000386786	ENSG00000196604	POTEF	Day 28		Day 1,7		Day 7
ENSP00000437301	ENSG00000137710	RDX		Day 3		Day 1	Day 1
ENSP00000262030	ENSG00000110955	ATP5B	Day 3,7	Day 28		Day 3,28	
ENSP00000330074	ENSG00000184357	HIST1H1B	Day 3	Day 28		Day 3	
ENSP00000441543	ENSG00000150991	UBC	Day 28	Day 3	Day 3		
ENSP00000376309	ENSG00000170144	HNRNPA3	Day 28		Day 3,28		Day 28
ENSP00000391592	ENSG00000111679	PTPN6			Day 28	Day 3	Day 3
ENSP00000263238	ENSG00000115091	ACTR3		Day 28	Day 7	Day 3	
ENSP00000431696	ENSG00000172757	CFL1		Day 7	Day 7		Day 7,28
ENSP00000394496	ENSG00000110880	CORO1C	Day 28		Day 7	Day 28	
ENSP00000228740	ENSG00000111144	LTA4H	Day 1	Day 7			
ENSP00000368646	ENSG00000123131	PRDX4	Day 1,3,28			Day 1	
ENSP00000439828	ENSG00000072110	ACTN1	Day 1,7			Day 3,7	
ENSP00000363071	ENSG00000175084	DES	Day 1,7,28		Day 7		
ENSP00000362413	ENSG00000102144	PGK1	Day 1				Day 7,28
ENSP00000462209	ENSG00000141522	ARHGDIA	Day 1	Day 3			
ENSP00000250559	ENSG00000127314	RAP1B		Day 1,3			Day 1
ENSP00000344419	ENSG00000005381	MPO	Day 7	Day 1			
ENSP00000246662	ENSG00000171403	KRT9		Day 1			Day 1
ENSP00000446252	ENSG00000112096	SOD2		Day 1	Day 28		
ENSP00000369475	ENSG00000057608	GDI2	Day 7	Day 1			

Table B-21 Continued.

Protein ID	Gene ID	Gene Name	B-cells	Monocytes	Neutrophils	NK-cells	T-cells
ENSP00000302393	ENSG00000171989	LDHAL6B		Day 1	Day 7		
ENSP00000262428	ENSG00000103187	COTL1		Day 7	Day 1		
ENSP00000359045	ENSG00000089820	ARHGAP4		Day 7	Day 1		
ENSP00000247470	ENSG00000103490	PYCARD		Day 7	Day 1		
ENSP00000327539	ENSG00000169045	HNRNPH1		Day 7		Day 1,28	
ENSP00000453508	ENSG00000171914	TLN2		Day 3		Day 1,3	
ENSP00000381736	ENSG00000152234	ATP5A1				Day 1,3,7	Day 3,28
ENSP00000302935	ENSG00000172349	IL16	Day 3			Day 1	
ENSP00000369315	ENSG00000133026	MYH10				Day 1	Day 1
ENSP00000228825	ENSG00000111229	ARPC3				Day 7	Day 1
ENSP00000264335	ENSG00000108953	YWHAE	Day 28				Day 1
ENSP00000365458	ENSG00000165119	HNRNPK	Day 3	Day 3			
ENSP00000349748	ENSG00000116560	SFPQ	Day 3	Day 3,7			
ENSP00000286788	ENSG00000156261	CCT8	Day 3			Day 3	
ENSP00000295470	ENSG00000152795	HNRNPDL	Day 3		Day 3		
ENSP00000324105	ENSG00000108515	ENO3	Day 3				Day 28
ENSP00000357076	ENSG00000158710	TAGLN2		Day 3	Day 7		
ENSP00000312999	ENSG00000114353	GNAI2		Day 3	Day 28		
ENSP00000386672	ENSG00000138069	RAB1A		Day 3	Day 7		
ENSP00000443053	ENSG00000150991	UBC	Day 28		Day 3		
ENSP00000387065	ENSG00000143933	CALM2		Day 7	Day 3		
ENSP00000270142	ENSG00000142168	SOD1		Day 28			Day 3
ENSP00000219169	ENSG00000102898	NUTF2	Day 7,28	Day 28			
ENSP00000455356	ENSG00000180209	MYLPF	Day 7	Day 7			
ENSP00000295897	ENSG00000163631	ALB	Day 28	Day 7,28			
ENSP00000350667	ENSG00000140416	TPM1		Day 7		Day 28	
ENSP00000398592	ENSG00000070831	CDC42		Day 28	Day 7,28		
ENSP00000380033	ENSG00000100201	DDX17	Day 28				Day 28

Table B-22 Significantly enriched MSigDB Reactome Pathways for B cells at day 7.

Category ID	Category Genes #	Significant Genes #(%) [#Protein Families]	Genes Up (AS03 vs. PBS) #(%)	Genes Down (AS03 vs. PBS) #(%)	P	FDR
<b>METABOLISM OF PROTEINS</b>	409	5 (1.2) [2]	4 (1)	1 (0.2)	<0.0001	0.0035
<b>ANTIGEN PRESENTATION FOLDING ASSEMBLY AND PEPTIDE LOADING OF CLASS I MHC</b>	20	2 (10) [2]	2 (10)	0 (0)	0.0001	0.0162
<b>SMOOTH MUSCLE CONTRACTION</b>	23	2 (8.7) [2]	2 (8.7)	0 (0)	0.0002	0.0176
<b>SEMA4D INDUCED CELL MIGRATION AND GROWTH CONE COLLAPSE</b>	24	2 (8.3) [2]	2 (8.3)	0 (0)	0.0002	0.0176
<b>SEMA4D IN SEMAPHORIN SIGNALING</b>	29	2 (6.9) [2]	2 (6.9)	0 (0)	0.0003	0.023

Table B-23 Significantly enriched MSigDB Reactome Pathways for B cells at day 28.

Category ID	Category Genes #	Significant Genes #(%) [#Protein Families]	Genes Up (AS03 vs. PBS) #(%)	Genes Down (AS03 vs. PBS) #(%)	P	FDR
<b>CELL CYCLE</b>	389	16 (4.1) [3]	0 (0)	16 (4.1)	<0.0001	<0.0001

Table B-24 Significantly enriched MSigDB Reactome Pathways for monocytes at day 3.

Category ID	Category Genes #	Significant Genes #(%) [#Protein Families]	Genes Up (AS03 vs. PBS) #(%)	Genes Down (AS03 vs. PBS) #(%)	P	FDR
<b>METABOLISM OF MRNA</b>	207	8 (3.9) [8]	6 (2.9)	2 (1)	<0.0001	<0.0001
<b>METABOLISM OF RNA</b>	252	8 (3.2) [8]	6 (2.4)	2 (0.8)	<0.0001	<0.0001
<b>ANTIGEN PROCESSING CROSS PRESENTATION</b>	72	5 (6.9) [5]	5 (6.9)	0 (0)	<0.0001	0.0002
<b>PEPTIDE CHAIN ELONGATION</b>	82	5 (6.1) [5]	3 (3.7)	2 (2.4)	<0.0001	0.0003
<b>INFLUENZA VIRAL RNA TRANSCRIPTION AND REPLICATION</b>	99	5 (5.1) [5]	3 (3)	2 (2)	<0.0001	0.0005
<b>3 UTR MEDIATED TRANSLATIONAL REGULATION</b>	101	5 (5) [5]	3 (3)	2 (2)	<0.0001	0.0005
<b>NONSENSE MEDIATED DECAY ENHANCED BY THE EXON JUNCTION COMPLEX</b>	101	5 (5) [5]	3 (3)	2 (2)	<0.0001	0.0005
<b>SRP DEPENDENT COTRANSLATIONAL PROTEIN TARGETING TO MEMBRANE</b>	105	5 (4.8) [5]	3 (2.9)	2 (1.9)	<0.0001	0.0005
<b>ER PHAGOSOME PATHWAY</b>	59	4 (6.8) [4]	4 (6.8)	0 (0)	<0.0001	0.001
<b>INFLUENZA LIFE CYCLE</b>	134	5 (3.7) [5]	3 (2.2)	2 (1.5)	<0.0001	0.0013
<b>TRANSLATION</b>	140	5 (3.6) [5]	3 (2.1)	2 (1.4)	<0.0001	0.0014
<b>REGULATION OF MRNA STABILITY BY PROTEINS THAT BIND AU RICH ELEMENTS</b>	83	4 (4.8) [4]	4 (4.8)	0 (0)	<0.0001	0.0026
<b>IMMUNE SYSTEM</b>	870	9 (1) [11]	9 (1)	0 (0)	0.0002	0.007
<b>CLASS I MHC MEDIATED ANTIGEN PROCESSING PRESENTATION</b>	228	5 (2.2) [5]	5 (2.2)	0 (0)	0.0002	0.007
<b>HOST INTERACTIONS OF HIV FACTORS</b>	118	4 (3.4) [4]	4 (3.4)	0 (0)	0.0002	0.007
<b>INTEGRATION OF ENERGY METABOLISM</b>	113	4 (3.5) [3]	2 (1.8)	2 (1.8)	0.0002	0.007
<b>FORMATION OF THE TERNARY COMPLEX AND SUBSEQUENTLY THE 43S COMPLEX</b>	46	3 (6.5) [3]	2 (4.3)	1 (2.2)	0.0002	0.007
<b>CDK MEDIATED PHOSPHORYLATION AND REMOVAL OF CDC6</b>	47	3 (6.4) [3]	3 (6.4)	0 (0)	0.0002	0.007
<b>AUTODEGRADATION OF THE E3 UBIQUITIN LIGASE COP1</b>	48	3 (6.2) [3]	3 (6.2)	0 (0)	0.0002	0.007
<b>P53 INDEPENDENT G1 S DNA DAMAGE CHECKPOINT</b>	49	3 (6.1) [3]	3 (6.1)	0 (0)	0.0002	0.007
<b>SCF BETA TRCP MEDIATED DEGRADATION OF EMI1</b>	50	3 (6) [3]	3 (6)	0 (0)	0.0002	0.007

Table B-24 Continued.

Category ID	Category Genes #	Significant Genes #(%) [#Protein Families]	Genes Up (AS03 vs. PBS) #(%)	Genes Down (AS03 vs. PBS) #(%)	P	FDR
VIF MEDIATED DEGRADATION OF APOBEC3G	50	3 (6) [3]	3 (6)	0 (0)	0.0002	0.007
DESTABILIZATION OF MRNA BY AUF1 HNRNP D0	52	3 (5.8) [3]	3 (5.8)	0 (0)	0.0003	0.0075
ACTIVATION OF THE MRNA UPON BINDING OF THE CAP BINDING COMPLEX AND EIFS AND SUBSEQUENT BINDING TO 43S	54	3 (5.6) [3]	2 (3.7)	1 (1.9)	0.0003	0.0075
P53 DEPENDENT G1 DNA DAMAGE RESPONSE	54	3 (5.6) [3]	3 (5.6)	0 (0)	0.0003	0.0075
SCFSKP2 MEDIATED DEGRADATION OF P27 P21	54	3 (5.6) [3]	3 (5.6)	0 (0)	0.0003	0.0075
CDT1 ASSOCIATION WITH THE CDC6 ORC ORIGIN COMPLEX	55	3 (5.5) [3]	3 (5.5)	0 (0)	0.0003	0.0076
REGULATION OF APOPTOSIS	56	3 (5.4) [3]	3 (5.4)	0 (0)	0.0003	0.0078
AUTODEGRADATION OF CDH1 BY CDH1 APC C	57	3 (5.3) [3]	3 (5.3)	0 (0)	0.0004	0.0079
ACTIVATION OF NF KAPPAB IN B CELLS	61	3 (4.9) [3]	3 (4.9)	0 (0)	0.0004	0.0091
METABOLISM OF PROTEINS	409	6 (1.5) [6]	3 (0.7)	3 (0.7)	0.0005	0.0092
CYCLIN E ASSOCIATED EVENTS DURING G1 S TRANSITION	63	3 (4.8) [3]	3 (4.8)	0 (0)	0.0005	0.0092
SIGNALING BY WNT	63	3 (4.8) [3]	3 (4.8)	0 (0)	0.0005	0.0092
INTERFERON SIGNALING	153	4 (2.6) [6]	4 (2.6)	0 (0)	0.0005	0.0093
ASSEMBLY OF THE PRE REPLICATIVE COMPLEX	64	3 (4.7) [3]	3 (4.7)	0 (0)	0.0005	0.0093
APC C CDH1 MEDIATED DEGRADATION OF CDC20 AND OTHER APC C CDH1 TARGETED PROTEINS IN LATE MITOSIS EARLY G1	65	3 (4.6) [3]	3 (4.6)	0 (0)	0.0005	0.0093
APC C CDC20 MEDIATED DEGRADATION OF MITOTIC PROTEINS	66	3 (4.5) [3]	3 (4.5)	0 (0)	0.0006	0.0093
ORC1 REMOVAL FROM CHROMATIN M G1 TRANSITION	66	3 (4.5) [3]	3 (4.5)	0 (0)	0.0006	0.0093
REGULATION OF MITOTIC CELL CYCLE	77	3 (3.9) [3]	3 (3.9)	0 (0)	0.0009	0.0138
ADAPTIVE IMMUNE SYSTEM	78	3 (3.8) [3]	3 (3.8)	0 (0)	0.0009	0.014
HIV INFECTION	494	6 (1.2) [6]	6 (1.2)	0 (0)	0.0013	0.0173
	190	4 (2.1) [4]	4 (2.1)	0 (0)	0.0012	0.0173

Table B-24 Continued.

Category ID	Category Genes #	Significant Genes #(%) [#Protein Families]	Genes Up (AS03 vs. PBS) #(%)	Genes Down (AS03 vs. PBS) #(%)	P	FDR
PLATELET ACTIVATION SIGNALING AND AGGREGATION	191	4 (2.1) [3]	2 (1)	2 (1)	0.0012	0.0173
REGULATION OF INSULIN SECRETION	87	3 (3.4) [2]	1 (1.1)	2 (2.3)	0.0013	0.0173
SYNTHESIS OF DNA	90	3 (3.3) [3]	3 (3.3)	0 (0)	0.0014	0.0187
DOWNSTREAM SIGNALING EVENTS OF B CELL RECEPTOR BCR	91	3 (3.3) [3]	3 (3.3)	0 (0)	0.0014	0.0189
METABOLISM OF CARBOHYDRATES	221	4 (1.8) [5]	3 (1.4)	1 (0.5)	0.0021	0.0262
G1 S TRANSITION	104	3 (2.9) [3]	3 (2.9)	0 (0)	0.0021	0.0262
S PHASE	106	3 (2.8) [3]	3 (2.8)	0 (0)	0.0022	0.0271
CELL CYCLE CHECKPOINTS	113	3 (2.7) [3]	3 (2.7)	0 (0)	0.0027	0.0314
SIGNALING BY THE B CELL RECEPTOR BCR	118	3 (2.5) [3]	3 (2.5)	0 (0)	0.003	0.0349
CYTOKINE SIGNALING IN IMMUNE SYSTEM	258	4 (1.6) [6]	4 (1.6)	0 (0)	0.0036	0.0413
MITOTIC G1 G1 S PHASES	127	3 (2.4) [3]	3 (2.4)	0 (0)	0.0037	0.0415
APOPTOSIS	137	3 (2.2) [3]	3 (2.2)	0 (0)	0.0046	0.0496

Table B-25 Significantly enriched MSigDB Reactome Pathways for monocytes at day 7. Results are sorted by FDR and number of significant protein families.

Category ID	Category Genes #	Significant Genes #(%) [#Protein Families]	Genes Up (AS03 vs. PBS) #(%)	Genes Down (AS03 vs. PBS) #(%)	P	FDR
SMOOTH MUSCLE CONTRACTION	23	4 (17.4) [3]	2 (8.7)	2 (8.7)	<0.0001	<0.0001
MUSCLE CONTRACTION	45	4 (8.9) [3]	2 (4.4)	2 (4.4)	<0.0001	0.0003
RESPONSE TO ELEVATED PLATELET CYTOSOLIC CA2	74	4 (5.4) [3]	2 (2.7)	2 (2.7)	<0.0001	0.0017
GLUCOSE METABOLISM	59	3 (5.1) [2]	1 (1.7)	2 (3.4)	0.0001	0.0185
PLATELET ACTIVATION SIGNALING AND AGGREGATION	191	4 (2.1) [3]	2 (1)	2 (1)	0.0003	0.0211
METABOLISM OF CARBOHYDRATES	221	4 (1.8) [3]	2 (0.9)	2 (0.9)	0.0005	0.0305
MRNA SPLICING	103	3 (2.9) [2]	3 (2.9)	0 (0)	0.0007	0.0345
PROCESSING OF CAPPED INTRON CONTAINING PRE MRNA	132	3 (2.3) [2]	3 (2.3)	0 (0)	0.0015	0.0456

**Table B-26 Significantly enriched MSigDB Reactome Pathways for monocytes at day 28.** Results are sorted by FDR and number of significant protein families.

Category ID	Category Genes #	Significant Genes #(%) [#Protein Families]	Genes Up (AS03 vs. PBS) #(%)	Genes Down (AS03 vs. PBS) #(%)	P	FDR
APOPTOTIC EXECUTION PHASE	48	5 (10.4) [3]	4 (8.3)	1 (2.1)	<0.0001	<0.0001
MRNA SPLICING	103	5 (4.9) [4]	5 (4.9)	0 (0)	<0.0001	0.0003
PROCESSING OF CAPPED INTRON CONTAINING PRE MRNA	132	5 (3.8) [4]	5 (3.8)	0 (0)	<0.0001	0.0005
APOPTOSIS	137	5 (3.6) [3]	4 (2.9)	1 (0.7)	<0.0001	0.0005
MRNA PROCESSING	151	5 (3.3) [4]	5 (3.3)	0 (0)	<0.0001	0.0007
RESPONSE TO ELEVATED PLATELET CYTOSOLIC CA2	74	4 (5.4) [4]	3 (4.1)	1 (1.4)	<0.0001	0.0008
PLATELET ACTIVATION SIGNALING AND AGGREGATION	191	5 (2.6) [5]	3 (1.6)	2 (1)	<0.0001	0.0017
CASPASE MEDIATED CLEAVAGE OF CYTOSKELETAL PROTEINS	12	2 (16.7) [2]	1 (8.3)	1 (8.3)	0.0002	0.0146

**Table B-27 Significantly enriched MSigDB Reactome Pathways for neutrophils at day 1.** Results are sorted by FDR and number of significant protein families.

Category ID	Category Genes #	Significant Genes #(%) [#Protein Families]	Genes Up (AS03 vs. PBS) #(%)	Genes Down (AS03 vs. PBS) #(%)	P	FDR
PROTEIN FOLDING	50	5 (10) [2]	2 (4)	3 (6)	<0.0001	<0.0001
PREFOLDIN MEDIATED TRANSFER OF SUBSTRATE TO CCT TRIC	27	4 (14.8) [2]	2 (7.4)	2 (7.4)	<0.0001	<0.0001
METABOLISM OF PROTEINS	409	7 (1.7) [4]	4 (1)	3 (0.7)	<0.0001	<0.0001
THE NLRP3 INFLAMMASOME	11	2 (18.2) [2]	2 (18.2)	0 (0)	<0.0001	0.0062
INFLAMMASOMES	16	2 (12.5) [2]	2 (12.5)	0 (0)	0.0001	0.0116



**Table B-28 Significantly enriched MSigDB Reactome Pathways for neutrophils at day 3.** Results are sorted by FDR and number of significant protein families.

Category ID	Category Genes #	Significant Genes #(%) [#Protein Families]	Genes Up (AS03 vs. PBS) #(%)	Genes Down (AS03 vs. PBS) #(%)	P	FDR
<b>SIGNALING BY THE B CELL RECEPTOR BCR</b>	118	6 (5.1) [3]	3 (2.5)	3 (2.5)	<0.0001	<0.0001
<b>ANTIGEN ACTIVATES B CELL RECEPTOR LEADING TO GENERATION OF SECOND MESSENGERS</b>	27	4 (14.8) [2]	3 (11.1)	1 (3.7)	<0.0001	<0.0001
<b>SIGNALING BY ERBB2</b>	96	5 (5.2) [2]	3 (3.1)	2 (2.1)	<0.0001	<0.0001
<b>SIGNALING BY EGFR IN CANCER</b>	103	5 (4.9) [2]	3 (2.9)	2 (1.9)	<0.0001	<0.0001
<b>SIGNALING BY FGFR</b>	107	5 (4.7) [2]	3 (2.8)	2 (1.9)	<0.0001	<0.0001
<b>SIGNALING BY FGFR IN DISEASE</b>	120	5 (4.2) [2]	3 (2.5)	2 (1.7)	<0.0001	<0.0001
<b>ADAPTIVE IMMUNE SYSTEM</b>	494	7 (1.4) [4]	4 (0.8)	3 (0.6)	<0.0001	<0.0001
<b>RESPONSE TO ELEVATED PLATELET CYTOSOLIC CA2</b>	74	4 (5.4) [2]	3 (4.1)	1 (1.4)	<0.0001	<0.0001
<b>PLATELET ACTIVATION SIGNALING AND AGGREGATION</b>	191	5 (2.6) [3]	3 (1.6)	2 (1)	<0.0001	<0.0001
<b>SIGNALING BY NGF</b>	201	5 (2.5) [2]	3 (1.5)	2 (1)	<0.0001	0.0001
<b>HEMOSTASIS</b>	440	6 (1.4) [4]	3 (0.7)	3 (0.7)	<0.0001	0.0002
<b>IMMUNE SYSTEM</b>	870	7 (0.8) [4]	4 (0.5)	3 (0.3)	<0.0001	0.0009
<b>ER PHAGOSOME PATHWAY</b>	59	3 (5.1) [2]	1 (1.7)	2 (3.4)	<0.0001	0.0009
<b>ANTIGEN PROCESSING CROSS PRESENTATION</b>	72	3 (4.2) [2]	1 (1.4)	2 (2.8)	<0.0001	0.0013
<b>CYTOKINE SIGNALING IN IMMUNE SYSTEM</b>	258	4 (1.6) [3]	1 (0.4)	3 (1.2)	0.0002	0.0026
<b>INTERFERON SIGNALING</b>	153	3 (2) [2]	1 (0.7)	2 (1.3)	0.0007	0.007
<b>CLASS I MHC MEDIATED ANTIGEN PROCESSING PRESENTATION</b>	228	3 (1.3) [2]	1 (0.4)	2 (0.9)	0.0022	0.0169
<b>MRNA SPLICING</b>	103	2 (1.9) [2]	1 (1)	1 (1)	0.0063	0.0355

**Table B-29 Significantly enriched MSigDB Reactome Pathways for neutrophils at day 7.** Results are sorted by FDR and number of significant protein families.

Category ID	Category Genes #	Significant Genes #(%) [#Protein Families]	Genes Up (AS03 vs. PBS) #(%)	Genes Down (AS03 vs. PBS) #(%)	P	FDR
<b>SEMAPHORIN INTERACTIONS</b>	62	3 (4.8) [3]	1 (1.6)	2 (3.2)	<0.0001	0.0095

**Table B-30 Significantly enriched MSigDB Reactome Pathways for neutrophils at day 28.** Results are sorted by FDR and number of significant protein families.

Category ID	Category Genes #	Significant Genes #(%) [#Protein Families]	Genes Up (AS03 vs. PBS) #(%)	Genes Down (AS03 vs. PBS) #(%)	P	FDR
HEMOSTASIS	440	5 (1.1) [4]	0 (0)	5 (1.1)	<0.0001	0.0097
ANTIGEN PRESENTATION FOLDING ASSEMBLY AND PEPTIDE LOADING OF CLASS I MHC	20	2 (10) [2]	2 (10)	0 (0)	0.0002	0.0162
INTEGRATION OF ENERGY METABOLISM	113	3 (2.7) [2]	0 (0)	3 (2.7)	0.0002	0.0162
PLATELET ACTIVATION SIGNALING AND AGGREGATION	191	3 (1.6) [2]	0 (0)	3 (1.6)	0.0008	0.0442

**Table B-31 Significantly enriched MSigDB Reactome Pathways for NK cells at day 3.** Results are sorted by FDR and number of significant protein families.

Category ID	Category Genes #	Significant Genes #(%) [#Protein Families]	Genes Up (AS03 vs. PBS) #(%)	Genes Down (AS03 vs. PBS) #(%)	P	FDR
FORMATION OF TUBULIN FOLDING INTERMEDIATES BY CCT TRIC	21	5 (23.8) [3]	5 (23.8)	0 (0)	<0.0001	<0.0001
PREFOLDIN MEDIATED TRANSFER OF SUBSTRATE TO CCT TRIC	27	5 (18.5) [3]	5 (18.5)	0 (0)	<0.0001	<0.0001
PROTEIN FOLDING	50	5 (10) [3]	5 (10)	0 (0)	<0.0001	<0.0001
POST CHAPERONIN TUBULIN FOLDING PATHWAY	18	4 (22.2) [2]	4 (22.2)	0 (0)	<0.0001	<0.0001
METABOLISM OF PROTEINS	409	8 (2) [6]	7 (1.7)	1 (0.2)	<0.0001	<0.0001
RESPIRATORY ELECTRON TRANSPORT ATP SYNTHESIS BY CHEMIOSMOTIC COUPLING AND HEAT PRODUCTION BY UNCOUPLING PROTEINS	91	3 (3.3) [3]	3 (3.3)	0 (0)	0.0001	0.0104
FORMATION OF ATP BY CHEMIOSMOTIC COUPLING	15	2 (13.3) [2]	2 (13.3)	0 (0)	0.0001	0.0104
TCA CYCLE AND RESPIRATORY ELECTRON TRANSPORT	124	3 (2.4) [3]	3 (2.4)	0 (0)	0.0003	0.0233

**Table B-32 Significantly enriched MSigDB Reactome Pathways for T cells at day 1.** Results are sorted by FDR and number of significant protein families.

Category ID	Category Genes #	Significant Genes #(%) [#Protein Families]	Genes Up (AS03 vs. PBS) #(%)	Genes Down (AS03 vs. PBS) #(%)	P	FDR
POST CHAPERONIN TUBULIN FOLDING PATHWAY	18	4 (22.2) [2]	4 (22.2)	0 (0)	<0.0001	<0.0001
FORMATION OF TUBULIN FOLDING INTERMEDIATES BY CCT TRIC PROTEIN FOLDING	21	4 (19) [2]	4 (19)	0 (0)	<0.0001	<0.0001
RAP1 SIGNALLING	50	4 (8) [2]	4 (8)	0 (0)	<0.0001	0.0001
LOSS OF NLP FROM MITOTIC CENTROSOMES	16	3 (18.8) [2]	2 (12.5)	1 (6.2)	<0.0001	0.0002
RECRUITMENT OF MITOTIC CENTROSOME PROTEINS AND COMPLEXES	54	3 (5.6) [2]	0 (0)	3 (5.6)	<0.0001	0.0051
MITOTIC G2 G2 M PHASES	61	3 (4.9) [2]	0 (0)	3 (4.9)	<0.0001	0.0063
ARMS MEDIATED ACTIVATION	76	3 (3.9) [2]	0 (0)	3 (3.9)	0.0001	0.0097
PROLONGED ERK ACTIVATION EVENTS	17	2 (11.8) [2]	1 (5.9)	1 (5.9)	0.0002	0.0131
SIGNALLING TO ERKS	19	2 (10.5) [2]	1 (5.3)	1 (5.3)	0.0003	0.0139
	36	2 (5.6) [2]	1 (2.8)	1 (2.8)	0.001	0.0411

**Table B-33 Significantly enriched MSigDB Reactome Pathways for T cells at day 7.** Results are sorted by FDR and number of significant protein families.

Category ID	Category Genes #	Significant Genes #(%) [#Protein Families]	Genes Up (AS03 vs. PBS) #(%)	Genes Down (AS03 vs. PBS) #(%)	P	FDR
SEMAPHORIN INTERACTIONS	62	2 (3.2) [2]	1 (1.6)	1 (1.6)	0.001	0.0462

**Table B-34 Combination of protein families differentiating between seroprotection status for monocytes at day 1.** Sorted by descending absolute logistic regression coefficient (log odds ratio).

Ensembl Protein ID	Ensembl Gene ID	Gene Name	Ensemble Gene Description	Coefficient
ENSP00000459921	ENSG00000262785	PKLR	pyruvate kinase, liver and RBC [Source:HGNC Symbol;Acc:9020]	2.2980
ENSP00000250559	ENSG00000127314	RAP1B	RAP1B, member of RAS oncogene family [Source:HGNC Symbol;Acc:9857]	1.4093
ENSP00000358162	ENSG00000183941	HIST2H4A	histone cluster 2, H4a [Source:HGNC Symbol;Acc:4794]	0.9855
ENSP00000446252	ENSG00000112096	SOD2	superoxide dismutase 2, mitochondrial [Source:HGNC Symbol;Acc:11180]	0.8463
ENSP00000344419	ENSG00000005381	MPO	myeloperoxidase [Source:HGNC Symbol;Acc:7218]	0.6826
ENSP00000381216	ENSG00000088247	KHSRP	KH-type splicing regulatory protein [Source:HGNC Symbol;Acc:6316]	0.1670
ENSP00000350667	ENSG00000140416	TPM1	tropomyosin 1 (alpha) [Source:HGNC Symbol;Acc:12010]	0.1489
ENSP00000371982	ENSG00000100453	GZMB	granzyme B (granzyme 2, cytotoxic T-lymphocyte-associated serine esterase 1) [Source:HGNC Symbol;Acc:4709]	0.0671

**Table B-35 Combination of protein families differentiating between seroprotection status for monocytes at day 3.** Sorted by descending absolute logistic regression coefficient (log odds ratio).

Ensembl Protein ID	Ensembl Gene ID	Gene Name	Ensemble Gene Description	Coefficient
ENSP00000216802	ENSG00000100911	PSME2	proteasome (prosome, macropain) activator subunit 2 (PA28 beta) [Source:HGNC Symbol;Acc:9569]	1.0332
ENSP00000373123	ENSG00000206509	HLA-F	major histocompatibility complex, class I, F [Source:HGNC Symbol;Acc:4963]	0.8873
ENSP00000324074	ENSG00000143401	ANP32E	acidic (leucine-rich) nuclear phosphoprotein 32 family, member E [Source:HGNC Symbol;Acc:16673]	0.7787
ENSP00000250559	ENSG00000127314	RAP1B	RAP1B, member of RAS oncogene family [Source:HGNC Symbol;Acc:9857]	0.5431
ENSP00000391481	ENSG00000163931	TKT	transketolase [Source:HGNC Symbol;Acc:11834]	0.4869
ENSP00000357076	ENSG00000158710	TAGLN2	transgelin 2 [Source:HGNC Symbol;Acc:11554]	0.3746
ENSP00000229270	ENSG00000111669	TPI1	triosephosphate isomerase 1 [Source:HGNC Symbol;Acc:12009]	-0.2424
ENSP00000372155	ENSG00000092010	PSME1	proteasome (prosome, macropain) activator subunit 1 (PA28 alpha) [Source:HGNC Symbol;Acc:9568]	0.2143
ENSP00000296181	ENSG00000082781	ITGB5	integrin, beta 5 [Source:HGNC Symbol;Acc:6160]	0.2064
ENSP00000300026	ENSG00000166794	PPIB	peptidylprolyl isomerase B (cyclophilin B) [Source:HGNC Symbol;Acc:9255]	0.1679
ENSP00000245932	ENSG00000125753	VASP	vasodilator-stimulated phosphoprotein [Source:HGNC Symbol;Acc:12652]	0.0888
ENSP00000279227	ENSG00000149781	FERMT3	fermitin family member 3 [Source:HGNC Symbol;Acc:23151]	0.0695

**Table B-36 Combination of protein families differentiating between seroprotection status for monocytes at day 7.** Sorted by descending absolute logistic regression coefficient (log odds ratio).

<b>Ensembl Protein ID</b>	<b>Ensembl Gene ID</b>	<b>Gene Name</b>	<b>Ensemble Gene Description</b>	<b>Coefficient</b>
<b>ENSP00000353129</b>	ENSG00000183783	KCTD8	potassium channel tetramerization domain containing 8 [Source:HGNC Symbol;Acc:22394]	1.4593
<b>ENSP00000270776</b>	ENSG00000142657	PGD	phosphogluconate dehydrogenase [Source:HGNC Symbol;Acc:8891]	0.8716
<b>ENSP00000455356</b>	ENSG00000180209	MYLPF	myosin light chain, phosphorylatable, fast skeletal muscle [Source:HGNC Symbol;Acc:29824]	0.7378
<b>ENSP00000279227</b>	ENSG00000149781	FERMT3	fermitin family member 3 [Source:HGNC Symbol;Acc:23151]	-0.5299
<b>ENSP00000346550</b>	ENSG00000197043	ANXA6	annexin A6 [Source:HGNC Symbol;Acc:544]	-0.4512
<b>ENSP00000264932</b>	ENSG00000073578	SDHA	succinate dehydrogenase complex, subunit A, flavoprotein (Fp) [Source:HGNC Symbol;Acc:10680]	0.4453
<b>ENSP00000388169</b>	ENSG00000241553	ARPC4	actin related protein 2/3 complex, subunit 4, 20kDa [Source:HGNC Symbol;Acc:707]	-0.4105
<b>ENSP00000295897</b>	ENSG00000163631	ALB	albumin [Source:HGNC Symbol;Acc:399]	0.3807
<b>ENSP00000273398</b>	ENSG00000114573	ATP6V1A	ATPase, H+ transporting, lysosomal 70kDa, V1 subunit A [Source:HGNC Symbol;Acc:851]	0.3463
<b>ENSP00000216802</b>	ENSG00000100911	PSME2	proteasome (prosome, macropain) activator subunit 2 (PA28 beta) [Source:HGNC Symbol;Acc:9569]	0.2992
<b>ENSP00000346921</b>	ENSG00000004455	AK2	adenylate kinase 2 [Source:HGNC Symbol;Acc:362]	-0.2647
<b>ENSP00000262030</b>	ENSG00000110955	ATP5B	ATP synthase, H+ transporting, mitochondrial F1 complex, beta polypeptide [Source:HGNC Symbol;Acc:830]	-0.1258

**Table B-37 Combination of protein families differentiating between seroprotection status for neutrophils at day 1.** Sorted by descending absolute logistic regression coefficient (log odds ratio).

Ensembl Protein ID	Ensembl Gene ID	Gene Name	Ensemble Gene Description	Coefficient
ENSP00000362089	ENSG00000148346	LCN2	lipocalin 2 [Source:HGNC Symbol;Acc:6526]	-6.5855
ENSP00000386786	ENSG00000196604	POTEF	POTE ankyrin domain family, member F [Source:HGNC Symbol;Acc:33905]	6.2142
ENSP00000216392	ENSG00000100504	PYGL	phosphorylase, glycogen, liver [Source:HGNC Symbol;Acc:9725]	-4.9844
ENSP00000236826	ENSG00000118113	MMP8	matrix metalloproteinase 8 (neutrophil collagenase) [Source:HGNC Symbol;Acc:7175]	-3.1220
ENSP00000221992	ENSG00000105388	CEACAM5	carcinoembryonic antigen-related cell adhesion molecule 5 [Source:HGNC Symbol;Acc:1817]	-2.9938
ENSP00000443475	ENSG00000167553	TUBA1C	tubulin, alpha 1c [Source:HGNC Symbol;Acc:20768]	-2.5615
ENSP00000250559	ENSG00000127314	RAP1B	RAP1B, member of RAS oncogene family [Source:HGNC Symbol;Acc:9857]	-2.1966
ENSP00000380334	ENSG00000100365	NCF4	neutrophil cytosolic factor 4, 40kDa [Source:HGNC Symbol;Acc:7662]	-2.1249
ENSP00000295897	ENSG00000163631	ALB	albumin [Source:HGNC Symbol;Acc:399]	2.0315
ENSP00000222553	ENSG00000105835	NAMPT	nicotinamide phosphoribosyltransferase [Source:HGNC Symbol;Acc:30092]	-2.0269
ENSP00000459921	ENSG00000262785	PKLR	pyruvate kinase, liver and RBC [Source:HGNC Symbol;Acc:9020]	-2.0072
ENSP00000279227	ENSG00000149781	FERMT3	fermitin family member 3 [Source:HGNC Symbol;Acc:23151]	1.8581
ENSP00000350667	ENSG00000140416	TPM1	tropomyosin 1 (alpha) [Source:HGNC Symbol;Acc:12010]	-1.8502
ENSP00000222286	ENSG00000105679	GAPDH5	glyceraldehyde-3-phosphate dehydrogenase, spermatogenic [Source:HGNC Symbol;Acc:24864]	-1.7305
ENSP00000401010	ENSG00000077549	CAPZB	capping protein (actin filament) muscle Z-line, beta [Source:HGNC Symbol;Acc:1491]	-1.2546
ENSP00000310219	ENSG00000173110	HSPA6	heat shock 70kDa protein 6 (HSP70B) [Source:HGNC Symbol;Acc:5239]	-1.2306
ENSP00000346550	ENSG00000197043	ANXA6	annexin A6 [Source:HGNC Symbol;Acc:544]	1.0741
ENSP00000371982	ENSG00000100453	GZMB	granzyme B (granzyme 2, cytotoxic T-lymphocyte-associated serine esterase 1) [Source:HGNC Symbol;Acc:4709]	-1.0695
ENSP00000384678	ENSG00000189403	HMGB1	high mobility group box 1 [Source:HGNC Symbol;Acc:4983]	-1.0413
ENSP00000466090	ENSG00000197561	ELANE	elastase, neutrophil expressed [Source:HGNC Symbol;Acc:3309]	-1.0067
ENSP00000263238	ENSG00000115091	ACTR3	ARP3 actin-related protein 3 homolog (yeast) [Source:HGNC Symbol;Acc:170]	-0.7432
ENSP00000354947	ENSG00000198898	CAPZA2	capping protein (actin filament) muscle Z-line, alpha 2 [Source:HGNC Symbol;Acc:1490]	-0.5263
ENSP00000369315	ENSG00000133026	MYH10	myosin, heavy chain 10, non-muscle [Source:HGNC Symbol;Acc:7568]	-0.5010
ENSP00000283195	ENSG00000153201	RANBP2	RAN binding protein 2 [Source:HGNC Symbol;Acc:9848]	0.2982
ENSP00000241052	ENSG00000121691	CAT	catalase [Source:HGNC Symbol;Acc:1516]	0.1718
ENSP00000394496	ENSG00000110880	CORO1C	coronin, actin binding protein, 1C [Source:HGNC Symbol;Acc:2254]	0.0231

## APPENDIX C

### ASSESSMENT OF INSTRUMENT STABILITY

Due to requiring the LTQ mass spectrometer to run 700 samples for quality control, a stability test was performed to determine the stability of it and the Thermo PAL autosampler. Ten aliquots of Pepmix (Table C-1) were loaded into the autosampler and run in triplicate using a 60 min gradient (5-45% acetonitrile). The raw files were converted to mxzml format and analyzed using X!Tandem. The number of peptides identified and the glufib peak area were plotted to observe any trends between the samples (Figure C-1).

**Table C-1 Components of Pepmix Samples**

Concentration (fmol/ $\mu$ L)	Peptide/Protein Digest	Company
50	BSA Digest Standard	Protea
50	Yeast ( <i>S. cerevisiae</i> ) alcohol dehydrogenase	Protea
50	Yeast ( <i>S. cerevisiae</i> ) enolase	Protea
50	Glu-1-Fibrinopeptide B	Protea
100	Angiotensin II	Sigma Aldrich
100	ACTH	Sigma Aldrich

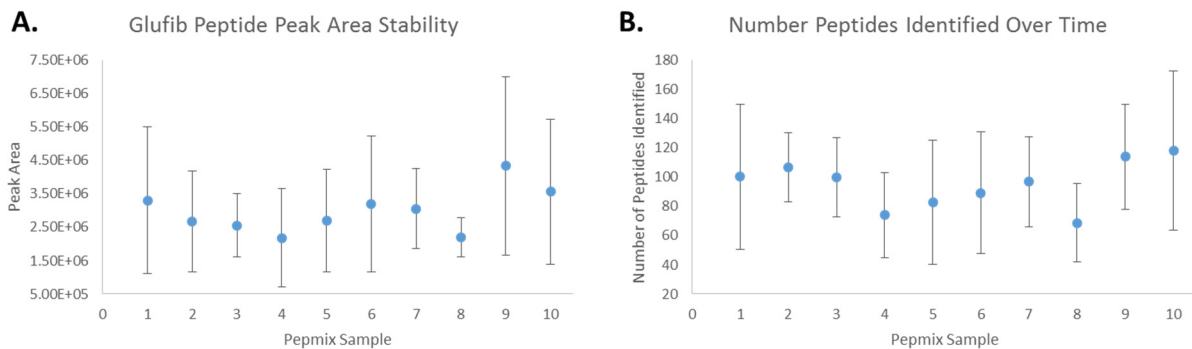


**Figure C-1 Assessment of stability in LTQ.** (A) Glufib peptide peak area and (B) number of peptides identified in triplicate experiments of 10 pepmix samples shows some variability across samples, but overall no significant differences between samples.

Glufib was chosen as the peptide to monitor for stability, as it is added to each sample prior to MS analysis to monitor the chromatography and instrument response. The peak area of glufib and the total number of peptides tracked similar patterns over the 10 pepmix samples. While there is variability across samples, there is no significant differences due to the overlap of the error bars. The high standard deviation was determined to be due to an issue in the autosampler picking up such a small volume (1  $\mu$ L). Overall, it was determined that the instrument and autosampler was stable enough to run the QC samples. Additional pepmix samples and blanks were run during QC experiments to ensure continued stability of the instrument.



# Allison C. Galassie

263 Wildberry Lane, Nashville, TN 37209 · Phone: 803-413-7871

Email: allison.c.galassie@gmail.com · Web: <https://www.linkedin.com/in/allisoncgalassie>

## EDUCATION

---

**Vanderbilt University** Nashville, TN  
**Ph.D., Chemistry** May 2017  
Advisor: Dr. Andrew J. Link  
Dissertation Title: Quantitative Proteomic Analysis of the Human Immune Response following Influenza Vaccination

**Eastern Kentucky University** Richmond, KY  
**B.S., Forensic Science**, concentration in Forensic Chemistry May 2012  
**B.S., Chemistry**, ACS certified May 2012  
**Minor: Statistics** **GPA: 3.97**  
Honors Diploma and *Summa Cum Laude*

## RESEARCH EXPERIENCE

---

**Graduate Research Assistant** April 2013 - Present  
Vanderbilt University Nashville, TN

- Performed sample preparation and shotgun proteomic analysis of human immune cell subtypes to investigate the changes made in regards to adjuvanted and non-adjuvanted influenza vaccines
- Collaborated across many disciplines (immunologists, microbiologists, statisticians, clinicians)
- Analyzed large datasets using various proteomics and systems biology software programs
- Maintained and troubleshot mass spectrometers and HPLC pumps
- Performed gel electrophoresis, western blotting, and co-immunoprecipitation to purify proteins

**Research Assistant, Organic and Analytical Lab** Jan 2011 – May 2012  
Eastern Kentucky University Richmond, KY

- Conducted novel synthetic developments towards ergovaline
  - Optimized the condensation of proline and valine into their diketopiperazine product
- Characterized synthesized compounds using DART-MS

**Student Intern/ Laboratory Technician, Veterinary Diagnostic Lab** May 2011 – May 2012  
University of Kentucky Veterinary Diagnostic Laboratory Lexington, KY

- Examined ergovaline stability in fescue grass over time and at different temperatures
  - Aided in the determination of superior sample collection and storage methods for fescue samples
- Perform other diagnostic tests as needed using various types of instrumentation (nitrate/nitrite levels in ocular fluid using colorimetric techniques, heavy metal levels using ICP-MS)

## PUBLICATIONS

---

Howard, L.H., Hoek, K.L., Goll, J. B., Samir, P., **Galassie, A. C.**, Allos, T.M., Niu, X., Gordy, L.E., Creech, C.B., Prasad, N., Jensen, T.L., Hill, H., Levy, S.E., Joyce, S., Link, A.J., Edwards, K.M. Cell-based systems biology analysis of AS03-adjuvanted H5N1 avian influenza vaccine responses: a phase I randomized controlled trial. PLoS ONE: 12(1): e0167488, doi: 10.1371/journal.pone.0167488.

**Galassie, A. C.**, Link, A. J. Proteomic contributions to our understanding of vaccine and immune responses. Prot. Clin. Appl., 9: 972-989. doi: 10.1002/prca.201500054.

Hoek, K. L., Samir, P., Howard, L. M., Niu, X., Prasad, N., **Galassie, A. C.**, Liu, Q., Allos, T. M., Floyd, K. A., Guo, Y., Shyr, Y., Levy, S. E., Joyce, S., Edwards, K. M., Link, A. J. A cell-based systems biology assessment of human blood to monitor immune responses after influenza vaccination. PLoS One. 2015 Feb 23; 10(2):e0118528. doi: 10.1371/journal.pone.0118528.

**Galassie, A. C.** Sound Quality of Stringed Instruments as Related to Price. 2012. Honors Theses. 50. [http://encompass.eku.edu/honors\\_theses/50](http://encompass.eku.edu/honors_theses/50)

## WORKS IN PROGRESS

---

**Galassie, A. C.**, Goll, J., Samir, P., Jensen, T., Hoek, K. L., Howard, L. M., Allos, T. M., Niu, X., Gordy, L. E., Creech, C. B., Hill, H., Joyce, S., Edwards, K. M., Link, A. J. Proteomics show antigen presentation processes in human immune cells after AS03-H5N1 vaccination. Proteomics – in revisions.

Browne, C. M., Samir, P., Gerbasi, V., Shen, B., Sun, M., **Galassie, A. C.**, Frank, J., Link, A. J. Yeast RACK1 regulates ribosome biogenesis during heat stress. In preparation.

## PRESENTATIONS

---

### Oral Presentations:

- **Galassie, A. C.**, Goll, J., Samir, P., Jensen, T., Hoek, K. L., Howard, L. M., Allos, T. M., Niu, X., Gordy, L., Creech, C. B., Hill, H., Joyce, S., Edwards, K. M., Link, A. J. Using Quantitative Proteomics to Profile Changes in Individual Immune Cell Types after an AS03-adjuvanted H5N1 Vaccine. Southeastern Regional Meeting of the American Chemical Society, Columbia, SC, October 2016.
- **Galassie, A. C.** Quantitative Proteomic Analysis of Immune Cells in Response to AS03-adjuvanted H5N1 Vaccination. Vanderbilt University Chemistry Forum, Nashville, TN, April 2016.
- **Galassie, A. C.** Quantitative Proteomic Analysis of Immune Cells in Response to AS03-adjuvanted H5N1 Vaccination. Vanderbilt University IBVSTP Inflammation Forum, Nashville, TN, February 2016.
- **Galassie, A. C.** Update on Immune System Responses to an Adjuvanted Influenza Vaccine. Vanderbilt University IBVSTP Inflammation Forum, Nashville, TN, May 2015.
- **Galassie, A. C.** Immune System Responses to an Adjuvanted Influenza Vaccine. Vanderbilt University Chemistry Seminar, Nashville, TN, Oct 2014.
- **Galassie, A. C.** Immune System Response to Adjuvanted and Nonadjuvanted Influenza Vaccines. Vanderbilt University IBVSTP Inflammation Forum, Nashville, TN, Jan 2014.
- **Galassie, A. C.** Sound Quality as Related to Price of Stringed Instruments. Eastern Kentucky University Honors Program Thesis Conference, Richmond, KY, April 2012.
- **Galassie, A. C.**, Jones, N., Van Zant, S., Wheeler, B. Learning Outcomes of Interdisciplinary Projects. Kentucky Honors Roundtable, Richmond, KY, Sept 2011.
- **Galassie, A. C.** Why are Stradivari Violins Superior? An Analysis of Varnish and Woods. Eastern Kentucky University Department of Chemistry seminar, Richmond, KY, 2010.

### Poster Presentations:

- **Galassie, A. C.**, Goll, J., Samir, P., Jensen, T., Hoek, K. L., Howard, L. M., Allos, T. M., Niu, X., Gordy, L., Creech, C. B., Hill, H., Joyce, S., Edwards, K. M., Link, A. J. Using Quantitative Proteomics to Profile Changes in Individual Immune Cell Types after an AS03-adjuvanted H5N1

Vaccine. Poster presentation at Vanderbilt Institute for Chemical Biology Student Research Symposium, Nashville, TN, August 2016.

- Gosline, S. J. C., Knight, P., Yu, T., Prasad, N., Jones, A., Shrestha, S., Boone, B., Levy, S. E., Link, A. J., **Galassie, A. C.**, Weinberg, H., Friend, S., La Rosa, S., Guinney, J., Bakker, A. The molecular landscape of dermal neurofibromatosis. 107<sup>th</sup> Annual Meeting of the American Association for Cancer Research, New Orleans, LA, April 2016.
- **Galassie, A. C.**, Goll, J., Samir, P., Jensen, T., Hoek, K. L., Howard, L. M., Allos, T. M., Niu, X., Gordy, L., Creech, C. B., Hill, H., Joyce, S., Edwards, K. M., Link, A. J. Using Quantitative Proteomics to Profile Changes in Individual Immune Cell Types after an AS03-adjuvanted H5N1 Vaccine. 64<sup>th</sup> ASMS Conference on Mass Spectrometry and Allied Topics, San Antonio, TX, June 2016.
- Howard, L.M., Hoek, K.L., Goll, J.B., Samir, P., **Galassie, A. C.**, Allos, T.M., Niu, X., Creech, C.B., Prasad, N., Jensen T.L., Hill, H., Levy, S.E., Joyce, S., Edwards, K.M., Link, A.J. Systems Biology of Vaccination for AS03-adjuvanted H5N1 avian influenza in humans. IDWeek 2015: The Annual Meeting of the Infectious Diseases Society of America. San Francisco, CA, Oct. 2015.
- **Galassie, A. C.**, Samir, P., Hoek, K. L., Niu, X., Link, A. J. Quantitative Proteomic and Systems Analysis of Cells in Response to External Stimuli. 63<sup>rd</sup> ASMS Conference on Mass Spectrometry and Allied Topics, St. Louis, MO, May-June 2015.
- **Galassie, A. C.**, Samir, P., Hoek, K. L., Niu, X., Link, A. J. Quantitative Proteomic and Systems Analysis of Cells in Response to External Stimuli. 62<sup>nd</sup> ASMS Conference on Mass Spectrometry and Allied Topics, Baltimore, MD, June 2014.
- Samir, P., Hoek K.L., Howard, L. M., Allos, T., **Galassie, A. C.**, Niu, X., Creech, C. B., Joyce, S., Edwards, K. M., Link, A. J. Optimizing the iTRAQ Multiplexing Strategy for Quantitative Proteomics Analysis of Immune Cell Subsets Fractionated from Whole Blood of Human Subjects. 61<sup>st</sup> ASMS Conference on Mass Spectrometry and Allied Topics, Minneapolis, MN, 2013.
- **Galassie, A. C.**, Wieliczko, M. B., Smith, D. L. *In situ* Analysis of the Synthesis of Ergovaline using Direct Analysis in Real Time Mass Spectrometry (DART-MS). American Chemical Society National Meeting, San Diego, CA, April 2012 and Undergraduate Presentation Showcase, Richmond, KY, April 2012.
- **Galassie, A. C.**, Wieliczko, M. B., Smith, D. L. Synthetic Developments towards Ergovaline. Kentucky Academy of Sciences Meeting, Murray, KY, Nov. 2011.
- **Galassie, A. C.**, Jones, N., Van Zant, S., Wheeler, B. Learning Outcomes of Interdisciplinary Projects. National Collegiate Honors Council Conference, Phoenix, AZ, Oct 2011.

## TEACHING EXPERIENCE

---

<b>Teaching Assistant, Analytical Chemistry</b> Department of Chemistry, Vanderbilt University	Aug. 2016 – Dec 2016 Nashville, TN
<b>Teaching Assistant, Forensic Analytical Chemistry</b> Department of Chemistry, Vanderbilt University	Jan 2013- May 2013 Nashville, TN
<b>Teaching Assistant, General Chemistry Lab</b> Department of Chemistry, Vanderbilt University	Aug 2012- Dec 2012 Nashville, TN
<b>Teaching Assistant, Forensic and Chemical Instrumental Analysis</b> Department of Chemistry, Eastern Kentucky University	Aug 2011-May 2012 Richmond, KY
<b>Teaching Assistant, Forensic Microscopy</b> Department of Chemistry, Eastern Kentucky University	Aug 2011-Dec. 2011 Richmond, KY

**Tutor and Grader**  
Department of Chemistry, Eastern Kentucky University

Aug 2010-May 2011  
Richmond, KY

---

**AWARDS AND FUNDING**

---

Top Poster at the Vanderbilt Institute for Chemical Biology Student Research Symposium	2016
NIH Training Grant: Immunobiology of Blood and Vascular Systems Training Program	2013 – 2016
ASMS Student Travel Award	2015, 2016
Vanderbilt Graduate School Travel Grant	2014, 2015, 2016
Top Senior in Forensics Award	2012
Top Junior in Forensics Award	2011
Top Junior in Chemistry Award	2010
Thomas Herndon Scholarship	2010
President's List	Fall 2008 – Spring 2010, Spring 2011 – Spring 2012
Dean's List	Fall 2008 – Spring 2012

---

**AFFILIATIONS**

---

American Chemical Society  
American Society for Mass Spectrometry  
Mu Sigma Rho National Statistics Honorary Society

---

**LEADERSHIP**

---

Chemistry Department Student Representative for the Dean	August 2011-May 2012
--	----------------------

---

**COMMUNITY SERVICE AND OUTREACH**

---

Adventure Science Center: Nanoday and Making Stuff Volunteer	March 2014
Vanderbilt Center for Science Outreach: Young Scientist Journal Editor	Fall 2014
Vanderbilt Center for Science Outreach: Poster Judge	July 2015, July 2016
Nashville Zoo Adult Volunteer Corps	August 2016 - Present